THE CLONING, CHARACTERISATION AND ENGINEERING OF AN IGF-I-BINDING SINGLE CHAIN FV

Anthony Simon Roberts B.App.Sc.(Hons.)

A thesis submitted for the degree of Doctor of Philosophy

Queensland University of Technology
School of Life Sciences

2004

QUEENSLAND UNIVERSITY OF TECHNOLOGY

DOCTOR OF PHILOSOPHY THESIS EXAMINATION

CANDIDATE NAME:	*Anthony Simon Roberts*
FACULTY:	*Science*
SCHOOL:	*Life Sciences*
CENTRE:	*Science Research Centre / CRC for Diagnostics*
PRINCIPAL SUPERVISOR:	*Dr Terry Walsh*
ASSOCIATE SUPERVISOR:	*Dr Robert Irving*
THESIS TITLE:	*The Cloning, Characterisation and Engineering of an IGF1-Binding Single Chain Fv*

Under the requirements of PhD regulations, Section 16, it is hereby certified that the thesis of the above-named candidate has been examined. On advice from the Principal Supervisor and Head of School, I recommend on behalf of the University that the thesis be accepted in fulfilment of the conditions for the award of the degree of Doctor of Philosophy.

.....

Professor R Wissler
Chair of Research Degrees Committee

21.7.04
.....
Date

Keywords

Antibody, IGF-I, single-chain Fv, error-prone PCR, scFv library, ribosome display, selection, enzyme-linked immunosorbent assay, BIAcore, DNA shuffling.

ABSTRACT

This thesis describes the construction and characterisation of an insulin-like growth factor (IGF-I)-binding single chain Fv (scFv) and the utilisation of this scFv as a model protein for the study of the application of DNA shuffling and ribosome display to antibody engineering.

The variable domain genes were isolated from the hybridoma cell line producing the monoclonal antibody and successfully joined by PCR for the construction of the scFv, named anti-GPE. Sequencing of the gene revealed an unusually short heavy chain CDR2 region. The cloned scFv was expressed in *E. coli* and purified. Expression levels were low and the protein has poor solubility, most likely due to a reduction in folding efficiency caused by the abbreviated CDR2. The purified monomeric form of the protein was analysed for binding to IGF-I using surface plasmon resonance on the BIAcore 1000 with the specificity of the IgG version of the antibody for the three N-terminal residues of IGF-I – Gly-Pro-Glu – reproduced. The scFv's calculated dissociation constant of 3.68 μM is a low affinity for an antibody and is approximately 36-fold weaker than was calculated for the Fab version of the antibody, but it is concluded that the calculated affinity for the scFv was an apparent affinity that may be an underestimation of true affinity due to the presence of non-functional or misfolded scFv species within the gel-filtration purified monomer peaks. A mutant version of anti-GPE with residues inserted in the CDR2 to restore it to normal length produced a protein with improved expression and solubility characteristics while retaining IGF-I-binding. It was concluded that the short CDR2 was due to deletions generated during the somatic mutation process and a model for this is described.

A ribosome display method using a rabbit reticulocyte lysate as a source of ribosomes was developed for specific selection of anti-GPE against IGF-I. Error prone PCR was used to produce a random point mutated library of anti-GPE (EPGPE). This was taken through several cycles of display and selection but selection for non-specifically binding scFvs was commonly observed. This was probably due to poor folding of ribosome-displayed proteins in the system used, possibly caused by the presence of DTT in the lysate and/or the low capacity of the anti-GPE framework to tolerate mutation while retaining stability. It is assumed misfolds, exposing hydrophobic regions, would have a tendency to non-specifically interact with the selection surface. Of the 64 EPGPE clones screened from four rounds

of display and selection, many were shown to have poor or non-specific binding, but one scFv was characterised that was affinity matured 2.6-fold over anti-GPE wild type affinity for IGF-I.

A DNA shuffling method was developed to produce libraries of chimaeric scFvs between anti-GPE and NC10 (anti-neuraminidase scFv) with the objective of isolating functional IGF-I-binding chimaeras. The NC10 scFv had its CDRs replaced with the anti-GPE CDRs prior to the shuffling to increase the likelihood of isolating IGF-I binders. Ribosome display was used for selection from the chimaera libraries. Selection strategies included elution of specific binders by GPE peptide and a GPE 10-mer peptide. Selection was also performed using IGF-I immobilised on a BIAcore sensorchip as a selection surface. Again, much non-specific selection was observed as seen for display of EPGPE, for what was expected to be the same reasons. Selected scFvs were genuinely chimaeric but with poor expression and solubility and mostly non-specific in their binding. One characterised selected chimaera, made up of three segments of each of the parental scFvs, was shown to bind specifically to IGF-I by BIAcore. Steps to improve the efficiency of the ribosome display system have been identified and are discussed.

The work contained in this thesis has not been previously submitted for a degree or diploma at any other higher education institution. To the best of my knowledge and belief, the thesis contains no material previously published or written by another person except where due reference is made.

Anthony Roberts
Date:

Part of the work presented in this thesis is found in the publication:

Irving, R.A., Coia, G., Roberts, A., Nuttall, S.D. and Hudson P.J., **2001**. Ribosome display and affinity maturation: from antibodies to single V-domains and steps towards cancer therapeutics. *J. Immunol. Methods*. 248:31-45.

Acknowledgements

Thank you to my supervisors Dr Bob Irving and Dr Terry Walsh for their time and effort, encouragement, intellectual input, and constructive criticism during the course of this work. I am fortunate to have been able to work in Prof Peter Hudson's laboratory at CSIRO and am grateful to him for the opportunity. As a mentor in the laboratory, Dr Peter Iliades was extremely generous and I thank him for his patience, friendship and first class technical assistance.

Dr Greg Coia, Dr Olan Dolezal, Mrs Meghan Hattarki, Dr John Atwell, Dr Maria Galanis, Dr Stewart Nuttall and Dr Alec Kortt were always happy to offer their expertise and advice and I thank them. Thanks to the many other friends I have made at CSIRO, Parkville, including Ms Anna Raicevic, Mr Tristan Wallis, Ms Suzy Juraja, Ms Aneta Todorovska, and all the people in the 'corner group' who have helped to create a productive work environment and make the experience enjoyable, even during the stressful times.

To Annie Edmonds, for your patience, understanding and love during the writing of this thesis, thank you. Special gratitude to my parents, Ray and Sue Roberts who have always nurtured and supported education and learning, financially and morally, thanks for your love, encouragement and assistance.

CONTENTS

List of Figures

List of Tables

Abbreviations

~	approximately
amp^R	amplicillin resistance
AMV	avian myoblastosis virus
A_{280nm}	absorbance at 280 nm
bp	base pairs
DEPC	diethylpyrocarbonate
DNA	deoxyribonucleic acid
dNTPs	deoxyribonucleoside triphosphates – dATP, dCTP, dGTP, dTTP (A = adenisine, C = cytidine, G = guanosine, T = thymidine)
EDC	N-ethyl-N/-(dimethylaminopropyl)carbodiimide
EDTA	ethylene diamine tetra acetic acid
ELISA	enzyme-linked immunosorbent assay
FACS	fluorescence activated cell sorting
g	acceleration due to gravity
IGF-I	insulin-like growth factor I
IgG	immunoglobulin G isotype
IPTG	isopropyl-β-D-thio-galactopyranoside
kD	kilodaltons
Mab	monoclonal antibody
MHC	major histocompatibility complex
MWCO	molecular weight cut off
mRNA	messenger RNA
NHS	N-hydroxysuccinimide
OD	optical density
PCR	polymerase chain reaction
PEG	polyethylene glycol
PBS	phosphate buffered saline
PVDF	polyvinyl-dinene difluoride
RBS	ribosome binding site
RNA	ribonucleic acid
RT	reverse transcription
SPR	surface plasmon resonance
SDS	sodium dodecyl sulphate
TAE	tris acetate EDTA buffer
TBS	tris buffered saline
TEMED	N,N,N,/N,/-tetramethylethylenediaminine
Tris	Tris(hydroxymethyl)aminomethane
UV	ultraviolet
V	antibody variable domain
V_H	heavy chain variable domain
V_L	light chain variable domain
wt	wild type
w/v	weight per volume
YT	yeast extract-tryptone

CHAPTER 1
INTRODUCTION

1.1 Introduction

This thesis describes experimental work to produce a recombinant antibody fragment from a novel monoclonal antibody, and using this as a model, the study of new molecular evolution approaches to select and improve these fragments. The work falls broadly into the field of antibody engineering. In the biomedical field it is necessary to produce binding molecules of high affinity and specificity to a target antigen or ligand. Antibodies and antibody fragments with such properties are of use in diagnostics and therapeutics or as research tools. A growing understanding of the mechanisms of diseases suggests that demand for these molecules will continue to increase. Improving the methods by which such proteins are designed, selected and produced is a constant challenge. Thus, methods for construction of libraries of variant binding molecules, selection of the best from these libraries, and their further evolution, need to be optimised, and novel improved methods developed. In recent years numerous techniques have been developed which have been used successfully to produce high affinity antibody-like molecules. Binding activities produced in nature can now be generated in the laboratory and even improved upon and engineered for possible use in science and medicine. The particular properties of the molecule being studied often dictates the method used. This chapter gives a brief introduction to antibodies and the antibody engineering field, and provides a general overview of some recent developments and current approaches used to isolate, engineer and affinity mature or evolve antibody fragments.

1.2 Antibodies

Antibodies, members of the immunoglobulin superfamily, are soluble proteins that are produced by B-lymphocytes as part of the immune response to bind foreign antigen and aid in its elimination (Roitt *et al.*, 1993). The immunoglobulin structure consists of two light polypeptide chains and two heavy polypeptide chains joined by disulphide bonds (Porter, 1973). The immunoglobulin molecule forms an approximate Y-shape, with both heavy and light chain N-terminal domains of variable sequence at the tips of the arms, binding antigen (Press and Hogg, 1969). The highly homologous C-terminal constant domains of the stem are responsible for the effector functions that aid in elimination of the antigen (Roitt *et al.,* 1993). Studies on the enzymic digestion of immunoglobulins

revealed that they can be reduced to two identical portions that are able to bind antigen, known as Fab fragments and an Fc portion, with no such antigen-binding activity (Palmer *et al.*, 1962). The two arms form the Fab portions while the stem is the Fc portion. The heavy and light chains of a Fab can associate to form an Fv, the region responsible for antigen binding (Inbar *et al.*, 1972). The Fab fragment consists of a complete light chain and the N-terminal half (Fd) of a heavy chain (Poljak *et al.*, 1973). Within the variable regions of the heavy (V_H) and light (V_L; V_κ or V_λ) chains there are three hypervariable regions which are close to each other in the folded protein, fully exposed to solvent, and which comprise the antigen binding site (Poljak *et al.*, 1973). These hypervariable regions are known as the complementarity determining regions (CDR1, CDR2 and CDR3). The diversity of antibody sequences is caused by a number of factors (Tonegawa, 1983). Essentially, each V_H region gene is made up of germline V_H, D and J_H sequences and each V_L of $V_{\kappa \text{ or } \lambda}$ and $J_{\kappa \text{ or } \lambda}$ sequences. These are joined in various combinations that can lead to great diversity, considering that there are around 300 V_H, 12 D and 4 J_H segments, thus many different combinations are possible. There also is junctional diversity as the precise site of joining can vary leading to different reading frames. Furthermore, almost any light chain can pair with any heavy chain. Finally, somatic mutation can cause amino acid substitutions that add variability. Thus, the immune system is equipped to cope with the vast diversity of antigens that it will be exposed to in a lifetime. A schematic representation of the immunoglobulin molecule is shown in Figure 1.1.

1.3 Recombinant antibody production

Monoclonal antibodies (Mabs) are single antibody species of desired specificity to a particular antigen, secreted from a cell line made by fusion of mouse myeloma and spleen cells from an immunised donor (Kohler and Milstein, 1975). They have been an important tool for scientists over the last two decades, having found many practical applications in research and medical and health sciences (Winter and Milstein, 1991).

The ability to manipulate antibody genes has opened up many new possibilities for the design and production of useful antibodies and their derivatives. It was shown initially that an antibody light chain variable region gene could be taken from a myeloma cell line, cloned into a plasmid vector and transformed into lymphoid cells for expression (Oi *et al.*, 1983). At the same time a heavy chain gene was cloned and expressed in a lymphoid line (Neuberger, 1983).

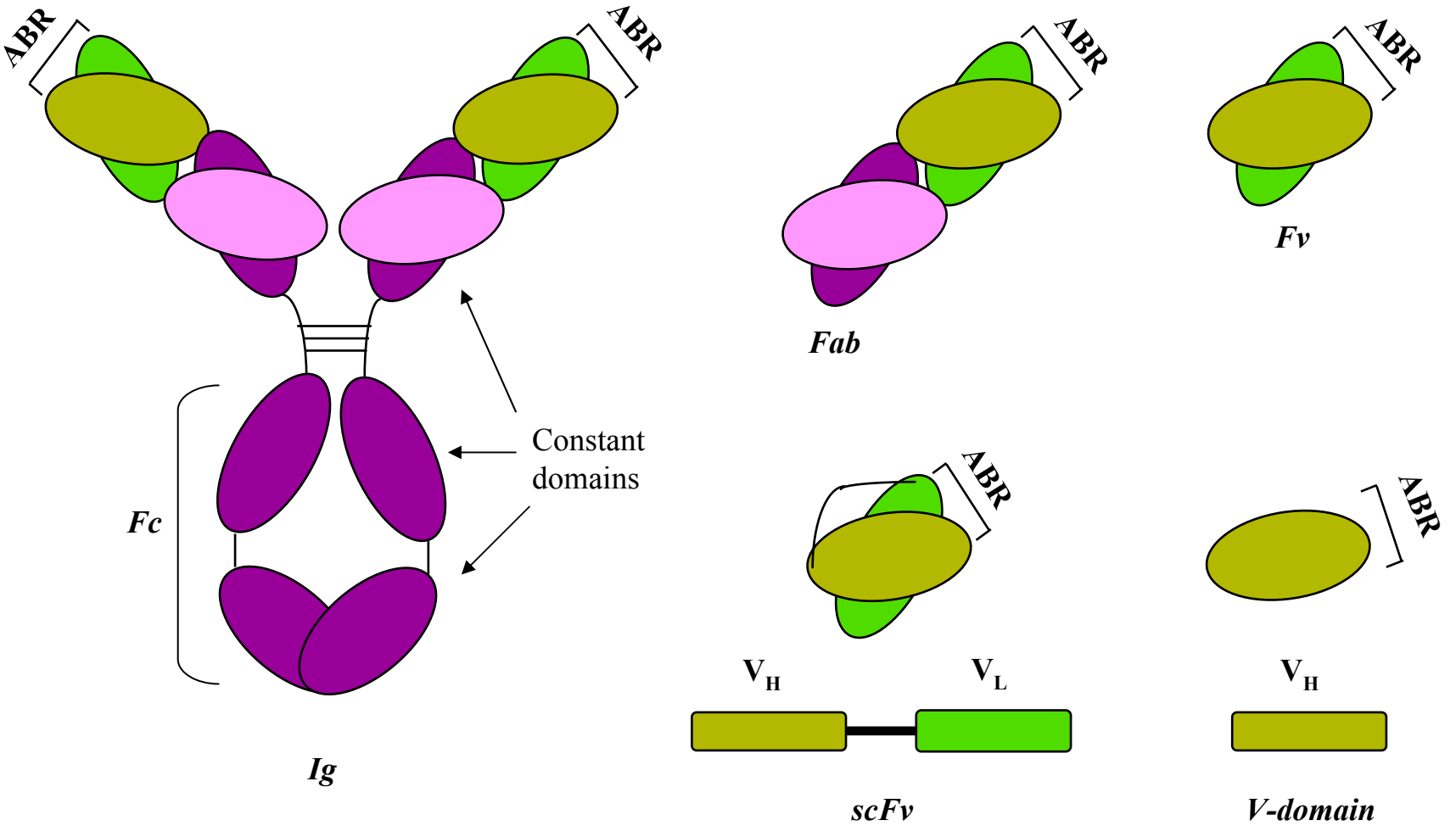

Figure 1.1 Schematic representation of immunoglobulin molecule and its derived fragments. ABR – antigen binding region.

The ability to produce antibodies by recombinant DNA technology and express them in bacteria opened up possibilities for their large-scale production and engineering. Cabilly *et al.*, (1984) cloned antibody heavy and light chains, from cDNA produced from hybridoma-extracted mRNA, and a Fab fragment was reconstituted from the *E. coli* extract and shown to retain antigen-binding activity. Similarly, Boss *et al.*, (1984) expressed antibody heavy and light chains from cDNA clones in *E. coli* for expression of an insoluble product whose binding affinity and specificity after solubilisation and refolding, was similar to that of the parent, hybridoma-produced IgM.

Skerra and Pluckthun, (1988) improved bacterial expression systems for the production of soluble Fv fragments that were able to correctly fold and associate to form a functional antibody-binding site. V_H and V_L domains were expressed from a vector that fused them to a signal peptide, directing the expressed fragments to the periplasm, mimicking transport in eukaryotic cells to the lumen of the endoplasmic reticulum where formation of functional antibody takes place. Affinity of the recombinant Fv fragments was identical to that of the parent antibody. A chimaeric Fab fragment, also linked to a signal peptide, was expressed in bacteria (Better *et al.*, 1988). This Fab, consisting of human Ig constant regions and mouse Ig variable regions, was shown to associate heavy and light chains in the periplasm and displayed the same binding activity as Fab fragments prepared proteolytically from the whole antibody.

It was then shown that the heavy and light chain variable regions (V_H and V_L) could be expressed as a single polypeptide chain by linking them with a flexible glycine-rich sequence of usually 15 amino acids (Huston *et al.*, 1988). In this structure, known as a single-chain Fv (scFv), the CDR loops are presented in such a way as to form a binding site of similar affinity to the parent monoclonal antibody. Bird *et al*., (1988) also developed a 'single-chain antigen binding protein' desiring to overcome the problems of expression of antibody genes in *E. coli* and to produce a better imaging or delivery molecule with low background and without the problems of dissociation of Fv fragments. These scFvs also were able to bind with affinity similar to that of the parent Mabs and were proposed to have advantages such as better penetration of the microcirculation, faster clearance rates and lower immunogenicity due to their size.

The ability to amplify variable domain genes by polymerase chain reaction (PCR), using a set of primers to conserved regions at the ends of V_H and V_L sequences, demonstrated an improvement in the efficiency of cloning (Orlandi *et al.*, 1989) which could now occur without cDNA library

construction, with inclusion of restriction sites in the PCR primers. It was now possible to clone directly from spleen or lymphocytes, thus bypassing hybridomas (Chiang *et al.*, 1989). Using PCR, a whole repertoire of V_H genes were amplified from the spleen cells of a mouse immunised with lysozyme and expressed in *E. coli* (Ward *et al.*, 1989). By screening these *E. coli* culture supernatants against lysozyme coated on microtiter plate wells, positive binders were isolated with affinities of up to K_D = 20 nM. When V_H region binders were expressed with V_K regions forming Fv fragments, affinities were improved further. Thus, the creation of antibody libraries had begun.

The development of methods to create antibody gene libraries was an important step in the bypassing of hybridomas, as this surveys the immunological repertoire more efficiently than is possible with the production of monoclonal antibodies (Sastry *et al.*, 1989). As spleen cell immunoglobulin mRNA is more diverse than that from hybridomas, this was used as the source of V_H genes for amplification and cloning of a library into phage vector (Sastry *et al.*, 1989). Sequencing of the amplified genes revealed a diverse library from a number of V_H subgroups. As V_H regions are generally not able to bind antigen with as high an affinity as a full antibody with an interacting V_L region, a Fab library was constructed to make use of the combined properties of heavy and light chains (Huse *et al.*, 1989). λ phage was used for this library with a large number of antigen binding clones being isolated. This was the start of the development of methods of antibody production that mimic the diversity of the immune system, suggesting future possibilities of antibody production without using animals. Fragments demonstrating reduction of antibody size are shown in Figure 1.1.

1.4 Phage display of antibody libraries

In order to efficiently select for useful antibody fragments from the libraries that were now being produced, methods employing display technology had to be developed. The use of filamentous phage for the display of antibody domains was a step closer to mimicking the clonal selection and amplification of antibodies displayed by B-cells of the immune system (McCafferty *et al.*, 1990). Filamentous phage were first used for the display of peptides by insertion of the encoding DNA fragments into the gene3 of the bacteriophage (Smith, 1985). The phage displays the peptide as a fusion to the gene3 protein at the tip of the virion, and this can be selected by antibody against the peptide for enrichment over non-specific phage. It was shown that one positive binding phage could be enriched from 10^8 non-specific phage (Parmley and Smith, 1988). This is a powerful technique,

the key being the linkage of the displayed peptide with its encoding genetic information within the phage particle. A random epitope library was constructed by ligation of degenerate fragments coding for approximately 10^9 possible nucleotide sequences into the gene3 of a phage vector (Scott and Smith, 1990). Phage were selected against an immobilised Mab of known epitope with binding phage eluted from the Mab and used to reinfect *E. coli* for amplification of the phage. After three rounds of this selection cycle, enriched phage were found to contain very similar sequences to the known epitope. The utility of this phage display and selection cycle was further demonstrated with a large epitope library screened against a number of different Mabs (Cwirla *et al.*, 1990).

With the principle of phage display proven, display of functional protein domains was then demonstrated by Bass *et al.*, (1990) with functional, properly folded human growth hormone displayed on phage when expressed as a gene3 fusion. An improved vector system was used that produced mostly monovalent display, negating avidity effects observed when multivalent display occurs on the four or five gene3 proteins expressed per virion, thus allowing better selection of binders based on their true affinities. The first antibody fragment to be displayed on phage was an anti-lysozyme scFv, expressed as a gene3 fusion (McCafferty *et al.*, 1990). Importantly, the antigen-binding site retained binding and specificity and phage antibody could be enriched by antigen even when diluted over 10^6-fold. It was then shown that scFv and Fab of the same antibody displayed on phage using phage or phagemid vectors retained binding function (Hoogenboom *et al.*, 1991). One chain of a Fab was expressed as a gene3 fusion, with the complementary chain secreted as a soluble chain to the periplasm, associating with the gene3-fused chain to form a Fab. The phagemid vector was designed with an amber stop codon so that it could be used for either phage display or soluble expression of the molecule, depending on whether suppressor or non-suppressor strains of *E. coli* respectively were used.

At around the same time the first libraries of antibody fragments were expressed on the phage surface as gene3 fusions. Clackson *et al.*, (1991) constructed a library of V_H and V_κ chains linked randomly as scFvs from mice immune to the hapten phOx and isolated a fragment with a dissociation constant of 10 nM. Barbas *et al.*, (1991) were able to express an anti-tetanus toxoid Fab library and isolated binders by panning against immobilised antigen. Subsequently, a human antibody library was constructed by amplification of V_H and V_L genes from peripheral blood lymphocytes and the random linkage of these genes as scFvs for display on phage (Marks *et al.*, 1991). The library of 10^7 clones was panned against different antigens and scFvs with affinities of

around $K_D = 10^{-7}$ M were selected. The library was similar in size to a mouse B-cell repertoire and the result was significant as specific antibodies were isolated without the need for immunisation.

Synthetic libraries were then produced where a rearranged V-gene pair was randomised in the V_H CDR3 with degenerate primers (Barbas *et al.*, 1992). A totally synthetic library for phage display was then created by using degenerate primers to add random CDR3 sequences and a J region to 49 unrearranged germline V_H genes and then linkage to a V_L for scFv display (Hoogenboom and Winter, 1992). Several antibodies against two haptens and a protein antigen were isolated from this library. Nissim *et al.*, (1994) enlarged this synthetic library by creating random CDR3 sequences of a greater range of lengths (4-12 residues). The resultant library was large (approximately 10^8 clones) with scFvs of a wide range of specificities to a diverse range of antigens isolated. This CDR mutagenesis is discussed further in section 1.5.4.

In an attempt to make the creation of larger phage antibody repertoires possible, thereby increasing the probability of isolating antibodies with higher affinities, Waterhouse *et al.*, (1993) developed a system for the *in vivo* recombination of heavy and light chains from two different replicons for packaging within the same phage particle. This involved using the *loxP*-Cre site-specific recombination system where *loxP* sites are placed at either end of the genes of interest and the Cre enzyme recognises these sites and catalyses recombination at these points. This strategy was used to create a very large library of Fab fragments (6.5×10^{10}) from which antibodies to a wide range of antigens were isolated with affinities approaching those of the secondary immune response (Griffiths *et al.*, 1994). The library was constructed by *in vivo* recombination of a heavy chain repertoire of 10^8 genes and a light chain repertoire of 8×10^5 genes, both created by randomisation of CDR3 (1.5.4). The heavy chain repertoire was encoded on a 'donor' plasmid and *E. coli* harbouring this repertoire was infected with 'acceptor' phage encoding the light chain repertoire. Antibodies with affinities higher than $K_D = 10$ nM were isolated (Griffiths *et al.*, 1994), compared to affinities of $K_D = 700$ nM from a smaller repertoire of 10^7-10^8 clones (Hoogenboom and Winter, 1992), showing that the larger the library, the better the chances of selecting higher affinity binders. A library of similar size (1.4×10^{10}) and diversity was constructed, with anti-fluorescein antibodies with affinities as high as $K_D = 0.3$ nM generated (Vaughan *et al.*, 1996). This library was made so large by pooling the genes from B-cells of 43 non-immunised donors, ligating large amounts of phagemid vector (100 μg) and insert DNA (10 μg) and a subsequent series of several hundred electroporations. It was expected that this library, as it comprised naturally rearranged V-genes as

scFvs, would have a larger number of functional fragments, less likely to be recognised as foreign, and be advantageous for expression as no subcloning would be needed. Production of a library of this size, however, would be laborious.

Thus, it can be seen that several of types of phage display libraries can be constructed. Libraries from antibody genes of immunised individuals (Clackson *et al.*, 1991) show a bias towards antibodies against the antigen in question so are in general not suited for use as a diverse source of antibodies. Thus, a new library would have to be prepared for each different antigen after time-consuming immunisation. Antibodies from large libraries (Griffiths *et al.*, 1994) have shown similar affinities to those from an immune repertoire. Therefore non-immune or naive libraries (Marks *et al.*, 1991) may be more useful as one library can be used for all antigens and if large repertoires are used, high affinity antibodies may be isolated. The unknown nature of the diversity of a naive repertoire can be partially overcome by the creation of a synthetic library (Hoogenboom and Winter, 1992) where diversity is introduced by randomisation of a defined area of the V-genes. Thus diversity can be added in a controlled manner. A drawback of this could be that some synthetic regions may appear foreign leading to an unwanted immune response (Hoogenboom, 1997). Antibodies of sufficient affinity for diagnostic and therapeutic application may be isolated from any of these libraries, but if libraries of sufficient size are not available, and these can be quite laborious and cumbersome to make, or the selected antibodies have low affinity, then the affinity maturation of selected molecules via the construction of synthetic libraries may be necessary.

1.4.1 Linkage of phage binding with infectivity

The panning procedure of cycling through successive rounds of selection, infection and amplification to obtain high affinity binders can be quite time-consuming and inefficient. A continuous culture strategy that links antigen recognition with phage replication can overcome this problem, reducing the need for separation of binders from non-binders. To achieve this, Duenas and Borrebaeck (1994) engineered M13 phage with deletions in the gene3 protein known to be necessary for attachment and infection of a host bacterium (Crissman and Smith, 1984), thus rendering the phage particles non-infective. This phage was used to display anti-hen egg lysozyme (HEL) antibody fragments as well as other antibodies as fusions to the truncated gene3 protein. After incubation with HEL antigen fused with the N-terminal domain of the gene3, the anti-HEL phage were enriched 10^{10}-fold, from an initial dilution of just one in 10^{11} non-specific phage, after two rounds of selection. Thus, in the same way that the humoral immune system produces high

affinity antibodies against a range of antigens by focussing selective pressure on individual B cells that each respond to one antigen, a linkage between recognition of the displayed antibody with phage replication and clonal amplification had been demonstrated (Duenas and Borrebaeck, 1994). Taking this work further, Duenas *et al.*, (1996) showed that by using this selection and amplification of phage (SAP) technology they could preferentially select and enrich for antibodies based on their kinetic parameters from a model library of six different Fab fragments with the same specificity.

A similar technology known as selectively infective phage (SIP) has been developed by Krebber *et al.*, (1995). In this system, the N-terminal domains have again been deleted from the antibody-displaying gene3 protein and the target antigen/N-terminal domain fusion is engineered into the same phage vector. The initial model system used was an anti-haemaglutinin scFv with the antibody antigen interaction actually occurring in the periplasm of the host cell. It is envisaged that this system may be useful for simultaneously selecting antibodies against members of antigen libraries with the possibility of mutagenesis of either partner in a continuous system. Subsequently, Krebber *et al.*, (1997), used an anti-fluorescein scFv model to further test the system, this time with the fluorescein antigen chemically coupled to the N-terminal domains. They observed up to 10^6 antigen specific binding events from an input of 10^{10} phage compared to only one antigen-independent event. Gramatikoff *et al.*, (1994) also devised a similar system, using a leucine zipper heterodimer interaction to link antigen recognition with phage infectivity. They hypothesised that the cytoplasm or periplasm may be more suitable for these physiological interactions to occur than an *in vitro* environment.

Eleven different residues of an anti-fluorescein scFv thought to be involved in hapten binding were mutated to create a suite of variants that were subjected to three rounds of the SIP process (Pedrazzi *et al*., 1997). The enriched molecules were shown to be within a factor of 2 of the best binding constant but SIP was also able to select for properties such as folding efficiency and stability. In the first demonstration of selection from a scFv library, Hennecke *et al*., (1998) constructed a library in the same scFv to produce a non-repetitive, partly random, 20 residue linker to replace the existing $(Gly_4Ser)_3$ linker. After just one selection round functional clones were obtained that showed comparable binding, expression, folding and solubility to the original scFv with elimination of non-functional linker sequences. A library in the three residues of the V_L kink was produced and SIP

similarly used with selected scFvs showing the same sequence as chosen in nature, showing that SIP can be an effective tool for protein optimisation (Spada et al., 1998).

Riechmann and Holliger, (1997) have shown that the N-terminal domain (N1) of the phage gene3 protein is the ligand for the C-terminal domain of the TolA periplasmic protein involved in infection of *E. coli* and that the adjacent gene3 protein domain (N2) binds the F-pilus. Thus, a further strategy for the linkage of binding and infectivity is the display of antigen on or near the F-pilus. If the corresponding scFv is displayed on phage in place of N2, binding of the scFv to the pilus-displayed antigen may facilitate interaction of N1 with TolA, allowing infection to take place. Malmborg *et al*., (1997) were the first to demonstrate such an *in vivo* selection by displaying 13-15 amino acid long epitopes of cytomegalovirus and HIV-1 V3 as fusions to pilin proteins of the *E. coli* F-pilus. These insertions blocked infection by wild type phage while phage displaying scFvs specific for these epitopes were able to infect the cells. Non-specific phage-scFvs were also shown to be non-infective.

1.5 Mutagenesis of antibody fragments for affinity maturation

After initial selection by the immune system of low affinity antibodies, drawn from the available repertoire at the time of immunisation, somatic mutation of selected genes occurs, followed by selection for antibodies of increased affinity (Griffiths *et al.*, 1984). Studies on sets of Mabs specific for one antigen have revealed that diversity is indeed due to somatic mutation that occurs sequentially with a high rate of about 10^{-3} mutations per base per generation (McKean *et al.*, 1984). Antibodies can be affinity matured *in vitro* by gradual incorporation of mutations that may improve affinity by influencing the position of side chains contacting antigen, by providing new contact residues, or by replacing low affinity contact residues (Hoogenboom, 1997). *In vitro* affinity maturation involves the introduction of diversity into the antibody V-genes to create a 'secondary' library, and selection of higher affinity variants, attempting to mimic the somatic mutation process of the immune system (Hoogenboom, 1997), or to further mature somatically matured molecules beyond levels that can be achieved by the immune system. This diversity can be introduced randomly, or in a more defined fashion by using the information available on immunoglobulin structures and the modelling of antigen binding sites, which reveal that all the hypervariable loops, bar the V_H CDR3, have a limited number of conformations, with sequence changes at a few specific sets of positions switching the chain to a different conformation (Chothia *et al.*, 1989). Thus,

affinity maturation seeks to produce strong binding molecules that will have the advantage in therapeutics of giving longer protection with much smaller dosage (Barbas and Burton, 1996). In diagnostics, high affinity reagents would add sensitivity to testing and would obviously be more cost effective. A number of different mutagenesis techniques exist to facilitate this. Rationally designed interface mutations in the CDR loops can be used to improve affinity (Dougan *et al*., 1998), however, in the absence of structural information, random or semi-rational approaches are necessary, and the best successes reported in the literature have been achieved by these means.

1.5.1 Error-prone PCR

Error-prone PCR utilises polymerases with low fidelity, such as Taq polymerase, to randomly misincorporate nucleotides, and reaction conditions to favour this, for the *in vitro* mutation of genes (Leung *et al.*, 1989), imitating somatic mutation of the immune system. After employing this mutagenesis strategy, a 100-fold increase in eluted phage-Fab relative to a non-mutant population was observed and a Fab of 30-fold higher affinity than the parent Fab was isolated (Gram *et al.*, 1992). Interestingly, this Fab had fewer mutations than the lesser-improved Fabs, suggesting that binding site conformation can be influenced by just a few key residues. An scFv was improved using error-prone PCR and phage display selection against soluble biotinylated antigen at a concentration lower than the K_D of the antibody (Hawkins *et al.*, 1992). Antibody-bound phage were then selected on streptavidin on the basis of their off-rates. Error-prone PCR can also be used to study the contribution of contact and non-contact residues to the affinity of an antibody (Hawkins *et al.*, 1993). Mutations introduced by this approach were able to improve affinity while not being part of the binding site, showing that binding site interactions can be modulated by mutations outside the binding site. It has since become a common method of mutagenesis, having been used in conjunction with phage display for improvements in binding of antibody fragments to a carbohydrate (Deng *et al*., 1994), a steroid (Saviranta *et al*., 1998) and changing specificity (Casson and Manser, 1995; Miyazaki *et al*., 1999) and has also been successfully used with other display technologies (1.6.3; Daugherty *et al*., 2000).

1.5.2 Mutator cells

Another strategy for introduction of random point mutations is the use of bacterial mutator cells. Passage of scFv genes through the *E. coli* mutD5 strain, which has an error-prone DNA polymerase III, has been shown to introduce mutations (Fowler *et al*., 1974), some of which lead to increases in affinity or solubility. Irving *et al.*, (1996) were able to frequently produce 10-fold increases in

apparent affinity of an anti-glycophorin scFv. The general phage display cycle is followed in this strategy with propagation of phage in each cycle carried out in the mutator strain instead of the usual bacterial strain. Using the same strain, Low *et al.*, (1996) were able to improve binding affinity of an anti-2-phenyl-5-oxazolone scFv 100-fold, from a dissociation constant of 320 nM to 3.2 nM. This was achieved by four sequentially acquired mutations. Coia *et al*., (1997) were able to use the same process to improve expression yields of scFvs by 10-fold. This is potentially quite an efficient mutagenesis approach, however, there is the problem that the entire genetic material of the vector harbouring the library is susceptible to mutation which may in some cases render the plasmid, or some genes, non-expressible (Irving *et al.*, 1996).

1.5.3 Chain Shuffling

Chain shuffling is a method of affinity maturation that maximises the potential of V_H and V_L pairing. The technique was first demonstrated by the construction of a phage display library of 2 x 10^5 clones of randomly assembled mouse V_H and V_L genes and selection against the phOx antigen, with sequenced clones showing the repeated occurrence of certain V_H and V_L chains (Clackson *et al.*, 1991). Consequently, a chain shuffling method was developed whereby these V_H and V_L domain binders were recloned with entire V_H and V_L gene repertoires (4 x 10^7 each) respectively, to elicit a much greater pool of strong binders - an early demonstration of high affinity antibodies being generated from phage display libraries. Starting with a human anti-phOx scFv isolated from a phage antibody library, Marks *et al.*, (1992) were able to produce affinity matured scFv by chain shuffling. Firstly, the heavy chain was shuffled with a light chain repertoire, eliciting an scFv of 20-fold greater affinity. Secondly, shuffling of the first two CDRs of the heavy chain against the V_L produced an antibody a further 15-fold improved, in the nanomolar affinity range, approaching that of a tertiary immune response. Kang *et al.*, (1991) also used chain shuffling to expand a family of antigen-binding Fab clones, optimising the pairing of heavy and light chains to produce redesigned antibodies of similar specificities. Likewise, panels of antibody fragments with common specificity to a target can be developed (Osbourne *et al*., 1996; Czerwinski *et al*., 1999). Chain shuffled human antibodies have been produced from an original mouse monoclonal antibody (Figini *et al.*, 1994). A repertoire of 10^7 human Fab heavy chains displayed on phage was mixed with soluble light chains of the mouse antibody for *in vitro* Fab assembly. After selection against antigen, a hybrid Fab of greater than 10-fold higher affinity than the parent was isolated. Selected human heavy chains were then cloned into a phagemid vector containing a human light chain repertoire for the selection of fully human Fabs. The similarity of human and mouse Fabs of this antibody suggested that the

mouse light chain guided the selection of human heavy chains of similar structure to the mouse heavy chain. However, successfully humanised antibodies by chain shuffling can diverge structurally from the original (Bieboer *et al*., 2000). It is proposed that chain shuffling between antibodies from different species may permit more extensive binding site variations (Figini *et al.*, 1994). Chain shuffling has also been used to convert a specificity of an scFv from an anti-hen egg lysozyme to an anti-T cell receptor V alpha (Ward *et al.*, 1995), or more subtly alter the specificity of a DNA-binding Fab (Bespalov *et al*., 1999). An scFv to the tumour antigen c-erB-2 has had its affinity increased sixfold by light chain shuffling and then a further fivefold by heavy chain shuffling (Schier *et al.*, 1996a). Other cancer targeting antibodies have been improved since (Kang *et al*., 2000; Klimka *et al*., 2000). This technique has also been applied to find neutralising antibodies to IL-5 (Ames *et al*., 1995) and antibodies against fibriotic disease targets (Thompson *et al*., 1999).

1.5.4 CDR mutagenesis

Mutagenesis of the CDRs of antibodies has been shown to be an effective approach in the affinity maturation of these molecules in a more focussed manner compared to randomly across the whole gene, as is the case with the use of error-prone PCR and mutator cells. Greater sequence diversity can be produced with this method than with chain shuffling of the V domains made available by the immune system. Essentially, a library of molecules with a randomised CDR is panned against antigen for binders. Selected clones may then be used for construction of a subsequent library where a different CDR has been randomised, known as CDR walking (Rader and Barbas, 1997). Generally, a degenerate primer mix is used that incorporates random nucleotides during PCR into the CDR region. The CDR3 region has been shown to contribute most to the total accessible surface area of an antibody combining site (Chothia and Lesk, 1987), hence the focus has been predominantly in this region. This process of creating antibodies *de novo,* without immunisation, has increased the likelihood of finding antibodies with useful medical applications (Lerner *et al.*, 1992). Changes in the CDRs are less likely to create immunogenic antibodies than changes in the more sequence constrained framework regions (Barbas and Burton, 1996).

CDR3 mutagenesis of an anti-tetanus toxoid Fab (Barbas *et al.*, 1992) resulted in a library of 5 x 10^7 antibodies containing clones with new specificities. By panning against fluorescein, antibodies were enriched showing affinities as good as K_D = 0.1 μM, approaching those of the secondary response of an immunised mouse. The anti-tetanus toxoid antibody had effectively been used as a

framework for mutation into an anti-fluorescein antibody. Sequence data revealed that selection against fluorescein had caused a bias toward the occurrence of certain residues and structural features known to be important in natural antibodies (Barbas *et al.*, 1992). Subsequent work by Barbas *et al.*, (1994) involved mutagenesis of the CDR1 of an antibody Fab and then further mutagenesis of the CDR3 of selected CDR1 clones. This was applied to a Fab against HIV1 envelope protein gp120. Not only was affinity increased eight-fold, but neutralising ability was improved and broadened, important properties in any HIV therapeutic molecule. When four different CDR loops of this antibody were randomised sequentially the affinity improved 420-fold, down to the picomolar range (Yang *et al.*, 1995). Randomisation of four CDRs of an anti-HER-2 Fab led to the isolation of a specific anti-insulin-like growth factor I (IGF-I) Fab (Garrard and Henner, 1993). A synthetic library prepared by randomisation of just six residues of the heavy chain CDR3 of an anti-IL1 beta antibody gave rise to a clone with 10-fold improvement in affinity (Jackson *et al*., 1995). Randomisation of CDRs for an antibody against the V3 loop of HIV has also been shown to improve affinity and broaden reactivity (Thompson *et al.*, 1996). This was achieved chiefly by a reduction in the off rates of the scFv that correlates with neutralisation potency. Again, mutations within CDR3, or those influencing its conformation, showed the greatest influence in improving affinity. An anti-testosterone Fab that had specificity improved by V_H CDR3 mutagenesis, was affinity improved over 10-fold by mutagenesis of other V_H and V_L CDRs (Hemminki *et al*., 1998). One of the greatest increases in affinity has been achieved using CDR mutagenesis (Schier *et al.*, 1996b). An anti-c-erB-2 scFv was increased in affinity 1230-fold by creating mutant libraries in both the V_H CDR3 and V_L CDR3. As c-erB-2 is a tumour antigen, this was a promising result for the development of tumour targeting molecules. In a novel means of producing new antibody specificities, Soderlind *et al*., (2000) created a large library of functional antibody fragments by shuffling diverse naturally occurring CDRs into a master scFv framework. A more complex library was created based on 49 master frameworks that account for 95% of human antibody diversity, with all CDRs randomised with synthetic sequences biased towards naturally occurring residues (Knappik *et al*., 2000). Many specificities have been isolated from this library with good affinities such as selection of an anti-insulin antibody with a dissociation constant of 83 pM (Hanes *et al*., 2000).

1.5.5 DNA shuffling

DNA shuffling is a means of protein evolution by random fragmentation of homologous genes and then their reassembly by PCR (Stemmer, 1994a). Essentially, the gene fragments prime off each

other in a primerless PCR before full-length genes are regenerated by PCR with flanking primers. This method allows for diverse populations of genes to be generated by recombination of any number of parental sequences. In the initial DNA shuffling experiments DNaseI was used to digest the TEM1 β-lactamase gene into 100-300 bp fragments and these homologous sequences were recombined by PCR that introduced point mutations at a rate similar to that of error-prone PCR. After rounds of shuffling and selection of point mutated variants of the one parental gene, the minimum inhibitory concentration of cefotaxime for clones containing shuffled sequences, selected against increasing concentrations of this target antibiotic, increased 32,000-fold (Stemmer, 1994b). It was reported that traditional mutagenesis conducted in parallel only yielded a 16-fold improvement.

The earliest demonstrations of the use and power of this technique were chiefly in improvements to various enzyme functions. An entire arsenate detoxifying pathway, coded for by an operon consisting of arsR, arsB and arsC genes, was DNA shuffled resulting in a 40-fold increase in resistance to arsenate (Crameri *et al.*, 1997). This showed that the method can be applied to large multigene determinants by complex and unexpected mutations that, because they aren't well understood, may be overlooked by more rational mutagenesis strategies. The same technology has seen the evolution of a beta-fucosidase from a beta-galactosidase (Zhang *et al.*, 1997) as well as large improvements in green fluorescent protein activity (Crameri *et al.*, 1996b). In the shuffling of a wild-type with a mutant subtilisin E, Zhao and Arnold (1997b) managed to enhance the number of clones retaining subtilisin activity from 20% up to 95%. This highlighted a key benefit of DNA shuffling in being able to reduce the number of incorporated point mutations which may often be deleterious or negate the effects of a beneficial mutation as would occur in clonal random mutagenesis (Zhao and Arnold, 1997a). This is important as mutations responsible for improved activity are often masked in a background of mutations that are neutral or detrimental to the behaviour being studied. Using these enhanced DNA shuffling strategies the same group substantially improved the activity of the enzyme para-nitrobenzyl esterase (Moore *et al.*, 1997).

An expansion of the method led to DNA shuffling of families of genes with Crameri *et al*., (1998) showing that by shuffling homologous cephalosporinase genes from four different bacterial species, much larger improvements (~50-fold) in enzyme function could be evolved than shuffling between mutants of one parent gene. This approach greatly increases the amount of genetic diversity available for evolution and has found common application. The method similarly has been used for

the shuffling of 11 different human interferon-αs with phage-displayed recombinants showing improved potency on human and murine cells (Patten *et al*., 1997). This work was pursued for the shuffling of 20 interferon-αs with chimaeras selected after two rounds that were up to 185 times more active than the most active parent (Chang *et al*., 1999). Also, Kumamaru *et al*., (1998) improved a biphenyl dioxygenase by shuffling the genes from two different species. Ness *et al*., (1999) family shuffled 26 protease genes and found multiple clones evolved to the four different enzymatic activities measured.

Similar methods to DNA shuffling have since been developed. Small gene fragments of two subtilisin E gene variants, generated by random sequence primers rather than by DNaseI digestion, were shuffled leading to improvements in the enzyme's stability (Shao *et al*., 1998). Another alternative developed by the same laboratory, known as staggered extension process (StEP), involves priming the template sequence, followed by very short extension times, so that the PCR products increase by small amounts with each cycle, with these growing fragments annealing to different templates based on homology until full length genes are regenerated (Zhao *et al*., 1998). By recombining two subtilisin genes this way, two rounds of the StEP process yielded variants with up to fifty times greater half life than the wild type. An alternative method that gives rise to progeny sequences with high levels of recombination, known as random chimaerogenesis on transient templates (RACHITT), involves single-stranded parental sequences being annealed onto a full-length single-stranded template (Coco *et al*., 2001).

The use of DNA shuffling as a method for the improvement of antibody properties is gaining popularity. Antibodies may be ideal candidates for this technique due to the large pools of relatively homologous genes available. This may be a better library construction strategy as in the normal high stringency library screening and selection of the best clones, potential for further improvement by recombination is lost. A PCR mix with fragmented wild-type scFv gene and oligonucleotides coding for randomised CDRs was recombined to produce a library of molecules with a mixture of wild-type and CDR mutant sequences (Crameri and Stemmer, 1995). An advantage of this system is that if one of the CDRs is not conducive to mutation and is replaced by a mutant sequence in 15% of cases, 85% of the library is still available for recovery of useful mutants in other CDRs. Once a pool of mutants is selected, fragmentation and recombination can continue without oligonucleotides to select for more useful permutations. A phage display scFv library created by CDR shuffling to construct the mutated molecules (Crameri *et al.*, 1996a) resulted in all six mutated

CDRs being efficiently incorporated (32-65%) in a wide variety of combinations, and after six rounds of shuffling and panning against granulocyte colony-stimulating factor, the percentage of phage bound increased 440-fold. However, no protein characterisation was undertaken.

Stability has been engineered into an scFv lacking its conserved cysteine residues using DNA shuffling (Proba *et al*., 1998). A scFv lacking one of the heavy chain cysteines was shuffled against variants with either the heavy chain cysteine residues or the light chain cysteine residues replaced. The resultant library yielded stable disulphide-free scFvs with comparable activity to the parent and able to be expressed cytoplasmically in bacteria. Thermodynamic stability has also been engineered into an scFv using DNA shuffling and selection at higher temperatures or in strong reducing environments (Jung *et al*., 1999; Jermutus *et al*., 2001). One of the highest affinity recombinant antibodies reported (K_D = 48 fM) has been evolved using error-prone PCR and DNA shuffling in combination over four rounds of panning (Boder *et al*., 2000). Also, three camel antibodies have been shuffled to generate chimaeras of improved affinity and expression levels (van der Linden *et al*., 2000).

All of the above applications of DNA shuffling to antibody engineering have involved the shuffling of point mutations of a sole parent sequence or shuffling of synthetic CDRs into such a sequence. Lorimer and Pastan (1995) reported the successful shuffling of two different scFvs. Five randomly chosen shuffled sequences showed that all contained a mix of fragments from both antibodies and that all were the result of different recombination events. This was a proof-in-principle at the genetic level only, with no protein characterisation reported. No other such shuffling of defined scFv sequences has been reported. However, two instances of DNA shuffling of whole libraries of V genes have been reported. A library of V_L domains amplified from peripheral blood lymphocytes was diversified by DNA shuffling in the presence and absence of spiking oligonucleotides coding for cytotoxic T-lymphocyte associated protein-4 (CTLA-4) CDR3, with selection of phage displayed binders to the natural CTLA-4 antigen B7.1 (van den Beuken *et al*., 2001). The V_L domains were very low affinity as binding could not be detected by SPR on the BIAcore. No information regarding recombination of different gene segments was provided with sequences selected described as being most closely related to one parental germline V_L gene. However, the numerous amino acid point mutations reported (up to 23.7 %) suggests that some segments from different genes may have been incorporated, but it is not stated in the literature. An scFv was

affinity matured for binding to a tumour antigen by DNA shuffling of a library of V_L domains (Huls *et al*., 2001) but again no evidence of crossovers in the selected genes was provided.

None of the affinity maturation methods described above are flawless but there have been good successes with all of these techniques. Though a more directed method such as CDR mutagenesis can give impressive results due to its focussed manner and the logic behind the mutations, where little structural information is known, the more random approaches, like DNA shuffling, should still be of some use. DNA shuffling has been used widely and very successfully for the improvement of enzymes but there is still much scope for its application to antibody engineering.

1.6 Other display methods

A number of alternative methods to phage display for the selection and evolution of binding reagents have been developed over the last decade indicating the search for methods not subject to the same limitations as phage display.

1.6.1 Ribosome Display

Teurk and Gold (1990) initially suggested the display of peptides or proteins on ribosomes and mutagenic amplification of their RNAs for evolution, after they produced a system for the selection and evolution of RNA ligands to T4 DNA polymerase from a randomised pool of mRNAs. In this system (SELEX), the same selected RNA molecule simultaneously represents genotype and phenotype. Libraries of RNAs have been mutagenised *in vitro* for the evolution of catalytic activity (Beaudry and Joyce, 1992; Bartel and Szostak, 1993). Display of peptides and proteins on ribosomes would link the mRNA genotype via the ribosome to the protein phenotype in a complex. Ribosome display of peptide or antibody libraries, due to its *in vitro* nature, can avoid the limitation of bacterial transformation (10^8-10^9 clones), making generation of libraries several orders of magnitude greater than is currently possible with phage display, as well as accelerating library construction and selection cycles, and minimising *in vivo* expression biases (Irving *et al*., 2001). Screening for toxic proteins should also be able to be demonstrated by this method. Furthermore, secretion, phage assembly and other cellular processes are not required, therefore greater diversity may be achievable (Mattheakis *et al.*, 1996) and selection focused on affinity over avidity due to the monovalent display of the *in vitro* system.

An early demonstration of the system involved a synthetic DNA library coding for random peptide sequences under control of a T7 promoter, incubated in an *E. coli* S30 ribosome transcription/translation system (Mattheakis *et al.*, 1994). The DNA was transcribed to mRNA, which bound to the ribosome for translation of the encoded peptide and a 31-residue spacer region to allow presentation of nascent peptides away from the ribosomal tunnel. Lack of a stop codon was used to stall the peptides and chloramphenicol added to stabilise the complexes. The complexes were selected against an antibody immobilised on ELISA microtiter wells with the message being retrieved for analysis and subsequent rounds of display and selection by reverse transcription. This process lead to enrichment for peptides that had similar sequences to the antibody's known epitope, with affinities in the nanomolar range. Mattheakis *et al*., (1994) suggested that libraries of up to 10^{14} sequences may be possible, a huge improvement from cell-based systems. This connection of genotype and phenotype and cycles of enrichment was obviously analogous to phage display. This work was followed by Gersuk *et al*., (1997) who selected high affinity peptide ligands to prostate specific antigen from a random peptide library. A schematic representation of the ribosome display cycle is shown in Figure 1.2.

There are several features of the ribosome display system that need to be fulfilled in order for display to be effective. For example, to select for protein domains such as antibody fragments, correct folding while attached to the ribosome is required. This assumes that the protein folds co-translationally or immediately at the completion of translation and does not need to be released before folding is initiated, however, there is evidence that both these mechanisms occur (Komar *et al*., 1997; Fedorov and Baldwin, 1997). Furthermore, ribosome displayed enzymes have been shown to retain activity (Kudlicki *et al*., 1995; Makeyev *et al*., 1996). A C-terminal tether of 23-residues was reported to be sufficient for nascent protein to protrude far enough away from the peptidyl transfer centre to exhibit activity (Makeyev *et al*., 1996). The first demonstration of ribosome display of correctly folded molecules was reported for the display of an anti-haemaglutinin scFv (Hanes and Pluckthun, 1997) which was enriched 10^8-fold over non-specific scFvs after five selection cycles. Over the course of five selection cycles, scFvs mutated *in vitro* which has implications for molecular evolution. A number of modifications were performed to achieve this result including: (a) uncoupling of the transcription and translation steps so that scFvs can fold without interference from a reducing agent like DTT which is required by T7 polymerase; (b) inclusion of stem loop structures at both ends of the constructs to minimise mRNA degradation; (c) addition of vanadyl ribonuclease complex (VRC) as a nuclease inhibitor; (d) use of protein

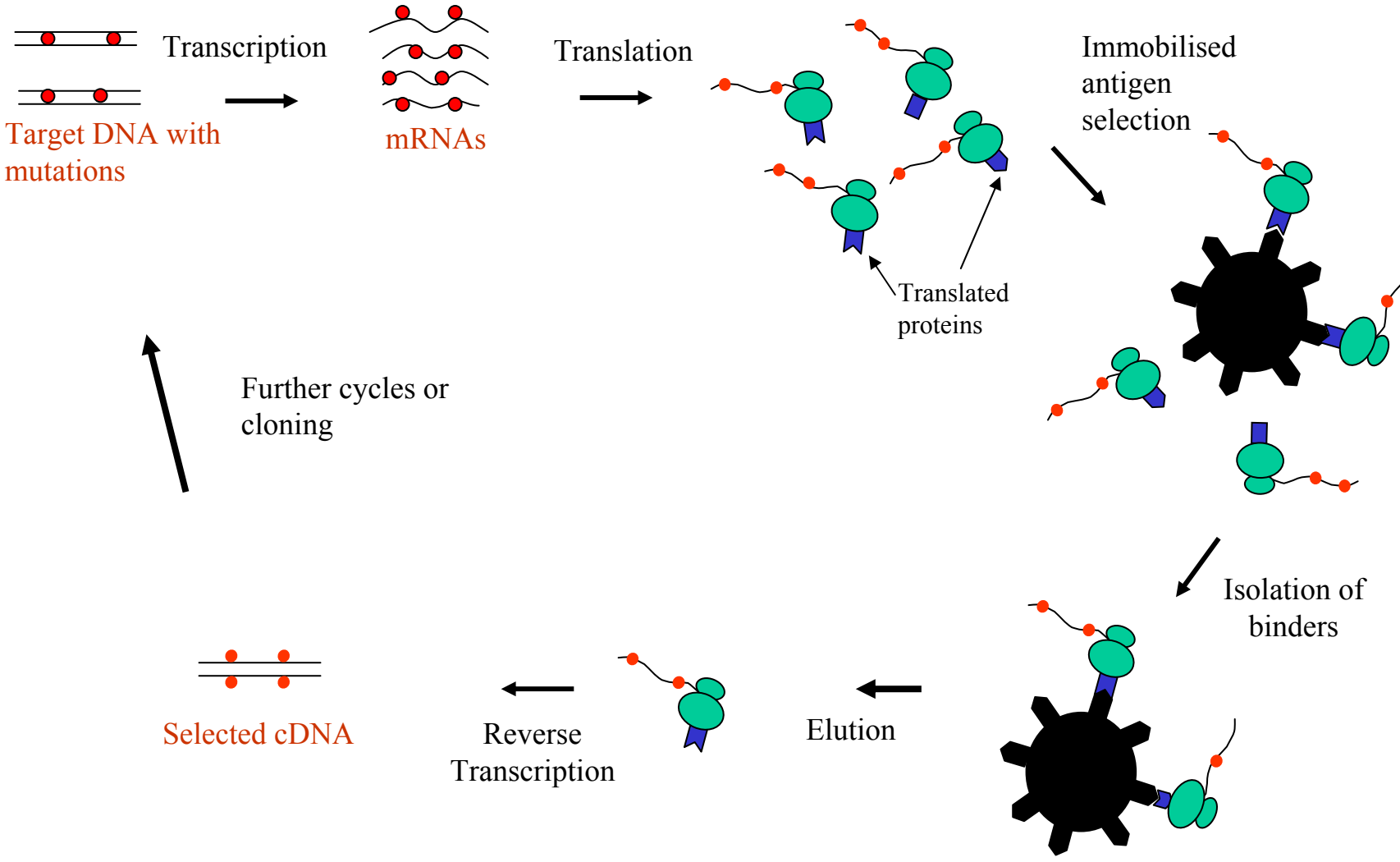

Figure 1.2 Schematic representation of the ribosome display cycle

disulphide isomerase (PDI) to assist folding; and (e) addition of an anti-ssrA oligonucleotide, as ssrA RNA codes for a peptide which marks the protein for degradation and is added to nascent proteins from mRNAs devoid of stop codons in the *E. coli* translation system.

The system developed by the Pluckthun group was applied in the first demonstration of selection from a full library (Hanes *et al*., 1998), where an scFv against the immunising GCN4 peptide of K_D = $4x10^{-11}$ M was selected, and evidence was presented for the existence of "in-built" affinity maturation over several display cycles due to use of non-proofreading polymerases in the RT-PCR amplification. This system has produced successes in a variety of applications since. Picomolar affinity antibodies have been isolated from a synthetic library described in 1.5.4 (Hanes *et al*., 2000), and lower affinity antibodies from the same library have been matured to the picomolar range with very slow off rates by selecting with long washing times, or evolved for higher stability with selection in reducing environments (Jermutus *et al*., 2001). ScFvs able to discriminate between different quadruplex conformations formed by the same DNA sequence motif have also been isolated (Schaffitzel *et al*., 2001), demonstrating the power of the technique in combination with a highly diverse library.

Other proteins have been successfully displayed and selected by ribosome display. Lamla and Erdmann, (2001) showed enrichment of a ribosome displayed protein based on the affinity of its N-terminal $(His)_6$ tag to Ni^{2+}-iminodiacetic acid resin. Their system was inefficient with nine rounds of display and selection required to achieve 10^8-fold enrichment of the specific binder. The selection of sialyltransferase with its immobilised natural substrate (Bieberich *et al*., 2000) was the first report of ribosome display and selection of an enzyme. Takahashi *et al*., (2002) were able to enrich for enzyme activity over three rounds of ribosome display by selecting for affinity to a substrate analog for dihydrofolate reductase (DHFR) with, in this instance, the source of ribosomes being a wheat germ cell free protein synthesis system. The most efficient enrichment for catalytic activity was reported for the ribosome display of a β-lactamase (Amstutz *et al*., 2002). Binding of a ribosome displayed enzyme to an enzyme substrate is not an effective means of capturing enzyme due to the constant substrate turnover, so a substrate analog for β-lactamase was used that is a mechanism-based inhibitor, binding covalently to the enzyme upon turnover, causing irreversible inhibition. In this way, active enzyme was enriched greater than 100-fold in one cycle. In a different application involving a mix of three non-antibody proteins with differing properties, ribosome display was used to enrich for soluble proteins by removal of aggregation-prone molecules using hydrophobic interaction chromatography in the selection step (Matsuura and Pluckthun, 2003).

An alternative eukaryotic system using commercial rabbit reticulocyte lysate as a source of ribosomes was first described for the enrichment of a specific scFv by a factor of 10,000 in one

round of selection from a mix of mutants (He and Taussig, 1997). Use of this system was extended to the selection of anti-progesterone antibody fragments from an immune mouse library (He *et al*., 1999). This system is simpler in concept than the prokaryotic system. The gene construct is simpler with no special loops engineered for minimising nuclease activity and anti-ssrA is not required. A low level of added magnesium and cold temperature are used to stabilise the complexes in this method. The transcription and translation steps are carried out in a coupled reaction, however, this has the potential to be detrimental to the folding of some disulphide bonded proteins, due to the presence of 2 mM DTT that is necessary for T7 polymerase activity. No chaperones or other molecules to aid in folding are included and the authors claim that 10 mM DTT was required to inhibit folding of nascent antibody fragments. However, Hanes *et al*., (1999) reported that the coupled reticulocyte system was several-fold less efficient than sequential transcription and translation in a side-by-side comparison, presumably because each step can be optimised, and it was significantly less efficient again compared to the *E. coli* system. Irving *et al*., (2001) reported specific selection of a number of antibody fragments using the eukaryotic system, with addition in some instances of oxidised glutathione, and selection of a lysozyme binder from a synthetic library based on a CTLA-4 framework, but no characterisation of binding beyond ELISA was presented. The systems described above utilise magnesium and low temperature to stabilise the ribosome display complex. A modified version of display using the rabbit reticulocyte lysate that aims to stabilise the ternary mRNA/ribosome/protein complex has been reported recently. In this case the gene for Ricin A chain protein is included in the ribosome display construct between the gene of interest and the spacer (Zhou *et al*., 2002). The de novo synthesised ricin subunit causes a specific depurination in the 28S RNA, inactivating the ribosome, stalling protein synthesis and causing the formation of a stable complex. This was achieved with binding of glutathione-S-transferase to glutathione, with reasonable recovery of input mRNAs (1-10%), although no selection from libraries has been demonstrated. The eukaryotic system needs to be developed for selection from naïve and synthetic libraries and improved for utility in affinity maturation.

1.6.2 mRNA display

An alternative *in vitro* display method involves a fusion between the nascent polypeptide synthesised from the ribosome and the encoding mRNA, with subsequent release from the ribosome (Nemoto *et al*., 1997). This is made possible by coupling puromycin to the mRNA, and as the puromycin resembles the 3′ end of an aminoacyl-tRNA molecule, it can be transferred to the polypeptide. Roberts and Szostak, (1997) independently achieved the same mRNA-protein fusion

and selection and enrichment for binding of this entity was demonstrated in principle. This method has the potential advantage of being more robust due to the covalent attachment, compared with ternary ribosome display complexes, but has the limitation that the puromycin-mRNA fusion needs to be repeatedly constructed for each cycle. The system was improved by Kurz *et al*., (2000) where manipulations were reduced with the preparation of the mRNA/DNA conjugates by the light induced crosslinking of the DNA-puromycin to the mRNA via a 5/ psoralen group. Wilson et al., (2001) demonstrated the potential of the mRNA display procedure, selecting 20 different streptavidin binding aptamers from a library of totally random 80 residue peptides. The best affinities were as low as K_D = 5 nM and a known streptavidin-binding motif was found in most sequences. The success was attributed to the diversity of the library (6 x 10^{12} individual sequences) and it was suggested that engineering of structural constraints into the library might improve selected affinities further. Further experiments lead to the isolation of ATP binders with affinities of up to K_D = 100 nM after multiple rounds of panning, including the use of error-prone PCR mutagenesis after initial enrichment (Keefe and Szostak, 2001). The technique has been used to demonstrate that in a sufficiently large library, many distinct peptide sequence motifs exist that can recognise a single target (Barrick *et al*., 2001), in this case a particular RNA structure. Baggio *et al*., (2002) showed the ability of mRNA display to display both constrained and non-constrained libraries to elucidate the specific recognition motifs of an enzyme and an antibody. Antibody-like mimics based on the tenth fibronectin type III domain were selected against tumour necrosis factor-α with dissociation constants in the nanomolar range, and after affinity maturation in the picomolar range (Xu *et al*., 2002), showing that mRNA display should be very useful in antibody evolution.

1.6.3 Surface display

Another alternative display system is the presentation of molecules on the surface of cells such as bacteria or yeast, coupled with fluorescence activated cell sorting (FACS) as a selection tool. For display on the surface of gram-negative bacteria such as *E. coli*, proteins must be exported from the cytoplasm and targeted to the outer membrane where special anchoring mechanisms have had to be designed to properly expose the protein without inactivating the native membrane proteins (Chen and Georgiou, 2002). A vector system that is able to express scFvs as fusions with part of the OmpA outer membrane and the Lpp signal peptide to direct the protein to the outer membrane of *E. coli* was used successfully to display copies of an anti-digoxin scFv (Francisco *et al*., 1993). A 10^5-fold enrichment from negative cells after two rounds of FACS was demonstrated. Also, in *E. coli*, Fuchs *et al*., (1996) expressed a mix of different scFvs as fusions to peptidoglycan-associated-

lipoprotein and selected antigen specific clones by FACS. Bacteria expressing this fusion were viable, however, it was noted that both large proteins and small peptides were not ideal as antigens in this system due to limited accessibility and non-specific binding respectively. This same group also expressed an anti-phOx scFv on mammalian cells by fusion with a membrane binding domain (Rode *et al*., 1996) and showed this could be used to attach a variety of moieties to cells via coupling with the hapten for the expressed antibody. Meanwhile, Chen *et al*., (1996) showed in principle that such surface expressed scFvs could be used to replace solid-supported antibodies in a quantitative immunoassay, thus providing a highly renewable source of antibody reagents. Another system for *E. coli* surface display has been reported using *Pseudomonas syringae* ice-nucleation protein as an outer membrane anchor for the functional display of various proteins (Jung *et al*., 1998; Lee *et al*., 2000). Libraries of peptides have been able to be displayed using the EaeA intimin from an enterohaemorrhagic *E. coli* (Christmann *et al*., 2001). Georgiou *et al*., (1997) have demonstrated the successful surface display of scFv libraries using the Lpp-OmpA system with FACS showing that the mean fluorescence intensity of cells varies as expected on the basis of the antigen affinity of the corresponding scFv antibodies in solution. This group then used this method to select affinity matured scFvs from a library of anti-digoxin variants with randomised heavy and light chain CDRs (Daugherty *et al*., 1998). Error-prone PCR was also used for affinity maturation with fine discrimination of affinities between the different mutants reported (Daugherty *et al*., 2000). The flagella of bacteria have recently also been used to display peptide libraries (Westerland-Wikstrom, 2000). Attachment of functional scFvs to the protein A of the gram-positive bacterium *Staphylococcus* has been reported (Gunneriusson *et al*., 1996). Novel binding proteins (affibodies) from a library based on the α-helical Z domain of this *S. aureus* protein A were then selected by phage display (Nord *et al*., 1997), and then the display of such functional affibodies on the bacterial surface demonstrated (Gunneriusson *et al*., 1999b).

The yeast *Saccharomyces cerevisiae* has been developed as an alternative cell surface display vehicle that provides eukaryotic protein folding and secretory machinery. Schreuder *et al*., (1993) were the first to display a heterologous protein on the surface of yeast, fusing an enzyme to an invertase signal sequence and the anchoring C-terminal half of α-agglutinin, an outer cell wall mannoprotein. A scFv library was then displayed as a fusion with the Aga2p subunit of α-agglutinin (Boder and Wittrup, 1997). A library of scFv molecules created by passage in a mutator strain of *E. coli* was screened by FACS which showed them to be accessible to antigen and was able to discriminate mutants with improved off rates to within a three-fold difference, an

improvement on phage display. Similarly, a library of $3x10^5$ mutants of an anti-T cell receptor scFv was screened with a 3-fold increase in affinity detected in one mutant (Kieke *et al*., 1997). These were promising initial results considering the small size of the libraries and that this new system was still being optimised for FACS selection and sorting conditions (Boder and Wittrup, 1998). The same scFv displayed on yeast has been shown, by its multivalent nature (~10^5 copies per cell), to induce biological activity by mimicking an antigen presenting cell, stimulating T cells to express CD69 and CD25 and downregulate TCR molecules (Cho *et al*., 1998). This suggested the system may be used to screen libraries for bioactive molecules and possible selection of co-receptors by the simultaneous display of several polypeptides. A number of recent impressive results employing this system have been reported. A >10,000-fold decrease in the rate of dissociation of a fluorescein-binding scFv was achieved by combining four cycles of yeast surface display with error-prone PCR and DNA shuffling (Boder and Wittrup, 2000). A single chain T-cell receptor with nanomolar affinity has been engineered using yeast display (Holler *et al*., 2000), and stability and expression have also been improved using the technique (Shusta *et al*., 1999). Overall, surface display looks as though it could be a viable alternative to phage display. The FACS selection allows binding in solution which appears to provide good enrichment factors and provides quantitative information during the screening, although for bacterial display, not a lot is known of susceptibility to surface proteases (Georgiou *et al*., 1997). Surface display may also help to overcome problems with phage such as selection due to avidity or reduced cell toxicity, and difficulty in elution of strong binders, and yeast display has the added advantage of eukaryotic folding machinery (Boder and Wittrup, 1997). Optimised FACS screening methodologies with surface display has allowed fine affinity discrimination between clones (as low as 2-fold) which is better than that offered by phage display (VanAntwerp and Wittrup, 2000).

1.7 Alternative binding formats

1.7.1.Scaffolds

The use of various scaffolds as frameworks on which to engineer particular binding activities has developed as a means of producing novel binding reagents. This can be useful if the particular scaffold maintains good soluble expression levels and exhibits stability and reliable folding after manipulation, which is not always the case with some recombinant antibody fragments. A further advantage can be the minimisation of the size of the binding fragment. If a protein has a stable

polypeptide conformation bringing together loops that form a solvent-accessible active site, and these features are structurally separate, then it may have potential as a scaffold (Skerra, 2000).

Immunoglobulin domains are highly successful scaffolds found in nature. Many recombinant antibody fragments, however, show poor expression and stability and so engineering of more robust and better expressing frameworks is desirable. The CDR fragments from an unstable, aggregation-prone anti-fluorescein scFv have been grafted onto a well characterised, stable and structurally similar antibody framework for this purpose (Jung and Pluckthun, 1997), with the resulting scFv having favourable properties and retaining fluorescein-binding activity. A number of examples of antibody frameworks being used as scaffolds for engineering of new binding affinities are discussed in 1.5.4. In a different application of antibody domain scaffolds, epitope insertion into the CDRs of antibodies have been able to illicit an immune response against the inserted epitope (Zanetti, 1992). The CDRs of these 'antigenised antibodies' have been able to display oligopeptides in an immunologically accessible and functional way superior to the use of the same synthetic free linear oligopeptide. A CDR3 loop of a self IgG expressing a viral T-cell epitope in a restricted conformation was 100 – 1000 more efficiently presented than the poorly immunogenic free synthetic peptide (Zaghouani *et al.*, 1993). The chimeric IgG was shown to induce virus-specific CD4+ cells. Similarly, the adhesion peptide RGD was introduced to an antibody CDR3 region and shown to bind to natural killer (NK) cells, thus inhibiting NK cytotoxic activity (Zanetti *et al.*, 1993). An antibody against the class II MHC molecule, involved in eliciting helper T-cell responses, has been used as a scaffold for presenting neutralising HIV1 epitopes, inserted into a specific loop of V_H framework three, in a conformationally constrained fashion (Cook and Barber, 1997). Anti-class II MHC binding activity was preserved and conformation-specific anti-envelope protein gp160 responses of high titre were induced, demonstrating the effective use of a molecular framework combined with an immunotargeting approach.

Single antibody and antibody-like domains can be used as scaffolds. The revelation that camelids have immunoglobulins devoid of light chains (Hamers-Casterman *et al.*, 1993) has opened the possibility of further reducing antibody size, using single V_H domains for engineering of binding molecules which could be advantageous due to better tissue penetration. Ward *et al.*, (1989) have previously shown that V_H domains of high affinity can be expressed in *E. coli* as described in section 1.3. Information on the increased surface hydrophilicity of these camel antibody domains, particularly in the region that would normally associate with V_L domains, and thus an area when

unpartnered could force the V domain to aggregate, has lead to the design of 'camelised' V_H domains (Davies and Reichmann, 1995). Phage libraries based on these camelised V_H domains have been used for successful selection of fragments against a variety of antigens (Davies and Reichmann, 1996; Martin *et al*., 1997). Libraries based on a shark antibody V domain that, like camelid domains, also exists in an unpaired state, have been created (Nuttall, *et al*., 2001). These libraries have been successfully panned against several antigens with selected binders displaying good stability and expression characteristics. CTLA-4 has also been used as an antibody-like scaffold (Nuttall *et al*., 1999). When somatostatin was substituted into the CDR3 of this protein the chimaeric molecule was detected by a somatostatin receptor and an anti-somatostatin antibody.

Antibody-like-molecules have been used as scaffolds with the construction of a stabilised and soluble 61-residue 'minibody', capable of displaying discontinuous epitopes (Tramontano *et al.*, 1994). This was achieved by deletion of three β strands from an immunoglobulin heavy chain variable domain and engineering of some of the newly exposed residues to reduce hydrophobicity. The two hypervariable regions (CDR1 and CDR2) were mutated to form a phage display library from which was selected a minibody with micromolar affinity to the cytokine hIL-6 and which was able to inhibit its biological activity (Martin *et al.*, 1994). The selected minibody CDR2 sequence is very similar to seven consecutive residues of the IL-6 receptor whereas a synthetic peptide of the H2 sequence was unable to inhibit IL-6 binding to its receptor, showing the importance of the constrained display of epitopes that the minibody provides. The specificity and affinity of this molecule was improved by mutagenesis of the H1 loop residues (Martin *et al.*, 1996) showing that the scaffold is suitable for manipulation, however there are still inherent solubility problems. The fibronectin type III domain (FN3), a member of the immunoglobulin superfamily without disulphide bonds that resembles these trimmed V_H domains has been used as a scaffold (Koide *et al*., 1998). This domain possesses seven β-strands instead of nine with three loops connecting the strands. Randomisation of residues in two of these loops, with phage display and selection against an ubiquitin led to the isolation of a specific binding clone. Initial problems of poor solubility of this framework were solved by engineering key residues (Koide *et al*., 2001) and its utility as a robust scaffold has been demonstrated with two of the three loops shown to be open to elongation without overly destabilising the protein (Batori et al., 2002).

Nord *et al.*, (1997) have utilised the Z-domain of the α-helical IgG binding protein A for the engineering of micromolar affinities to a variety of targets including Taq polymerase and human

insulin. This was achieved by randomisation of solvent accessible residues and display on phage for affinity selection. These engineered domains display good soluble expression and efficient folding, have no cysteines while retaining a highly stable structure, and their flat binding surface makes them ideal for selection of proteins, as opposed to smaller haptens. Initially selected binders were low in affinity but affinity maturation lead to nearly 1000-fold improvements (Gunneriusson *et al*., 1999a). It is suggested that two or more of these domains with different target specificity, could be linked as happens in nature, as an immunotargeting strategy. Minimisation of this framework from a three helix 59 residue domain to a truncated two helix 33 residue domain has been reported (Braisted and Wells, 1996) with the binding function of a discontinuous epitope being preserved. Three different phagemid libraries were constructed for the randomisation of three different regions to produce a smaller domain with similar binding affinity to the parent Z-domain.

The β-barrel of lipocalins supports four exposed loops that form a binding pocket that has been shown to be amenable to protein engineering. Initially a metal-binding site was engineered into this pocket of a lipocalin, based on structural information, proving its potential as a scaffold (Muller and Skerra, 1994). Subsequently, libraries were produced by randomisation of residues across all four loops resulting in high affinity fluorescein binders being isolated (Beste *et al*., 1999). Additionally, a digoxigenin binder from the same library was affinity matured nearly 10-fold (Schlehuber *et al*., 2000).

Even smaller potential scaffolds found in nature have been investigated. The knottin EETI-II, a highly stable triple-disulphide bonded trypsin inhibitor of just 28 amino acids, has been shown to tolerate the insertion of epitopes of up to 17 residues with the scaffold recognised by antibodies to these epitopes (Christmann *et al*., 1999). Vita *et al.*, (1995) introduced metal-binding sites of high affinity into the knottin-related 37 residue scorpion toxin charybdotoxin which maintained its stable triple disulphide-bonded natural structure, displaying tolerance of sequence mutation. The engineered binding sites mimicked the Zn^{2+} binding site found in carbonic anhydrase. Other functional sites have since been engineered (Vita *et al*., 1998). A scaffold of similar size, the GCN4 leucine zipper, has been designed with foreign biological activity (Butcher *et al.*, 1997). The stable and precise conformation of GCN4 was used for incorporation of four lysine residues, thought to be required for the heparin binding activity of the protein, platelet factor 4 (PF4). These residues in the zipper, mimicked the positions in PF4, whose helices show close similarity in orientation to those

of the zipper, resulting in native PF4 activity. The small size of scaffolds such as knottins and leucine zippers may make them useful in biological systems and allow ease of chemical synthesis.

The use of some protease inhibitors as scaffolds, as many are highly stable with an exposed peptide section, has been employed predominantly for the selection of new enzyme inhibitors (Roberts *et al*., 1992; Dennis and Lazarus, 1994; Markland *et al*., 1996). However, the scope of these scaffolds in selection of novel binding reagents may be limited due to the possession of only one or two loops. The potential to use a scaffold to direct high affinity molecules to selected targets was demonstrated with the CDR3 of an α-integrin antibody replacing a surface loop of a plasminogen activator (Smith *et al.*, 1995). Mutagenesis of the antibody peptide sequence for affinity maturation using phage display was performed before grafting. The resulting protein was able to bind platelet integrin while retaining enzymatic activity. MalE, an *E. coli* maltose binding protein has been used as a scaffold to express CD4 (the T cell receptor for HIV) domains of up to 99 residues as well as reduced domains, retaining CD4 activity by inhibiting HIV binding to $CD4^+$ cells (Clement *et al.*, 1996). This scaffold expresses well in the periplasm, is easy to produce and purify and is more stable than recombinant soluble CD4.

1.7.2 Humanisation

As rodent monoclonal antibodies often induce an anti-globulin response when used in humans, they can be of limited therapeutic value. Thus, engineering of these Mabs to construct 'human' antibodies is sometimes necessary. As discussed in section 1.5.3, the chain shuffling technique has been used to humanise a murine antibody by display of the light chain with a library of human heavy chains and then the selected human heavy chain displayed with a library of human light chains to select a totally human antibody (Figini *et al.*, 1994; Bieboer *et al*., 2000). The most common method of humanisation is to graft the selected CDRs from the rodent antibody onto a human scaffold of similar structure. This was demonstrated with the grafting of heavy-chain CDRs of a mouse Mab against the hapten NP-cap onto the corresponding CDRs of the human myeloma protein NEWM (Jones *et al.*, 1986). This humanisation by CDR grafting was successful with the new antibody showing only a small decrease in affinity. This showed that the transfer of important binding residues from a mouse to a convenient human framework could conserve the binding function of the parent molecule. However, CDR grafting doesn't always lead to a human antibody of the same affinity or function as the related mouse antibody. Riechmann *et al.*, (1988) grafted the heavy and light chain CDRs from a rat Mab against lymphocyte antigen CAMPATH-1, onto human

frameworks connected to constant effector function domains. The parent antibody can cause both complement-mediated and antibody-dependent cell-mediated cytotoxicity. The initially engineered 'human' antibody lost most of its binding ability and also its lytic ability. Restoration of one important framework residue from the original Mab restored binding and the new antibody was equivalent to the rodent Mab in complement lysis and more effective in cell-mediated lysis. This demonstrates the importance of some framework residues in influencing conformation of the hypervariable regions. This was further demonstrated by Kettleborough *et al*., (1991) when they produced a number of different versions of a humanised antibody with the same CDR grafts, but varying framework region alterations based on molecular modelling, in an attempt to determine which residues may be important for antigen binding. One or two appropriate changes were all that was necessary to cause the largest increases in binding. One of the humanised versions showed close to the binding capabilities of the mouse Mab, but the human version would be expected to be more efficient *in vivo* due to the reduction in immunogenicity. Carter *et al.*, (1992) demonstrated that a CDR grafted humanised antibody with seven framework residue mutations showed a 250-fold greater affinity than the antibody with CDR grafts alone. The antibody also showed a three-fold increase in affinity over the murine parent and had the same cytostatic and cell-mediated cytotoxic effect on a tumour cell presenting its target antigen. Thus it appears that along with CDR grafting, engineering of key residues affecting the CDRs is important for effective humanisation. This approach has lead to effective humanisation of murine antibodies against OKT4 (Pulito *et al.*, 1996), TNF-α (Nagahira *et al*., 1999), α-4 integrin (Saldanha *et al*., 1999), and CD40 (Wu *et al*., 1999). Monovalent phage display has also been used in the humanisation process (Baca *et al.*, 1997). By randomising a small set of 11 framework residues thought to have most influence on antigen binding, and displaying the resultant library on phage, a humanised antibody was recovered of 125-fold higher affinity than the same antibody humanised by CDR grafting alone. In an improved procedure, abbreviated CDRs with only the minimum specificity determining residues have been grafted to humanise an antibody (De Pascalis *et al*., 2002), with the minimal graft showing much less immunogenicity than a full CDR graft.

Another humanisation approach is resurfacing of a non-human antibody, only changing the solvent exposed residues that are not essential for the structural integrity of the hypervariable regions (Roguska *et al.*, 1994). An anti-CD56 and anti-CD19 were humanised in this way and found to retain the specificity and binding affinity of the parent, but it is not clear if they could totally escape the immune response in humans. A comparison with CDR grafting humanisation of both these

antibodies suggested that the resurfacing technique was a less laborious approach (Roguska et al., 1996). An antibody to human protein C was successfully humanised by this approach (O'Connor *et al*., 1998). However, a resurfaced neutralising antibody retained affinity in its humanised form but lost biological activity (Delagrave *et al*., 1999). As methods for the construction of human antibody libraries is improved, these humanisation strategies may become redundant.

1.7.3 Multivalency

The avidity or functional affinity of a molecule can be improved significantly if given an increased valency and so this is another approach for improving antibodies and their derivatives. In fact, binding of a bivalent Mab can enhance functional affinity up to 1000-fold over that of the monovalent species (Pluckthun and Pack, 1997). Essig *et al.*, (1993) observed that dimeric as well as higher multimeric forms were often present when producing scFvs, confirmed by the fact that purified dimer-sized fragment could bind two antigen molecules and by the ability to generate functional heterodimers from two non-active scFvs whose V_H and V_L domains are derived from antibodies of different specificity. Building on similar observations that some scFv fragments existed as dimer species, Holliger *et al.*, (1993) showed that by reducing the linker length they could encourage the equilibrium towards formation of dimers over monomers. This was presumably due to the fact that the shortened linkers made it difficult for normal pairing of V_H and V_L on the same chain, forcing pairing of complementary domains from different chains. These dimers were dubbed 'diabodies' with molecules of a 10 residue linker length showing greatest improvement in functional affinity over parent antibody. This proposed orientation of V_H and V_L pairing from different chains has been confirmed from crystal structure studies (Perisic *et al.*, 1994). Whitlow *et al.*, (1994) also produced dimers with an increased functional affinity and showed that the degree of multimerisation was linker length dependent with a 12 residue linker showing greatest propensity to dimerise. A similarly constructed scFv dimer against T cell receptor was shown to have a 10-fold higher functional affinity than the monomeric form and was also more active in inhibiting T cell activity (Schodin and Kranz, 1993). Improved tumour targeting was achieved by an anti-CEA non-covalent dimer (Wu *et al*., 1996). Kortt *et al.*, (1997) have also shown that reducing linker lengths to five and ten residues can cause exclusive formation of anti-neuraminidase scFv dimers and that further reduction to zero residue linker length caused formation of trimers. The dimers were shown to be bivalent and the trimers trivalent, having three active binding sites, each able to bind an anti-idiotype Fab to form a complex of the expected size and showing a marked increase in binding affinity due to avidity. Stable trimers of an anti-idiotype scFv

11-G10 have also been formed (Iliades *et al.*, 1997). It was proposed that a trimer was the preferred conformation for zero-linker scFvs and the expected increase in avidity of the trivalent molecule was implicated as being advantageous in imaging and immunotherapy. It has recently been shown that non-covalent tetramers can be formed from some zero-linker scFvs (Dolezal *et al*., 2000; Dolezal *et al*., 2003).

A number of alternative means of multimerising recombinant antibodies have been investigated. When scFvs have been produced as fusions to association domains such as helix bundles (Regan and DeGrado, 1988) or coiled coils (leucine zippers) (O'Shea *et al.*, 1991), dimeric binding molecules have been formed. These association domains are able to pack together closely in a tight formation. Such scFv/association domain fusions were expressed in *E. coli* and shown to associate into dimers *in vivo* (Pack and Pluckthun, 1992). A hinge region for flexibility was expressed between the Fv and helix and the gain in avidity of these dimers was detected by ELISA. Constructs with an extra cysteine containing sequence were shown to bind best but the cysteine was not essential for dimerisation. Thus, the bivalency of an antibody has been achieved with a beneficially huge reduction in size, hence the term 'miniantibodies'. By creating a series of mutants in GCN4 leucine zipper through altering some of the buried residues, two, three and four helix structures have been produced (Harbury *et al.*, 1993). The tetramer is a parallel 4-stranded coiled coil and was utilised as an association domain to create tetravalent miniantibodies (Pack *et al.*, 1995). ScFvs were connected genetically via a flexible hinge to a helix so that when expressed in *E. coli*, tetramerisation occurred in the periplasm. When compared to the dimeric form of the same scFv, the tetramer was produced in much lower quantities, but after engineering to exchange three amino acids important for efficient folding, this problem was overcome. It was shown that the tetramer gave enhanced binding over the dimer in a manner dependent on the surface epitope density. The human transcription factor p53 has also been used as a tetramerisation domain to create a tetravalent scFv against the tumour carbohydrate antigen Lewis Y (Rheinnecker *et al.*, 1996). Comparisons were made with monomeric and dimeric forms of the scFv, with the tetramer showing greatest functional affinity. Streptavidin has also been used as a tetramerisation domain (Kipriyahov *et al.*, 1995). A tetramer of improved affinity due to four scFv binding sites was produced which also had biotin binding activity. However, as each streptavidin subunit is 15-kDa it leads to a bulky protein.

1.7.4 Bispecificity

Bispecific antibodies have been made from two different antibodies by reduction and reoxidation of hinge cysteines (Nisinoff and Mandy, 1962) and by fusion of hybridomas producing antibodies of two different specificities (Milstein and Cuello, 1983). They have even been produced chemically to recognise two different epitopes on the same antigen (Cheong *et al.*, 1990). However it is difficult to obtain large amounts of homogenous material by these methods and so recombinant methods appear more useful.

When diabodies were produced as discussed above (Holliger *et al.*, 1993; Essig *et al.*, 1993; Whitlow *et al.*, 1994), it was also observed that heterodimeric molecules or bispecific diabodies could be formed. This was achieved by linkage of a V_H from one antibody with the V_L of another in the formation V_HA-V_LB/V_HB-V_LA where A and B are antibodies of different specificities. Such bispecific molecules could have great potential such as in the direction of an effector cell to a tumour site (Pluckthun and Pack, 1997). The diabody strategy was used to create an antibody-like molecule with specificity for both a marker on a mouse B-cell lymphoma and mouse CD3 (Holliger *et al.*, 1996). The compact diabody binding sites are separated by less than half the distance than those of the corresponding IgG which should theoretically bring T-cells closer to target cells. This diabody was able to mediate specific killing of lymphoma by cytotoxic T-cells and was 10-fold more active in killing than the parent bispecific IgG, most likely due to this increased affinity and longer half-life. A diabody of two humanised antibodies consisting of an anti-tumour and an anti-CD3 scFv linked in the V_HA-V_LB/V_HB-V_LA formation was produced by Zhu *et al.*, (1996). Co-expression led to a highly produced diabody with bispecific high affinity binding sites able to retarget activated T-cells against the tumour cells. Phage display has also been utilised for the screening of bispecific diabody repertoires (McGuinness *et al.*, 1996). This involved fusing one scFv pair to a phage gene3 protein and secreting the other to the periplasm for association of the diabody. Selection against both antigens enabled screening of the best binding combination.

Genetically linking two scFvs by joining the C-terminus of one scFv to the N-terminus of another via a flexible hydrophilic peptide has proved to be effective. Hayden *et al.*, (1994) made a bispecific construct consisting of an anti-human CD3 scFv linked by a 27 residue helical linker to an anti-L6 tumour scFv with a human IgG1 Fc domain linked to the C-terminus. This was an attempt to resemble a miniature antibody molecule and was shown to simultaneously bind cells expressing both antigens and display biological activity. Mallender *et al.*, (1994) showed that such a tandem bispecific scFv was a flexible protein suggesting that such a design could be used to bind

two epitopes on the same macromolecule. Similar biologically active bispecific constructs have been shown to be effective with linkers of only 15 residues such as $(Gly_4\text{-}Ser)_3$ (De Jonge *et al.*, 1995; Kurucz *et al.*, 1995; Mack *et al.*, 1995). Such an approach was used to enhance selectivity for a particular cell type by producing a molecule bispecific for neighbouring epitopes on the same cell surface (Neri *et al.*, 1995) and this approach with linkage to an endotoxin is also possible (Schmidt *et al.*, 1996). Introduction of cysteines to form disulphide bonds for the stabilisation of Fv fragments to form a dsFv (Glockshuber *et al.*, 1990) and for the stabilisation of scFv molecules (Young *et al.*, 1995) has been performed. This approach has also been used for a recombinant bispecific immunotoxin consisting of an unstable Fv linked to *Pseudomonas* exotoxin (Brinkmann *et al.*, 1993). The dsFv immunotoxin showed identical specificity and activity to an scFv counterpart indicating that binding site conformation was retained. Association domains like the Fos and Jun leucine zipper have also been used to create bispecific molecules (deKruif and Logtenberg, 1996). showing a greater tendency to form heterodimers over homodimers. Engineering of antibody-like molecules to introduce multivalency and multispecificity will often be necessary for their *in vivo* application and the methods described above to achieve this are showing much promise, particularly in tumour targeting.

1.8 An antibody to the N-terminal GPE domain of insulin-like growth factor I (IGF-I)

The experiments in this thesis exploit an antibody that binds to the insulin-like growth factor I (IGF-I) and more specifically the three N-terminal residues of this protein Gly-Pro-Glu. IGF-I is a 70-amino acid protein, structurally similar to insulin, that promotes cell proliferation and differentiation in multiple tissues, with growth-promoting effects prominent in the nervous system, qualifying it as a neurotrophin (Anlar *et al*., 1999). IGF-I is transported in biological fluids and its activity regulated by the IGF binding proteins IGFBPs (Baxter, 1994). Des(1-3)IGF-I is a truncated form of IGF-I lacking the three N-terminal residues Gly-Pro-Glu and appears to have enhanced potency relative to IGF-I in stimulation of body growth in mice (Gillepsie *et al*., 1990). IGFBP3 has been shown to possess a 25-50-fold lower affinity to des(1-3)IGF-I than full-length IGF-I (Heding *et al*., 1996). Baxter *et al*., (1992) showed that the serum concentration of IGF-I and IGFBP3 is roughly equimolar and that residues three and four appear to be important for IGFBP3 binding while residues two and three were implicated as important for IGFBP1 binding (Jansson *et al*., 1998). Des(1-3)IGF-I appears to have greater growth promoting potency than IGF-I due to its decreased affinity for IGFBPs (Baxter, 1994), thus increasing the amount of free protein that can

bind to cell receptors (Ross *et al*., 1989; Bagley *et al*., 1989). The cleaved GPE peptide has been shown to be neuroactive, stimulating release of the neurotransmitters acetylcholine and dopamine, the latter via interaction with NMDA receptor (Sara *et al*., 1989). Acetylcholine release was stimulated by GPE at a much lower concentration than full length IGF-I, and not at all by des(1-3)IGF-I (Nilsson-Hakansson *et al*., 1993). In brain injury IGF-I is strongly expressed and has been shown in rats to inhibit apoptosis at a 10-fold higher level than des(1-3)IGF-I suggesting that IGFBPs are required for transport to site of injury (Gluckman *et al*., 1998). The GPE peptide alone appears to be neuroprotective (Gluckman *et al*., 1998; Saura *et al*., 1999; Sizonenko *et al*., 2001) with the IGFBPs possibly regulating this effect (Bourguignon *et al*., 1999). Des(1-3)IGF-I has been reported to have its own specific neuroprotective properties (Scheepens *et al*., 2000). The neuroprotective effect of GPE extends to an animal model of Huntington's disease (Alexi *et al*., 1999) and Parkinson's disease (Guan *et al*., 2000). GPE may be a potential marker of neurodegenerative disease and brain injury and thus a specific antibody may be an assay for this peptide and provide information regarding its biological significance, regulation and distribution. A specific antibody could also distinguish between IGF-I and des(1-3)IGF-I. An antibody with specificity to IGF-I, but not des(1-3)IGF-I has been produced (Craven 1999). An antibody with such a well-defined specificity was seen as a good model for antibody engineering studies.

1.9 Nature of this study

The overall aim of this study was to clone a functional recombinant version of the anti-GPE antibody in the scFv format and gain further insight into the engineering approaches of ribosome display and DNA shuffling using this anti-GPE scFv as a model. The work of the thesis is described in three broad sections. Firstly, cloning of the genes encoding the variable regions of the anti-GPE monoclonal antibody in the scFv format with the objective of regenerating the affinity and specificity of the parent, creating a recombinant antibody that could then serve as a model in molecular evolution strategies. A site-directed mutagenesis was performed on this anti-GPE scFv due to its shortened HCDR2 sequence. This work is described in Chapter 3. Secondly, random point mutations were introduced into the anti-GPE scFv gene by error-prone PCR with the objective of developing ribosome display with a rabbit reticulocyte system that could be used to isolate affinity matured scFvs from a pool of mutants. Such a development with this system has not been reported in the literature to date. This work is described in Chapter 4. Thirdly, the objective was to develop DNA shuffling of two antibody frameworks to investigate this as a means of

producing a functional chimaeric scFv. The CDRs from anti-GPE were grafted onto the NC10 scFv (anti-neuraminidase) framework and the two scFvs were recombined by DNA shuffling, with ribosome display used for selection, including use of BIAcore for selection against immobilised IGF-I. A functional chimaera generated from two different DNA shuffled scFvs has not been reported in the literature to date. This work is described in Chapter 5.

CHAPTER 2
MATERIALS AND METHODS

General chemicals and other buffer components and reagents used in this work were purchased from Sigma (St. Louis, MO, USA) and BDH (Poole, England) unless otherwise stated. The sequences of oligonucleotide primers used in this thesis are shown in Table 2.1

2.1 Molecular Biology

2.1.1 Isolation of RNA

Cell pellets of a hybridoma cell line (5C6/B3) that expresses the anti-GPE monoclonal antibody (Mab) were provided by The School of Life Sciences, Queensland University of Technology (QUT). These cells were used as the source of RNA for the cloning of the variable region genes. This RNA was isolated from ~ 10^6 hybridoma cells using TRIZOL reagent (Life Technologies, Rockville, MD, USA) according to manufacturer's instructions. Essentially, this reagent is a mono-phasic solution of phenol and guanidine isothiocyanate that maintains the integrity of RNA while disrupting the cells and dissolving cell components. The cells were lysed in 400 μL of the TRIZOL reagent and then 80 μL of chloroform was added, which, after centrifugation at 12,000 x *g* for 15 min at 4^{o}C, produced an organic phase and an RNA-containing aqueous phase. RNA was precipitated with 200 μL of isopropyl alcohol and centrifuged at 12,000 x *g* for 10 min at 4^{o}C. A visible RNA pellet was produced. This was washed with 0.5 mL of 75% ethanol and then dissolved in 50 μL of diethylpyrocarbonate (DEPC)-treated H_2O. To produce DEPC-treated water for elimination of RNases, DEPC (Sigma) was added to 0.1 %, and the solution incubated for 2 h at 37^{0}C and then autoclaved.

2.1.2 Purification of mRNA

Isolation of mRNA from the total RNA preparation (2.1.1) was performed using Oligo$(dT)_{25}$ Dynabeads (Dynal, Oslo, Norway) according to manufacturer's instructions. Essentially, this involved application of the whole RNA sample to the beads for binding of mRNAs, with non-binding species being washed away. Prior to binding, the RNA was heated to 65^{o}C to destroy secondary structures. mRNA was eluted from the beads at 65^{o}C in 20 μL 10 mM Tris-HCl pH 7.5.

2.1.3 Generation of cDNA by reverse transcription

The mRNA preparation (2.1.2) was used as template for reverse transcription to cDNA. 10 μL of the mRNA sample was brought to 40 μL with DEPC-treated H_2O. This was heated at 65°C for 3 min and then quenched on ice for 1 min. To this was added 25 μL H_2O, 5 μL 10 mM dNTPs (equimolar mix of each dNTP; Invitrogen, Life Technologies, San Diego, CA, USA), 10 μL 10X first strand buffer (Table 2.2), 10 μL 0.1 M DTT, 2 μL 10 μM $(dT)_{15}$ primer, and 5 μL RNasin (33 units/μL; Promega, Madison, WI, USA). Then, 4 μL of AMV reverse transcriptase (Promega) was added and the reaction incubated for 1 h at 42°C. The reaction was boiled for 3 min, centrifuged at 20,000 x g for 5 min, and the supernatant stored at –20°C.

2.1.4 Polymerase chain reaction (PCR)

Genes and gene fragments were amplified by PCR (Saiki *et al*., 1988) using either Vent polymerase (New England Biolabs (NEB), Beverly, MA, USA) for high fidelity replication, or *Taq* polymerase (Biotech International, Bentley, WA, Australia) when lower fidelity was acceptable. Reactions contained template DNA sample mixed with 0.2 mM of each dNTP, 1-2 mM $MgCl_2$ (*Taq*) or $MgSO_4$ (Vent), the reaction buffer supplied with the enzyme (Table 2.2), 0.5 mM each of the oligonucleotide primers homologous to the 5′ and 3′ ends of the DNA to be amplified, 1-2 units of the enzyme, and H_2O to a total volume of 50 μL. The reaction was performed in a thermocycler (Perkin-Elmer, Norwalk, CT, USA) with an initial 3 min denaturation step, followed by 30-40 cycles of a 94°C denaturation for 30 s, a 55-66°C primer-annealing step for 30 s, and a 72°C elongation step. The elongation step varied in duration depending on the length of the fragment to be amplified with a rule of about 1 min per 1000 bp being applied. After cycling, a final elongation incubation of 72°C for 5 min followed. Cycling conditions for PCR isolation of the V genes were different (see 3.2.3) to encourage primers of best fit from the pool to preferentially amplify. PCR primers (Table 2.1) were often designed with overhangs encoding restriction enzyme sites for subsequent cloning. Primers were synthesised using a model 382A DNA synthesizer (Applied Biosystems, Foster City, CA, USA) by the CSIRO, analytical services group, Parkville.

2.1.4.1 Error-prone PCR

Random point mutations were introduced into genes by a modified PCR amplification (Leung *et al*., 1989). Standard PCR conditions (2.1.4) were followed except that the fidelity of *Taq* polymerase was reduced by the introduction of $MnCl_2$ at 0.5 mM, increasing the level of Mg^{2+} by the addition

of $MgCl_2$ up to 5 mM, and biasing of nucleotide levels whereby dATP concentration was kept at 0.2 mM and the concentration of the other three dNTPS was raised to 1 mM.

2.1.4.2 Splice Overlap Extension (SOE) PCR

In some instances, PCR was used to join two DNA segments together. SOE PCR (Horton *et al*., 1989) was used in these instances, such as in the joining of two V genes into an scFv, where the V gene fragments have been PCR (2.1.4) amplified to have overlapping regions of homology. SOE PCR with Vent polymerase was performed initially for 12 – 20 cycles as for standard PCR (2.1.4), but without addition of primers, allowing annealing of the regions of homology of the fragments, so that they prime off each other. The flanking 5′ and 3′ primers for a full scFv were then introduced for a further 30 cycles of PCR to complete amplification of the full-length gene.

2.1.4.3 Reverse transcription (RT)-PCR

RT-PCR was used to detect selected mRNAs in ribosome display (2.4) experiments. A Titan one tube RT-PCR kit (Roche, Mannheim, Germany) was used, which contains both the reverse transcriptase and polymerase enzymes to allow the RT and PCR reactions to proceed in the one tube. Reactions were performed according to the manufacturer's instructions with 1-2 μL of the ribosome display eluate (2.4.4) used as template in the reaction. The reactions conditions were as for standard PCR (2.1.4) but with a preceding 94°C denaturation for 2 min and 48°C incubation for 45 min for reverse transcription. PCR (2.1.4) was also performed on eluates in parallel to confirm that RT-PCR products were genuinely amplified from mRNAs, and not residual DNAs.

2.1.5 Agarose electrophoresis

DNA fragments were isolated and analysed by electrophoresis on 0.9-2.0% agarose gels (Progen, Darra, QLD, Australia) made in TAE buffer (Table 2.2) with 0.1 μg/mL ethidium bromide added for visualisation of bands under UV light. Samples were mixed with a 1/6 volume of 6X loading buffer (Table 2.2) and electrophoresis performed at about 100 Volts for 30-40 min in a mini-sub cell GT electrophoresis tank (BioRad, Hercules, CA, USA) filled with TAE buffer. Sizes of DNA fragments were determined by comparison with known DNA size markers loaded in a separate well of the gel, such as *Hae*III-digested ϕX174 DNA (NEB) *Hind*III-digested λ DNA (Fermentas, Hanover, MD, USA), 1 kb plus DNA ladder (Life Technologies) or 100 bp ladder (Life Technologies).

2.1.6 Purification of DNA

2.1.6.1 Purification from agarose gels

DNA fragments to be further manipulated were excised from the body of the gel with a scalpel blade. A gel extraction kit (Qiagen, Hilden, Germany) was used to melt the agarose and purify the DNA according to manufacturer's instructions. The kit works on the principle of DNA within the melted agarose binding to a silica gel that is then washed before the bound DNA is eluted in a small volume of H_2O or 10 mM Tris, pH 8.5.

2.1.6.2 Purification from enzymatic reactions

When DNA from enzymatic reactions such as restriction digests (2.1.7) and ligations (2.1.9) needed to be purified to remove protein, oligonucleotide, or buffer components, before use in subsequent experiments, a PCR purification kit (Qiagen) that works by the same principle of the gel extraction kit (2.1.6.1) was used according to manufacturer's instructions.

2.1.7 Restriction digestion of DNA

To create cohesive ends for ligation reactions (2.1.9), DNA fragments were digested with restriction enzymes that recognise specific nucleotide motifs, either existing or engineered into the sequence by PCR (2.1.4). Restriction enzymes were purchased from New England Biolabs and used essentially according to manufacturer's instructions, with the enzyme used to digest the particular DNA in the presence of the recommended buffer (Table 2.2) supplied with the enzyme, and sometimes with the addition of Bovine Serum Albumin (BSA, Sigma) to 0.1 mg/mL when specified by the manufacturer. Reactions were allowed to proceed for 2-3 h at the recommended temperature and were then gel-purified (2.1.6.1) or purified directly (2.1.6.2) prior to further enzyme digests or ligation (2.1.9) reactions. Digested vector DNA was dephosphorylated prior to ligation to prevent self-ligation. This was achieved by adding 5-10 units of calf intestinal alkaline phosphatase (CIP; NEB) to the completed restriction digest and incubating for 1 h at 37^{o}C.

2.1.8 Quantitation of DNA

The concentration of DNA samples was determined by measuring absorbance at 260 nm in a spectrophotometer using the estimations that an absorbance reading of 1 corresponds to 50 μg/mL of double stranded DNA and 20 μg/mL of oligonucleotide primer (Sambrook *et al*., 1989).

2.1.9 Ligation of insert and vector DNA

Restriction digested gene fragments were joined with likewise digested vector DNA by ligation with T4 DNA ligase (Gibco, Life Technologies, Rockville, MA, USA) according to manufacturer's instructions. Generally, about 100-200 femtomoles of the insert DNA was ligated into vector at a 3:1 molar ratio. The reaction, in a volume of 10-20 μL, was performed overnight at 16^{o}C or for 1-2 h at room temperature with 10 units of the enzyme in the presence of its supplied buffer (Table 2.2). The ligated DNA was purified (2.1.6.2) prior to transformation of *E. coli* (2.1.11).

2.1.10 Preparation of electrocompetent E. coli cells

To increase the permeability of *E. coli* cells for uptake of plasmid vector DNA, the cells were made electrocompetent prior to transformation (2.1.11). A single colony was inoculated into 10 mL of 2YT broth (Table 2.2) and incubated overnight at 37^{o}C. 2.5 mL of the overnight culture was used to inoculate 0.5 L of 2YT/0.4% glucose/10 mM $MgCl_2$ and this was incubated at 37^{o}C until the optical density at 600 nm (OD_{600nm}) reached ~ 0.7-1.0. The culture was then immediately chilled on ice for 15 min and centrifuged at 4000 x *g* for 20 min at 4^{o}C. The supernatant was removed and the cells washed by resuspension in 250 mL of ice-cold 10% glycerol (BDH). This was centrifuged at 4000 x *g* for 20 min at 4^{o}C and the supernatant removed. This wash was repeated. The cells were then resuspended in 12.5 mL of ice-cold 10% glycerol and centrifuged at 4000 x *g* for 15 min at 4^{o}C. Most of the supernatant was removed and the remaining cells resuspended in a minimum of the glycerol solution. The cells were then immediately snap frozen by pipetting in 50 μL aliquots into tubes placed in dry ice. The cells were stored at –80^{o}C.

2.1.11 Electroporation of DNA into E. coli

Plasmid DNA was introduced into the *E. coli* cells by electroporation. 50 μL of electrocompetent cells (2.1.10) were thawed on ice and mixed with ~ 1 μL of the DNA sample to be electroporated. This mix was pipetted into an ice-cold electroporation cuvette (Biorad) with a 2 mm gap width and pulsed at 2.5 Volts and 25 mF capacitance using a Gene Pulser (BioRad) apparatus, then returned to ice. The cells were then flushed with 1 mL of prewarmed 2YT and allowed to recover at 37^{o}C for

30 min. Transformed cells were selected by plating on YT agar (Table 2.2) supplemented with ampicillin (Sigma) to 100 μg/mL and glucose to 1.0 % and incubated overnight at 37^{o}C.

2.1.12 Screening for positive clones by colony PCR

Cells were tested for presence of gene insert by a colony screen PCR. Standard PCR conditions (2.1.4) using Taq polymerase were followed except that the template was in the form of cells picked from colonies using a pipette tip. These cells were transferred into the reaction mix with primers to the 5$^{/}$ and 3$^{/}$ ends of the gene insert for identification of putative positive clones. PCR products were analysed by agarose electrophoresis (2.1.5).

2.1.13 Plasmid DNA isolation

For plasmid DNA isolation, cells from single colonies were inoculated into 3 mL of YT broth supplemented with ampicillin to 100 μg/mL and glucose to 0.5% and incubated overnight at 37^{o}C. Plasmid 'minipreps' were made from cell pellets of these cultures using a plasmid mini kit (Qiagen) according to manufacturer's instructions.

2.1.14 DNA sequencing

DNA sequencing was outsourced to SUPAMAC, Sydney, Australia. Plasmid DNA samples were mixed with RSP and USP primers (Table 2.1) for sequencing using Dye-terminator chemistry and analysis with an ABI 3700 Genetic Analyser (Applied Biosystems). An ABI PRISM Dye-Terminator Cycle Sequencing Ready Reaction kit was used according to manufacturer's instructions (Applied Biosystems) when sequencing reactions were performed in-house.

2.1.15 Desalting of nucleic acid samples

Nucleic acid samples such as DNaseI gene digests for DNA shuffling (2.1.16.1) and ribosome display mRNA eluates (2.4.4) were desalted using MicroSpin Sephadex G25 columns (Amersham Biosciences, Piscataway, NJ, USA) according to manufacturer's instructions. This allowed buffer exchange to water, enabling subsequent enzymatic reactions to proceed with optimal new buffer conditions.

2.1.16 DNA shuffling

DNA shuffling of genes involved the random fragmentation of the PCR amplified (2.1.4) genes by DNaseI digestion, primerless PCR regeneration of the genes from these digested fragments, and PCR with flanking primers for amplification of full-length shuffled genes (Stemmer, 1994a).

2.1.16.1 DNaseI digests

The genes were digested using DNaseI (Boehringer Mannheim GmbH, Mannheim, Germany). Reactions were in a total of 100 μL containing 1-2 μg of DNA, 50 mM Tris-HCl pH 7.4, 1 mM $MgCl_2$, and 1 unit of the enzyme. The reaction proceeded for 25 min at room temperature to achieve an acceptable level of digestion to a median fragment size of about 50 base pairs. The digested fragments were desalted (2.1.15) and then vacuum concentrated to 50 μL. To assess the effectiveness of the digest, 20 μL of the reaction was analysed on an agarose gel (2.1.5).

2.1.16.2 Primerless PCR

Fragments were randomly reassembled in a primerless PCR using Taq polymerase with the following differences from standard PCR (2.1.4). The DNaseI-digested fragments served as both template and primer with 5-15 μL of this sample added to the reaction. The annealing temperature was lower (35^{o}C or 50^{o}C as specified in text of thesis) to encourage crossovers. 45 PCR cycles were undertaken, as the extra cycles were needed in order to generate an easily visible smear when 25 μL of this reaction was analysed on an agarose gel (2.1.5).

2.1.16.3 Flanking PCR

Full-length shuffled genes were generated by standard PCR (2.1.4) with primers specific to the 5/ and 3/ ends of the gene using 1 μL of the primerless PCR as template. This PCR was run on an agarose gel and the gene bands gel-purified (2.1.6.1) before cloning.

2.2 Cell culture

2.2.1 Small and large-scale E. coli expression culture

E. coli HB2151 (Hoogenboom *et al*., 1991) transformed with the plasmid vector pGC (Coia *et al*., 1996; 3.2.1; Figure 3.1) was used for the expression of recombinant scFvs. Cell colonies were grown on YT agar supplemented with 100 μg/mL ampicillin, to select for presence of the β-lactamase gene product encoded by pGC, and 0.5% glucose, to suppress the *lacZ* promoter. Cells

from a single colony were used to inoculate 1-2 mL for small-scale, and 30-40 mL for large-scale expression, of 2YT supplemented with 100 μg/mL ampicillin and 0.5 % glucose. This was incubated overnight at 37°C with shaking in an orbital shaker. This overnight culture was used to inoculate 5-10 mL at a 1:100 dilution for small-scale, and 1-2 L to an OD_{600nm} ~ 0.1 for large-scale, of 2YT supplemented with 100 μg/mL ampicillin but with no added glucose. Large-scale cultures were grown in shake flasks holding 500 mL of broth each. Cultures were grown at 37°C until an OD_{600nm} of 0.7-1.0 was reached and then the incubation temperature was dropped to 30°C and isopropyl-β-D-thio-galactopyranoside (IPTG; Promega) was added to 0.5 mM to induce expression of scFv. The cells were induced for 3-4 h for small-scale, and ~ 2 h for large-scale expression, before analysis and/or purification of expressed products.

2.2.2 Harvesting of culture supernatant, lysate, and periplasmic fractions

After expression, cultures were centrifuged at 5000 x *g* for 15 min. Supernatant was removed but a small sample was kept for analysis. The cell pellets were harvested for the periplasmic fractions. The method for this extraction was a modification of the method of Minsky *et al*., (1986) by Iliades *et al*., (1997) essentially utilizing the osmolarity of sucrose. The cells from a 1 L expression were resuspended in 40 mL of ice-cold spheroplast buffer (50 mM Tris-HCl, pH 8.0, 0.5 M sucrose, 0.5 mM EDTA, 100 μg/mL lysozyme (Sigma)). Two Complete protease inhibitor cocktail tablets (Roche Diagnostics GmbH, Mannheim, Germany) were added and the suspension was left on ice for 10 min. Then, 26.7 mL of ice-cold weak spheroplast buffer (50 mM Tris-HCl, 1 mM EDTA) was mixed in with the suspension and this left on ice for 15 min. The amounts used were scaled up or down according to the volume of the expression culture. This was centrifuged at 75,000 x *g* for 30 min at 4°C, and the supernatant containing the periplasmic fraction was collected. If not processed immediately this was stored at –20°C. Cell lysate fractions of small-scale cultures were obtained by resuspending the spheroplast pellets remaining after periplasmic extraction in 100 μL of 4% sodium dodecyl sulphate (SDS) in phosphate buffered saline (PBS; Table 2.2). This was sonicated with a short pulse, centrifuged at 20,000 x *g* for 10 min, and the supernatant collected.

2.2.3 Microtiter well screening cultures

To produce culture supernatants from multiple clones for screening of expressed binding scFvs by enzyme-linked immunosorbent assay (ELISA; 2.3.13), cells were grown in the wells of Microwell 96F microtiter plates (Nunc, Roskilde, Denmark). In this way up to 96 colonies could be screened at a time in one plate. Wells were filled with 200 μL of 2YT supplemented with 100 μg/mL ampicillin and 0.5 % glucose. Cells from individual transformant colonies were used to inoculate these wells. The plate was then sealed and incubated overnight at 37^{o}C with shaking. The wells of a new plate were filled with 200 μL of 2YT supplemented with 100 μg/mL ampicillin but no glucose. 5 μL from each well of the overnight cultures were used to inoculate the new plate. This was incubated for 2.5 h at 37^{o}C with shaking and then the temperature was reduced to 30^{o}C and 10 μL of 10 mM IPTG was added to each well to a final concentration of 0.5 mM. These cultures were incubated for a further 2.5 h and then the plates were centrifuged for 15 min at 4000 x *g* at 4^{o}C. The supernatants were removed and then placed into new wells coated with antigen for ELISA analysis of binding as described (2.3.13).

2.2.4 Culture of hybridoma cells

Hybridoma cells producing the anti-GPE and anti-FLAG (WEHI) monoclonal antibodies were maintained and cultured by the CSIRO, fermentation group, Parkville.

2.3 Protein chemistry

2.3.1 Sodium dodecyl sulphate polyacrylamide gel electrophoresis (SDS-PAGE)

Protein samples were analysed by SDS-PAGE (Laemmli *et al*., 1970) using a Protean II mini-gel apparatus (BioRad). Resolving gels were made at 10-12.5% of a 29:1 mix of acrylamide/bis-acrylamide (BioRad) in 0.375 M Tris-HCl, pH 8.8, 0.1% SDS, and 0.1% ammonium persulphate (BioRad), with 0.05% N,N,N$^{/}$,N$^{/}$-tetramethylethylenediamine (TEMED; BioRad) added for cross-linking. This was poured between glass plates in the apparatus to set. A stacking gel consisting of 5% of the acrylamide mix in 0.25 M Tris-HCl, pH 6.8, 0.1% SDS, 0.2% ammonium persulphate and 0.1 % TEMED was overlaid. Protein samples were mixed with an equal volume of loading buffer (Table 2.2) and these were boiled for 2 min before loading into wells of the gel. Electrophoresis was carried out for 45-60 min at 150 V in electrophoresis buffer (Table 2.2). Proteins in the gel were visualised by staining with Coomassie blue R-250 (BioRad) for 2-3 h. The gels were destained with 40% methanol/10% acetic acid with 2 or 3 changes of the destain until

clear, leaving the stained protein bands. The sizes of the bands were estimated by comparison with protein standards such as prestained SDS-PAGE low range protein standards (BioRad) and Benchmark prestained standards (Gibco, Life Technologies).

2.3.2 Western Blotting

Expressed proteins were detected immunologically by Western blotting (Towbin *et al*., 1979). Proteins separated by SDS-PAGE (2.3.1) were transferred electrophoretically to a nitrocellulose membrane (Osmonics, Westborough, MA, USA) at 250 mA for 45 min in transfer buffer (Table 2.2) using a mini trans-blot apparatus (BioRad). The membrane was blocked with 5% skim milk in PBS for 1 h. To detect FLAG epitope-tagged recombinant proteins the membrane was incubated with an anti-FLAG antibody provided by the Walter and Eliza Hall Institute (WEHI) at ~ 2 μg/mL in 1% skim milk in PBS for 30 min. The membrane was then washed with PBS, then PBS/0.05% Tween-20 (Sigma), then PBS for 5 min each. To detect the anti-FLAG antibody the membrane was incubated with goat anti-mouse IgG (GαM)-horse radish peroxidase (HRP) conjugate (BioRad) at 1:1000 in 1% skim milk in PBS for 30 min. The membrane was then washed as above. For development of protein bands the membrane was incubated with the substrate for HRP consisting of 30 mg of 4-chloro-1-naphthol dissolved in 5 mL methanol and mixed with 45 mL PBS and 10 μL 30% H_2O_2. After bands had developed the membrane was washed in H_20. Molecular weights of the protein bands were estimated by comparison with protein standards as done for Coomassie-stained polyacrylamide gels.

2.3.3 Dot blotting

For detection of expressed recombinant proteins without size estimation, supernatant or periplasmic fraction proteins from expression cultures were transferred to nitrocellulose membranes using a dot blotting apparatus (BioRad). The membranes were blocked, washed, and developed for visualisation of recombinant protein exactly as described for Western blotting (2.3.2).

2.3.4 IgG purification

The anti-FLAG (WEHI) Mab used in Western blotting (2.3.2), dot-blotting, and for coupling to resin (2.3.7) for affinity chromatography (2.3.8), and the anti-GPE Mab (5C6/B3) used for production of Fab fragments (2.3.5) for BIAcore studies (2.3.13), were both purified from their respective hybridoma culture supernatants (2.2.4). Purified anti-GPE Mab was also provided by School of Life Sciences, QUT, for N-terminal amino acid sequencing of the heavy and light chains

(2.3.6) and for use as a control in ELISA (2.3.12). The antibodies were purified based on the affinity of the Fc portion of the IgG to Protein A. 2-3 L of culture supernatant (2.2.4) was applied to a 25 mL column of Protein A-coupled resin (Pharmacia Biotech, Uppsala, Sweden) equilibrated in PBS at a flow rate of 3 mL/min throughout the procedure using a BioLogic LP chromatography system (BioRad) at 4^{o}C. The column was then washed with 10 column volumes of PBS. Bound IgG was eluted using 0.1 M Glycine pH 3. Eluted protein was monitored by absorbance at 280 nm (A_{280nm}). Elution peaks of ~ 60 mL were collected and immediately neutralised with drops of saturated Tris base. Anti-FLAG Mab was dialysed against 5 L PBS at 4^{0}C. Anti-GPE Mab was dialysed against 5 L of 50 mM Tris, 3 mM EDTA, pH 7.0 prior to preparation of Fab fragments (2.3.5). The samples were filtered by passing through a 0.45 μm nitrocellulose membrane (Millipore, Bedford, MA, USA) under vacuum pressure using a bottle-top filtration unit (Nalge, Rochester, NY, USA). The samples were concentrated (2.3.9) and the integrity of the IgG was analysed by gel filtration chromatography on a Superose 12 HR 10/30 column (2.3.10). The concentration of the protein was determined as described (2.3.11).

2.3.5 Fab production

Fab fragments of the anti-GPE Mab were prepared by papain digestion of the IgG. 150 μL of a papain solution (~ 18.5 mg/mL; Sigma) was activated by mixing with 350 μL of 50 mM Tris-HCl, 3 mM EDTA, pH 7.0 and 10 μL 0.1 M DTT and incubating for 40 min at 37^{o}C. The papain was desalted by applying to a Sephadex G25 column (Pharmacia, Uppsala, Sweden) and the collected protein quantitated by measuring the A_{280nm} with calculations based on 1 mg/mL of papain corresponding to an A_{280nm} of 2.5. 1.5 mL (~ 9 mg) of the IgG was digested. Activated papain was added at 1.8% of the IgG weight (0.16 mg in 200 μL) and the mixture incubated for 5 h at 37^{o}C. The digestion was stopped by addition of 50 μL of 0.1 M iodoacetic acid (i.e. ~ 1 μL/3μg papain). The papain digested IgG was loaded onto a protein A column equilibrated in PBS to bind the Fc fragments and uncut IgG. The unbound fraction containing Fab was collected. The bound Fc and IgG were eluted with 0.1 M Glycine pH 3.0 and this was also collected. The unbound Fab fraction was concentrated (2.3.9) to ~ 2 mL and 100 μL of this analysed by gel filtration on Superose 12 HR 10/30 (2.3.10). 3 x 0.5 mL of this unbound fraction was loaded on the same column and the peak corresponding in size to a Fab fragment was collected for purification.

2.3.6 N-terminal amino acid sequencing

N-terminal amino acid sequencing was performed using a Hewlett Packard Protein Sequencer G1000A by the CSIRO, analytical services group, Parkville. Starting material was either gel filtration peak-purified (2.3.10) protein, or the protein chains of interest on polyvinyl-dinenedifluoride (PVDF; Micron Separations Inc., Westboro, MA, USA) membrane that had been separated by SDS-PAGE (2.3.1) and then transferred electrophoretically as for Western blotting (2.3.2), except that CAPS transfer buffer (Table 2.2) was used.

2.3.7 Preparation of anti-FLAG affinity resin

Purified anti-FLAG IgG (2.3.4) was coupled to N-hydroxysuccinimide (NHS)-activated Sepharose 4 fast flow resin (Pharmacia Biotech, Uppsala, Sweden) to make columns for affinity chromatography. 15 mL of the antibody in PBS at ~ 1-2 mg/mL was mixed with 10 mL of a coupling buffer of 30% polyethylene glycol (PEG) 20000 (Sigma), 0.3 M $NaHCO_3$, and this was brought to pH 6.0. The resin (25 mL) was poured in a column for washing with 15 volumes of 1 mM HCl and then removed and mixed with the 25 mL antibody solution. This mixture was brought to pH 6.0 and the coupling allowed to proceed overnight at 4^{o}C in 50 mL tubes with rotation. The resin was poured into an Econo column (BioRad) and the unbound antibody drained and collected. Unreacted NHS-ester groups were blocked with 2 column volumes of 0.2 M ethanolamine pH 8.5. The resin was washed with 5 column volumes of 100 mM Tris pH 9, 200 mM NaCl and then 5 column volumes of 10 mM Sodium Acetate pH 4.5, 200 mM NaCl. The anti-FLAG column was stored at 4^{o}C in TBS (Table 2.2) with addition of 0.02% NaN_3.

2.3.8 Affinity chromatography

FLAG-tagged recombinant proteins (2.2.2) were purified from expression culture periplasms by affinity chromatography on an anti-FLAG column (2.3.7). Prior to loading on the column the samples were given 2 or 3 short bursts of sonication on ice and then were filtered through 0.45 μm nitrocellulose membranes (Millipore) by vacuum pressure using a bottle-top filtration unit (Nalge). The column was equilibrated with TBS and protein monitored at A_{280nm}. A constant pressurised flow rate, generally at 2-3 mL/min for all steps, was applied using a BioLogic LP chromatography system (BioRad) and all solutions were kept cold on ice. Once a stable A_{280nm} base line was achieved the periplasm sample was loaded onto the column to bind FLAG-tagged proteins. The column was then equilibrated with TBS until a stable baseline was again reached. The bound protein was eluted by passing Immunopure Gentle Ag/Ab Elution Buffer (GEB, Pierce, Rockford,

IL, USA) through the column. An A_{280nm} elution peak was collected and then the column equilibrated with TBS/0.02% NaN_3 before storage at 4°C. Eluted protein was dialysed against either TBS or HEPES buffered saline containing 0.005% P20 surfactant (HBS/P20; Table 2.2). The protein sample of 15-25 mL was pipetted into Spectropor dialysis membrane tubing (Spectrum Laboratories, Rancho Dominguez, CA, USA) with a molecular weight cut off (MWCO) of 3 kD or 6-8 kD and this was clamped and placed into ~ 2 L of the buffer and allowed to rock gently overnight at 4°C. The dialysed protein sample was collected from the tubing and centrifuged to remove any precipitate.

2.3.9 Concentration of protein samples

Larger volume protein samples of >10 mL were concentrated using an Amicon 50 mL tangential flow ultrafiltration cell (Millipore). Samples were placed into the apparatus fitted with a cellulose ultrafiltration membrane (Millipore) with MWCO of 3 or 10 kD and concentrated under nitrogen pressure of 75 kPa at 4°C with magnetic stirring until the desired volume was reached. Smaller volume samples were concentrated using Microsep microconcentrator columns (Pall Gelman Sciences, Ann Arbor, MI, USA) of MWCO of 3 or 10 kD. The sample was placed in the column and centrifuged at 7000 x *g* at 4°C until the desired volume remained. Concentrated samples were centrifuged afterwards to remove any precipitate.

2.3.10 Gel filtration chromatography

Affinity purified protein samples (2.3.8) were subjected to gel filtration chromatography on Superose 12 HR 10/30 or Superdex 200 HR 10/30 columns (Pharmacia Biotech) for analysis of the quality of the preparations and for peak purification. The columns were equilibrated with TBS, PBS, or HBS/P20 at at a flow rate of 0.5 mL/min which was maintained throughout the procedure using either a Model 700 workstation (BioRad) or an AKTAbasic chromatography system (Amersham Biotech, Uppsala, Sweden), and calibrated with gel filtration protein standards (BioRad). The affinity-purified samples were concentrated to 1-2 mL (2.3.9) and 400-500 µL was injected and the relevant scFv peaks collected. Repeat injections were undertaken and the peaks pooled.

2.3.11 Estimation of protein concentration

Proteins to be analysed for binding kinetics were quantitated using a method reported by Gill and von Hippel (1989). This involves calculation of the molar extinction coefficient ε_M due to tryptophan and tyrosine residues in the protein. The molar concentration of the protein is given by A_{280nm}/ε_M where ε_M = (5690W) + (1280Y). W = number tryptophan residues; Y = number of tyrosine residues.

2.3.12 Enzyme-linked immunosorbent assay (ELISA)

The binding of antibody fragments was assessed using ELISA. Antigen was coated onto the well surface of Maxisorp microtiter plates (Nunc). For IGF-I (Gropep, Thebarton, SA, Australia), 50 μL of a 10 μg/mL solution of the protein in PBS was dispensed into the wells and left to coat overnight at 4^{o}C or for 2-3 h at room temperature. Negative control antigens such as lysozyme and/or α-amylase (Sigma) were coated likewise at a roughly equimolar concentration. All other steps were at room temperature. The antigen solution was removed and the wells were rinsed once with PBS. The wells were then blocked with either 5% skim milk in PBS or 2% BSA in PBS. The blocking reagent was left in the well for 2-3 h and then removed. The samples containing the proteins to be tested such as 100 μL of culture supernatant or periplasm were applied as a 3:1 mix with blocking reagent to the wells and incubated for 1 hour. Anti-GPE Mab used as a positive control was at ~ 2.5 μg/mL in ¼ strength of the blocking reagent. After this binding, the wells were washed 3 times with PBS, PBS/0.05% Tween-20, and PBS respectively. Bound protein was detected with 50 μL anti-FLAG antibody at ~ 2 μg/mL in ¼ strength of the blocking reagent for 20 min. During this step the anti-GPE Mab well was incubated with ¼ strength of the blocking reagent. The wells were washed again as above. Anti-FLAG antibody was detected with 50 μL of GαM-HRP at a 1:1000 dilution in ¼ strength of the blocking reagent for 20 min. The wells were washed again as above. 2,2$^{/}$-azino-di(3-ethylbenzothiazoline sulphonate) (ABTS; Roche, Indianapoulos, IN, USA), was used as substrate for HRP. ABTS was prepared at 0.5 mg/mL in 0.1 M citrate/phosphate buffer pH 4.0, 0.03% H_2O_2, with 50 μL dispensed into the wells for colour development, the absorbance of which was measured at 405 nm.

2.3.13 Binding analysis using the BIAcore 1000

Surface plasmon resonance was employed to study binding kinetics of protein interactions using the BIAcore 1000 optical biosensor. All reagents used with the machine were purchased from BIAcore AB (Uppsala, Sweden). One of the interacting proteins is immobilised to the sensor surface with the

other protein introduced to the system by flowing it over this surface, allowing real time analysis of the binding event between antibody fragments and antigen (Jonsson *et al*., 1991). Binding is monitored by a change in refractive index of the solution, which is proportional to the mass associated with the surface. The data generated can be analysed for kinetics with the BIAevaluation 3.0 software provided.

2.3.13.1 Immobilisation of antigen

Antigen was immobilised to the carboxymethylated dextran flow cell surface of a CM5 sensorchip by standard NHS/N-ethyl-N$^{/}$-(dimethylaminopropyl)carbodiimide [EDC] chemistry (Johnsson *et al*., 1991). The standard BIAcore running buffer of HBS/P20 was allowed to run over the flow cell surface at 5 μL/min until the response unit (RU) baseline was stable. All injections for immobilisation were done at 5 μL/min. The surface was activated with an injection of 35 μL of a NHS/EDC mixture to form NHS esters. This activation allows covalent coupling of the antigen via primary amine groups, mainly from lysine residues on the protein, to the flow cell surface. The optimal concentration of antigen injected over the activated surface was determined empirically. Generally the antigen was diluted to between 20 and 100 μg/mL in 10 mM sodium acetate buffer and 50 μL of this injected over the activated flow cell. The pH of acetate buffer for this injection was also determined empirically but is related to the pI of the protein. This procedure generally produced an increase of 500-2000 RUs on the chip, depending on the antigen. The RU increase is proportional to the mass immobilised on the chip surface. Remaining NHS-ester groups on the surface were then deactivated with an injection of 35 μL of 1 M ethanolamine-HCl, pH 8.5.

2.3.13.2 Binding to antigen

The protein samples to be injected over the immobilised antigen were gel filtration peak-purified monomers. This was so that analysis could be done for 1:1 binding, excluding avidity effects. Injections were done at 5, 10 or 20 μL/min with the latter being the best flow rate for kinetic determinations. HBS/P20 was allowed to run over the flow cell until a stable base line was reached. Then the protein of interest was injected for 7 min for the association phase. Immediately at the end of the association phase the HBS/P20 was passed over the chip for the dissociation phase until the response returned to base line. The association and dissociation phases together represent the sensorgram for the binding event. Consecutive sensorgrams were obtained for a range of concentrations of the protein sample, with dilutions made in the HBS/P20. Regeneration of the surface without any loss of activity to the immobilised antigen could be undertaken with an

injection of 25 mM HCl for 1-2 min but this was generally not required as the interactions being studied returned to the baseline level during dissociation phase in reasonable time. Proteins samples that were not in HBS/P20 from the gel filtration purification were dialysed into this buffer using MWCO 3.5 kD Slide-A-lyzer mini dialysis units (Pierce).

2.3.13.3 Analysing binding kinetics using BIAevaluation 3.0 software

The BIAevaluation 3.0 software was used to gain information on the binding kinetics from the sensorgrams derived from the binding experiments. The sensorgrams representing the different concentration runs were overlaid and brought to the same zero point so association and dissociation curves could be analysed simultaneously. Data from the curves were selected for fitting to the Langmuir model, which is a theoretical model for 1:1 binding. The initial 10-20 s of association and dissociation were disregarded as initial refractive index change in passing from HBS/P20 to the sample could distort the data. Therefore the data 3-4 min after the first 20 s of each phase was selected for analysis. The evaluation program calculates the best fit of the selected regions of the experimental curves to the theoretical model and provides values for the on and off rates, and the dissociaton constant (K_D). The quality of the data fit was assessed by visually comparing the closeness of the experimental and theoretical curves, by looking at the standard error (SE) values for the data set provided by the program, with a T value for the particular figure (T=X/SE; where X = value of parameter such as off-rate) of greater than 10 considered satisfactory, and by looking at the χ^2 value given by the program. The χ^2 value gives a measure of the goodness of fit, with a figure below 2 being ideal, and a figure below 10 being generally acceptable according to the manufacturer.

2.4 Ribosome display

2.4.1 Preparation of ribosome display templates

The ribosome display DNA templates for use in coupled transcription/translation experiments for the production of ribosome display complexes, prepared by standard cloning procedures as described in section 4.2, were amplified by standard PCR (2.1.4), gel purified (2.1.6.1), and quantitated (2.1.8).

2.4.2 Transcription and translation

All H_2O and PBS solutions used for making wash solutions and blocking reagents for use in ribosome display experiments were DEPC-treated as described in 2.1.1. For ribosome display of antibody fragments, a TNT T7 quick coupled transcription and translation system (Promega) was used. This is based on a rabbit reticulocyte lysate as a source of ribosomes and also contains T7 polymerase for transcription of the DNA template. 0.5-1.0 μg of the template was mixed with 20 μL of the TNT master mix, 1.0 μL of a complete amino acid mix (1 mM; Promega), magnesium acetate to 0.5 mM, with H_20 added to bring the total volume to 24 μL. Reactions were undertaken in siliconised RNase-free microfuge tubes (Ambion, Austin, TX, USA). In some instances oxidized glutathione (GSSG) was included at 2.5 mM where indicated. The coupled reaction was incubated for 1 h at 30^{o}C to produce stalled complexes consisting of the ribosome, the translated protein, and its encoding mRNA produced by the T7 polymerase. To remove DNA from the mixture prior to selection, 3 μL of DNaseI (Promega) and 3 μL of 10X DNaseI buffer were added and this incubated for 15 min at 30^{o}C.

2.4.3 Selection of translated ribosome complexes

During attempts to optimise the procedure for specific selection of ribosome display complexes a number of different experimental conditions were altered. The particular conditions that were altered from one experiment to the next are specified in the text in the description of the experiments. Antigen for selection was immobilised on tosylactivated magnetic beads (Dynal) or, more routinely on the well surface of Maxisorp microtiter wells (Nunc). Antigen (IGF-I and lysozyme or α-amylase) was coupled to tosylactivated beads according to manufacturers instructions (Dynal). Antigen was coated to the well surface by dispensing a 10 μg/mL solution of IGF-I in PBS into the well and leaving overnight at 4^{o}C or for 2-3 h at room temperature. Lysozyme and α-amylase, were coated in the same way at an approximately equimolar concentration. After coating, the well surface was blocked with either skim milk or BSA solutions in PBS. Skim milk concentration used was 5-10%. BSA concentration used was 2-3%. Torula Yeast RNA (Sigma) was sometimes included in the block at a concentration of 50-100 μg/mL. Wells were filled with the blocking solution for 2-3 h and then removed and the wells rinsed with PBS. The translated ribosome mixture was cooled on ice and diluted to 90 μL with the addition of 60 μL of ice-cold PBS and Mg Acetate to 0.5 mM. Blocking reagent was sometimes included in this solution. In the case of skim milk the concentration was 2.0%, BSA was at 0.67-2.0%, and the yeast RNA was at 0-66 μg/mL, as indicated in the text for the experiments. This mixture was then split into 2 x 45 μL

portions, and for binding of complexes, each was incubated with a different antigen at 4°C for 1 h with agitation. In the case of antigen-coated beads, 1 μL of beads were added to the translated mix in a 0.5 mL siliconised tube. Unbound complexes were removed by washing 2-3 times with a wash solution of PBS, 5 mM Mg Acetate with Tween-20 at 0-1.0%, then once with PBS, 5 mM Mg Acetate. Each wash involved the dispensing of 100 μL of the washing solution into the well, or mixed in with the beads, pipetting up and down 5 times and then removal of the solution.

2.4.4 Recovery of selected complexes

After washing, elution of the complexes was performed. This was achieved by disruption of complexes using EDTA or by elution of whole complexes with peptide. For EDTA elution, 50 μL of a solution of 20 mM EDTA in PBS was incubated in the wells, or with the beads for 15 min at room temperature. The eluate was removed, desalted using G25 columns (2.1.15) and vacuum concentrated to 10-20 μL. For peptide elution, 50 μL of a range of concentrations of the peptide (GPE (3.5.2), GPE 10mer (3.1.2), or whole IGF-I) in PBS, 5 mM Mg Acetate were incubated in the wells for 2-3 min on ice. The eluates were vacuum concentrated to ~ 15 μL and used as templates (0.2-2 μL) in RT-PCR (2.1.4.3). RT-PCR products were analysed on agarose gels (2.1.5) to assess the success of the ribosome display experiment and also for isolation of DNA for cloning and subsequent display and selection rounds.

2.4.5 Use of BIAcore for ribosome display selection

To attempt to inactivate any RNases that may be remaining after the BIAcore 1000 was desorbed and washed, a solution of 1 unit/μL RNasin (Promega), 1 mM DTT in HBS/P20 was injected. Two 30 μL transcription/translation reactions (2.4.2) were pooled and their volume brought to 180 μL with HBS/P20/0.5 mM MgAcetate. As the concentration of DTT in 20 μL reticulocyte lysate is 2 mM, the concentration in the final volume of 180 μL is 0.22 mM. The translated complexes were injected over immobilised antigen (2.3.13.1) at 20 μL/min for 7 min. Untranslated complexes were prepared and injected in the same way except that DNA template was not added to the reaction. When translated complexes were to be dialysed prior to injection, the transcription/translation reaction was dialysed against 300 mL of HBS/P20/0.5 mM MgAcetate at 4^0C for 1 h using Slide-A-lyser minidialysis units (Pierce) with MWCO 10 kD, immediately before injection. Fractions were collected during the dissociation phase using the fraction collection function of the BIAcore 1000, normally at 15 s intervals. Selected fractions were analysed by their use as template in RT-PCR (2.1.4.3).

Table 2.1 Oligonucleotides used in this thesis

(All primer sequences listed 5′ to 3′)

Mouse V_L primers:

VLF1- TCTGGCGGTGGCGGATCGGATGTTTTGATGACCCAAACT

VLF2- TCTGGCGGTGGCGGATCGGATATTGTGATGACGCAGGCT

VLF3- TCTGGCGGTGGCGGATCGGATATTGTGATAACCCAG

VLF4- TCTGGCGGTGGCGGATCGGACATTGTGCTGACCCAATCT

VLF5- TCTGGCGGTGGCGGATCGGACATTGTGATGACCCAGTCT

VLF6- TCTGGCGGTGGCGGATCGGATATTGTGCTAACTCAGTCT

VLF7- TCTGGCGGTGGCGGATCGGATATCCAGATGACACAGACT

VLF8- TCTGGCGGTGGCGGATCGGACATCCAGCTGACTCAGTCT

VLF9- TCTGGCGGTGGCGGATCGCAAATTGTTCTCACCCAGTCT

VLR1- ATGAGTTTTTGTTCTGCGGCCGCCCGTTTCAGCTCCAGCTTG

VLR2- ATGAGTTTTTGTTCTGCGGCCGCCCGTTTTATTTCCAGCTTGGT

VLR3- ATGAGTTTTTGTTCTGCGGCCGCCCGTTTTATTTCCAACTTG

VLR4- ATGAGTTTTTGTTCTGCGGCCGCGGATACAGTTGGTGCAGCATC

Other primers:

5325 forward primer to anti-GPE V_H with *SfiI* site overhang-

TTATTACTCGCGGCCCAGCCGGCCATGGCCGAGGTCCAGCTGCAACAGTCTGGACC

5304 reverse primer to anti-GPE V_H-

TGAACCGCCTCCACCTGAGGAGACGGTGACCGTGGT

2643 reverse primer to V_H to add $(Gly_4Ser)_3$ linker sequence-

CGATCCGCCACCGCCAGAGCCACCTCCGCCTGAACCGCCTCCACCTGAGGAGAC

2950 forward primer to V_L to add $(Gly_4Ser)_3$ linker sequence-

GTCTCCTCAGGTGGAGGCGGTTCAGGCGGAGGTGGCTCTGGCGGTGGCGGATCG

6248 forward primer for engineering insertions into anti-GPE V_H CDR2-

GGAGGTATTATTCCAGGAAATGGTGATACTTCCTACAACCAGAAATTCAAGGGCAAGGCC

6249 reverse primer for engineering insertions into anti-GPE VH CDR2-

CTGGTTGTAGGAAGTATCACCATTTCCTGGAATAATACCTCCAATCCACTCAAG

RSP forward sequencing primer for genes inserted in pGC-

AACAGCTATGACCATG

USP reverse sequencing primer for genes inserted in pGC-

GTAAAACGACGGCCAGT

5998 forward primer to anti-GPE scFv to add T7 promoter and RBS for ribosome display-

GCGCGAATACGACTCACTATAGAGGGACAAACCGCCATGGCCGAGGTCCAGCTGCAACAGTCTGG

5385 reverse primer to 3′ end of C_H3 domain-

GCCCTTGGGCCGGGAGATGGTCTGCTTCAGTGGCGAGGGCAGGTCTGTGTG

Table 2.1 continued.

5386 reverse primer to C_H3 internal to 5385-

CGAGGGCAGGTCTGTGTGGGTCACGGTGCACGTGAACCTCTCCCCGGAG

5387 reverse primer to C_H3 internal to 5386-

CGTGAACCTCTCCCCGGAGTTCCAGTCATCCTCGCAGATGCTGGCCTCACC

6232 reverse primer to C_H3 internal to 5387-

GACGGCGCTGAAAGTGGCATTGGGG

6321 forward primer to C_L domain with *Not*I site overhang-

CTGAAACGGGCGGCCGCTGATGCTGCACCAACTGTA

6322 reverse primer to C_L domain with *Sac*II overhang-

TTTATAATCCGCGGCACACTCTCCCCTGTTGAAGCT

5267 reverse primer to 3/ end of C_L domain-

CATCATCATCATCTTTATAATCTGCGGCCGCACACTCTCCCCTGTTGAAGCTCTTGAC

5268 reverse primer to C_L internal to 5267-

CCCCTGTTGAAGCTCTTGACAATGGGTGAAGTTGATGTCTTGTGAGTGGCCTCACAG

5269 reverse primer to C_L internal to 5268-

CTTGTGAGTGGCCTCACAGGTATAGCTGTTATGTCGTTCATACTCG

5942 reverse primer to C_L internal to 5269-

GCTGTTATGTCGTTCATACTCG

6188 forward primer to 4T10-

GCAGCTAATACGACTCACTATAGGAACAGACCACCATGGACCTGCAGCTGCAGGCCTCCG

6227 forward primer to NC10 with *Sfi*I site overhang-

TTATTACTCGCGGCCCAGCCGGCCATGGCCCAGGTCAAACTGCAGGAGTCTGGGGC

6228 reverse primer to NC10 with *Not*I site overhang-

ATGAGTTTTTGTTCTGCGGCCGCCCGTTTTAGTTCCAGCTTTG

6221 forward primer for grafting anti-GPE V_H CDR1 onto NC10-

TCTGGCTACACATTTACCGATTACACCATGCACTGGGTAAAACAGTCACCT

6240 reverse primer for grafting anti-GPE V_H CDR1 onto NC10-

CCCAGTGCATGGTGTAATCGGTAAATGTGTAGCCAGAAGC

6261 forward primer for grafting anti-GPE V_H CDR2 onto NC10-

GCCTGGAATGGATTGGAGGTATTATTCCAGGAAATGGTGATACTTCCTAC

6291 reverse primer for grafting anti-GPE V_H CDR2 onto NC10-

GGAAGTATCACCATTTCCTGGAATAATACCTCCAATCCATTCCAGGCCCTGTCC

6222 forward primer for grafting anti-GPE V_H CDR3 onto NC10-

GTCTATTACTGTGCAAGAAATTACTACGGAGTGGACTGGTTCTTCGATGTCTGGGGCCAAGGGACCACG

6241 reverse primer for grafting anti-GPE V_H CDR3 onto NC10-

GACATCGAAGAACCAGTCCACTCCGTAGTAATTTCTTGCACAGTAATAGACCGC

6305 forward primer for grafting anti-GPE V_L CDR1 onto NC10-

CAGAGCATTGTACATAGAAATGGAAACACCTATTTAGAGTGGTATCAACAGAATCCAGATGG

Table 2.1 continued

6306 reverse primer for grafting anti-GPE V_L CDR1 onto NC10-
CCACTCTAAATAGGTGTTTCCATTTCTATGTACAATGCTCTGACTTGCCCTGCAACTGATG
6351 forward primer for grafting anti-GPE V_L CDR2 onto NC10-
CTCCTGATCTACAAAGTTTCCAACCGATTTTCAGAAGTCCCATCACGGTTC
6352 reverse primer for grafting anti-GPE V_L CDR2 onto NC10-
GAAAATCGGTTGGAAACTTTGTAGATCAGGAGTTTAACGGTTCC
6449 forward primer for grafting anti-GPE V_L CDR3 onto NC10-
TGCTTTCAAGGTTCACATGTTCCGTGGACGTTCGGAGGGGGCACA
6450 reverse primer for grafting anti-GPE V_L CDR3 onto NC10-
CGTCCACGGAACATGTGAACCTTGAAAGCAAAAGTAAGTGGCAATATCTTCTTG
6904 forward primer to NC10 scFv to add T7 promoter and RBS for ribosome display-
GCGCGAATACGACTCACTATAGAGGGACAAACCGCCATGGCCCAGGTCAAACTGCAGGAGTCTGG

Table 2.2 Buffers, Solutions and Media

First strand buffer (10X): 0.65 M KCl, 0.25 M Tris-HCl, pH 8.1, 2.1 mM $MgCl_2$

Vent polymerase buffer: 10 mM KCl, 10 mM $(NH_4)_2SO_4$, 20 mM Tris-HCl, pH 8.8, 2 mM $MgSO_4$, 0.1% Triton X-100

Taq polmerase buffer: 67 mM Tris-HCl, pH 8.8, 16.6 mM $(NH_4)_2SO_4$, 0.45% Triton X-100, 2 mg/mL gelatin

TAE buffer: 40 mM Tris-Acetate, 1 mM EDTA

DNA gel-loading buffer (6X): 0.25% bromophenol blue, 40% (w/v) sucrose in H_2O

Restriction enzyme digest buffers (10X):

NEB1: 0.1 M Bis Tris Propane-HCl, 0.1 M $MgCl_2$, 10 mM DTT, pH 7.0

NEB2: 0.1 M Tris-HCl, 0.1 M $MgCl_2$, 0.5 M NaCl, 10 mM DTT, pH 7.9

NEB3: 0.5 M Tris-HCl, 0.1 M $MgCl_2$, 1 M NaCl, 10 mM DTT, pH 7.9

NEB4: 0.2 M Tris-Acetate, 0.1 M Mg Acetate, 0.5 M K Acetate, 10 mM DTT, pH 7.9

T4 DNA ligase buffer (5X): 0.25 M Tris-HCl, pH 7.6, 50 mM $MgCl_2$, 5 mM ATP, 5 mM DTT, 25% (w/v) polyethylene glycol-8000

Media:

All media ingredients purchased from Oxoid (Hampshire, UK)

YT broth: 0.8% (w/v) bacto-tryptone, 0.5% (w/v) bacto-yeast extract, 0.5% (w/v) NaCl

YT agar: as for YT broth but with addition of 1.5% bacto-agar

2YT broth: 1.6% (w/v) bacto-tryptone, 1.0% (w/v) bacto-yeast extract, 0.5% (w/v) NaCl

Phosphate buffered saline (PBS; 10X): 8% (w/v) NaCl, 0.2% (w/v) KCl, 1.44% (w/v) Na_2HPO_4, 0.24% (w/v) KH_2PO_4, pH 7.4

SDS-PAGE gel-loading buffer: 50 mM Tris-HCl, pH 6.8, 100 mM DTT, 2% SDS, 0.1% bromophenol blue, 10% glycerol

SDS-PAGE electrophoresis buffer: 15.1 g/L Tris base, 72 g/L Glycine, 5 g/L SDS

Transfer buffer: 5.8 g/L Tris base, 2.9 g/L Glycine, 0.37 g/L SDS, 20% methanol

CAPS transfer buffer: 10 mM 3-(cyclohexylamino)-1-propanesulfonic acid (CAPS), pH 11, 0.25% SDS, 20% methanol

Tris buffered saline (TBS; 10X): 3% (w/v) Tris base, pH 7.4, 8 % (w/v) NaCl, 0.2% (w/v) KCl

HBS/P20: 10 mM N-(2-hydroxyethyl)piperazine-N$^{/}$-(2-ethanesulphonic acid) [HEPES], pH 7.4, 150 mM NaCl, 3.4 mM EDTA, 0.005% surfactant P20

CHAPTER 3
CLONING AND CHARACTERISATION OF THE ANTI-GPE SCFV AND A HCDR2 MUTATED VARIANT

3.1 Introduction

3.1.1 General

The first objective of this work was to develop and characterise the model protein for use in molecular evolution strategies. Antibodies have been some of the most studied molecules in protein engineering as discussed in Chapter One. Various fragments have been used in antibody engineering, such as Fabs (Better *et al*., 1988; Huse *et al*., 1989), V-domains (Ward *et al*., 1989; Power *et al*., 1992), antibody-like frameworks (Tramontano *et al*., 1994; Nuttall *et al*., 1999), and the scFv, which has been chosen as the model in this project.

Since the cloning of an scFv was first reported (Huston *et al*., 1988; Bird *et al*., 1988) many antibodies have been produced as scFv fragments and scFv libraries have been constructed. By linking the antibody variable domains together with a flexible linker, the scFv format is able to closely reproduce a binding site of the parent antibody in a compact size that can be easily expressed and manipulated. The binding affinity of the scFv fragment to its cognate antigen can be measured to allow easy comparison between affinity matured and wild type molecules. In gauging the efficacy of new affinity maturation strategies the use of the scFv will allow comparison with existing methods.

This chapter describes the construction, cloning and characterisation of an IGF-I-binding scFv (anti-GPE) and its HCDR2 mutated variant as a model protein for new molecular evolution strategies.

3.1.2 Antecedent work

The monoclonal antibody used as a model in this project was raised at Queensland University of Technology, School of Life Sciences (Craven, 1999). The antibody was elicited against a 10-mer peptide with the objective of having specificity to the GPE tripeptide that is the N-terminal cleavage product from IGF-I in the formation of the residual molecule des(1-3)IGF-I (Craven, 1999). The 10-mer peptide consisted of Gly-Pro-Glu at the N-terminus, then 3 β-Alanine residues as an inert spacer to Asp-Tyr-Lys for solubility, with a Cys residue at the C-terminus for possible coupling of

the peptide to a carrier protein. The hybridoma clone producing the antibody was named 5C6/B3. ELISA studies on the monoclonal antibody demonstrated that it binds to IGF-I and this binding can be inhibited by free GPE peptide. There is however, virtually no binding to des(1-3)IGF-I (Craven,1999). This suggests the antibody has specificity to the N-terminal (GPE) end of IGF-I.

In addition to the Mab, an scFv version of the parent antibody had been constructed and isolated at QUT using the 'recombinant phage antibody system' marketed by Pharmacia Biotech. This scFv was provided in the vector pCANTAB 5 E. This scFv was named anti-GPE(QUT).

In BIAcore binding studies described in 3.5.4, the N-terminal fragment of IGF-I-binding protein-3 (N-BP3) was used. This protein fragment was cloned and characterised previously (Galanis *et al*., 2001). This fragment was provided in affinity-purified (FLAG) form by Dr. M. Galanis (CSIRO, Parkville).

3.2 Cloning of an anti-GPE scFv

3.2.1 Subcloning of the phage-isolated anti-GPE(QUT) scFv

In order for the anti-GPE scFv to be compatible with our laboratory expression and purification protocols, the construct was subcloned into the pGC expression vector (Coia *et al*., 1996; Figure 3.1). This vector allows periplasmic extracts to be harvested for soluble protein by the introduction of a *pelB* signal peptide to the N-terminus. It also allows detection and affinity purification of expressed protein by FLAG-tagging (Hopp *et al*., 1988) the C-terminus. Expression from pGC is under the control of the *lacZ* promoter with an ampicillin resistance gene for selection of pGC-transformed cells.

The anti-GPE(QUT) scFv gene was PCR amplified (2.1.4) out of the pCANTAB plasmid supplied by QUT with a restriction site primer mix (supplied with the Pharmacia Biotech kit) containing primers that code for a *Sfi*I site at the 5′ end of the gene and a *Not*I site at the 3′ end. The amplified DNA was subjected to agarose electrophoresis (2.1.5), gel purified (2.1.6.1), restriction digested with *Sfi*I and *Not*I (2.1.7), and ligated into the likewise digested vector pGC (2.1.9). This ligation was electroporated (2.1.11) into competent *E. coli* HB2151 cells (2.1.10) and five clones positive for the scFv insert by colony PCR (2.1.12) were sequenced (2.1.14) from plasmid preparations (2.1 13). The DNA sequences received correlated well with the sequence data provided with the original clones, indicating that subcloning was successful (data not shown). The one discrepancy in the

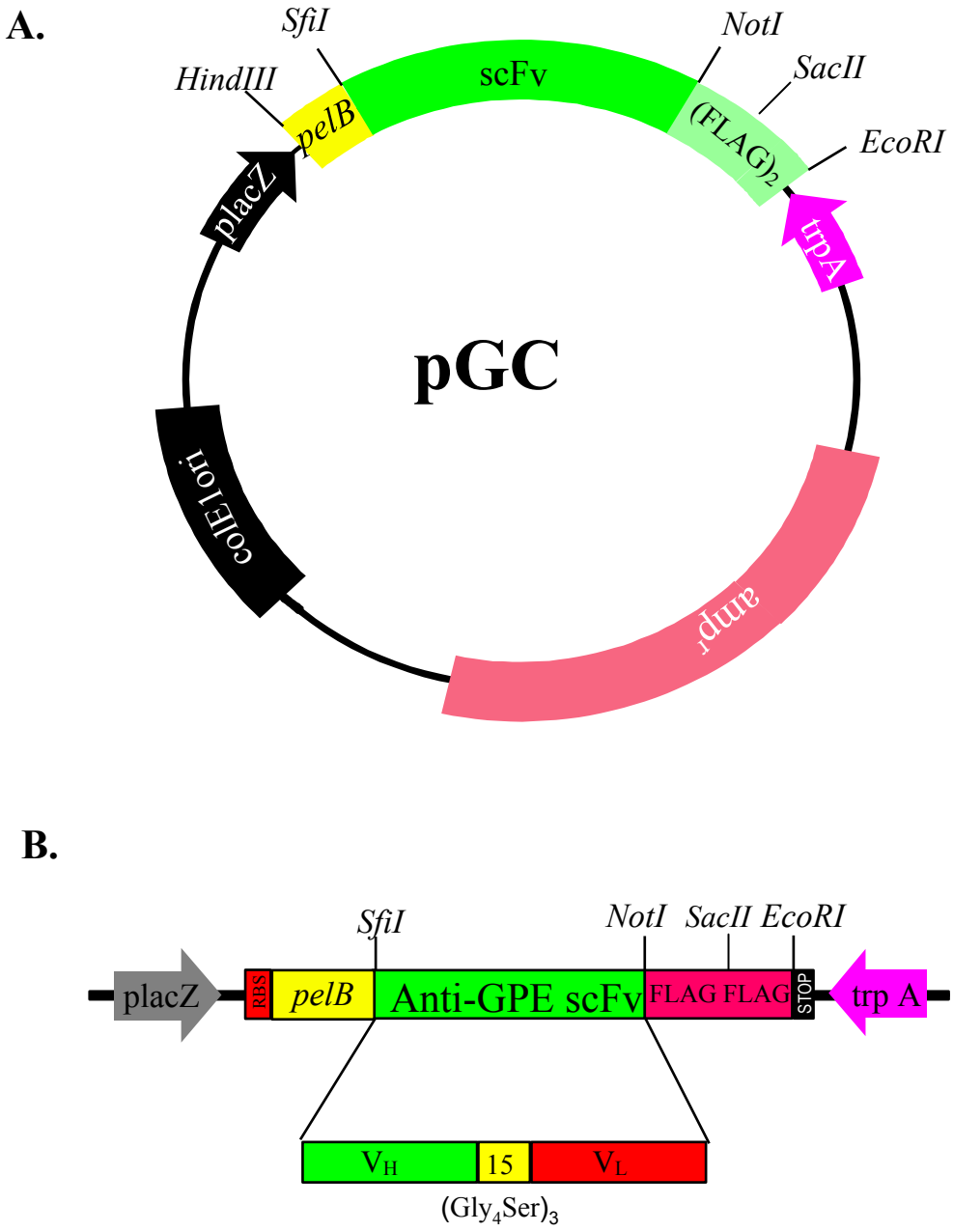

Figure 3.1 Schematic diagram of the *E. coli* expression vector pGC. Expression is under the control of the lac promoter. The gene is expressed with a *Pel*B signal sequence and two C-terminal FLAG octapeptide tag sequences separated by two alanine residues. A. pGC expression vector and B. the cloning cassette.

sequence data being that the codon for the third amino acid varied in the clones - reading CAG for two clones, AAG for two clones, and AAA for one clone. This led to the deduced amino acid sequence reading Gln for two clones and Lys for three clones. These discrepancies would most probably be the result of the degeneracy in the sequences of the primer mix used to amplify the anti-GPE scFv.

3.2.2 N-terminal amino acid sequencing

N-terminal sequencing of the heavy and light chains of the purified Mab was undertaken to verify that the cloned anti-GPE V gene sequences correctly matched those of the parent antibody. The heavy and light chains of the purified 5C6/B3 Mab provided by QUT were resolved by SDS-PAGE (2.3.1) under reducing conditions and transferred to PVDF membrane for sequencing to be performed (2.3.6). Ten residues of sequence for each chain were obtained. This sequence was compared to that deduced from DNA sequencing data (Table 3.1)

Table 3.1 N-terminal amino acid sequence for anti-GPE monoclonal antibody

Heavy Chain:

E V Q L Q Q S G P E – data from N-terminal amino acid sequencing.

Q V Q L Q E S G P E – data deduced from DNA sequence of anti-GPE clones.
K

Light Chain:

D V L M T Q T P L S – data from N-terminal amino acid sequencing.

D I E L T Q S P T I – data deduced from DNA sequence of anti-GPE clones.

There are discrepancies in the sequence for the heavy chain in residues 1 and 6 but apart from this the data matches. These two discrepancies are probably due to degeneracy in the sequences of the primer mix. Residues 7-10, outside the realm of binding of the primers, are a match and therefore it appears the authentic V_H has been amplified. However, there appears to be enough of a discrepancy with the light chain sequence data, with only four matches, to suggest that the incorrect V_L domain may have been amplified.

3.2.3 Isolation of V genes

Due to the inconsistencies between the amino acid and DNA sequence data it was decided to attempt to amplify the V-genes individually from the hybridoma 5C6/B3 provided by QUT (Craven, 1999). Total RNA was extracted from hybridoma cells using Trizol reagent (2.1.1) and mRNA purified using magnetic $(dT)_{25}$ Dynabeads (2.1.2). Reverse transcription was performed (2.1.3) to produce a cDNA pool, which was used as template for PCR amplification (2.1.4) of V genes.

A suite of primers to the 5′ and 3′ ends of the known mouse V-gene sequences (Table 2.1; Zhou *et al*., 1994) was employed in the PCR to amplify the V_L gene. With this primer library comprising nine forward (5′) primers and four reverse (3′) primers there were a total of 36 possible PCR reactions that could be attempted to amplify the gene. The first nine PCRs used all nine forward primers, each with reverse primer VLR1. In the set up of PCR temperature conditions, it was decided to have just two initial cycles with an annealing step at 59°C, then 40 cycles with denaturing and elongation steps only. This was to encourage the primer of best fit to the gene to be favoured, and reduce chances of contaminating sequences being amplified. These PCRs were electrophoresed in an agarose gel (2.1.5), revealing that just one reaction, with primers VLF1 and VLR1, amplified a strong V gene-size band (data not shown). Of the nine forward primers, the VLF1 primer is the closest in sequence to that deduced from the light chain N-terminal amino acid data. PCRs with two of the other primers produced very faint bands. It was decided to test the amplification of the other reverse primers with VLF1 under the same PCR conditions. Electrophoresis again showed VLR1 and VLF1 to amplify V_L. The combination with VLR2 also gave some weak amplification (data not shown).

The VLR1/VLF1 fragment was DNA sequenced (2.1.14) prior to cloning in scFv format to verify the fidelity of the amplification. The deduced amino acid sequence of this DNA sequence (data not shown) matched with the sequence of the first ten residues of the light chain as revealed by the N-terminal sequencing (Table 3.1). The sequence did not match with any existing V_L sequences in use or previously used in our laboratory. This gave some confidence to proceed with cloning of this gene as part of the anti-GPE scFv.

Based on the available heavy chain amino acid sequence data and the DNA sequence data of the scFv, forward (5325) and reverse (5304) primers for amplification of the V_H gene were designed (Table 2.1), rather than using the general mouse primer library. The V_H gene was amplified from

cDNA by the same process as that for the V_L with primers 5325 and 5304 and the amplified fragment used directly for construction of an scFv.

3.2.4 Construction of the anti-GPE scFv gene

The first step in the construction of the scFv was the PCR (2.1.4) addition of linker fragments to the V genes with primers 2643 and 2950 (Table 2.1) coding for a $(Gly_4Ser)_3$ flexible linker. The agarose gel-purified (2.1.6.1) V_L gene fragment was PCR amplified with primers 2950 (linker) and VLR1 (flanking). The agarose gel-purified V_H gene fragment was PCR amplified with primers 5325 (flanking) and 2643 (linker). These added linker overhangs enabled joining of the two domains in the V_H-V_L orientation by SOE PCR (2.1.4.2). Gel-purified V gene + linker fragments were allowed to prime off each other due to homology of the linker overhangs in 20 cycles of PCR before flanking primers (5325 & VLR1) were introduced for a further 30 cycles of amplification for full length scFv (Figure 3.2).

3.2.5 Cloning and sequencing of the anti-GPE scFv gene

The flanking primers 5325 and VLR1 code for *Sfi*I ($5^{/}$) and *Not*I ($3^{/}$) restriction sites respectively in the overhangs at the ends of the gene. This enables cloning into the plasmid expression vector pGC (Figure 3.1). The newly constructed anti-GPE scFv fragment was gel purified (2.1.6.1) and digested with *Not*I and *Sfi*I restriction enzymes respectively (2.1.7), as was pGC. The digested scFv fragment was ligated into pGC (2.1.9). The ligated DNA was then electroporated into competent *E.coli* HB2151 cells (2.1.11) and these were selected on YT plates supplemented with ampicillin at 100 μg/mL. Random colonies were screened by colony PCR (2.1.12) for scFv insert using the flanking primers 5325 and VLR1. A selection of positive clones was grown for plasmid preparation (2.1.13). DNA sequencing of the inserts was performed (2.1.14). Analysis of the sequence revealed that an scFv had been properly constructed (Figure 3.3). The deduced amino acid sequences of both V_H and V_L fragments correlated well with the N-terminal sequence data and *pelB*, V_H, linker, V_L and FLAG tags all appeared to be in frame. The deduced amino acid sequence data revealed a short heavy chain CDR2 which is six residues briefer than most other mouse subgroup II(A) sequences (Kabat *et al*., 1991) of which this V domain is a member.

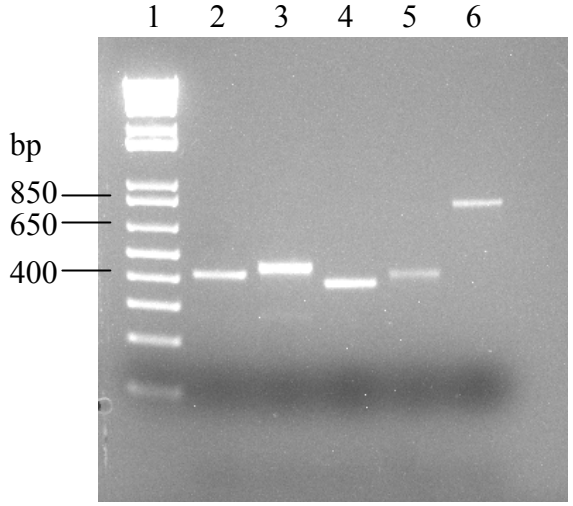

Figure 3.2 Agarose gel electrophoresis of fragments for anti-GPE scFv gene construction. Lane 1, 1 kb plus DNA ladder; 2, V_H; 3, V_H + linker; 4, V_L; 5, V_L + linker; 6, ScFv.

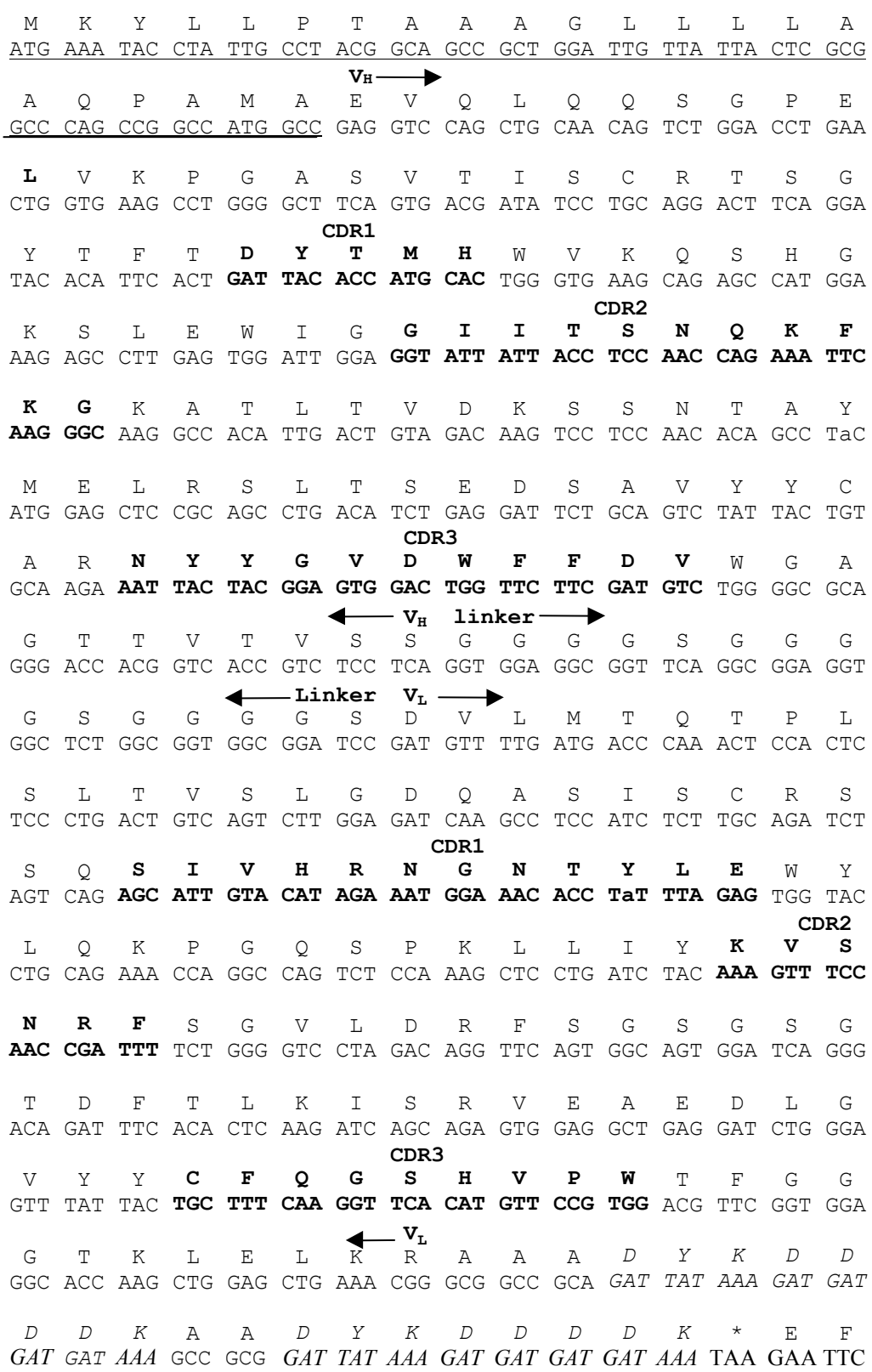

Figure 3.3 Nucleotide sequence and deduced amino acid sequence of the anti-GPE scFv. *Pel*B sequence is underlined; CDRs in bold; FLAG tags italicised.

3.3 Expression and purification of the anti-GPE scFv

3.3.1 Small and large scale expression

Small-scale expressions of the anti-GPE scFv clone were performed initially as described (2.2.1) to test if sufficient scFv was being expressed for detection by SDS-PAGE and Western blotting. After 4 hours IPTG induction periplasms and supernatants were harvested (2.2.2) from the 5 mL cultures. Proteins from both the supernatant and periplasmic extract were separated by reducing SDS-PAGE (2.3.1) and transferred to nitrocellulose for Western blot (2.3.2). The Western blot showed a FLAG-tagged protein migrating at ~ 33 kD in both periplasmic extracts and supernatant (data not shown). It was therefore decided to proceed with larger scale expression for purification of the scFv. The migration of the scFv at ~ 33 kD is about 4 kD more than the expected size of the FLAG-tagged anti-GPE scFv, an anomaly that has been observed for other scFvs in our laboratory.

Large scale expressions of anti-GPE scFv were generally performed in 1 to 2 litres as described (2.2.1). It was observed that soon after induction the cell growth decelerated markedly with the culture failing to reach an OD_{600nm} much above 1.0, and this reading on the decline and below the induction reading after 2 hours (data not shown). The induction temperature of 30^{o}C appeared to be optimal for cell growth and expression levels (data not shown). It is assumed that expression of the cloned scFv is quite toxic to the bacterial cells resulting in the low cell densities reached during expression. It was therefore decided to harvest bacterial culture periplasms no later than 2 hours after induction, before extensive lysis had occurred, and while expressed scFv may still be associated with the periplasmic fraction. Expression was monitored by Coomassie blue staining of SDS-PAGE gels and Western blotting (Figure 3.4) where it can be seen that expressed scFv is detected in the periplasmic fraction (lane 2) as also seen for small-scale expression.

The anti-GPE construct was transformed (2.1.11) into another six competent *E.coli* cell lines (TOPP2, TOPP6, HB101, TOPP10, TG1, XL1-Blue) to determine if a more resilient strain was available for expression of the scFv. Parallel 10 mL expressions (2.2.1) of colony PCR (2.1.12) positive clones were monitored for OD_{600nm} reached (data not shown) and expression levels into supernatant (Figure 3.5) and periplasmic fraction by dot blotting (2.3.3). HB2151 reached the second highest OD_{600nm} (higher for small-scale culture than shake flask culture) but clearly expressed scFv to higher levels than the other strains so it was decided to continue with this strain. Periplasmic expression levels (data not shown) reflected the supernatant levels.

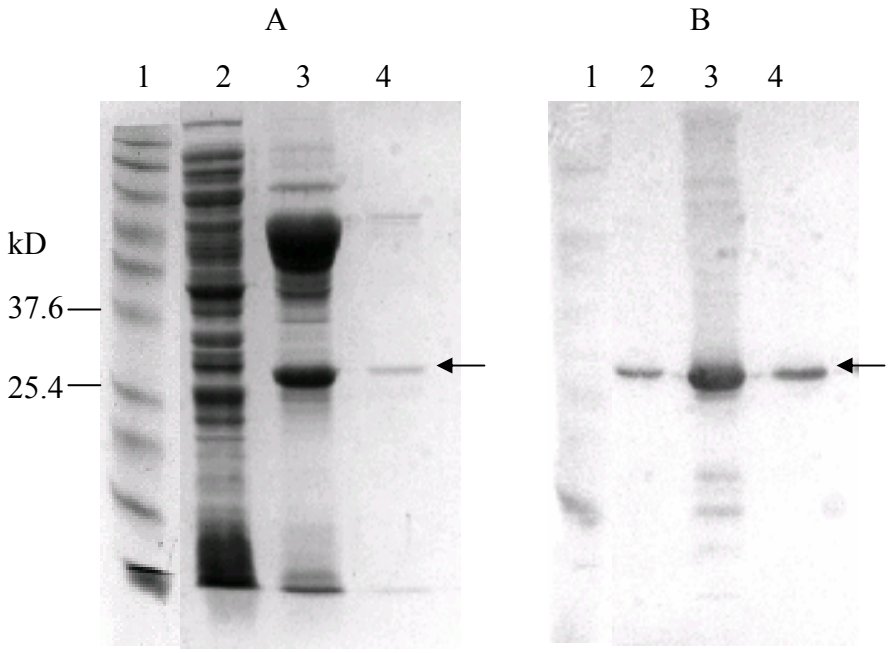

Figure 3.4 A. SDS-PAGE (Coomassie-stained) and B. Western blot of expression and purification of anti-GPE scFv. Lane 1, Benchmark protein standards; 2, periplasmic extract; 3, FLAG affinity-purified material; 4, purified monomeric scFv from gel filtration on Superose 12. Arrows indicate migration of scFv.

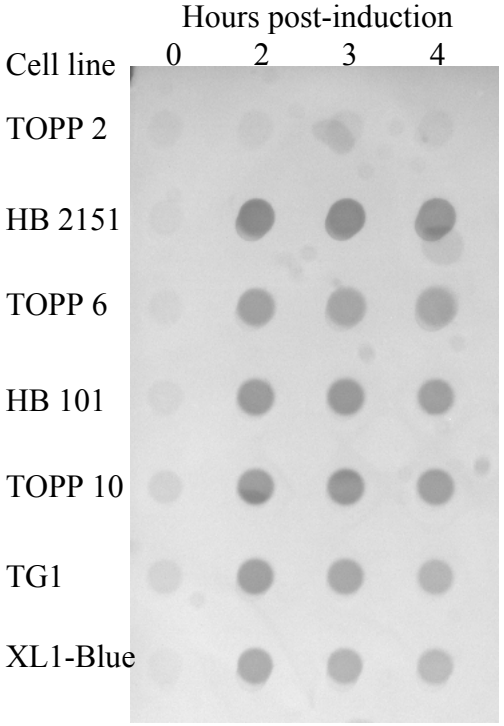

Figure 3.5 Dot blot of time course of expression of anti-GPE scFv in pGC in a selection of *E. coli* host strains.

3.3.2 Affinity purification of the anti-GPE scFv

The anti-GPE scFv was initially purified from periplasmic extract based on the affinity of the C-terminal FLAG tag epitopes on the expressed protein to the anti-FLAG (WEHI) Mab. Affinity chromatography of periplasmic extract was performed as described (2.3.8). FLAG-tagged protein that was bound to the column was easily visualised as an A_{280nm} peak when eluted with GEB and this was collected. Collection of the elution peak generally resulted in a sample volume of 20-25 mL and this was dialysed into TBS in preparation for gel filtration chromatography. FLAG-purified scFv was detectable by SDS-PAGE and Western blot (Figure 3.4, lane 3) with large amounts of an ~ 60kD protein copurifying with the scFv. This has been observed previously and is most likely GroEL (Iliades *et al*., 1998) but was not investigated further.

3.3.3 Gel filtration chromatography of the scFv

Affinity purified eluate in TBS was concentrated to ~ 1-2 mL (2.3.9). Analysis and further purification was performed by gel filtration chromatography on calibrated Superose 12 or Superdex 200 columns (2.3.10). Protein peaks (A_{280nm}) corresponding to the expected size of monomeric scFv were collected for binding analysis. The Superose 12 profile (Figure 3.6) shows monomer and higher molecular weight peaks corresponding to oligomeric and aggregated material. Monomer collected from one gel filtration run was concentrated (2.3.9) and then loaded onto the column again for further purification to ensure the highest purity of monomeric protein possible was obtained without contamination of higher molecular weight forms from earlier peaks (Figure 3.6). Purified scFv was quantitated (2.3.11). N-terminal sequencing (2.3.6) of the first 10 amino acid residues of the scFv was performed and corresponded to the expected sequence, verifying the identity of the anti-GPE scFv monomer (data not shown). The amount of soluble, monomeric scFv purified was quite low (<100 μg per Litre of culture). This appeared to be due to the protein being quite prone to oligomerisation, aggregation, and precipitation. This low monomer solubility saw substantial amounts of protein lost through precipitation during concentration and freeze/thaws. Concentration had to be done nonetheless to get adequate levels for binding analysis on the BIAcore. Also, the observed toxicity of expressed scFv to the bacterial cells (3.3.1), causing lysis and therefore low cell densities, resulted in low amounts of scFv being produced in cultures. The Superose 12 profile (Figure 3.6) shows the large proportion of higher molecular weight forms to monomer. SDS-PAGE and Western blot of the purification (Figure 3.4) also demonstrates the poor recovery of soluble monomer when comparing the periplasmic band (lane 2) with the affinity-purified band (lane 3) and the scFv monomer band from Superose 12 (lane 4). The periplasmic sample is an ~ 15-fold

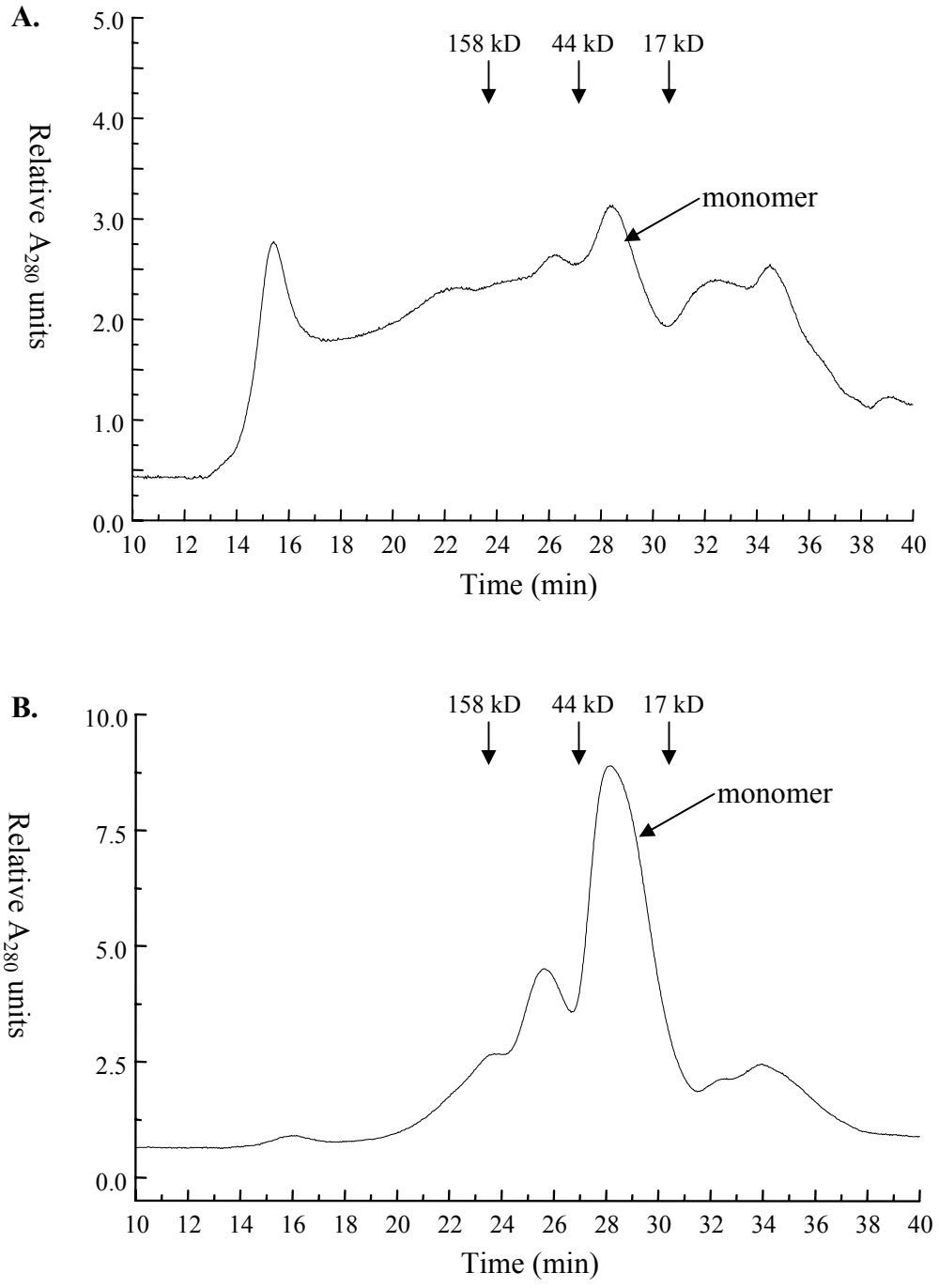

Figure 3.6 Gel filtration chromatography of anti-GPE scFv on a Superose 12 column. A. Anti-FLAG affinity-purified *E. coli* periplasmic extract and B. scFv monomer peak from A. concentrated and reinjected for further purification. Collected monomer peaks and elution times of Biorad protein standards indicated by arrows.

concentration from the original culture volume, the FLAG-pure sample is an ~ 100-fold concentration, and the soluble monomer band is an ~ 1000-fold concentration. Equal volumes of each sample were loaded on the gel. Therefore, if 100% of the periplasmic band was recovered as monomer, the band for the monomer sample would be expected to be 1000/15 = 66.7-fold more intense than the band for the periplasmic sample. Estimating that the Western blot monomer band (Figure 3.4.B, lane 4) is twice as intense as the periplasmic band (lane 2), one can approximate that 2/66.7 x 100 = 3% of periplasmic expressed protein was recoverable as soluble monomer. Often the yield from expressions was lower than this.

3.4. Production of the 5C6/B3 monoclonal antibody and its Fab

For analysis of binding of the anti-GPE IgG antibody freshly prepared protein was required. The 5C6/B3 hybridoma cell line was obtained from QUT and grown by the CSIRO Parkville fermentation group (2.2.4). IgG expressed into the hybridoma culture supernatant (~2.5 L) was purified using a Protein A column (2.3.4). The purified IgG was estimated to be at a concentration of 6 mg/mL in ~ 4 mL based on calculation of molar extinction coefficient at A_{280nm} (2.3.11) giving a yield of ~ 9.6 mg per litre of culture. For comparison of the purified scFv monomer fragment to its parent, Fab fragments needed to be produced so that monomeric binding could be analysed. Fab fragments of anti-GPE were made by papain digestion as described (2.3.5). Essentially, papain was activated and desalted then used to digest the IgG for the release of Fab fragments. After the digestion reaction material was loaded on a Protein A column to bind uncleaved IgG and cleaved Fc. The Fab and other cleaved products were in the flow through fraction and were collected. Bound material was also eluted as a potential source of more anti-GPE IgG for future applications such as in ELISA. The unbound material migrated as two main peaks on a Superose 12 column, with sizes consistent with Fab′2 and Fab fragments (data not shown). These peaks were collected and the concentration of purified Fab was estimated (2.3.11). The purity and homogeneity of the Fab was confirmed by running a sample on a SDS-PAGE gel under reducing and non-reducing conditions (Figure 3.7) and by rerunning a sample on the Superose 12 column (Figure 3.8).

3.5. Characterisation of binding of the anti-GPE scFv and Fab

3.5.1 Immobilisation of IGF-I to the CM5 BIAsensor chip

The binding analysis of these antibody fragments was achieved by surface plasmon resonance using the BIAcore 1000 (2.3.13). The binding interaction involved IGF-I being immobilised to a flow cell

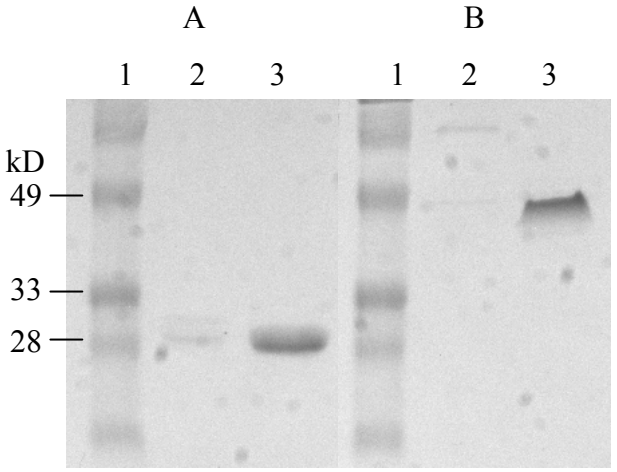

Figure 3.7 SDS-PAGE of purified anti-GPE Fab fragment. A. reducing and B. non-reducing conditions. Lane 1, Markers; 2, Superose 12 peak 24.5 min (Fab/2); 3, Superose 12 peak 27.4 min (Fab).

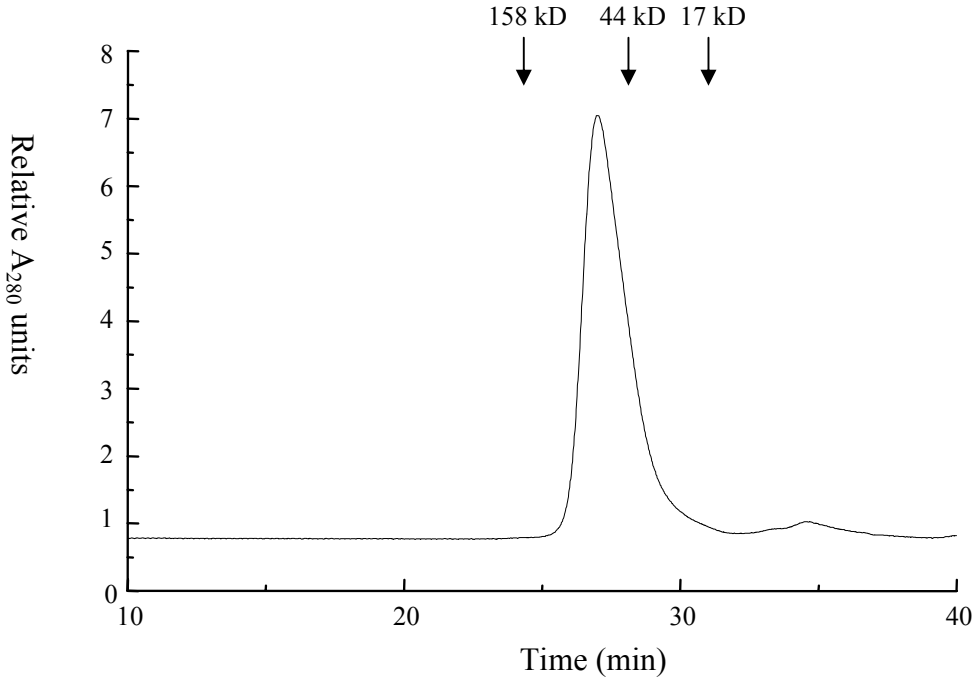

Figure 3.8 Gel filtration chromatography of purified anti-GPE Fab fragment on a Superose 12 column. Elution times of BioRad protein standards are indicated.

of a CM5 BIAsensor chip (2.3.13.1) with the antibody fragments being passed over this surface in solution. The NHS/EDC chemistry that couples the antigen to the surface of the chip involves reaction of mostly lysine residues of the protein with the carboxymethylated dextran layer (Johnsson *et al*., 1991). The IGF-I molecule has three lysine residues as potential points of coupling to the chip and these are distant from the binding epitope. It was determined that a pH of 4.5 was optimal for immobilisation of the IGF-I. The IGF-I was immobilised at 50-100 μg/mL in 50 μL of 10 mM Sodium Acetate pH 4.5. Routinely this method immobilised 500-1000 response units (RUs) on the chip. Once IGF-I was coupled to the chip a stable RU baseline was achieved.

3.5.2 Binding of the Fab to IGF-I

Purified scFv and Fab were either dialysed into the BIAcore running buffer of HBS/P20 or collected from columns equilibrated in this buffer to limit the bulk refractive index changes on the sensorgrams due to the bulk refractive buffer change effect. The kinetics of association were determined by binding to immobilised IGF-I at Fab concentrations of 284, 568, 1136, 2272 nM (2.3.13.2; data not shown). The sensorgrams confirmed the ELISA data (Craven, 1999) that the anti-GPE antibody binds to IGF-I. Using the BIAevaluation software to fit the data to a 1:1 binding model (2.3.13.3), an affinity corresponding to a $K_D = 1.02 \times 10^{-7}$ M was calculated (Table 3.2). This affinity figure was determined by simultaneous fitting of the 284-1136 nM curve data. However, strong confidence in the accuracy of the number is not possible due to the large χ^2 values (> 10) generated in the data analysis, suggesting a relatively poor fit to the theoretical model, although standard errors for the data were low. The poor fit could be due to mass transfer, where rebinding of dissociated Fabs occurs due to high density of the IGF-I immobilised on the flow cell surface. This affinity is however in the normal range of affinities for antibodies generated by an immune response (Griffiths *et al*., 1994).

The ELISA data produced by Craven (1999) showed inhibition of the antibody's binding to IGF-I when the antibody was preincubated with increasing concentrations of GPE peptide. This was confirmed by binding studies using the BIAcore. The GPE peptide was manufactured and provided by Mr. A. Kirkpatrick of the CSIRO, analytical services group, Parkville. A visual representation of this is shown in Figure. 3.9.A. A fixed concentration of the anti-GPE Fab was mixed with specified concentrations of the GPE peptide for 5 minutes at room temperature before being passed across immobilised IGF-I. The presence of the GPE peptide was shown to inhibit this binding but needed to be in great molar excess to achieve significant inhibition. For example, 20 μM GPE peptide

could only inhibit binding of 1 μM anti-GPE Fab by approximately one third (maximum RUs bound) compared to the amount bound in absence of peptide. This evidence suggests that the antibody has a preference for binding to the GPE domain of IGF-I. Binding of the anti-GPE Fab to des(1-3)IGF-I, the IGF-I analogue without the N-terminal GPE residues, was also attempted. The des(1-3)IGF-I was immobilised on a CM5 sensorchip under the same conditions as for whole IGF-I. The sensorgram showed negligible binding (Figure 3.15), further suggesting a specificity for the GPE domain.

3.5.3 Binding of the scFv to IGF-I

Prior to running on the BIAcore the scFv concentration was estimated (2.3.11). It was observed that a flow rate of 20 μL/min was optimal for passing these antibody fragments over the chip-immobilised IGF-I, minimising the mass transfer effect and generating binding curves that gave a better fit to theoretical curves than slower flow rates (data not shown). The kinetics of binding of anti-GPE scFv to immobilised IGF-I were determined by analysis of binding of the scFv at 250, 500, 1000 and 2000 nM. The resultant sensorgrams clearly showed a binding event with association and dissociation phases, providing more evidence that the correct V domains have been cloned. These sensorgrams are shown as overlaid plots in Figure 3.10.A. BIAevaluation 3.0 software was used to assess binding affinities from the curves simultaneously using the Langmuir 1:1 model (2.3.13.3). A K_D of 3.7 x 10^{-6} M was calculated (Table 3.2) by globally fitting the data of all curves. This analysis of data generated a χ^2 value (a measure of the goodness of fit) of about 3, an acceptable figure as a value of 2 and under is generally considered an ideal fit for BIAcore analysis according to the manufacturer. Further, the standard errors for the data were quite low (Table 3.2). A dissociation constant of 3.7 μM is in the weaker end of the range for antibody affinities, due to a moderate off rate and slow on rate, and suggests the anti-GPE scFv could be an ideal candidate for affinity maturation experiments. This is quite a discrepancy between the binding affinities (~36-fold) of the scFv and Fab and is greater than that generally observed for other scFvs and their parents, suggesting that the binding surface presented to antigen is not identical for the Fab and scFv or that there are problems with the binding reactions in the BIAcore environment. The off-rate of the Fab is similar for the scFv, although the on-rate for the scFv is much slower (Table 3.2). The scFv was also tested on immobilised IGF-II (data not shown) and des(1-3)IGF-I (both immobilised under the same conditions as IGF-I) and showed negligible binding (Figure 3.10.B), further demonstrating the specificity of this antibody. As performed for the anti-GPE Fab, inhibition of binding of the scFv to IGF-I in the presence of GPE peptide was demonstrated (Figure 3.9.B).

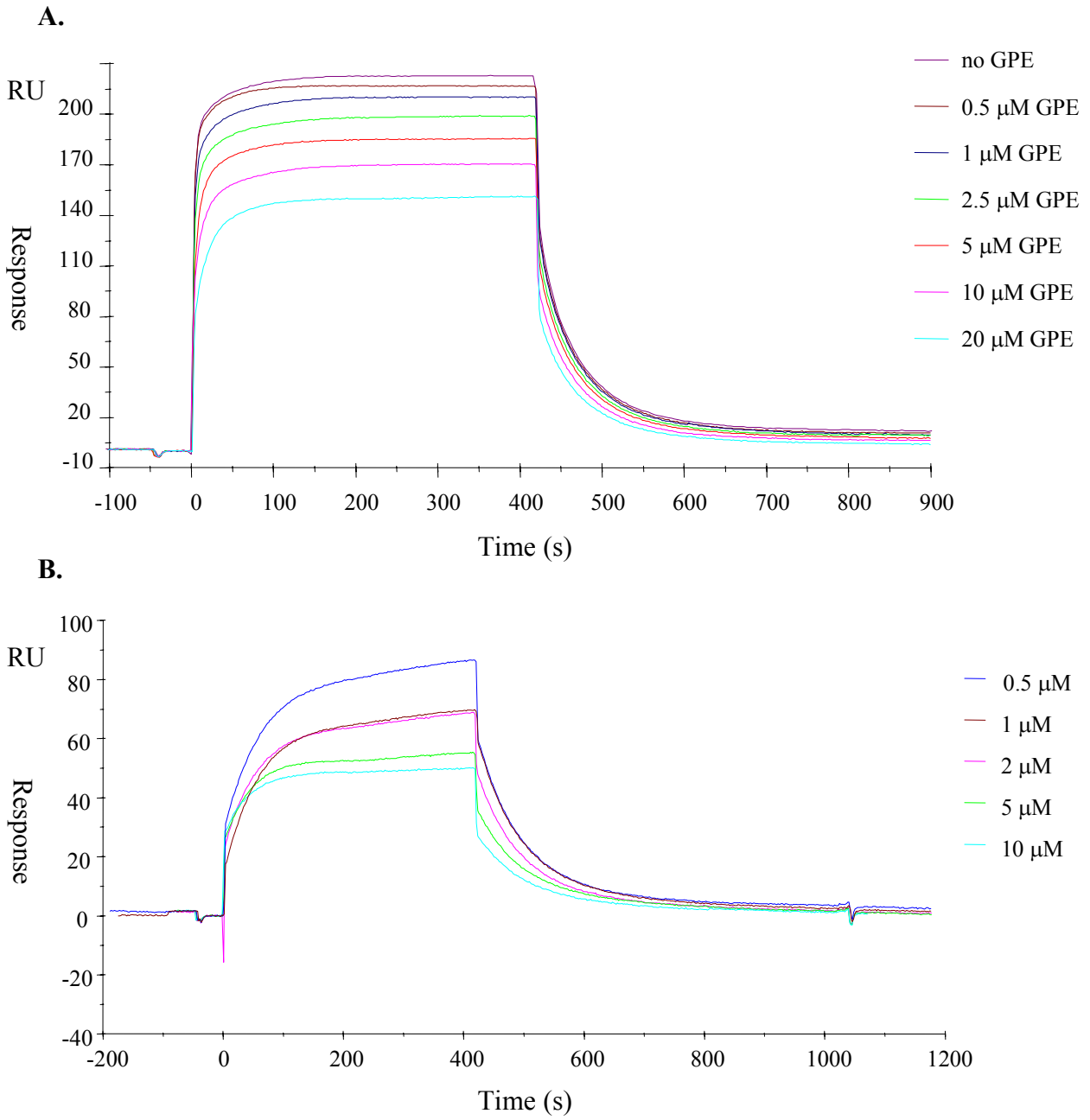

Figure 3.9 Inhibition of binding of anti-GPE to IGF-I by GPE peptide. A. 1µM anti-GPE Fab B. 1 µM antiGPE scFv. Concentrations of GPE peptide indicated in legend.

A.

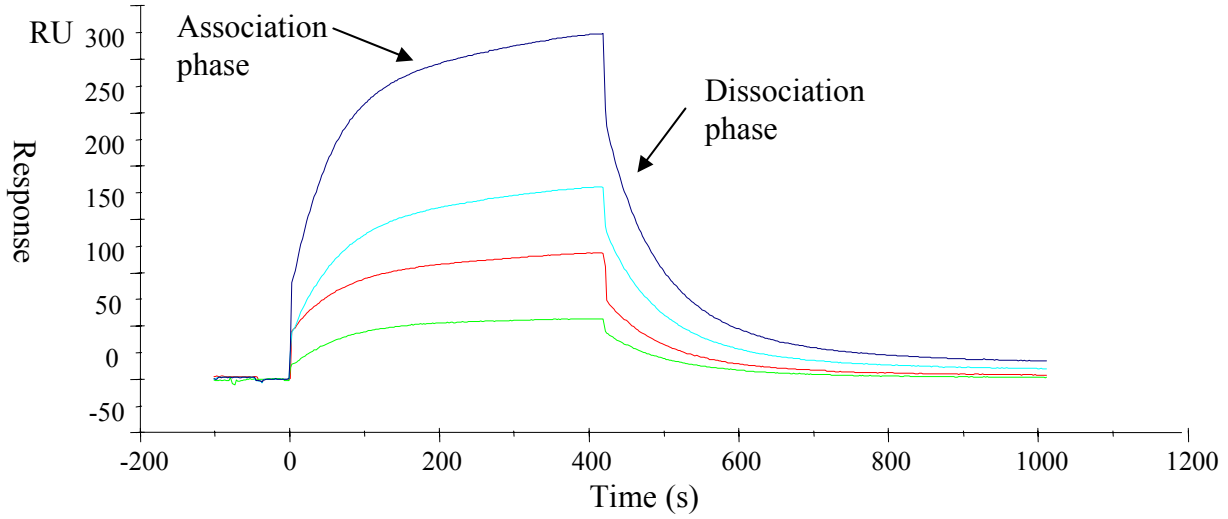

B.

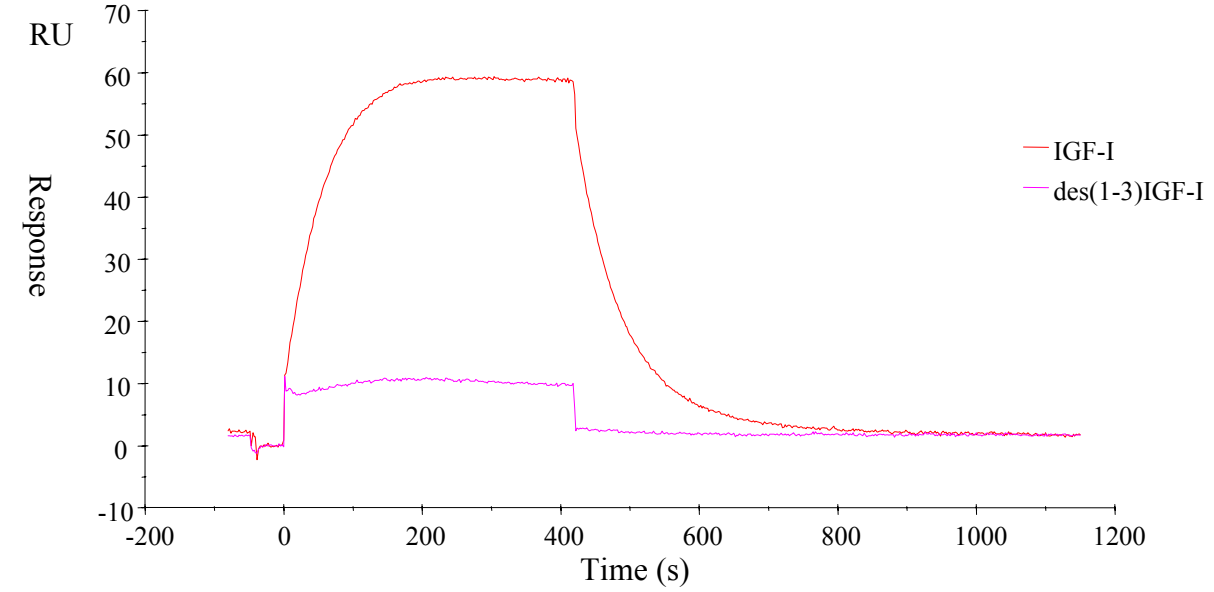

Figure 3.10 BIAcore analysis of binding of anti-GPE scFv to IGF-I and des(1-3)IGF-I. A. Overlaid sensorgrams of the interaction of a series of concentrations of anti-GPE scFv with IGF-I immobilised on the BIAcore (250 nM - green, 500 nM - red, 1000 nM – light blue, and 2000 nM – navy blue). B. Comparison of binding of 0.5 μM scFv to immobilised IGF-I and des(1-3)IGF-I showing specificity to the GPE epitope.

Table 3.2 Kinetic data for interactions of anti-GPE wild type and anti-GPE H2M scFvs, and anti-GPE Fab with immobilised IGF-I.

	k_a(1/Ms)	SE**	k_d(1/s)	SE	K_D(μM)
Anti-GPE scFv	2.20×10^3	28	8.11×10^{-3}	2.52×10^{-5}	3.68
Anti-GPE Fab	1.50×10^5	2.1×10^3	1.53×10^{-2}	1.68×10^{-4}	0.102
Anti-GPE H2M scFv*	4.21×10^3	164	8.67×10^{-3}	1.22×10^{-4}	2.06

* see section 3.8

** standard errors for on and off rate calculations

3.5.4 Binding interactions involving the N-terminal IGFBP3 fragment and the IGF-I receptor ectodomain

The binding interactions of other known IGF-I-binding molecules were also assessed using the BIAcore. IGF-I binding protein 3 (IGFBP3) which consists of cysteine-rich N- and C-terminal regions, binds to IGF-I, and has been shown to have a much lower affinity for des(1-3)IGF-I (Gluckman *et al*., 1998). This suggests the GPE residues may make up part of the epitope. In our laboratory the bacterially expressed N-terminal domain of IGFBP3 (N-BP3) has been shown to bind to IGF-I on the BIAcore but with a reduced affinity compared with the full-length protein (Galanis *et al*., 2001). The N-BP3 was obtained in affinity-purified form from culture supernatant and this was concentrated (2.3.9) and monomer peak purified by gel filtration chromatography on a Superose 12 column (2.3.10). When anti-GPE Fab and N-BP3 were injected over immobilised IGF-I simultaneously, the maximum RUs appeared to be additive when compared to when they were injected individually (Figure 3.11). This was also demonstrated when using the coinject function of the BIAcore (2.3.13) to sequentially inject these molecules (Figure 3.12) with the order of injection showing no significant difference in overall binding. Using coinject, first one protein was allowed to interact with the immobilised IGF-I for 5 minutes, and then the second protein was injected for 7 minutes in the presence of the first so that the equilibrium of the first interaction could be maintained. These observations suggest that these proteins can recognise different epitopes on IGF-I, but is contradicted by the data showing that the anti-GPE Fab and the N-BP3 (Figure 3.15) show virtually no binding to des(1-3)IGF-I on the BIAcore which suggests that they at least partly share an epitope.

Binding interactions involving IGF-I receptor ectodomain (IGF-IRED; Garrett *et al*., 1998) were also performed. Again substantial additivity could be seen in binding interactions with immobilised IGF-I. IGF-IRED showed strong binding on its own and when coinjected with anti-GPE Fab

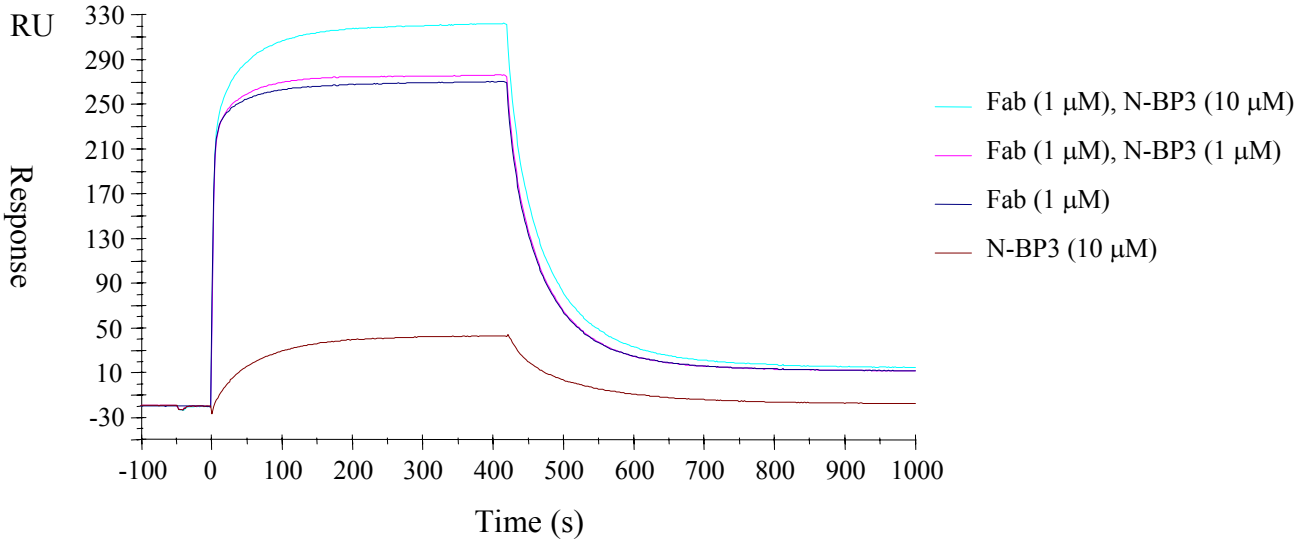

Figure 3.11 BIAcore analysis of additive binding of N-BP3 and anti-GPE Fab to immobilised IGF-I.

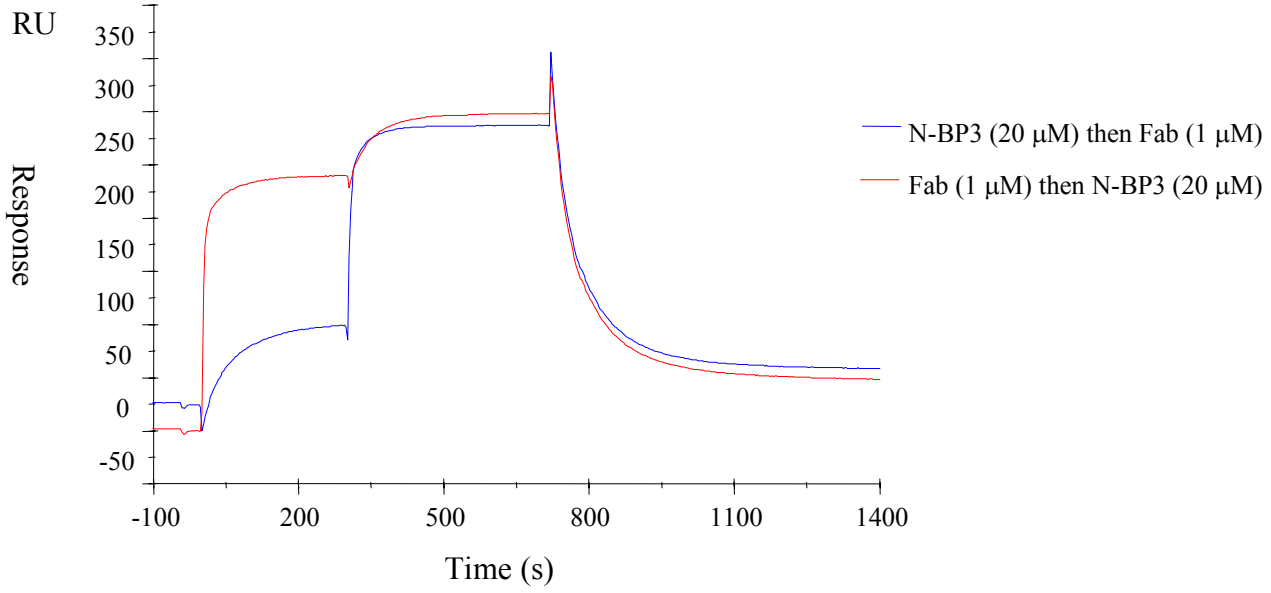

Figure 3.12 BIAcore analysis of additive binding of anti-GPE Fab and N-BP3 to immobilised IGF-I using coinject function.

(Figure 3.13) or N-BP3 (Figure 3.14). It is apparent that these molecules are able to simultaneously bind to IGF-I which could be expected as the proposed epitope for receptor binding is well away from that for the binding protein (Bayne *et al*., 1989). This is also further evidence that the immobilised IGF-I on the CM5 chip is functional. Maximum RUs achieved was significantly higher when IGF-IRED was the first species injected. This is probably due to the fact that this bivalent species is simply the stronger binder, and when it is the first species injected there is 12 minutes instead of 7 minutes interaction time, thus allowing a lot more of the protein to bind. The fact that N-BP3 and Fab were injected at 100-fold and 5-fold higher concentrations respectively, to obtain these sensorgrams, is indicative of the strength of binding of IGFRED to IGF-I. Further to this, the reverse orientation of this interaction was attempted with IGFRED immobilised on the sensor chip. Despite substantial bulk refractive index change, a good binding curve was obtained (Figure 3.16). Finally, IGFRED was shown to bind very strongly to immobilised des(1-3)IGF-I (Figure 3.15), as expected, due to its binding epitope being away from the N-terminus. This confirmed the activity of the immobilised des(1-3)IGF-I on the chip surface, further substantiating the specificity of both anti-GPE and N-BP3, which showed negligible binding.

3.6 Cloning of an anti-GPE HCDR2-mutated (H2M) scFv

3.6.1 Design of the anti-GPE H2M gene

As the anti-GPE scFv has poor stability and low bacterial expression levels, it was postulated that the unusually short HCDR2 area may be a factor in these characteristics, and that reintroducing these 'missing' residues may favour proper folding and stability of the molecule. Therefore this heavy chain CDR2 was seen as a likely area for mutagenesis and six residues that are normally found in this CDR of mouse heavy chain variable region class IIA (Kabat, 1991) were targeted to be engineered back into the sequence. The reduction in size of the CDR2 may decrease the potential surface area for binding, therefore leading to a low affinity, or conversely, it may provide a valley or pocket into which the IGF-I epitope for anti-GPE can fit.

The design of anti-GPE H2M scFv is shown in Figure 3.17. It was decided to insert the residues found in the corresponding positions in the NC10 scFv, an influenza neuraminidase binding antibody fragment characterised in our laboratory (Malby *et al*., 1993) that has good solubility and expression. The six residues are P, G, N, G and D at positions 52A to 56 (Kabat, 1991) and Y at position 59. All are the consensus residues of mouse subclass IIA for their respective positions, except the D, with the P and Y both highly conserved. D is not the consensus residue, but it is not

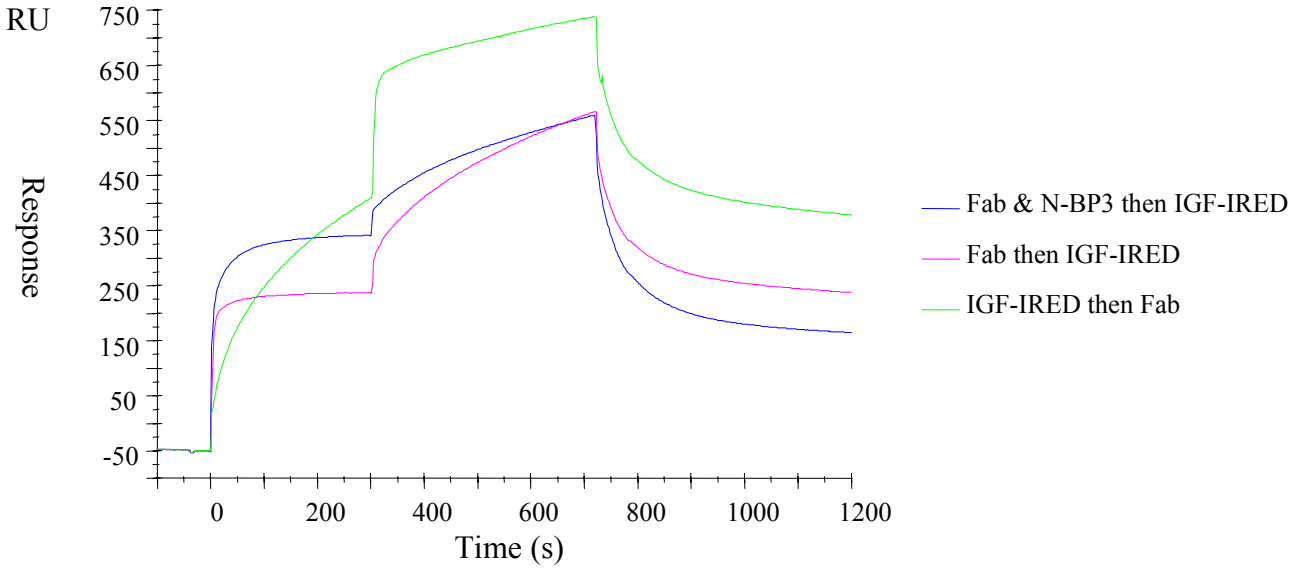

Figure 3.13 BIAcore analysis of additive binding of anti-GPE Fab (1 μM), IGF-IRED (0.2 μM) and N-BP3 (20 μM) to immobilised IGF-I using coinject function.

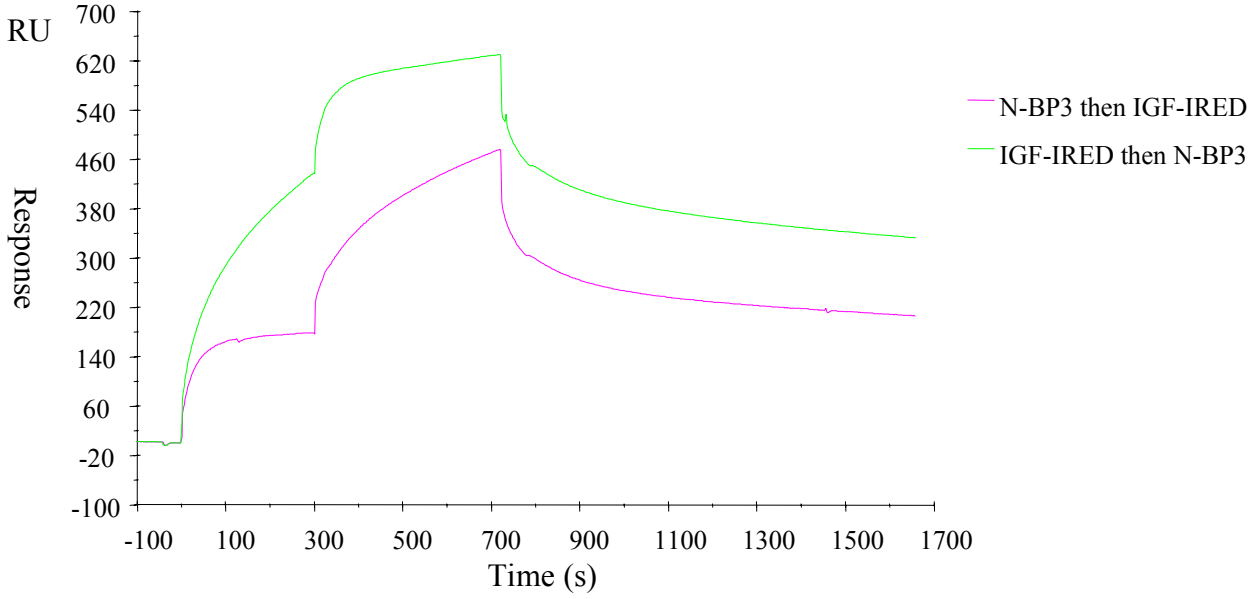

Figure 3.14 BIAcore analysis of additive binding of N-BP3 (20 μM) and IGF-IRED (0.2 μM) to immobilised IGF-I using coinject function.

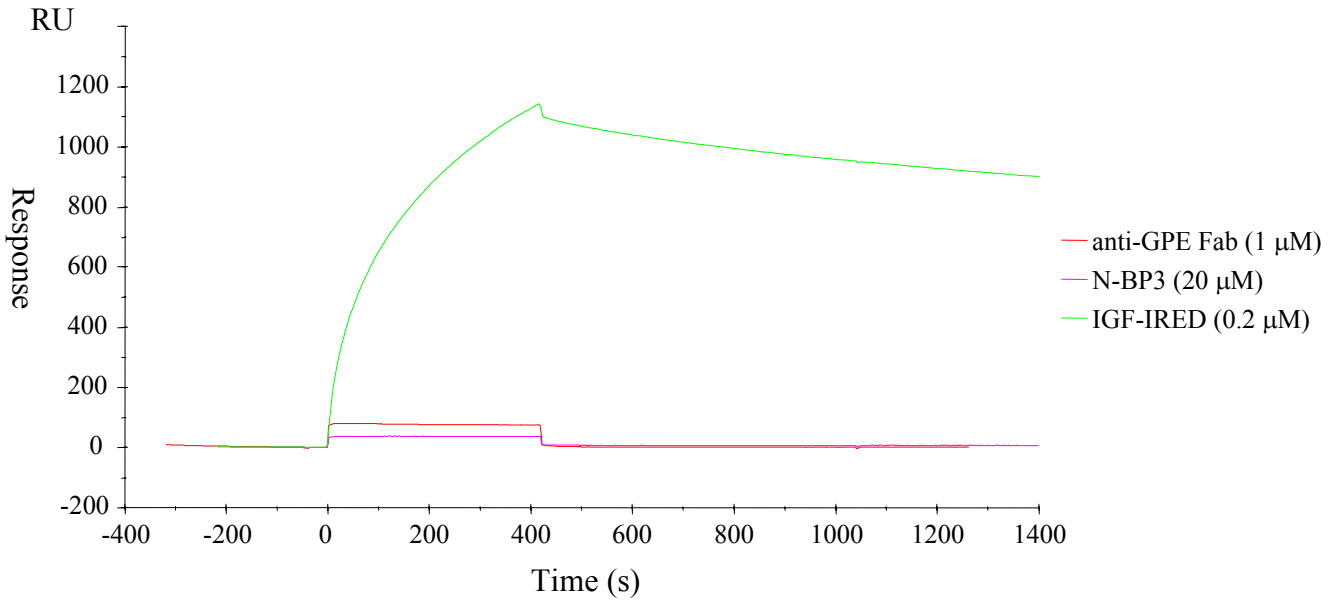

Figure 3.15 BIAcore analysis of interaction of anti-GPE Fab, N-BP3 and IGF-IRED to immobilised des(1-3)IGF-I.

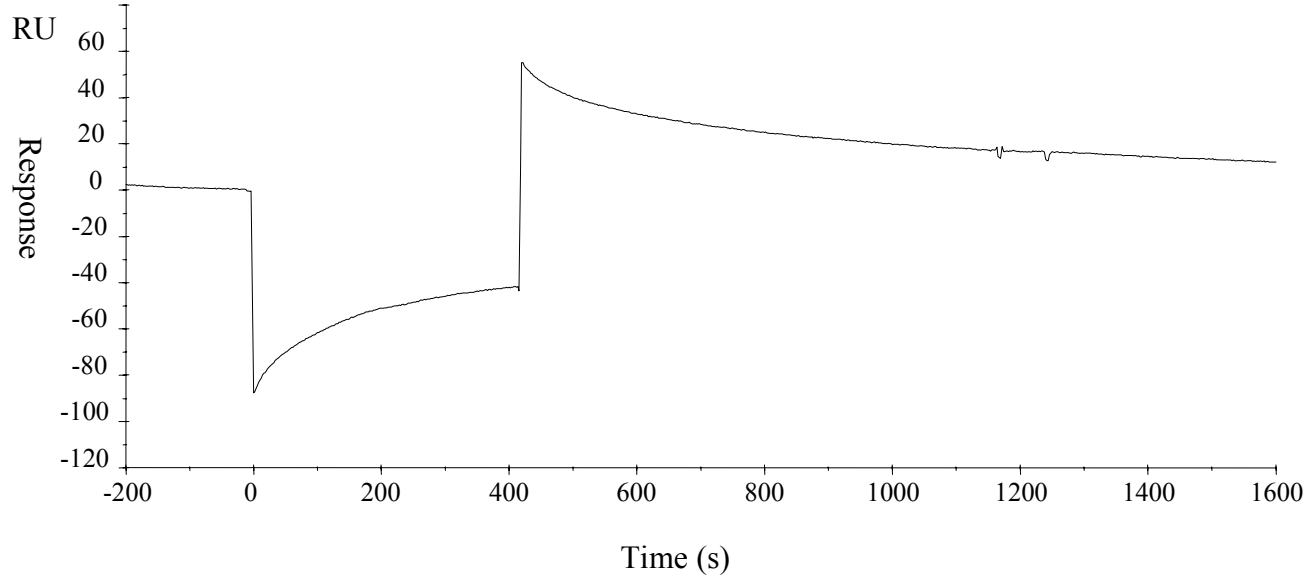

Figure 3.16 BIAcore analysis of binding of IGF-I (10μM) to immobilised IGF-IRED.

uncommon in this position, and could possibly aid in solubility. Insertions into a HCDR2 have been tolerated for improvement of another antibody (Lamminmaki *et al*., 1999). By constructing this mutant version of anti-GPE an alternative binding molecule (scFv) for affinity maturation may be developed.

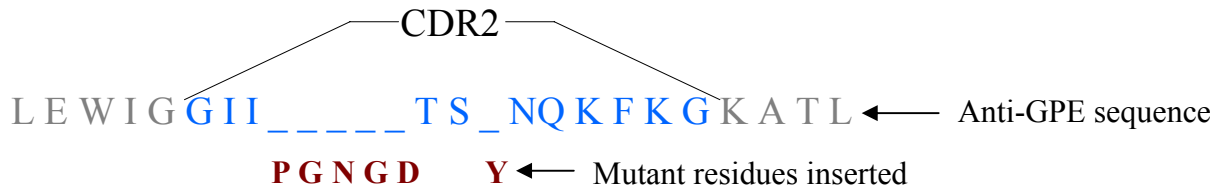

Figure 3.17 Design of anti-GPE H2M. Anti-GPE V_H CDR2 residues shown in blue. Engineered residues (insertions) in red.

3.6.2 Construction of the anti-GPE H2M gene

Two primers were designed (Table 2.1) to amplify from the anti-GPE scFv template DNA with overhangs coding for the amino acid residues to be added to the HCDR2. The primers 6248 (forward) and VLR1 were used to PCR amplify a fragment from the HCDR2 to the 3′ (V_L) end of the scFv gene. The primers 5325 and 6249 (reverse) were used to PCR amplify a fragment from the 5′ (V_H) end of the gene to HCDR2. This produced two fragments that had overlapping HCDR2 regions coding for the mutant residues to be inserted into the gene (Figure 3.18). These gel purified fragments were allowed to prime off their regions of homology for 12 cycles of SOE PCR (2.1.4.2) before flanking primers 5325 and VLR1 were introduced for a further 35 cycles for full length scFv amplification. This process is analogous to that of the construction of the anti-GPE scFv represented in Figure 3.2, however the sizes of the two fragments to be joined for anti-GPE H2M (Figure 3.18) are significantly different due to one encompassing only the front part of V_H, and the other covering the rest of the V_H, the linker, and the entire V_L.

3.6.3 Cloning and sequencing of the anti-GPE H2M scFv

The amplified gene was cloned in pGC as described for the wild type anti-GPE scFv gene (3.2.5). *Sfi*I/*Not*I digested scFv and vector were ligated together and this transformed into *E.coli* HB2151. Plasmid preparations of selected clones were sequenced. Sequencing revealed that the mutagenesis of the gene had been successful as shown in Figure 3.19.

3.7 Expression and purification of anti-GPE H2M scFv

3.7.1 Small and large scale expression

The anti-GPE wild type and anti-GPE H2M scFvs were expressed initially in small-scale culture (2.2.1). Periplasmic, cell lysate, and culture supernatant fractions (2.2.2) were analysed by SDS-PAGE (2.3.1) and Western blot (2.3.2). A FLAG-tagged protein was detected in all fractions migrating at ~ 33 kD and the intensity of the bands suggested that there was more protein being expressed by the mutant in all fractions (data not shown). It was decided to proceed to large scale expression (2.2.1) of both the mutant and wild type clones. IPTG induction again resulted in a deceleration in cell growth, which was in decline at two hours post-induction when cultures were harvested. However, the decline in cell growth was less marked in the mutant (data not shown). Periplasmic extracts and supernatant samples from these cultures were analysed by Western blot (Figure 3.20). Again, increased expression levels were observed for the mutant. The Western blot shows substantially stronger bands appearing in the mutant supernatant (lane 1) and periplasm (lane 2), suggesting stronger expression levels than the parental scFv.

3.7.2 Affinity purification and gel filtration chromatography of the anti-GPE H2M scFv

The anti-GPE H2M scFv was purified from the periplasm by anti-FLAG affinity chromatography (2.3.8) as described for anti-GPE wild type (3.3.2). Affinity purified material was analysed and further purified by gel filtration chromatography on a calibrated Superose 12 column (2.3.10). Monomer peaks at ~ 28 min and dimer peaks at ~ 26 min for both clones were collected (Figure 3.21). These were concentrated (2.3.9), reapplied to the same column, and peaks collected again. Purified samples were applied to SDS-PAGE and detected by Western blotting (Figure 3.20). It can be clearly seen that the amount of purified mutant scFv is larger than parental scFv (lane 4). Significantly, the proportion of soluble monomer in the affinity-purified material is much higher in the mutant than the wild type (lane 5), suggesting an improvement in solubility as a result of the HCDR2 modification. The overlaid Superose 12 profiles (Figure 3.21) show again that there are higher levels of expression for the mutant than the wild type anti-GPE. There is also a clear increase in the ratio of monomer over higher molecular weight forms and aggregate for the mutant suggesting that the mutations to the scFv may have improved folding efficiency and stabilised the structure. The purified monomer peaks were quantitated (2.3.11). The concentration of the mutant was 5.71 μM and the wild type was 2.22 μM, again demonstrating the improvement as both samples were in the same volume.

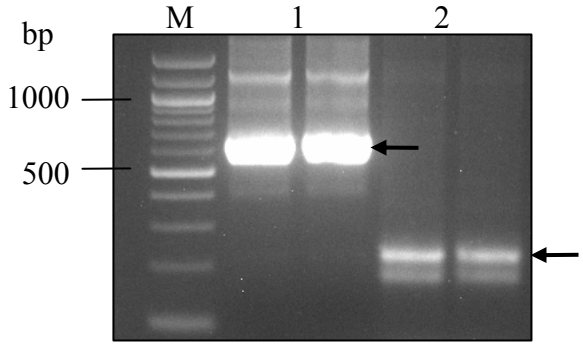

Figure 3.18 Agarose electrophoresis of PCR amplified fragments for the construction of anti-GPE H2M scFv. M. 100 bp DNA ladder. Lanes 1, HCDR2 to 3′ V_L fragment; 2, 5′ V_H to HCDR2 fragment.

K	S	L	E	W	I	G	G	I	I	**P**	**G**	**N**	**G**	**D**	T
AAG	AGC	CTT	GAG	TGG	ATT	GGA	GGT	ATT	ATT	**CCA**	**GGA**	**AAT**	**GGT**	**GAT**	ACT
S	**Y**	N	Q	K	F	K	G	K	A	T	L	T	V	D	K
TCC	**TAC**	AAC	CAG	AAA	TTC	AAG	GGC	AAG	GCC	ACA	TTG	ACT	GTA	GAC	AAG

Figure 3.19 DNA sequence and deduced amino acid sequence of the heavy chain CDR2 region of anti-GPE H2M. The CDR2 is underlined and introduced residues (and codons) are in bold.

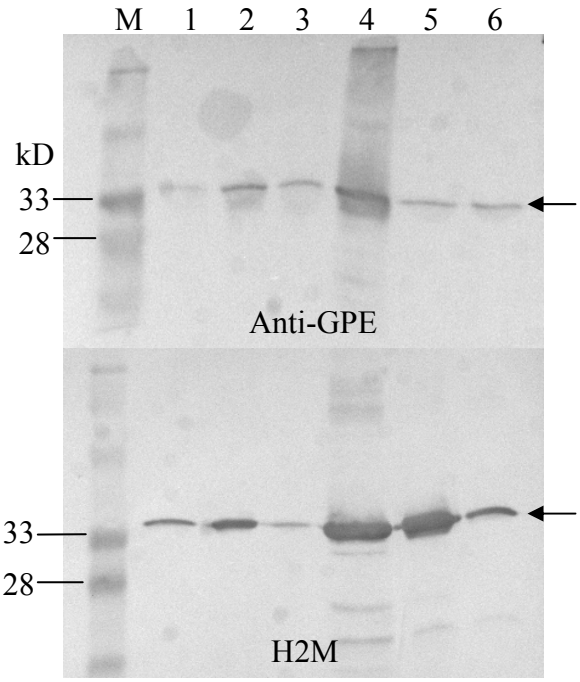

Figure 3.20 Western blot of comparative expression and purification of anti-GPE (wild type) and anti-GPE H2M scFvs showing enhanced expression levels for the mutant. M. Markers. Lane 1, culture supernatant; 2, periplasm (pre-FLAG column); 3, flow-through (post-FLAG column); 4, FLAG-purified; 5, Superose 12-purified monomer; 6, Superose 12 purified dimer.

3.8 Characterisation of the binding of the anti-GPE H2M scFv

As described previously for anti-GPE wild type (3.5.3), BIAcore was used to analyse the binding of the anti-GPE H2M scFv to immobilised IGF-I (2.3.13.2). A series of concentrations (250, 500, 1000, and 2000 nM) of the purified mutant monomer in HBS/P20 were tested for binding to IGF-I. The sensorgrams show that the mutagenesis has not prevented this protein from binding to IGF-I (Figure 3.22). BIAevaluation 3.0 software was used to analyse the data (2.3.13.3) with the results summarised in Table 3.2 (p. 77). An affinity of K_D = 2.06 μM was determined and the data was a reasonably good fit to the experimental model. Repeat experiments produced a similar result. The off rate is similar to the wild type scFv and the Fab, but the on rate of the mutant is nearly two-fold better than the scFv, accounting for the higher affinity value. However, this is still in excess of an order of magnitude slower than the Fab. These figures suggest that the insertions have not negated the ability of the scFv to bind to IGF-I but have made subtle changes to the nature of binding. Negligible binding to des(1-3)IGF-I (data not shown) shows that specificity is retained. These data suggest that the HCDR2 loop contributes, but is not critical in binding to the IGF-I.

3.9 Proposed mechanism of deletion in HCDR2

3.9.1 Alignment of anti-GPE with germline sequence

The anti-GPE sequence is unusual. A search of the Sequences of Proteins of Immunological Interest database (Kabat *et al*., 1991) revealed no antibody heavy chain variable domains with such a large deletion in the CDR2. In fact, the entire H2 region responsible for one of the four described canonical loop structures linking adjacent strands of β-sheet, according to Chothia and Lesk (1987), is missing. It has been reported that somatic insertions and deletions can sometimes be added to variable region genes in the CDR regions to add to the diversity of the gene repertoire (Ohlin and Borrebaeck, 1998; de Wildt *et al*., 1999). Thus the sequence of the anti-GPE V_H gene was analysed to determine how such a deletion might have come about.

The mouse V_H germline gene repertoire has not been completely described, but a listing of all reported mouse V_H gene segment sequences has been compiled on the web at http://www.ibt.unam.mx/vir/V_mice (Almagro *et al*., 1997) and the anti-GPE sequence was compared against sequences in this database. The sequence closest to the anti-GPE antibody is

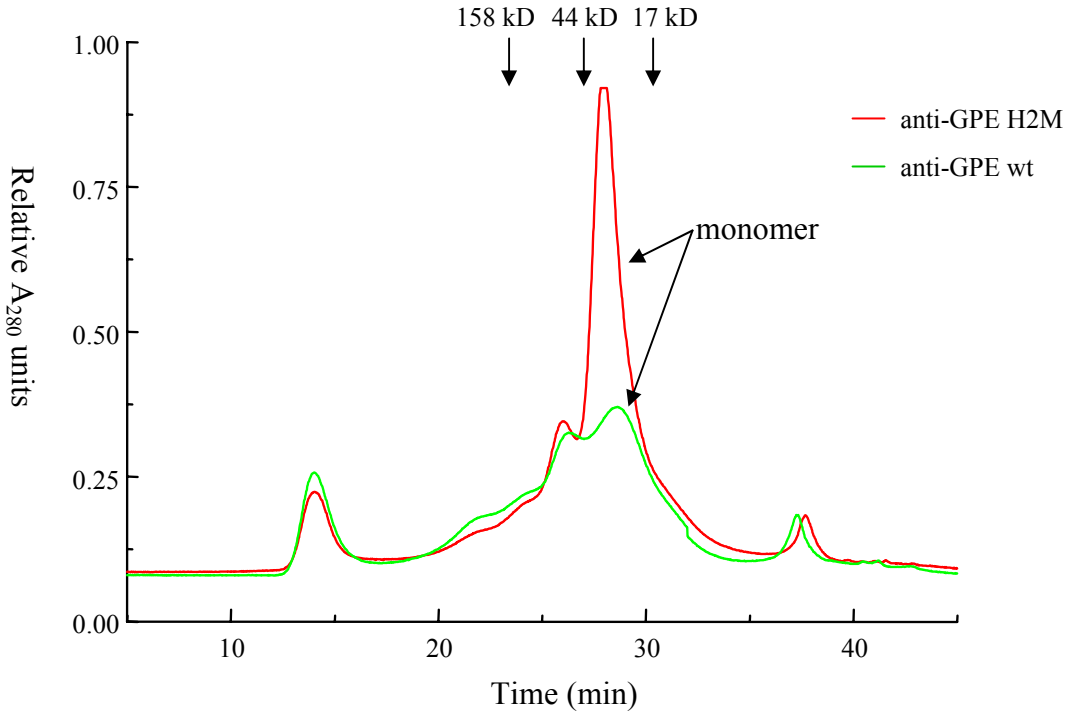

Figure 3.21 Gel filtration chromatography profiles on a Superose 12 column of FLAG-purified material from parallel expressions of anti-GPE (wild type) and anti-GPE H2M. Elution times of BioRad protein standards are indicated.

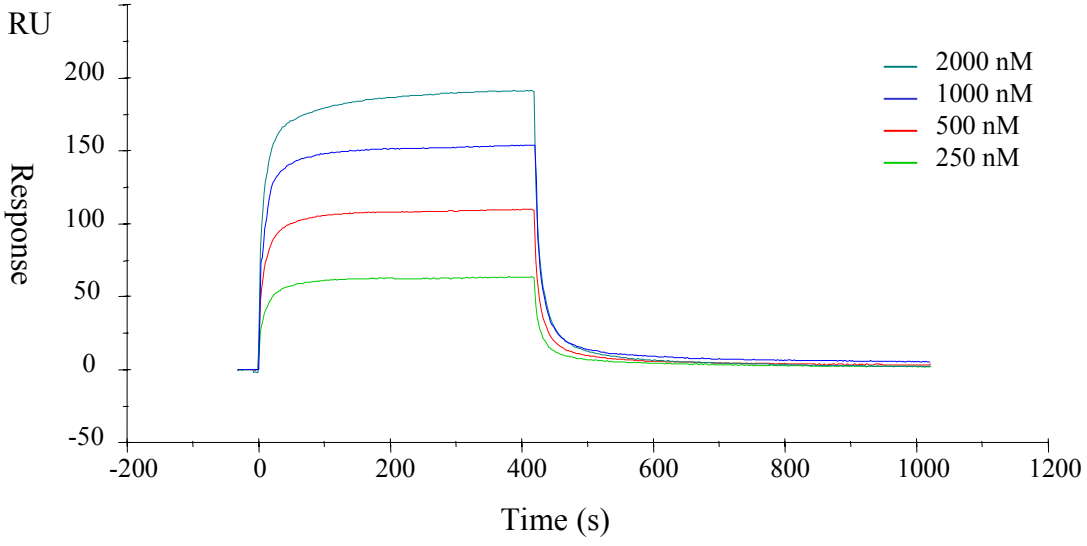

Figure 3.22 Overlaid sensorgrams of the binding of anti-GPE H2M scFv with IGF-I immobilised on the BIAcore at specified concentrations.

musbalb17V (locus), accession number L33954 (Rothenfluh 1994; unpublished). Assuming that this is the germ-line from which anti-GPE is derived, there appear to be 11 somatic nucleotide changes (4.35%) leading to 5 amino acid changes (5.95%) in the 84 residue fragment reported (not including deletions). The deduced amino acid and nucleotide alignments are shown in Figure 3.23.

3.9.2 Mechanism of deletion

The amino acid and nucleotide alignments in the CDR2 shown in Figure 3.23.C allow analysis of a possible mechanism for the deletion of residues. Homologous sequences can be seen within this CDR2 area that may be responsible for incorrect pairing during DNA extension. A proposed mechanism for these deletions similar to that described by de Wildt *et al.*, (1999) is shown in Figure 3.24. The codon AAT, coding for N at position 52, is repeated nine bps downstream (Figure 3.24.a.). If there is a breakage (Figure 3.24.b.), and this downstream codon misaligns with the corresponding codon on the antisense strand, a three-codon loop is formed on the sense strand (Figure 3.24.c.). If the misaligned codon then serves to prime for DNA extension, the corresponding residues – N, P, and N (52, 52A and 53) – are deleted (Figure 3.24.d.). The following two codons – GGT GGT – at positions 55 and 56, are also deleted from anti-GPE. It can easily be seen how position 55 could be deleted, due to the repeated codon, by the same mechanism, causing a one-codon loop (Figure 3.24.e. and f.). The deletion of the Y residue at position 59 (codon TAC) is assumed to occur due to a somatic point mutation of the first nucleotide of this codon from T to A. This would cause a consecutive AAC repeat, therefore allowing misalignment of the codon for N at position 60 (Figure 3.24.g. and h.). This proposed mechanism doesn't easily explain the deletion of the G residue at position 56. It is not shown in Figure 3.24 but from the mechanism described a double nucleotide change would have to occur at the corresponding codon, changing it from GGT to ACT, thus allowing for misalignment of the codon for T at position 60. The somatic mutation of the middle nucleotide of the codon at position 52 from A to T, changing the residue from N to I is shown Figure 3.24.i.). This must have occurred after the deletion involving this codon.

A.

i. EVQLQQSGPELVKPGASVKISCKTSGYTFTEYTMHWVKQSHGKSLEWIGGINPNNGGTSYNQKFKGKATLTVDKSSSTAYMELR
ii. EVQLQQSGPELVKPGASVTISCRTSGYTFTDYTMHWVKQSHGKSLEWIGGII-----TS-NQKFKGKATLTVDKSSNTAYMELR

B.

i. GAG GTC CAG CTG CAA CAG TCT GGA CCT GAG CTG GTG AAG CCT GGG GCT TCA GTG AAG ATA TCC TGC AAG ACT TCT GGA TAC ACA TTC
ii. GAG GTC CAG CTG CAA CAG TCT GGA CCT GAA CTG GTG AAG CCT GGG GCT TCA GTG ACG ATA TCC TGC AGG ACT TCA GGA TAC ACA TTC

i. ACT GAA TAC ACC ATG CAC TGG GTG AAG CAG AGC CAT GGA AAG AGC CTT GAG TGG ATT GGA GGT ATT AAT CCT AAC AAT GGT GGT ACT
ii. ACT GAT TAC ACC ATG CAC TGG GTG AAG CAG AGC CAT GGA AAG AGC CTT GAG TGG ATT GGA GGT ATT ATT --- --- --- --- --- ACC

i. AGC TAC AAC CAG AAG TTC AAG GGC AAG GCC ACA TTG ACT GTA GAC AAG TCC TCC AGC ACA GCC TAC ATG GAG CTC CGC A
ii. TCC --- AAC CAG AAA TTC AAG GGC AAG GCC ACA TTG ACT GTA GAC AAG TCC TCC AAC ACA GCC TAC ATG GAG CTC CGC A

C.

	48	49	50	51	52	52A	53	54	55	56	57	58	59	60	61	62	63	64
i.	I	G	G	I	N	P	N	N	G	G	T	S	Y	N	Q	K	F	K
	ATT	GGA	GGT	ATT	AAT	CCT	AAC	AAT	GGT	GGT	ACT	AGC	TAC	AAC	CAG	AAG	TTC	AAG
ii.	I	G	G	I	I	-	-	-	-	-	T	S	-	N	Q	K	F	K
	ATT	GGA	GGT	ATT	ATT	---	---	---	---	---	ACC	TCC	---	AAC	CAG	AAA	TTC	AAG

Figure 3.23 Sequence alignments of musbalb17V (i) and anti-GPE (ii) V gene segments. Mutations are underlined. Dashes represent deleted residues. A. Deduced amino acid sequence alignment. B. Nucleotide sequence alignment. C. Nucleotide and deduced amino acid sequence of area of deletions in HCDR2. Numbering according to Kabat (1991).

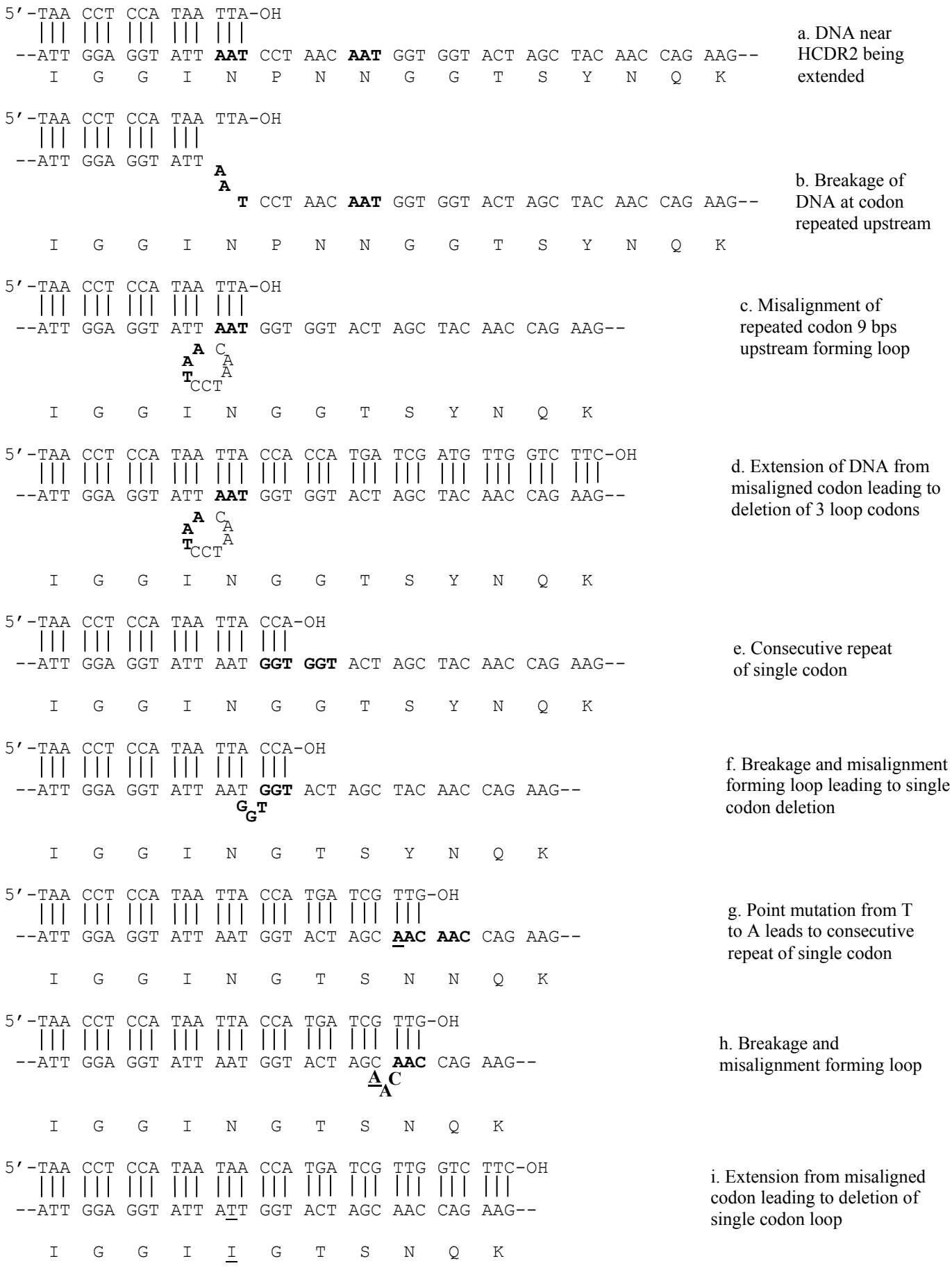

Figure 3.24 Proposed mechanism for deletion of residues in anti-GPE heavy chain CDR2. DNA strands and deduced amino acid residues are shown. Repeated sequences are in bold. Mutations are underlined.

3.10 Discussion

3.10.1 Cloning of anti-GPE scFv

The anti-GPE scFv was chosen as the model for molecular evolution studies as it was a novel antibody with a unique specificity and the binding of its IgG form was well characterised by ELISA. In comparing the deduced amino acid sequence of the phage-isolated anti-GPE(QUT) scFv with the N-terminal amino acid sequence of the monoclonal antibody expressed by the hybridoma 5C6/B3, it was apparent that the V_H domain gene fragment was consistent with the cloned gene being able to code for the V_H domain of the antibody. However, there were sufficient differences between the deduced amino acid sequence of the V_L gene fragment and the N-terminal amino acid sequence of the V_L to suggest that this V_L gene fragment did not encode the monoclonal antibody V_L domain. Despite the fact that the V_H is the generally more important domain in conferring the binding affinity and specificity of an antibody (Collet *et al*., 1992), it was decided to independently clone the V genes, which resulted in a better match of the sequences. As the initial scFv was not generated in our laboratory, the possible origin of the non-matching sequence was not investigated further, although when using PCR to isolate V genes, amplification of contaminant V genes is not uncommon, presumably due to the degeneracy of the primers used and the sensitivity of this enzymatic reaction.

Sequencing of the constructed scFv showed that cloning of the required V-domains had been successful. Furthermore, characterisation of this clone by expression of the scFv and binding to antigen would be further confirmation of correct cloning. The unusually large deletion in HCDR2 was of some interest as to the implications this may have on the expression and binding of the scFv. Selection of such a short HCDR2 may be due to the fact that the antibody was raised against a small peptide (10-mer). Some antibodies can display a cavity-like structure defined by the HCDR1 and 2 sequences for binding of its antigen (Babino *et al*., 1997). Perhaps the shortened HCDR2 of the anti-GPE forms such a binding pocket. It is generally considered that an antigen needs to be larger than an epitope to elicit an antibody response (Craven, 1999) and so perhaps an unusual antibody selection has occurred in response to challenge from this small peptide. The residues 52 to 56 form the hairpin loop referred to as the H2 region that is responsible for one of four described canonical structures for the HCDR2 in human V_H segments (Chothia and Lesk, 1987). As five residues from 52A to 56 are missing (Figure 3.23.C.ii), the turn between the two strands would be different compared to that found in other antibodies and might be expected to have deleterious implications for folding of the protein.

3.10.2 Expression and purification of anti-GPE scFv

Expression levels of scFv in *E. coli* vary between micrograms per litre to milligrams per litre in culture and may result from any one of several factors known to affect expression levels in *E. coli*. For example, hydrophobic patches at the variable/constant domain interface may be exposed, making the protein susceptible to aggregation (Nieba *et al*., 1997). Differences in the translation machinery and folding pathways for a eukaryotic protein in a bacterial system can cause poor expression (Duenas *et al*., 1995). Also, primer encoded mutations can disrupt crucial residues, for example residue six of V_H has been shown to be critical for expression levels in some scFvs (Kipriyanov *et al*., 1997; de Haard *et al*., 1998). It has been shown that the most important factor influencing the bacterial expression of antibody fragments is the primary sequence of these variable domains (Knappik and Pluckthun, 1995).

The poor growth characteristics of *E. coli* expressing the anti-GPE scFv was an early indication of the toxicity of the molecule. The fact that the transformed cells could not be grown after induction for extended periods of time before cell lysis occurred meant that expression was restricted to short periods and high levels of periplasmic accumulation could not be achieved. A number of different *E. coli* strains were tested for scFv expression (3.3.1) but HB2151 was the best strain. Even though substantial amounts of scFv were detected in the culture supernatant it was decided that harvesting early in the expression (2 h post-induction) from periplasms was the best approach. This was because processing the large volumes of the viscous supernatant would be laborious, would expose the scFv to potential proteolytic degradation, and would be unnecessary as adequate amounts for characterisation could be gained from the periplasm.

It has been noted that a large deletion of four residues in the HCDR1 has been tolerated in a functional antibody (de Wildt *et al*., 1999) leaving a short three residue H1 perhaps just long enough to form a β-turn. However, the H2 of anti-GPE is missing the relevant residues. Other residues to those normally present would have to be involved for the formation of a β-turn for proper folding of the molecule. It would be expected that this deletion in the loop residues of the CDR2 would be extremely detrimental to proper folding of the protein and is the most likely explanation for the poor solubility of this molecule. This poor solubility was evidenced in the precipitation of purified protein upon dialysis, concentration, freeze/thawing, and the gel filtration profile displaying aggregate and higher molecular weight peaks (Figure 3.6). Soluble monomer

made up only a small proportion (generally < 3%) of the total original fraction (Figure 3.5). Techniques for refolding recombinant proteins produced in *E. coli* can be successful (Lilie *et al*., 1998). However, it was assumed that refolding of this scFv may be difficult due to the unusual sequence. Misfolded scFv aggregating within the cell is a possible reason for the toxicity to *E. coli*, with hydrophobic surfaces of the partially folded species, or folded intermediates, promoting self-association (Georgiou and Valax, 1996), and the resulting aggregation causing a host stress response accompanied by cell lysis (Suominen *et al*., 1987). Some amino acid mutations in antibody fragments have been shown to increase their solubility and expression (Knappik and Pluckthun, 1995; Kipriyanov *et al*., 1997; Neiba *et al*., 1997; Chowdhury *et al*., 1998; Coia *et al*., 1997). It would then follow that there is some scope for engineering approaches to improve the biophysical characteristics of the anti-GPE scFv and this would be highly desirable to obtain a more robust scaffold.

3.10.3 Binding of anti-GPE

Monoclonal antibody affinities are generally towards the nanomolar range which is reflected in the calculated affinity of the parent 5C6/B3 Fab of 0.102 μM. It has been shown here that the scFv version of this antibody has an affinity of 3.68 μM. ScFvs are generally expected to reproduce the affinity of the parent antibody fairly closely, so the approximately 36-fold difference reported here seems to be somewhat excessive, although it is not unusual for there to be some drop in affinity displayed by the scFv version. The initial scFv cloning by Bird *et al*., (1988) reported a 4-fold reduction in affinity compared with the parent antibody and Huston *et al*., (1998) reported a 6-fold reduction. An anti-estradiol scFv has been reported with a 10-fold weaker affinity than its parent (Coulon *et al*., 2002). Huston *et al*., (1988) suggested that the slight reduction in affinity might be due to the elimination of charge at the V_L α-amino group that may be close enough to the binding site to influence affinity. Further, it was suggested that the initial two residues of the V_H can influence affinity of some antibodies and these residues may be affected by the linker. The HCDR2 deletion discussed above, may cause greater instability to the scFv version than the Fab version of the antibody which has the stabilising effect of the interaction of the constant regions, thereby altering the tightness of binding, or the particular linker used may not be optimal in allowing the V domains to associate naturally. The BIAcore data collected for the anti-GPE scFv (Table 3.2) may not give a true indication of its real affinity as the concentration of the peak purified protein may not be indicative of the active scFv concentration. Due to possible instability of the protein, there may be a mix of active and incorrectly folded non-active forms of the scFv present within the

collected peak, which may have an effect on the kinetic data collected on the BIAcore biosensor (Zeder-Lutz *et al*., 1999), and may therefore be part of the reason for the lower than expected affinity. Due to the uncertainties in the calculated affinity figures for the scFv and Fab, the real discrepancy may not be as significant as indicated here. Interestingly the calculated off rates are similar. Importantly, the BIAcore can give an indication of apparent affinities of samples and these values can be used to compare the binding of one species to another with respect to interaction with a particular antigen, which is adequate for the purposes of this study. There appears to be much scope for improvement of this low affinity anti-GPE scFv, as well as potential to engineer improvements in stability, expression and solubility, by evolutionary approaches.

The binding data for both N-BP3 and IGF-IRED are significant as they are both well characterised IGF-I binders and therefore gives confidence that the immobilised IGF-I is active and that the anti-GPE binding is real. The IGF-IRED binding to des(1-3)IGF-I gives further confidence in the immobilisation of this species in an active form which helps to confirm that anti-GPE specificity does lie towards the GPE domain of IGF-I. The contradiction of additive binding of N-BP3 and Fab to IGF-I described in 3.5.4 may be explained by the fact that the IGF-I could be immobilised in up to three different orientations due to its three lysine residues. One such orientation may be suitable for the N-BP3 to bind to the IGF-I N-terminal region, but the Fab may not be able to access the N-terminus in this particular IGF-I orientation, perhaps due to steric constraints, while finding another orientation of IGF-I on the chip in which it can access its N-terminal region. This could explain the observed additive binding effect despite recognition of similar epitopes as indicated by the lack of binding of either species to des(1-3)IGF-I. The lack of N-BP3 binding to des(1-3)IGF-I confirms that the N-terminal region of IGF-I is important for binding of this species (Ross *et al*., 1989), explaining the enhanced *in vivo* potency of des(1-3)IGF-I as its activity is not attenuated by complexed binding protein (Bagley *et al*., 1989).

3.10.4 Cloning of anti-GPE H2M

The design of the anti-GPE H2M gene was based on ‘filling in’ the deleted residues so that the CDR2 would be of the same length as most other antibodies of this class. It was thought that this may confirm that the deletion is at least in part responsible for the poor solubility and expression of the anti-GPE scFv and should assist in proper folding of the molecule. Residues from HCDR2 of NC10 were chosen as this is an scFv well characterised in our laboratory, contains most of the residues of this subclass, and the Asp residue may aid solubility. The question would be whether such an addition would change the binding characteristics of the purified scFv. All six CDRs are

not always involved in the antibody-binding site (Malby *et al*., 1994), although the insertion in the HCDR2 may cause enough subtle change in the orientation of the other CDRs in relation to the epitope, that affinity and or specificity may be affected.

3.10.5 Expression and purification of anti-GPE H2M

The mutated version of the anti-GPE scFv described here may be a useful alternative target for molecular evolution due to its improved solubility and expression properties (Figures 3.20 & 3.21). The increased expression levels out of *E. coli* are beneficial, making purification of adequate amounts for characterisation of binding easier. Likewise, the increased levels of soluble monomeric material produced also aids purification. The expression and solubility problems encountered with the anti-GPE wild type scFv may indeed be partly due to the shortened HCDR2. The restoration of 'missing' residues described here appears to have somewhat improved the stability of this molecule. The shortened nature of the wild type HCDR2 may hinder proper folding of the molecule leading to large amounts of the expressed molecule existing as misfolded aggregates. The improved physiology of *E. coli* during expression of anti-GPE H2M shows that there is a reduced toxicity to the cells, probably due to the higher ratio of molecules folding correctly.

3.10.6 Binding of the anti-GPE H2M scFv

The fact that the anti-GPE H2M scFv still binds to IGF-I with a similar low affinity to the wild type presents it as an alternative model for affinity maturation, especially as it appears to be a more robust scaffold. The nature of the binding of the mutant as tested by BIAcore analysis is different to the wild type scFv in that the 'on rate' is faster, which suggests that even though the HCDR2 is not absolutely essential for binding to IGF-I, the shortened wild type loop did have some effect on the way the antibody bound. Interestingly, the off rate of the molecule is little changed by the insertions. Randomisation of the newly inserted loop residues, followed by selection, may yield a CDR2 sequence more beneficial for tighter IGF-I binding. The slight improvement in affinity calculated here may only be an apparent effect due to improved levels of properly folded functional protein in the purified sample for anti-GPE H2M compared to that of the wild type scFv, and thus may not be significant. This more robust scaffold may permit mutations into other CDRs of the molecule for achieving affinity enhancements.

3.10.7 Mechanism of deletion in HCDR2

It is likely that the large deletion in the HCDR2 of anti-GPE has occurred as part of the somatic mutation process. In humans, V genes containing insertions or deletions contain large numbers of

somatic point mutations and the processes appear to be closely associated (Klein *et al*., 1998; Wilson *et al*., 1998; de Wildt *et al*., 1999). In vertebrate IgV genes, nucleotide changes that result in amino acid replacements are concentrated in CDRs (Rothenfluh *et al*., 1995), which is observed in the anti-GPE sequence (Figure 3.23.B). In functional, properly folded human antibody genes, almost all insertions and deletions are found in or near CDRs, suggesting they have been subjected to antigen selection (de Wildt *et al*., 1999). Murine V genes also appear to have hotspots in CDR regions, with a bias towards non-silent mutation (Rothenfluh and Steele, 1993; Rothenfluh *et al*., 1995) and there is evidence this hypermutation process is antigen-driven (Steele *et al*., 1997). Human V genes have more nucleotide repeats in the loop regions than the frameworks, and insertions and deletions occur at recognised 'hot spots' for somatic point mutation, and so both processes are probably created by the same enzymatic machinery (de Wildt *et al*., 1999; Lantto and Ohlin, 2002). Such nucleotide repeats are also observed in the CDR2 region of the musbalb17V germline segment (Figure 3.23.B and C). The deletion mechanism presented here, involving chain breakage misalignment and extension (Figure 3.24), is one possible model for the genesis of the anti-GPE scFv sequence. It is concluded that the unusual anti-GPE sequence arose as part of the somatic mutation process subjected to antigen selection. The large deletion has rendered the scFv version of the antibody with poor solubility properties but it does have a specific affinity for the GPE domain of IGF-I. Molecular evolution may be used to improve the properties of the anti-GPE wild type and anti-GPE H2M scFvs and is part of the focus of the next two chapters.

CHAPTER 4
RIBOSOME DISPLAY OF ANTI-GPE SCFV AND ITS POINT MUTATED LIBRARY

4.1 Introduction

4.1.1 General

The objectives of this chapter were: (i) to optimise ribosome display to enable its use for specifically selecting the anti-GPEwt scFv and anti-GPE H2M against IGF-I; (ii) to create a library of point mutants of anti-GPE scFv using error-prone PCR; and (iii) to use ribosome display to select for affinity matured scFvs from this mutant library against IGF-I.

The ribosome display system used is based on the method of He and Taussig (1997), utilising a rabbit reticulocyte coupled transcription/translation system as the source of ribosomes. Phage display (Hoogenboom and Winter, 1992) has been the initial method of choice in antibody engineering for selection of improved molecules from libraries. Other methods such as yeast or bacterial surface display have recently begun to gain some popularity (Wittrup, 2001), and the development of ribosome display as a robust selection tool is in its early stages. It was decided to employ ribosome display, since its *in vitro* nature could potentially allow greater numbers of variants to be displayed, as well as being potentially a less laborious technique as discussed in 1.6.1. Little has been reported on the use of the reticulocyte lysate system for affinity maturation. Random point mutation for the improvement of antibody fragments has been successfully applied in antibody engineering, predominantly by error-prone PCR (1.5.1), although mutator cells have also been employed (1.5.2). In keeping with the *in vitro* nature of ribosome display, error-prone PCR was used.

This chapter describes the experimental approaches taken to develop a ribosome display system for the specific selection of the anti-GPE scFv and its HCDR2 mutant, and of the improved point mutated variants. Optimisation of the system for specific selection of the anti-GPE wt and H2M scFvs was first demonstrated. Then a library (EPGPE) was generated by error-prone PCR of anti-GPE. Multiple cycles of selection and display were performed on this library. Several fourth round selected clones from display of this library were expressed and purified for characterisation of binding.

4.1.2 Antecedent work

The constant heavy chain domain three (C_H3) used as a spacer for ribosome display was previously cloned by Dr. J. L. Atwell at CSIRO, Parkville (personal communication). It is a human IgM domain and was initially cloned in the plasmid pGC as a chimaera with a mouse scFv 13C11. The constant light chain (C_L) domain used was previously cloned by Coia *et al*., (1996). It was also cloned in pGC, as part of an entire light chain (V_L and C_L) linked to the V_H domain from a hybridoma producing the anti-glycophorin antibody 1C3. 4T10, a PCR assembled camelid V_H domain (Gharoudi *et al*., 1997) with a C_H3 spacer and specificity to lysozyme, was provided by Dr. S. Nuttall (CSIRO, Parkville) to be used as a lysozyme-binding control in ribosome display selection.

4.2 Construction of ribosome display cassettes

4.2.1 Design of cassettes

Ribosome display cassettes were designed with a 5′ T7 promoter sequence for transcription by the DNA dependent polymerase T7 RNA polymerase and included the ribosome-binding site (RBS). Following this were the gene encoding the protein to be displayed, and a spacer sequence which had the function of distancing the nascent protein from the ribosome complex to improve the potential for proper folding of the translated scFv. Two different spacers were used: a C_H3 domain and a C_L domain (4.1.2). The design also omitted a translation stop codon, which causes the ribosome to stall at the 3′ end of the transcribed mRNA without dissociation, leaving the translated protein attached to the ribosome (He and Taussig, 1997; Irving *et al*., 2001). The resulting complex (translated protein, ribosome, mRNA) links genotype and phenotype, and allows selection of functional scFvs with recovery of their respective encoding mRNAs. The process for the construction of these cassettes is shown schematically in Figure 4.1.

4.2.2 Construction of C_H3 cassettes

The 13C11 scFv was removed from pGC-13C11-CH3 provided by Dr. J. L. Atwell (CSIRO, Parkville), by *Sfi*I/*Not*I restriction digestion (2.1.7) and the cut pGC-C_H3 vector was gel purified (2.1.6.1). Likewise digested coding sequences for anti-GPE scFv, anti-GPE H2M scFv, or mutant library were ligated (2.1.9) into this vector. The *Not*I site codes for three Alanine residues between the scFv and the C_H3. The C_H3 can be removed and inserted as a *Not*I/*Sac*II fragment. The 3′ *Sac*II restriction site codes for two Alanine residues between the C_H3 domain and the FLAG tag. A primer (5998; Table 2.1) that recognises the 5′ end of the anti-GPE and that codes for the T7

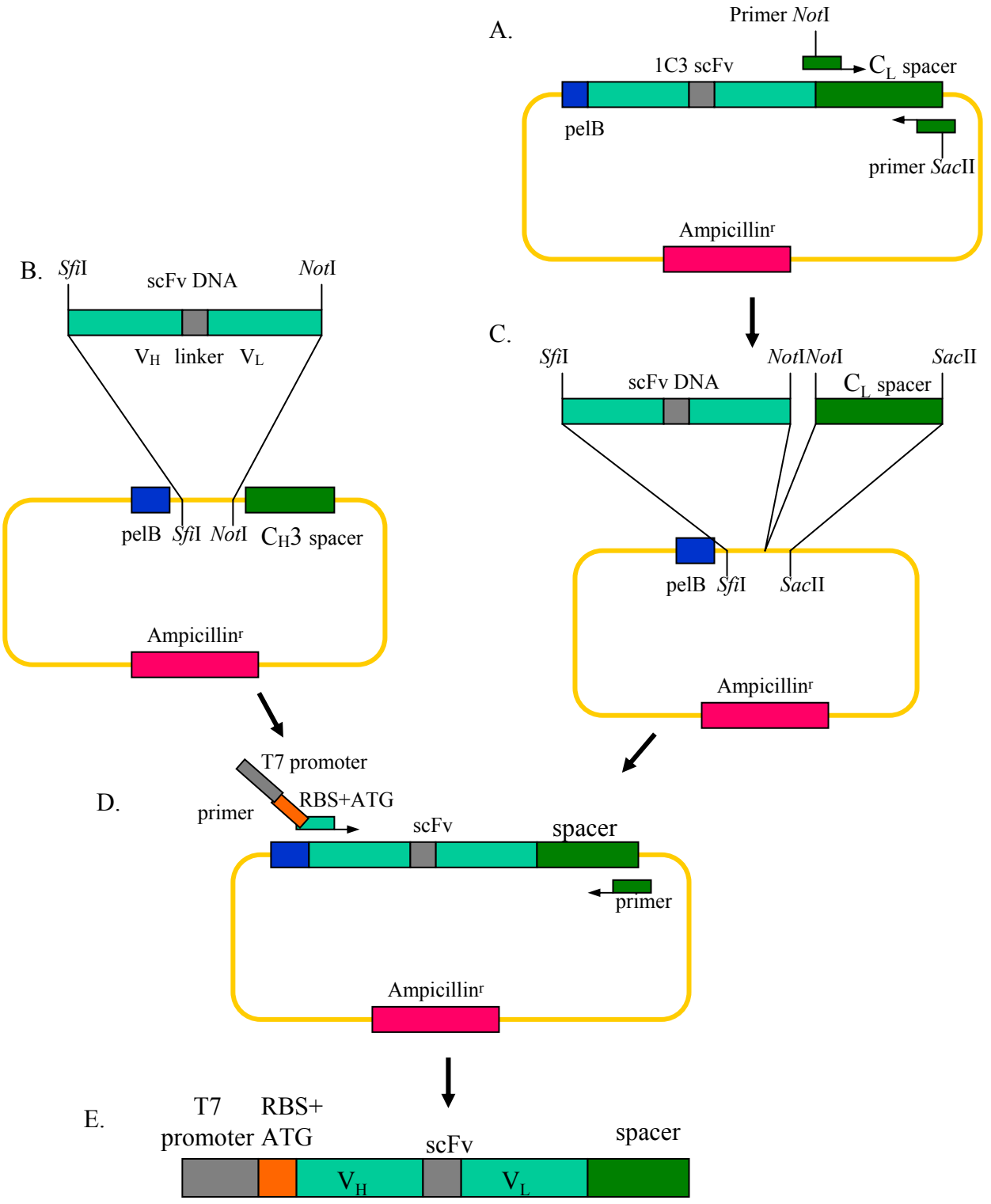

Figure 4.1 Construction of ribosome display cassettes. A. PCR amplification of C_L from pGC-1C3-C_L. B. Ligation of scFv into pGC-C_H3. C. Ligation of scFv and C_L into pGC. D. PCR amplification of template using T7+RBS primer and primer to C_H3 or C_L spacer. E. Amplified ribosome display cassette.

promoter, RBS and ATG codon was designed. This was used with 5385, (3/ primer to C_H3 gene Table 2.1) in PCR (2.1.4) to amplify the ribosome display cassette from vector pGC-GPE-C_H3.

4.2.3 Construction of C_L cassettes

Primers (Table 2.1) to the C_L domain were designed to amplify (2.1.4) this fragment from pGC-1C3-C_L (Coia *et al*., 1996), as this vector did not have a convenient restriction site for insertion of an scFv fragment in front of the C_L. The 5/ primer (6321) coded for a *Not*I restriction site and the 3/ primer (6322) coded for a *Sac*II restriction site. The gel purified (2.1.6.1) PCR amplified C_L fragment was restriction digested with *Sac*II and *Not*I (2.1.7) and this was purified (2.1.6.2). *Sfi*I/*Not*I digested pGC-C_H3 was digested with *Sac*II to remove the C_H3 coding sequence, and the cut plasmid was verified and purified by electrophoresis (2.1.6.1). These restricted and purified pGC, C_L and anti-GPE scFv fragments were ligated (2.1.9) in the one reaction. Purified ligation (2.1.6.2) was electroporated into *E. coli* HB2151 (2.1.11) and transformants screened by colony PCR (2.1.12) for anti-GPE-C_L insert using primers 5325 and 6322 (Table 2.1). Plasmid preparations (2.1.13) on three positive clones were sequenced (2.1.14) to confirm correct cloning (Figure 4.2). As the codon for Alanine is the first residue of the C_L domain, there are only two Alanines between the inserted scFv and the C_L at the *Not*I site, compared with three for the C_H3 version. In the same way as for the C_H3 vector, other scFvs or libraries could now be inserted into this vector as a *Sfi*I/*Not*I fragment. PCR (2.1.4) with primers 5998 and 6322 (C_L) was used to amplify the ribosome display cassette. This process is shown schematically in Figure 4.1.

4.3 Ribosome display and selection of anti-GPE wild type and anti-GPE H2M scFvs

The general method used for ribosome display and selection of antibody fragments is described in 2.4 and is broadly based on that developed by He and Taussig, (1997). Essentially, the ribosome display cassette coding for 5/ T7 promoter, RBS, antibody fragment and spacer was used as template in the T7 coupled transcription/translation reaction (2.4.2). DNA template was then removed from the reaction by DNaseI digestion and the complexes selected against immobilised antigen (2.4.3). Unbound complexes were removed with washing and bound complexes eluted with either EDTA or peptide (2.4.4). Selection of eluted complexes was monitored by RT-PCR (2.1.4.3) using reverse primer VLR1, or a number of different primers that anneal to various parts of the C_H3 and C_L genes (Table 2.1). These primers, and the positions they anneal on the genes are shown schematically in Figure 4.3. Due to the DNaseI removal of DNA any RT-PCR bands would be amplified exclusively from mRNA. The immediate goals in utilizing this system were then to

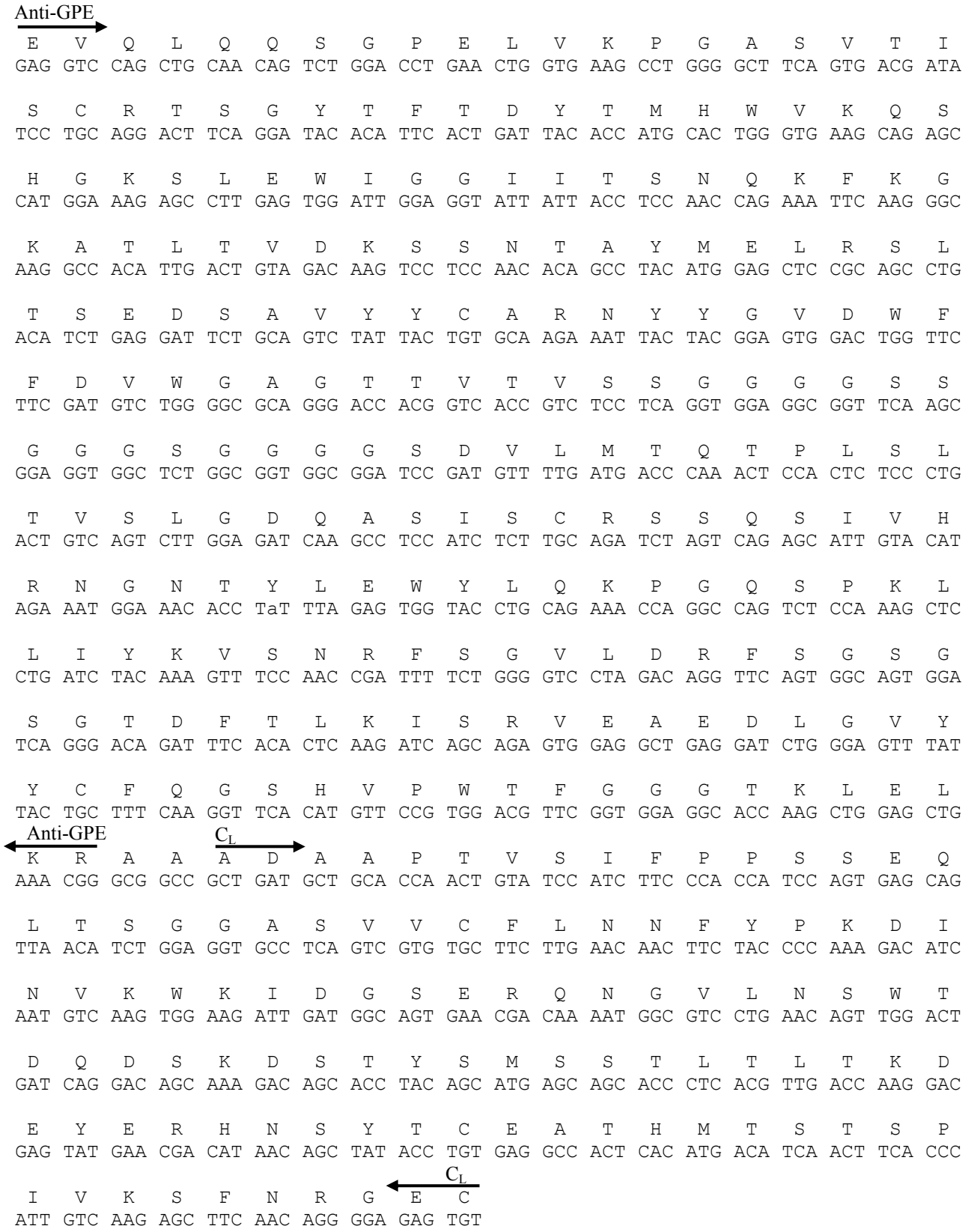

Figure 4.2 DNA sequence and deduced amino acid sequence of anti-GPE scFv fusion with 1C3 C_L domain for ribosome display.

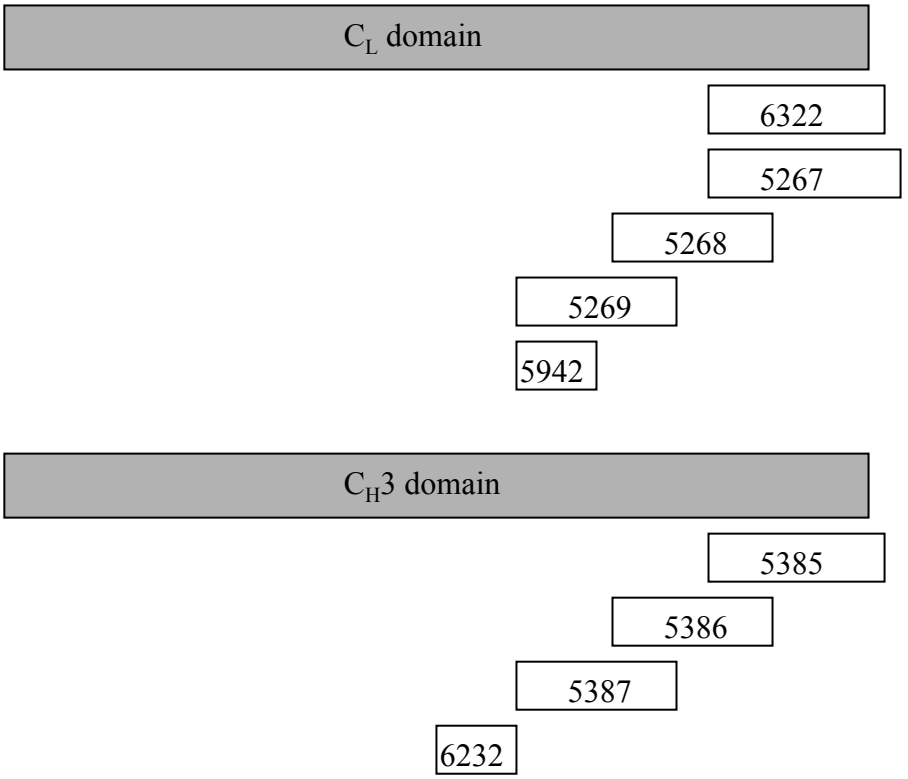

Figure 4.3 Schematic representation of the relative annealing positions of primers to the C_H3 and C_L domains used in ribosome display.

develop a method to specifically select anti-GPE by its ability to bind IGF-I in preference to other antigens (lysozyme, in this case) as an index of correct folding of the scFv on the ribosome complex, and to use these conditions to select for affinity-matured scFvs generated by random mutation.

4.3.1 Effect of selection surface and oxidised glutathione (GSSG)

With all ribosome display experiments the initial coupled transcription and translation reactions were carried out as described (2.4.2). The first selections of antibody fragments were performed against IGF-I and lysozyme that had been coupled to tosylactivated magnetic beads or adsorbed to microtiter wells (2.4.3). The blocking reagent here was 5% skim milk, no blocking reagent was included in the selection, and no Tween-20 was included in the wash buffers (2.4.3). Complexes were eluted with EDTA (2.4.4). The latter selection surface (microtiter wells) indicated more promising and easier selection, as no RT-PCR bands could be achieved with selection on beads (data not shown), and so was therefore used for subsequent display experiments. Under the same experimental conditions, the addition of GSSG (Coia *et al*., 2001) in the coupled transcription/translation reactions (2.4.2) prevented the apparent selection of functional scFvs, as tested by RT-PCR, with no DNA bands generated, despite the low stringency of binding by omission of Tween-20 from the wash buffers (Figure 4.4.A). The target antibody fragments included 4T10-C_H3, anti-GPE H2M-C_H3, anti-GPE H2M-C_L, anti-GPEwt-C_H3, and anti-GPEwt-C_L; primers for the anti-GPE constructs were the standard amplification primers 5325 and VLR1 (Table 2.1) and, for 4T10, the 5/ primer 6188 and the C_H3 primer 5387 (Table 2.1). The omission of GSSG from the coupled reactions on the same templates, and change of washing temperature from ambient to 4^oC resulted in significant but apparently non-specific capture of products (Figure 4.4.B). PCR (2.1.4) without prior treatment with reverse transcriptase of the eluates confirmed the absence of contaminating residual DNA, which may have escaped the DNaseI digestion (Figure 4.4.C). The omission of GSSG was incorporated into subsequent experiments designed to reduce the non-specific binding observed here.

4.3.2 Increasing stringency of washes with Tween 20

The first measure taken to focus on reducing the non-specific recovery seen in the display shown in Figure 4.4B was increasing stringency of selection. This was achieved by returning the wash step to ambient temperature with the inclusion of Tween-20 in the wash buffer (2.4.3). The first selections were done with Tween 20 at 0.1% in the wash buffer on the display of 4T10-C_H3, anti-GPEwt-C_L, and anti-GPE H2M-C_L. Each reaction was selected against both lysozyme and IGF-I. RT-PCR

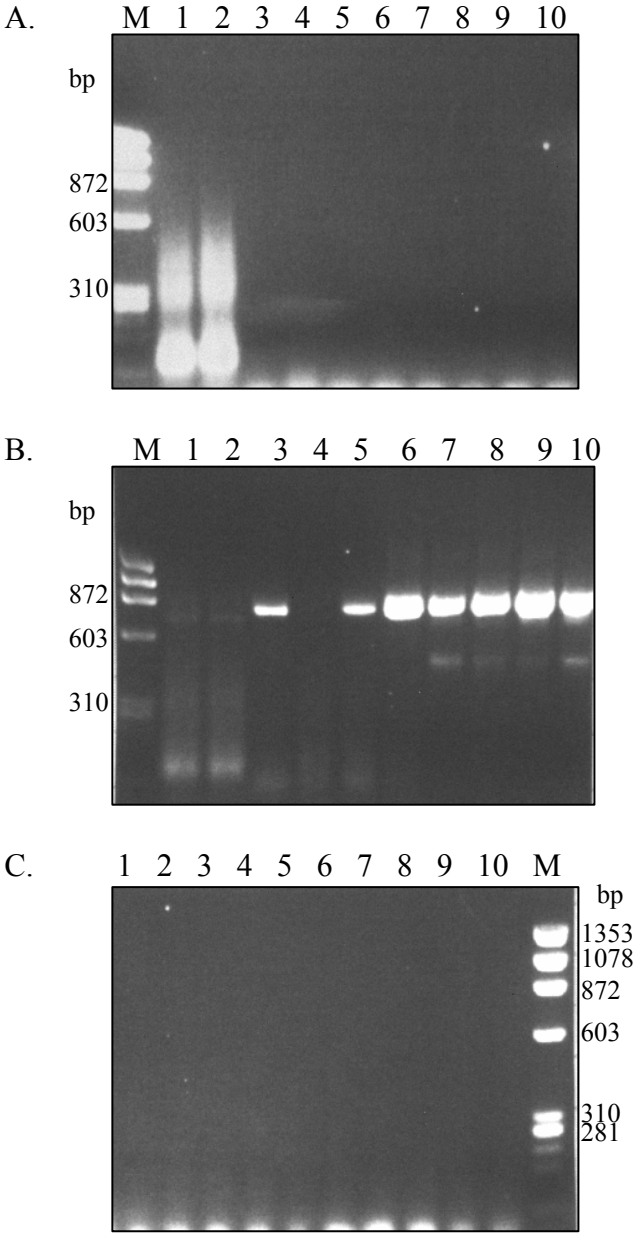

Figure 4.4 RT-PCR from ribosome display and selection in the presence (A) and absence (B) of oxidised glutathione, and PCR (C) showing the effectiveness of the DNaseI digestion in removing DNA post-transcription/translation. M, ϕX174 DNA markers. Lane 1, 4T10-C_H3 selected against lysozyme and 2, against IGF-I; 3, anti-GPE H2M-C_H3 selected against lysozyme and 4, against IGF-I; 5, anti-GPE H2M-C_L selected against lysozyme and 6, against IGF-I; 7, anti-GPEwt-C_H3 selected against lysozyme and 8, against IGF-I; 9, anti-GPEwt-C_L selected against lysozyme and 10, against IGF-I.

(2.1.4.3) using 5325 as forward primer and VLR1 as the reverse primer showed that this served overall to reduce the intensity of the bands seen previously, but had no impact on specificity of selection (Figure 4.5.A). Recovery for anti-GPEwt was particularly weak compared to anti-GPE H2M. A subsequent display of the same constructs, plus the C_H3 versions of the anti-GPE constructs, with Tween-20 raised to 0.2% in the washes was tried. RT-PCR on the anti-GPE constructs was performed using the T7 forward primer 5998 and the reverse primer VLR1 for the C_L constructs and the C_H3 reverse primer 5387 for the C_H3 constructs. Still no improvement in the specificity could be seen and no retrieval of the C_H3 constructs or 4T10 was seen at all (Figure 4.5.B). It was decided at this stage to focus on optimising the system using only one of the spacer domains. As the better recovery was achieved here with the use of the C_L domain, and this is the domain that naturally follows the V_L domain in antibodies, it was chosen for use in subsequent experiments.

4.3.3 Comparing C_L primers

An investigation of the influence of the reverse (C_L) primer on the ability to amplify cDNA from selected complexes was undertaken. It was possible that some primers would not be effective because of digestion by contaminant nucleases of part of the selected mRNAs, or perhaps some primers would anneal more strongly than others to selected mRNAs, possibly influenced by secondary RNA structures. RT-PCR (2.1.4.3) was performed on the selected eluates from the anti-GPEwt-C_L and anti-GPE H2M-C_L displays above (Figure 4.5.A). The reverse primers used for RT-PCR were VLR1, 5942, 5269, 5268 and 5267 as shown in Figure 4.3. For both anti-GPE H2M (Figure 4.6.A) and anti-GPEwt (Figure 4.6.B), RT-PCR with 5269 reverse primer produced the strongest bands although with no specific recovery. Apart from weak amplification seen for use of the reverse anti-GPE primer VLR1, the other primers gave no, or extremely faint products. The same experiment with a panel of primers for 4T10-C_H3 was performed with some primers showing recovery of DNA bands, albeit non-specific (data not shown).

4.3.4 Altering blocking and washing conditions for specific selection

To improve specificity of selection as indicated by RT-PCR, a number of experimental conditions were altered. Torula yeast RNA at 50 μg/mL was included in the blocking solution of 5% skim milk, to prevent non-specific adsorption of mRNA of the translated complexes to the well surface. Skim milk was added to the mix at 2% in the binding step, and the concentration of Tween 20 in the wash was further increased to 0.4%. After displaying the 4T10-C_H3, anti-GPEwt-C_L and anti-GPE

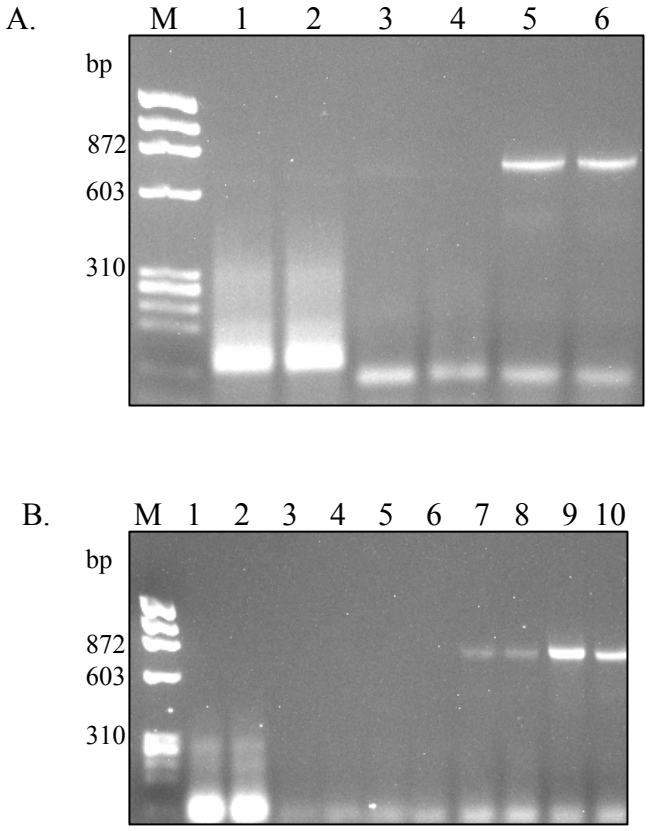

Figure 4.5 RT-PCR of ribosome display showing the effects of Tween-20 in the wash steps. A. 0.1% Tween-20. M, ϕX174 DNA markers. Lane 1, 4T10-C_H3 against lysozyme and 2, against IGF-I; 3, anti-GPEwt-C_L against lysozyme and 4, against IGF-I; 5, anti-GPE H2M-C_L against lysozyme and 6, against IGF-I. B. 0.2% Tween 20. M, ϕX174 DNA markers. Lane 1, 4T10-C_H3 against lysozyme and 2, against IGF-I; 3, anti-GPEwt-C_H3 against lysozyme and 4, against IGF-I; 5, anti-GPE H2M-C_H3 against lysozyme and 6, against IGF-I; 7, anti-GPEwt-C_L against lysozyme and 8, against IGF-I; 9, anti-GPE H2M-C_L against lysozyme and 10, against IGF-I.

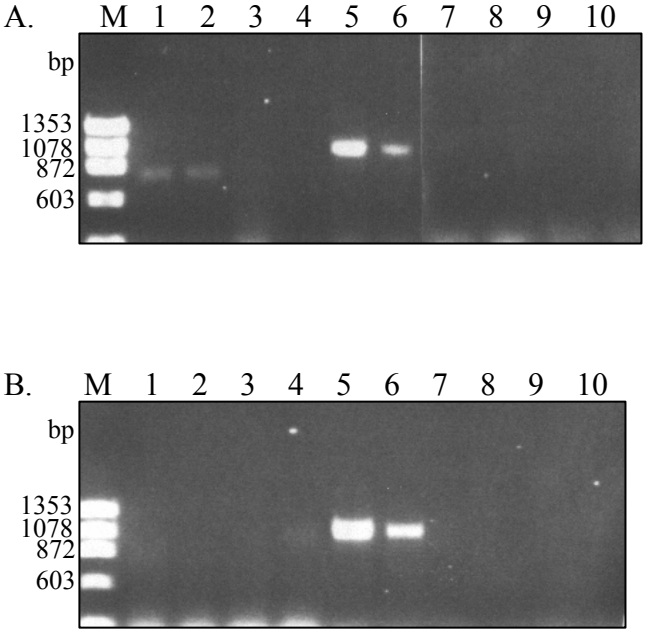

Figure 4.6 RT-PCR on selected ribosome display eluates of A. anti-GPE H2M-C_L and B. anti-GPEwt-C_L using different reverse primers. M, ϕX174 DNA markers. Lane 1 and 2, VLF1; 3 and 4, 5942; 5 and 6, 5269; 7 and 8, 5268; 9 and 10, 5267. Odd lanes, selections against lysozyme; even lanes, selections against IGF-I.

H2M-C_L constructs, RT-PCR (2.1.4.3) on eluted material using the reverse primers 5387 or 5385 for 4T10 and 5269 or VLR1 for the anti-GPE constructs, showed there was still no selection for 4T10, but there was some improvement for the anti-GPE constructs (Figure 4.7). There was specific selection for anti-GPEwt (lanes 9, 10) when using reverse primer VLR1 although the band is weak. The reverse primer 5269 (lanes 5-8) produced strong bands for both constructs and, even though there was some cross-selection against lysozyme, the bands for selection against IGF-I appear stronger.

Extra modifications to the overall selection process were taken to reduce non-specific binding. Doubling the concentration of the blocking solution (i.e. the skim milk concentration increased from 5% to 10% and the RNA concentration increased from 50 μg/mL to 100 μg/mL), and increasing the concentration of Tween 20 in the wash to 1.0% resulted in the loss of most of the RT-PCR bands seen in Figure 4.7 (Figure 4.8). However, a specific selection could be seen for one of the anti-GPEwt selections (Figure 4.8, lanes 5, 6). This result suggested that a level of blocking and washing somewhere in between the strength of those used in the displays shown in Figures 4.7 and 4.8 might be needed to produce the desired specificity.

A ribosome display of anti-GPEwt-C_L and anti-GPE H2M-C_L was performed with the block strength remaining at 10% skim milk / 100 μg/mL RNA, skim milk omitted from the binding step, and the concentration of Tween-20 in the washes reduced to 0.5%. RT-PCR (2.1.4.3) using both the 5267 and 5269 C_L primers resulted in no obvious bands with the 5267 primer (data not shown) but good specific bands (Figure 4.9) using the 5269 primer. Having established conditions that enabled specific selection of translated complexes, as measured by RT-PCR, the application of this system to select and enrich for affinity matured proteins from a pool of mutants was undertaken.

4.4 Mutagenesis of anti-GPE scFv by error-prone PCR

4.4.1 Error-prone PCR

The error-prone PCR method developed (2.1.4.1) is based on that of Leung *et al.*, (1989). It is reliant on the infidelity of Taq polymerase and the manipulation of reaction conditions to reduce this fidelity. By using dATP at one fifth the level of the other dNTPs, and using $MnCl_2$ as a source of Mn^{2+} ions at 0.5mM, Leung *et al.*, (1989) were able to achieve a random DNA mutation rate of

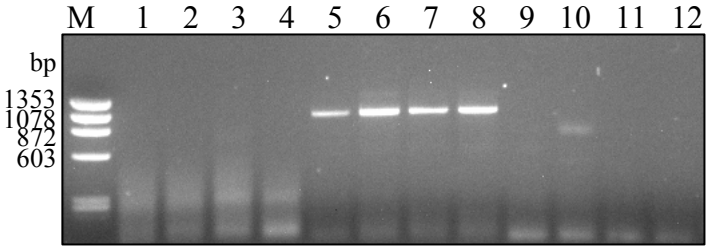

Figure 4.7 RT-PCR on ribosome display eluates showing the effect of RNA in the blocking solution, skim milk in the binding step, and 0.4% Tween-20 in the washes. M, ϕX174 DNA markers. Lane 1, 4T10 against lysozyme (primer 5387); 2, 4T10 against IGF-I (primer 5387); 3, 4T10 against lysozyme (primer 5385); 4, 4T10 against IGF-I (primer 5385); 5, anti-GPEwt-C_L against lysozyme (primer 5269); 6, anti-GPEwt-C_L against IGF-I (primer 5269); 7, anti-GPE H2M-C_L against lysozyme (primer 5269); 8, anti-GPE H2M-C_L against IGF-I (primer 5269); 9, anti-GPEwt-C_L against lysozyme (primer VLR1); 10, anti-GPEwt-C_L against IGF-I (primer VLR1); 11, anti-GPE H2M-C_L against lysozyme (primer VLR1); 12, anti-GPE H2M-C_L against IGF-I (primer VLR1).

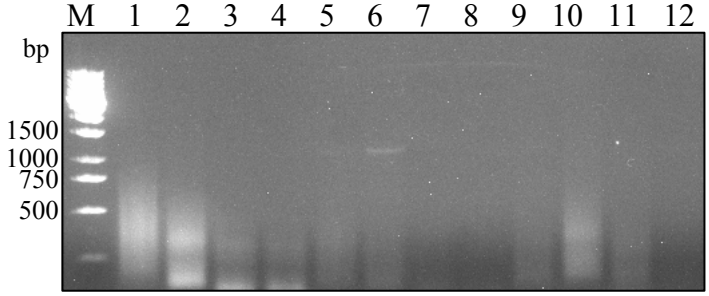

Figure 4.8 RT-PCR on ribosome display eluates showing effect of doubling the strength of blocking solution and increasing Tween-20 concentration to 1%. M, markers. Lanes 1-12 as shown in Figure 4.7.

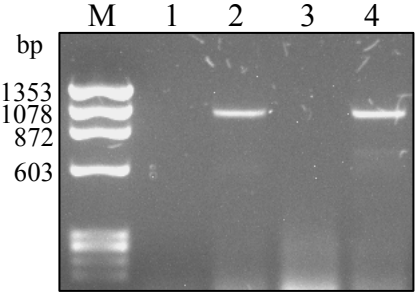

Figure 4.9 RT-PCR on ribosome display eluates showing the effect of reducing the Tween 20 concentration to 0.5% and eliminating skim milk from the selection step. M, ϕX174 DNA markers. Lane 1, anti-GPEwt-C_L against lysozyme and 2, against IGF-I; 3, anti-GPE H2M-C_L against lysozyme and 4, against IGF-I.

about 2%. Error-prone PCR fragments amplified from anti-GPE scFv template in this way (2.1.4.1) were analysed and isolated using agarose electrophoresis (2.1.5; data not shown).

4.4.2 Cloning of PCR fragments

Gel purified (2.1.6.1) error-prone PCR fragments were digested with *Sfi*I and *Not*I restriction enzymes (2.1.7) and ligated (2.1.9) into likewise digested pGC. Purified ligated DNA (2.1.6.2) was electroporated into *E.coli* HB2151 (2.1.11), and a selection of clones were picked from plates and screened for inserted scFv by colony PCR (2.1.12).

4.4.3 Sequencing of error-prone PCR generated clones

Plasmid preparations (2.1.13) were made for five of the positive clones. These were DNA sequenced (2.1.14) and the deduced amino acid sequences aligned (Figure 4.10) to check for the effectiveness of the error-prone PCR. The five clones had 2, 5, 6, 5, and 3 amino acid changes respectively for an average of 4.2 mutations per scFv gene. This equates to a mutation rate of 1.74% at the amino acid level which is in line with effective mutation rates observed in previous studies where error-prone PCR has been used (Daugherty *et al*., 2000). It was decided to use this error-prone PCR derived library in the ribosome display system to isolate evolved anti-GPE variants.

4.5 Ribosome display and selection of anti-GPE mutant library (EPGPE)

The *Sfi*I and *Not*I digested error-prone anti-GPE DNA library (EPGPE) was ligated into likewise digested pGC-C_L vector at an insert to vector ratio of approximately 3:1 (2.1.9). The ribosome display cassette was amplified by PCR (2.1.4) from this ligation using the 5/ primer 5998 (Table 2.1) for addition of the T7 promoter and RBS, and the 3/ C_L primer 6322. The amplified cassette was gel purified (2.1.6.1) and quantitated (2.1.8). The C_L construct was preferred as success was achieved with this construct in the ribosome display of the anti-GPE constructs.

4.5.1 First round of EPGPE display

The transcription and translation of EPGPE library for ribosome display was carried out as described (2.4.2). Selection of translated complexes was performed against IGF-I and lysozyme as described (2.4.3) with modifications as indicated. The conditions that led to successful specific selection of anti-GPEwt and anti-GPE H2M (4.3.4; Figure 4.9) were initially used for EPGPE ribosome display, but these were unsuccessful in achieving specific selection (data not shown). It was anticipated that there may be a significant proportion of misfolded non-functional scFvs

```
w.t.  EVQLQQSGPELVKPGASVTISCRTSGYTFTDYTMHWVKQSHGKSLEWIGGIITSNQKFKGKATLTVDKSSNTAYMELRSLTSEDSAVYYCARNYYGVDWFFDVWGAGTTV
1.1   EVQLQQSGPELVKPGAPVTISCRTSGYTFTDYTMHWVKQSHGKSLEWIGGIITSNQKFKGKATLTVDKSSNTAYMELRSLTSEDSAVYYCARNCYGVDWFFDVWGAGTTV
1.3   EAQLQQSGPELVKPGASVTISCRTSGYTFTDYTMHWVKQSHGKSLEWIGGIITSNQKFRGKATLTVDKSSNTAYMELRSPTSGDSAVYYCARNYYGVDWFLDVWGAGTTV
1.4   EVQLQQSGPELVKPGASATISCRTSGYTFTDYTMHWVKQSHGKSLEWIGGIITSNQKFKGKATLTVDKSSNTAYMELRSLTSEDSAVYYCARNYYGVDWFFDVWGAGTTV
1.8   EVLLQQSGPELVKPGASVTISCRTSGYTFTDYTMHWVKQSHGKSLEWIGGIITSNQKFKGKATLTVDKSSNTAYMELRSLTSEDSAVYYCARNYYGVDWFFDAWGAGTTV
1.9   EVQLQQSGPELVEPGATVTISCRTSGYTFTDYTMHWVKQSHGKSLEWIGGIITSNQKFKGKATLTVDKSSNTAYMELRSLTSEDSAVYYCARNYYGVDWFFDVWGAGTTV

w.t.  TVSSGGGGSGGGGSGGGGSDVLMTQTPLSLTVSLGDQASISCRSSQSIVHRNGNTYLEWYLQKPGQSPKLLIYKVSNRFSGVLDRFSGSGSGTDFTLKISRVEAEDLGVY
1.1   TVSSGGGGSGGGGSGGGGSDVLMTQTPLSLTVSLGDQASISCRSSQSIVHRNGNTYLEWYLQKPGQSPKLLIYKVSNRFSGVLDRFSGSGSGTDFTLKISRVEAEDLGVY
1.3   TVSSGGGGSGGGGSGGGGSDVLMTQTPLSLTVSLGDQASISCRSSQSIVHRNGNTYLEWYLQKPGQSPKLLIYKVSNRFSGVLDRFSGSGSGTDFTLKISRVEAEDLGVY
1.4   TVSSGGGGSSGGGSGGGGSGVLMTQTPPSLTVSLGDQASISCRSGQSIVHRNGNTYLEWYLQKPGQSPKLLIYKVSNRFSGVLDRFSGSGSGTDFTLKISRVEAEDLGVY
1.8   TVSSGGGGSGGGGSGGGGSDVLMTQTPLSLTVSPGDQASISCRSSQSIVHRNGNTYLEWYLQKPGQPPKLLIYKVSNRFSGVLDRFSGSGSGTDFTLKISSVEAEDLGVY
1.9   TVSSGGGGSGGGGSGGGGSDVLMTQTPLSLTVSLGDQASISCRSSQSIVHRNGNTYLEWYLQKPGQSPKLQIYKVSNRFSGVLDRFSGSGSGTDFTLKISRVEAEDLGVY

w.t.  YCFQGSHVPWTFGGGTKLELKR
1.1   YCFQGSHVPWTFGGGTKLELKR
1.3   YCFQGSHVPWTFGGGTKLELKR
1.4   YCFQGSHVPWAFGGGTKLELKR
1.8   YCFQGSHVPWTFGGGTKLELKR
1.9   YCFQGSHVPWTFGGGTKLELKR
```

Figure 4.10 Deduced amino acid sequences of five randomly chosen clones (preselection) from the EPGPE library. Mutations are indicated in bold and underlined.

displayed within the library, due to some of the mutations having a deleterious effect on the framework. These could potentially be involved in non-specific interaction with the selection surface. Therefore, selection of the displayed EPGPE library using stronger blocking and washing conditions (i.e. blocking with 10% BPBS / 100 μg/mL RNA, adding 2% skim milk to the binding step, and using 1% Tween in the washes) was undertaken to prevent this. Anti-GPEwt-C_L, anti-GPE H2M-C_L, and EPGPE-C_L were displayed with RT-PCR (2.1.4.3) on eluted mRNA (Figure 4.11) showing good specific bands generated for EPGPE using reverse primers 5267 and 5268 (lanes 10 and 12). A weak specific band was also evident for anti-GPEwt (lane 2). The outermost 3/ primers, 5267 and 5268 were used in the RT-PCR to allow retrieval of the largest amount of spacer region possible as it was intended to take selected EPGPE scFvs through further rounds of display and selection. These RT-PCR bands were excised and gel-purified (2.1.6.1).

4.5.2 Second round of EPGPE display

Using the same conditions employed for the first round described above (4.5.1), gel-purified RT-PCR bands, either directly or following secondary PCR amplification (2.1.4) to obtain higher levels of template, in a second round of ribosome display and selection, failed to generate any selected second round bands (data not shown), apart from a weak specific response for anti-GPE H2M against IGF-I. While the first round display experiments used 0.5 – 1.0 μg template in the transcription/translation reaction, within the range of 0.1 – 1.0 μg specified by the reticulocyte system manufacturer, these second rounds of display and selection used RT-PCR and PCR bands without quantitation, and it is possible that such optimal levels of template were not achieved. Freshly amplified template was prepared from the first round RT-PCR product by PCR (2.1.4) using the 5/ T7 promoter/RBS primer 5998, and either 5267 or 5269 C_L primers, to give constructs of two different spacer lengths, referred to below as EPGPE-5267 and EPGPE-5269 respectively (Figure 4.12). These were quantitated (2.1.8) for optimisation of template concentration. In this experiment the blocking strength was reduced to 5% BPBS / 50 μg/mL RNA, skim milk was left out of the selection step, and Tween-20 was reduced to 0.5% in the wash, in an attempt to lower overall stringency to enhance recovery of selected bands. RT-PCR (2.1.4.3) on selected material was performed using both primers 5267 and 5269. RT-PCR using 5267 was unsuccessful (data not shown), but RT-PCR with 5269 showed good specific amplification for both anti-GPE constructs, a weak non-specific band for the EPGPE-5267, and a weak specific band for the EPGPE-5269 (Figure 4.13). In order to obtain enough T7-EPGPE-CL DNA template for use in a third round of display and selection, the RT-PCRs on the second round selection of EPGPE-5269 against

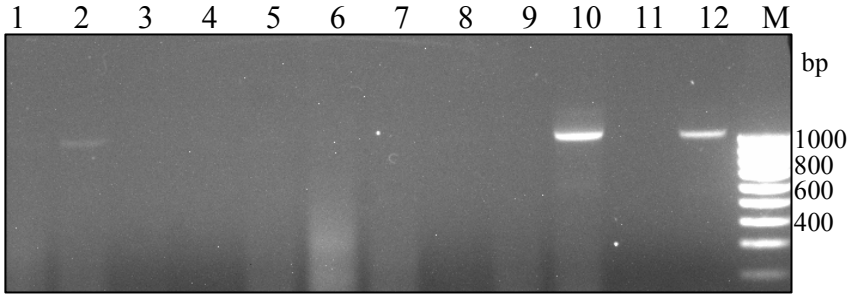

Figure 4.11 RT-PCR on ribosome display eluates showing specific selection of EPGPE against IGF-I. Lane 1, anti-GPEwt-C_L against lysozyme and 2, against IGF-I using 5267; 3, anti-GPEwt-C_L against lysozyme and 4, against IGF-I using 5268; 5, anti-GPE H2M-C_L against lysozyme and 6, against IGF-I using 5267; 7, anti-GPE H2M-C_L against lysozyme and 8, against IGF-I using 5268; 9, EPGPE-C_L against lysozyme and 10, against IGF-I using 5267; 11, EPGPE-C_L against lysozyme and 12, against IGF-I using 5268. M, 100bp ladder.

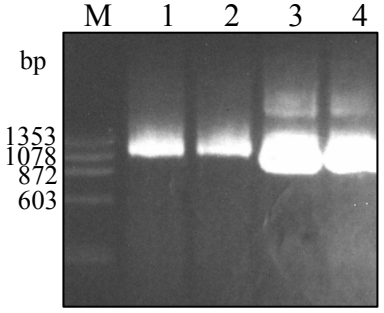

Figure 4.12 PCR reamplification of RT-PCR generated DNA selected from EPGPE in a first round of ribosome display. M, ϕX174 DNA markers. Lanes 1 and 2, amplified using primer 5267; 3 and 4, amplified using primer 5269.

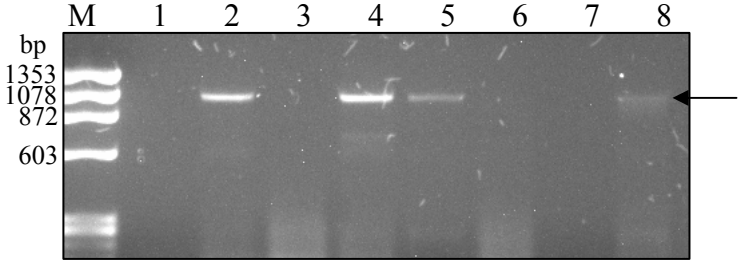

Figure 4.13 RT-PCR on eluates from a second round of ribosome display of EPGPE. M, ϕX174 DNA markers; Lane 1, anti-GPEwt-C_L against lysozyme and 2, against IGF-I; 3, anti-GPE H2M-C_L against lysozyme and 4, against IGF-I; 5, EPGPE-5267-C_L against lysozyme and 6, against IGF-I; 7, EPGPE-5269-C_L against lysozyme and 8, against IGF-I.

lysozyme and IGF-I were repeated with levels of IGF-I-eluate of 0.2, 0.5, 1.0, and 2.0 μL used as template (Figure 4.14). It is noteworthy that the bands generated in this RT-PCR were still specific but much stronger than they appear in Figure 4.13. A possible reason for this is that the selected material used as template had been stored frozen overnight and the freeze/thaw may have allowed more efficient amplification, possibly by freeing mRNA from complexes thereby improving primer accessibility, or modifying secondary structure in the mRNA. The levels of template did not appear to titrate out over the range used, suggesting a good concentration of mRNA in the selected eluate.

4.5.3 Further rounds of EPGPE display

The round two EPGPE RT-PCR bands were gel purified (2.1.6.1), quantitated (2.1.8), and used in parallel with 4T10-C_H3 in a third round of ribosome display and selection against IGF-I and lysozyme. RT-PCR on selected eluates showed weak specific selection for both 4T10-C_H3 and EPGPE-5269 (Figure 4.15.A). However, there appeared to be little enrichment for binders, where one would expect an increase in intensity of selected bands over the course of multiple rounds, analogous to enrichment indicated by increasing phage titres after multiple rounds of phage display (McCafferty *et al*., 1990). The RT-PCR for the weak specific band for EPGPE selected against IGF-I was repeated and showed much stronger bands than the original, suggesting again that the freeze/thaw step may be helpful (data not shown).

These round three RT-PCR bands were gel purified, quantitated, and subjected to a fourth round of ribosome display in parallel with 4T10-C_H3, as performed for the third round. RT-PCR on selected material showed that no specific band could be seen for 4T10-C_H3 (Figure 4.15.B), demonstrating difficulty in achieving reproducibility with this system, as a band had been achieved from this contruct under the same conditions in the previous display. A band could be seen for EPGPE-C_L against IGF-I, but a non-specific band against lysozyme had also developed, although this was a little weaker than the IGF-I band. Fourth round selected sequences were taken through two further rounds of ribosome display and selection. RT-PCR analysis showed that non-specific bands against lysozyme were increasing in strength compared to bands against IGF-I (data not shown). It appears therefore that some sort of enrichment for non-specific binders was occurring.

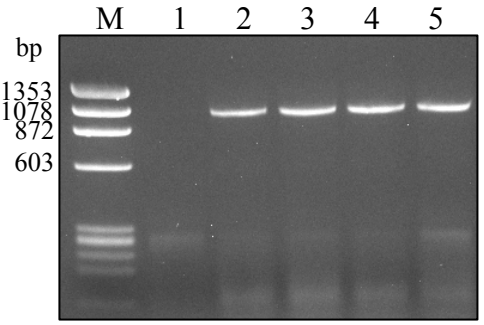

Figure 4.14 Repeated RT-PCR of second round ribosome display of EPGPE-C_L (5269 fragment). M, ϕX174 DNA markers; Lane 1, against lysozyme; 2-5 against IGF-I at 0.2, 0.5, 1.0, and 2.0 μL respectively.

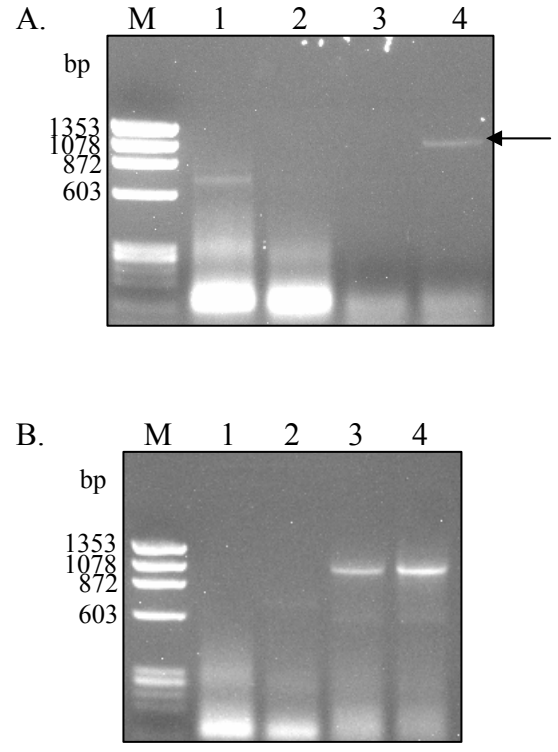

Figure 4.15 RT-PCR on eluates from a third (A) and fourth (B) round of ribosome display of EPGPE. M, ϕX174 DNA markers; Lane 1, 4T10-C_H3 against lysozyme and 2, against IGF-I; 3, EPGPE-CL (5269 fragment) against lysozyme and 4, against IGF-I.

4.6 Screening of selected EPGPE clones

The interpretation of the increase in non-specific binders against lysozyme amongst the later-round EPGPE selection cycles was that there was an increase in poorly folded scFvs which bound through incorrectly exposed surfaces that might include, for example, hydrophobic patches. It would be expected that such phenomena would also create increased aggregation in cell expression systems. Sequences from the sixth round of display/selection were amplified by PCR (2.1.4) using primers 5325 and VLR1, restriction digested with *Sfi*I and *Not*I (2.1.7), and ligated (2.1.9) into likewise digested pGC. The ligated DNA was electroporated (2.1.11) into *E. coli* HB2151. Plasmid preparations (2.1.13) from a selection of seven clones positive for insert by colony PCR (2.1.12) were sequenced (2.1.14), and revealed scattered amino acid point mutations as well as silent nucleotide changes (data not shown). Two of the sequences had single amino acid deletions, one showed the loss of a large proportion of the scFv insert, and one had a mutation leading to a stop codon, while three had 9, 12, and 4 scattered amino acid changes respectively, the latter also with a three residue deletion of V_H residues 4-6. The latter three clones were cultured and induced as 1 L shake flask cultures (2.2.1), and periplasmic extracts (2.2.2) were affinity-purified on a FLAG column (2.3.8). Gel filtration chromatographic analysis (2.3.10) of FLAG-pure proteins showed that nearly all migrated in the aggregate fraction, with negligible soluble monomeric species (data not shown), even though they were detected by Western blotting (2.3.2) migrating as FLAG-tagged scFvs (data not shown). These data are compatible with the interpretation that these sequences result in poorly folding protein prone to aggregation, possibly due to non-specific association of exposed hydrophobic regions. The sequence data of the round six clones also supported this with the high number of mutations in some of the clones and deletions in others expected to be more harmful than beneficial to the stability of the framework.

On the basis of these results with the sixth-round selected clones, DNAs from the fourth round of display, the last round where RT-PCR bands were still stronger for selection against IGF-I than lysozyme, were cloned as described for the sixth round selection above. Prior to screening of these clones, ELISA (2.3.12) using BSA as the blocking reagent was optimised for detection of IGF-I-binding of the anti-GPE parent Mab, and anti-GPEwt and anti-GPE H2M scFvs (Figure 4.16). Purified Mab was used at ~ 2 μg/mL, and the scFvs were expressed from small-scale cultures (2.2.1) with the supernatants used undiluted for binding. Four controls were included using the anti-GPEwt scFv sample (4.16). The Mab response against IGF-I, was strong and specific. The anti-

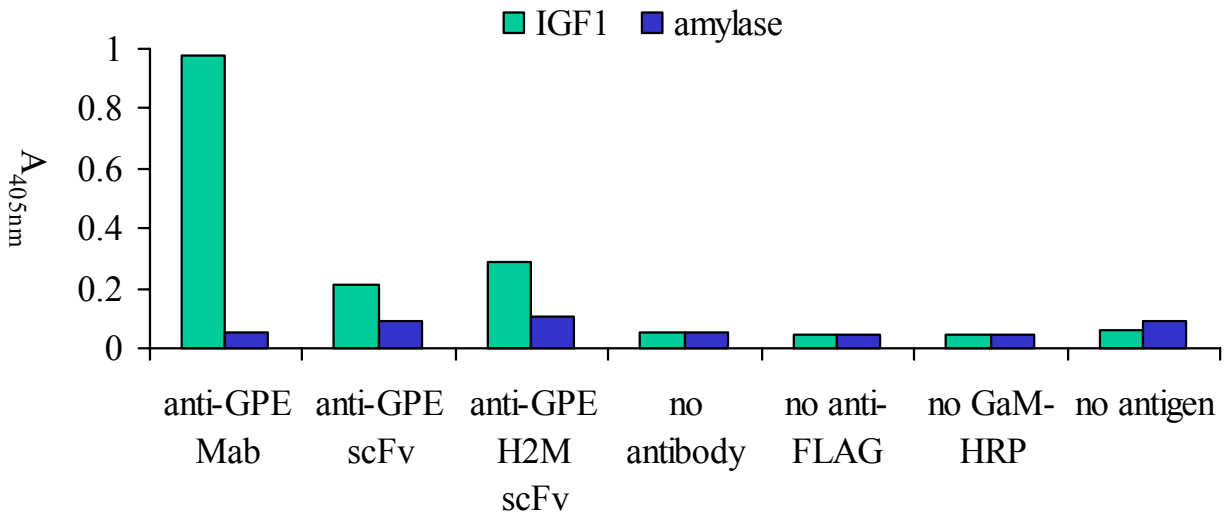

Figure 4.16 ELISA comparing binding of recombinant anti-GPE scFv with the parent Mab 5C6/B3.

GPEwt and anti-GPE H2M scFvs have particularly low responses, due to their monovalency and relatively weak (micromolar) affinity, however, direct comparisons of binding can not be made as protein concentrations were not normalised. The non-specific background is probably higher in the scFvs due to their 'stickiness' compared with the stable parent, either from hydrophobic regions that are normally masked in IgG, or from hydrophobic regions exposed in misfolded species. Sixty-four mutant fourth round clones were randomly picked and screened for binding. These clones were cultured in microtiter wells for expression of scFvs (2.2.3) and the culture supernatants tested by ELISA (2.3.12). Most clones showed negligible or poor binding when compared to that of the anti-GPEwt (data not shown), although eleven clones that showed a reasonable degree of binding when compared to the wild type anti-GPE scFv were analysed further (Figure 4.17) for ELISA-binding from small-scale culture (2.2.1) supernatants. Most of these clones showed a response against IGF-I comparable to that of the wild type scFv with fairly low cross-reactivity to α-amylase but higher cross-reactivity to lysozyme.

The six clones with the best binding to IGF-I relative to that of the wild type were chosen for DNA sequencing (2.1.14). The deduced amino acid sequences of these clones are shown in Figure 4.18 and they appear to be genuine random error-prone PCR mutants. The overall amino acid mutation rate of the selected scFvs was higher than for random representatives from the unselected library (6.7/gene compared to 4.2/gene). Three clones were chosen for expression and purification based on the strength of ELISA signals compared to that of anti-GPEwt scFv. These were EP50 (4 mutations), EP58 (10 mutations), and EP62 (7 mutations). Due to its strong cross-reactivity with lysozyme, EP37 was disregarded.

4.7 Expression and purification of selected scFvs

4.7.1 Expression and affinity purification

Expression cultures (1 L) of clones EP50, EP58, EP62, and anti-GPEwt scFv were carried out as described (2.2.1). It was noted that the mutant cultures exhibited poor growth within 1-2 hours of induction, as indicated by low maximal OD_{600nm} readings, as was observed and described for the anti-GPEwt in Chapter 3. Periplasmic fractions (2.2.3) from these cultures were harvested and affinity purified (2.3.8) on an anti-FLAG column. Affinity purified material was dialysed into HBS/P20 and concentrated (2.3.9) to ~ 1 mL. Expression of scFvs was verified by Western blot (see 4.7.4; Figure 4.21).

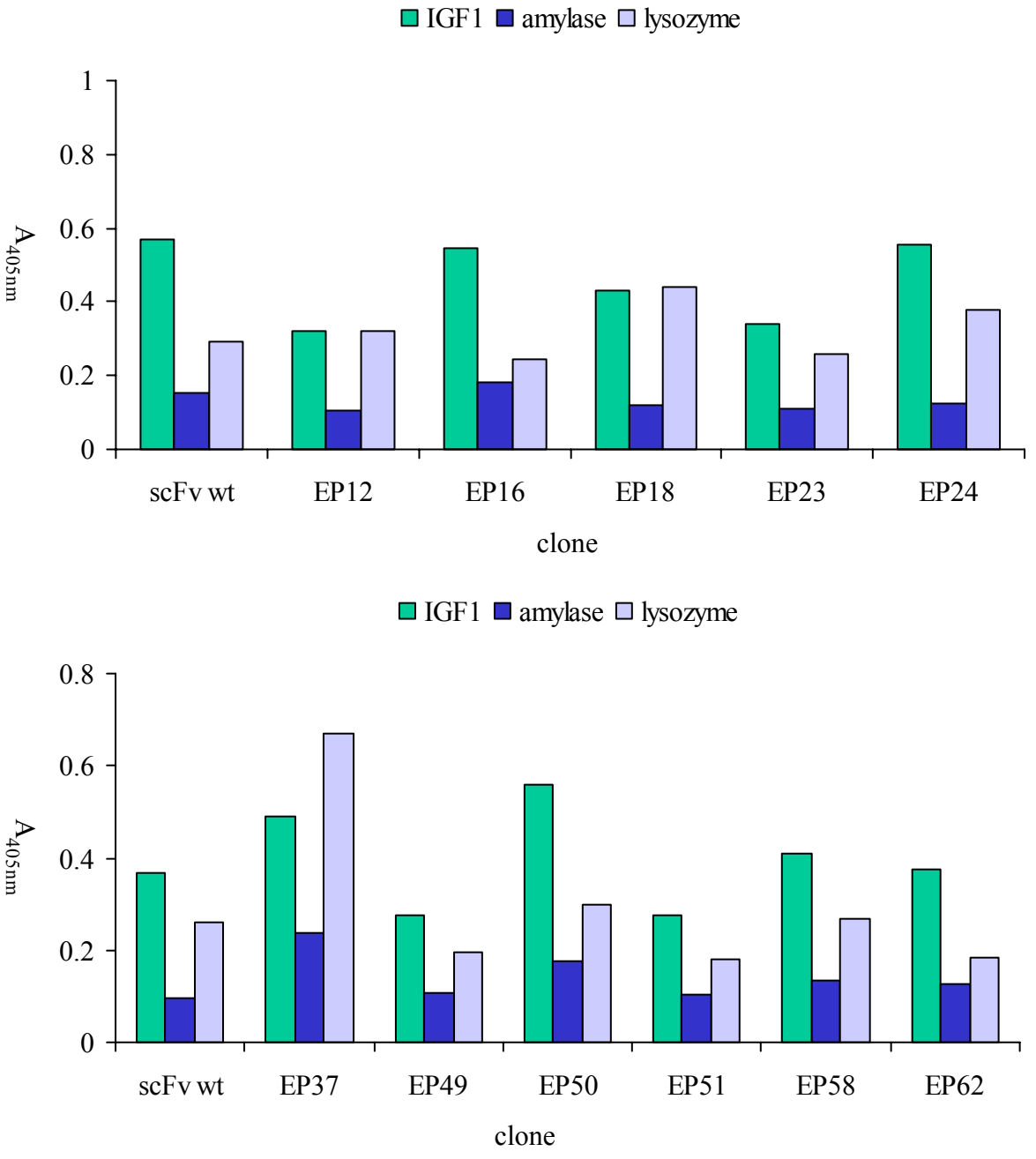

Figure 4.17 ELISA of best binding EPGPE clones compared with anti-GPEwt scFv.

```
w.t.  EVQLQQSGPELVKPGASVTISCRTSGYTFTDYTMHWVKQSHGKSLEWIGGIITSNQKFKGKATLTVDKSSNTAYMELRSLTSEDSAVYYCARNYYGVDWFFDVWGAGTTV
16    EVQLQQSGPELVKPGASVTISCRTSGYTFTDYTMYWVKQSHGKGLERIGGIITSNQKFKGKATLTVDKSSNTAYMELRSLTSEDSAVYYCARNYYGVDWFFDVWGAGTTV
24    EVQLQQSGPELVKPGASVTISCRTSGYTFTDYTMHWVKQSHGKSLEWIGGIITSNQKFKGKATLTVDKSSNTAYMELRSLTSEDSAVYYCARNYYGVDWFFDVWGAGTTV
37    AVQLQQSGSELLKPGASVTISCRTSGYTFTDYTMHWVKQSHGKSLEWIGGIITSNQKFKGKATLTVDKSSNTAYMELRSLTSEDSAVYYCARNYYGVDWLFDVWGAGTAV
50    EVQLQQSGPEPVKPGASVTISCRTSGYTFTDYTMHWVKQSHGKSLEWIGSIITSNQKFKGKATLTVDKSSNTAYMELRSLTSEDSAVYYCARNYYGVDWFFDIWGAGTTV
58    EVQLQQSGPELVKPGASVTISCRTSGYTFTDYTMHWVRQSHGTGLEWIGGIITSNQKFKGKATLTVDKSSSTAYMELRSLTSEDSAVYYCARDYYGVDWLFDVWGAGTTV
62    EVQLQQSGLELVKHGASVTISCRTSGYTFTDYTMHWVKQSHGKSLEWIGGIITSNQKFKGKATLTVDKSSNTAYMELRSLTSEDSAVYYCARNYYGVDWFFDVWGAGTMV

w.t.  TVSSGGGGSGGGGSGGGGSDVLMTQTPLSLTVSLGDQASISCRSSQSIVHRNGNTYLEWYLQKPGQSPKLLIYKVSNRFSGVLDRFSGSGSGTDFTLKISRVEAEDLGVY
16    TVSSGGGGSGGGGSGGGGSDVLMTQTPLSLTVSLGDQASISCRSSQSSVHRSGNTYLEWYLRKPGQSPKLLIYKVSNRFSGVLDRFSGSGSGTDFTLKISRVEAEDLGVY
24    TVSSGGGGSGGGGPGGGGSGVLMTQTPLSLTVSLGDQASISCRSSQGIVHRNGNTYLEWYLQKPGQSPKLLIYKVSNRSSGVLDRFSGDGSGADFTLKISRVEAEDLGVY
37    TVSSGGGGSGGGGSGGGGSDVLMTQTPLSLTVSLGDQASISCRSSQSIVHRNGNTYLEWYLQKPGQSPKLLIYKVSNRFSGVLGRFSGSGSGTDFTLKISRVEAEDLGVY
50    TVSSGGGGSGGGGSGGGGSDVLMTQTPLSLTVSLGDQASISCRSSQSIVHRNGNTYLEWYLQKPGQSPKLLIYKVSNQFSGVLDRFSGSGSGTDFTLKISRVEAEDLGVY
58    TVSSGGGGSGGGGSGGGGSDVLMTQTPLSLTVSLGDQASISCRSSQSIVHRNGNTYLEWYLQKPGQSPKLLIYKVSSRFSGVLDRFSGSGSGTDFTLKISRVEAEDLGVY
62    TVSSGGGGSGGGGSGGGGSDVLMTQTPLSLTVSLGDQASISCRSSQSIVHRNGNTYLEWYLQKPGQSPKLLIYKVSNRFSGVLDGFSGSGSGADFALEISRVEAEDLGVY

w.t.  YCFQGSHVPWTFGGGTKLELKR
16    YCFQGSHVPWTFGGGTKLELKR
24    YCFQGSHVPWTFGGGTKLELKR
37    YCFQGSHVPWVFGGGTKLELKR
50    YCFQGSHVPWTFGGGTKLELKR
58    YCFQGSHVPWTFGGGPQLELPR
62    YCFQGSHAPWTFGGGTKLELKR
```

Figure 4.18 Deduced amino acid sequence alignment of best IGF1-binding (by ELISA) EPGPE scFvs selected by four cycles of ribosome display. Mutations indicated in bold and underlined.

4.7.2 Gel filtration chromatography analysis and purification

Affinity purified (4.7.1) samples were then subjected to gel filtration chromatography on a Superose 12 column (2.3.10) for comparative size profile analyses and scFv monomer peak collection. There are some differences in the multimerisation states of the selected EPGPE clones and the anti-GPEwt (Figure 4.19). These profiles show that large proportions of all these scFvs exist as multimers and higher aggregates. The ratios of monomer to other states vary for each of these clones. All mutants appear to have a slightly increased expression of monomer compared to the wild type. There appears to be an improvement in the ratio of monomer to dimer in all the mutants compared with the wild type. All mutants however displayed a tendency to precipitate out of solution during the purification process, as described in Chapter 3 for the anti-GPE scFv. Pooled monomer peaks were concentrated and then reapplied to the Superose 12 column to ensure highest purity peaks. In some instances, Superdex 200 was used to prepare monomer fractions since it provides a larger separation in the region of molecular weights of interest (about 4 min separation between 17 kD and 44 kD BioRad protein standards, compared to about 3 min for Superose 12; data not shown). An example of this is shown for a 2 L expression (2.2.1) of EP50 in Figure 4.20 although no substantial improvement in monomer peak separation from possible breakdown products eluting at approximately 38 min and higher molecular weight oligomeric peaks was achieved. The monomer and oligomer peaks indicated were collected, concentrated (2.3.9), reapplied to the same column, and collected again to improve purity.

4.7.3 Western Blot analysis

Western blots (2.3.2) detected FLAG-tagged proteins migrating at ~ 34-35 kD for all clones (Figure 4.21). The corresponding Coomassie-stained gels (2.3.1) revealed the relatively low expression, reflected as very faint bands (data not shown). In the Western blots (Figure 4.21), a comparison of the periplasmic samples (lane 1) with the post-FLAG column flow throughs (lane 2) shows that the affinity purifications were effective in sequestering most FLAG-tagged protein, showing that the column was working efficiently. A comparison of the supernatant samples (lane 3) with the periplasmic samples (lane 1) shows that for all clones a large proportion of expressed scFvs are leaking into the medium, considering that the periplasmic sample is a total volume of 67 mL, a 15-fold concentration of the total culture volume (1L), yet the bands from both fractions are of similar intensity. The leakage into the cell culture medium most probably reflects a toxicity of the recombinant proteins to the host cells similar to that observed for the wild type, which might be causing cell lysis during the course of the expression. Dialysis into HBS/P20 caused material to precipitate from solution for all clones, and is shown in Figure 4.21 lane 4 for both anti-GPEwt and

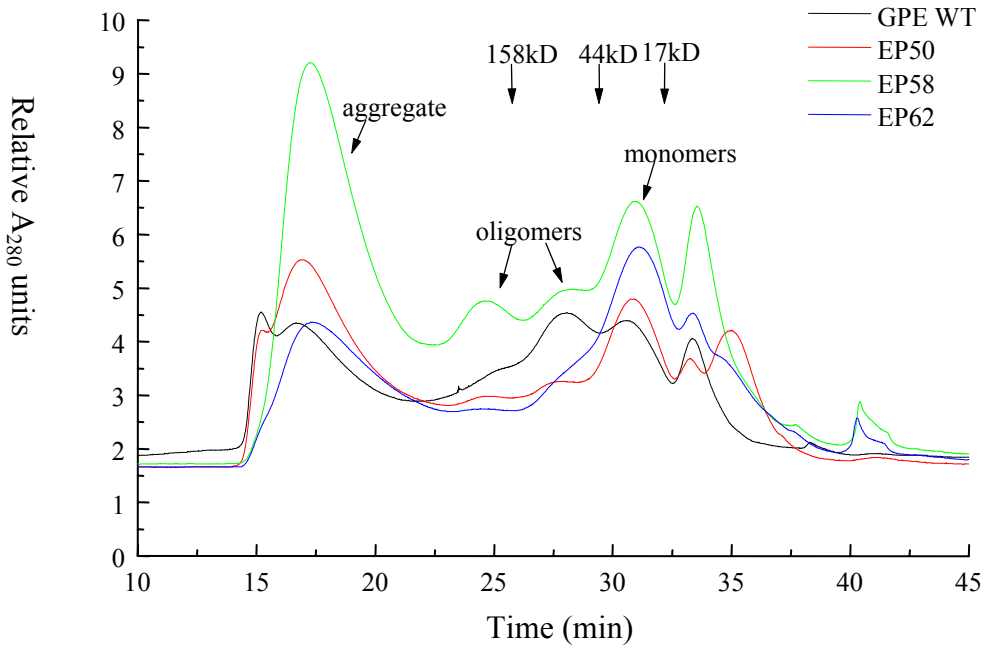

Figure 4.19 Gel filtration chromatography on a Superose 12 column of affinity purified anti-GPEwt, EP50, EP58 and EP62. Retention times of Biorad molecular weight standards during column calibration are indicated.

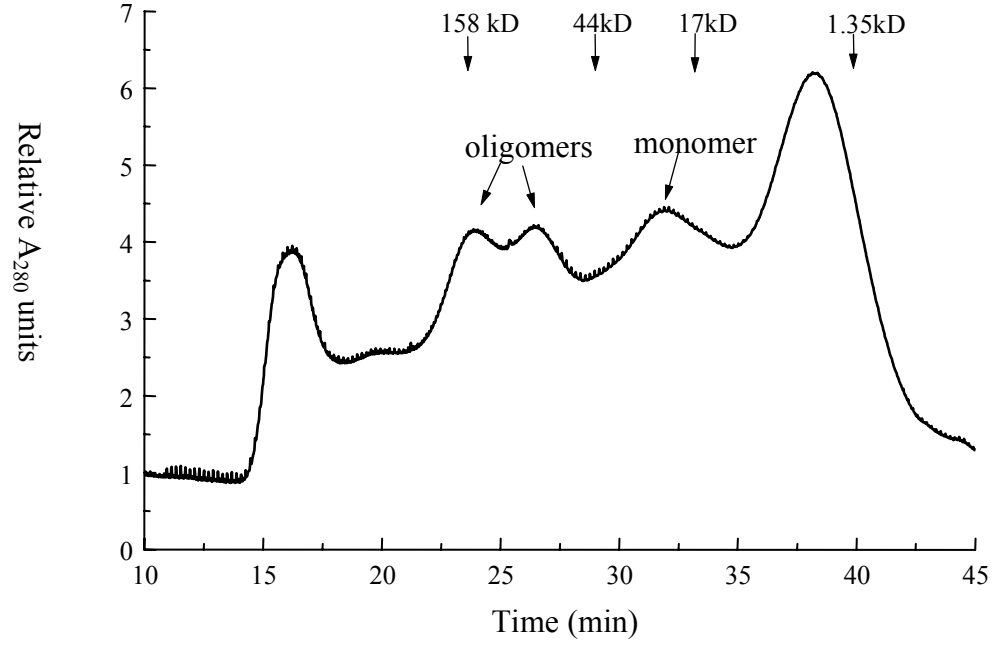

Figure 4.20 Gel filtration chromatography on a Superdex 200 column of affinity purified EP50. Retention times of Biorad molecular weight standards during column calibration are indicated.

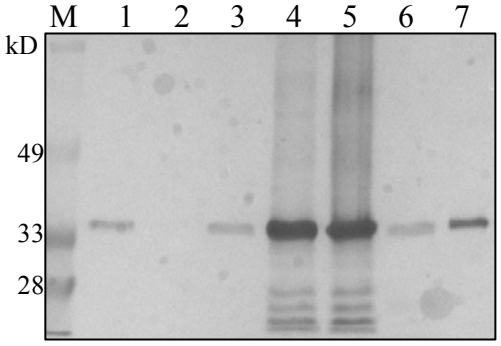

Anti-GPEwt.
M, Bio-Rad low range protein standards;
Lane 1, periplasm (pre-FLAG column);
2, flow through (post-FLAG column);
3, culture supernatant;
4, FLAG-pure dialysis precipitate;
5, FLAG-pure concentration precipitate;
6, scFv monomer peak (Superose 12);
7, aggregate peak (Superose 12).

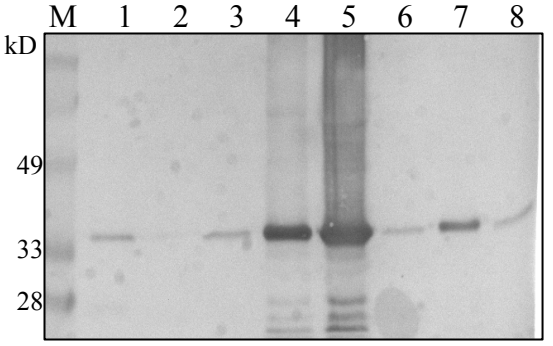

EP50.
M, Bio-Rad low range protein standards;
Lane 1, periplasm (pre-FLAG column);
2, flow through (post-FLAG-column);
3, culture supernatant;
4, FLAG-pure dialysis precipitate;
5, FLAG-pure concentration precipitate;
6, oligomer peak (Superose 12);
7, aggregate peak (Superose 12);
8, scFv monomer peak (Superose 12).

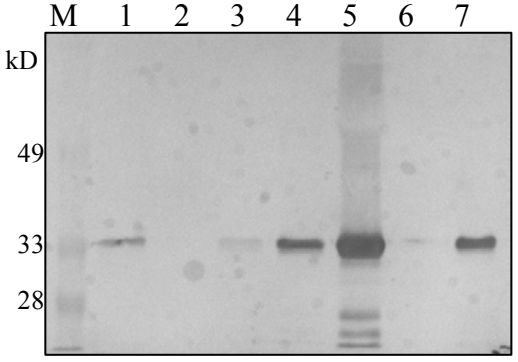

EP58.
M, Bio-Rad low range protein standards;
Lane 1, periplasm (pre-FLAG column);
2, flow through (post-FLAG column);
3, culture supernatant;
4, FLAG-pure;
5, FLAG-pure concentration precipitate;
6, scFv monomer peak (Superose 12);
7, aggregate peak (Superose 12).

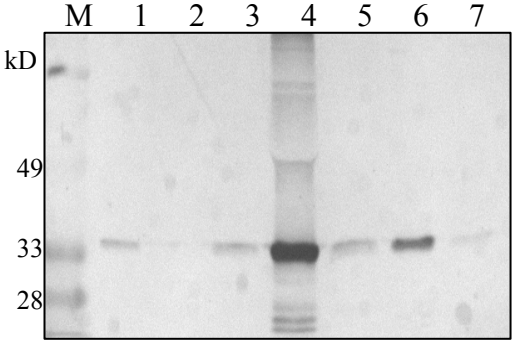

EP62.
M, Bio-Rad low range protein standards;
Lane 1, periplasm (pre-FLAG column);
2, flow through (post-FLAG column);
3, culture supernatant;
4, FLAG-pure concentration precipitate;
5, oligomer peak (Superose 12);
6, aggregate peak (Superose 12);
7, scFv monomer peak (Superose 12).

Figure 4.21 Western blots of expression and purification of anti-GPEwt, EP50, EP58 and EP62 scFvs.

the EP50 mutant. Similarly, concentration resulted in precipitates shown in Figure 4.21 lanes 5 for anti-GPEwt, EP50, and EP58, and lane 4 for EP62. These precipitates were resuspended in 100 μL 10% SDS for this analysis. As the amount of the precipitate sample loaded represented about 5% of the entire precipitate from affinity-purified protein, and the monomer peaks loaded (lanes 6 for anti-GPEwt and EP58, lane 8 for EP50, and lane 7 for EP62) corresponded to about 5% of the total monomer from affinity-purified protein, it can be concluded that a large proportion of purified protein is precipitating, showing the low solubility of these scFvs. When looking at the amount of scFv running in the aggregate peak (Figure 4.21 lanes 7 for anti-GPEwt, EP50 and EP58, and lane 6 for EP62) compared with that of the scFv monomer peaks (Figure 4.21 lanes 6 for anti-GPEwt and EP58, lane 8 for EP50, and lane 7 for EP62), it is clear that a low proportion of soluble purified protein exists as monomer. Likewise, a Western blot of the expression and purification of EP50 utilising the Superdex 200 column showed similar results (data not shown).

4.8 Characterisation of binding of selected scFvs

The wild type and mutant scFvs were assessed for their binding to IGF-I immobilised on a BIAsensor chip (2.3.13.1) as described in 3.5 for anti-GPE wt. The EP58 and EP62 scFvs showed some evidence of weak binding but the data were a poor fit to the theoretical model (not shown) and were not analysed further. The EP50 mutant scFv monomer eluted from the Superose 12 column (4.7.2; Figure 4.19) clearly exhibited binding over a range of concentrations (Figure 4.22.A). Only enough monomer was produced to analyse a concentration series of 0.125, 0.25, and 0.5 μM. Thus, the 2 litre expression was performed, using a Superdex 200 column for purification, as described in 4.7.3, to produce enough scFv for a concentration series of 0.5, 1.0, and 2.0 μM to be analysed on the BIAcore (Figure 4.22.A). The data from the Superdex 200-purified EP50 were analysed using BIAevaluation software 3.0 (2.3.13.3) to determine the association and dissociation rates (Table 4.1). Likewise the purified anti-GPEwt scFv was analysed for comparison at the concentrations of 0.25, 0.5, and 1.0 μM (Figure 4.22.B). The data were a reasonably good fit to the Langmuir theoretical model for 1:1 binding with low standard errors, yielding K_D = 1.44 μM for the mutant EP50 scFv and K_D = 3.73 μM for the anti-GPEwt scFv. This equates to a 2.6-fold improvement in affinity for the error-prone PCR generated mutant that appears to be chiefly due to an improvement in the on rate as the off rate calculated is close to that of the wild type scFv. The affinity calculated for the wild type concurs closely to that determined initially as described in 3.5.2. Data for Superose

A.

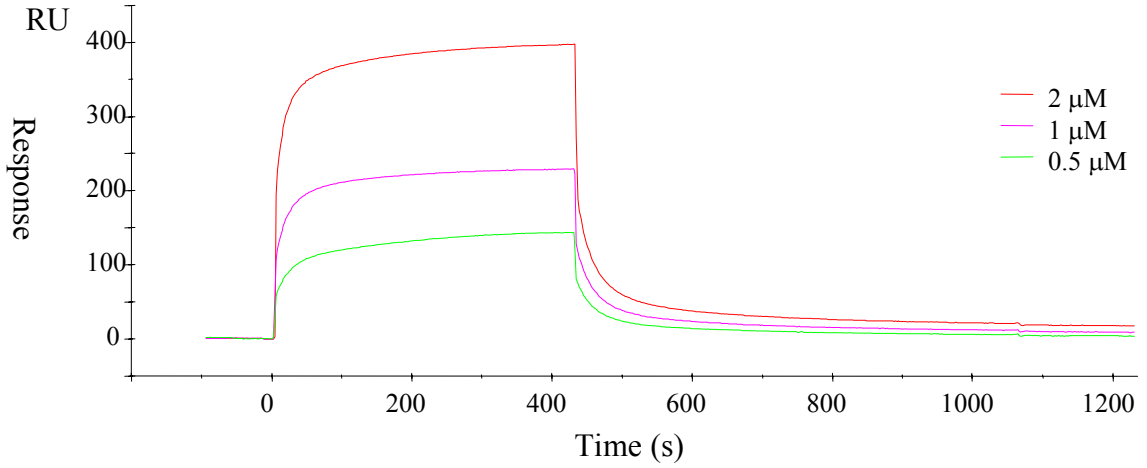

B.

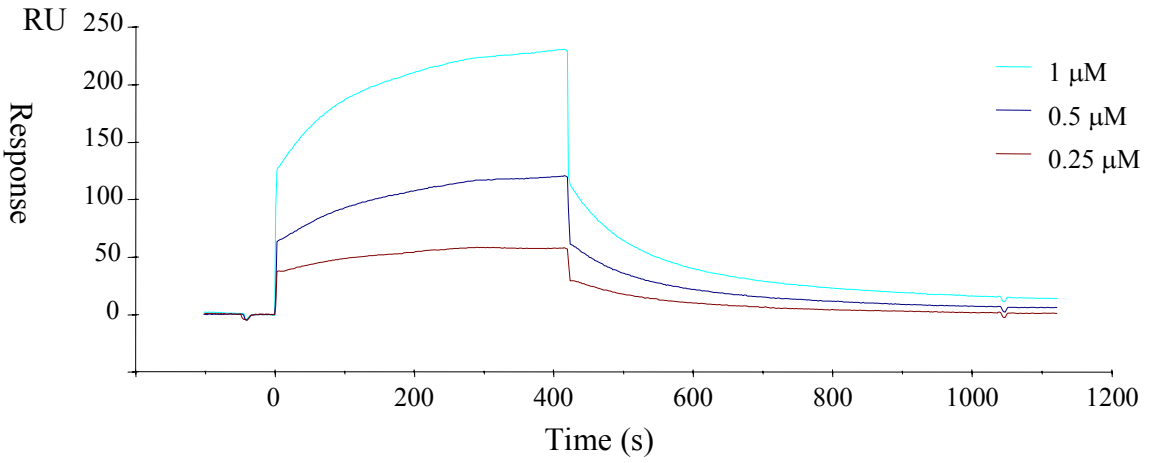

Figure 4.22 Overlaid BIAcore sensorgrams showing concentration series of purified scFvs binding to immobilised IGF-I on the BIAcore. A. EP50 (Superdex 200-purified), B. anti-GPEwt.

12-purified EP50 were also analysed (not shown) and the calculated on and off rates correlated well with the Superdex 200-purifed EP50.

Table 4.1 Kinetic data for BIAcore interactions of EP50 and anti-GPE wild type scFvs with immobilised IGF-I.

	k_a (1/Ms)	SE*	k_d (1/s)	SE	K_D (μM)
EP50	3.55×10^3	113	5.11×10^{-3}	5.95×10^{-5}	1.44
Anti-GPEwt	1.41×10^3	44	5.25×10^{-3}	2.17×10^{-5}	3.73

* standard errors for on and off rate calculations

4.9 Discussion

4.9.1 Ribosome display and selection of anti-GPE wild type and anti-GPE H2M scFvs

One feature of the coupled transcription translation system used is the presence of 2 mM DTT required for activity of the T7 polymerase. It was thought that this level of DTT could possibly hinder the formation of the intra-domain disulphide bonds that are required for the correct folding of the immunoglobulin domains (Glockshuber *et al*., 1992), and the presence of GSSG may assist folding in this environment. The initial ribosome display experiments (4.3.1) showed inclusion of GSSG did not assist in selection of ribosome complexes, and He and Taussig (1997) reported specific selection of folded scFvs in a coupled system containing 2 mM DTT without GSSG. However, it could not be concluded that this mRNA was from selected complexes, or non-specific complexes, or even that the mRNA was ribosome-associated at all.

A possible cause of the non-specific selection shown by RT-PCR (4.4.B) in early experiments was that a proportion of ribosome-displayed proteins produced in the transcription/translation system were misfolded and therefore able to non-specifically interact with the selection surface. Optimisation of blocking and washing conditions were used to overcome this, and therefore measures to attempt to improve the folding of ribosome-displayed proteins such as uncoupling of the transcription and translation steps, or the addition of substances to assist folding were not required. It is assumed that the use of skim milk at 10% in the blocking reagent, along with inclusion of RNA, to achieve the specific selection observed (Figure 4.9) was sufficient to minimise non-specific interaction with the selection surface. In turn, the Tween-20 at 0.5% in the wash buffer was able to disrupt any remaining non-specific hydrophobic interactions, while still allowing

properly folded ribosome-displayed anti-GPE scFvs to bind to IGF-I. This Tween-20 percentage seems high, yet He *et al*., (1999) used Tween-20 at a level of 1% in their wash buffers to reduce non-specific binding. This may be an indication of the high amount of misfolded proteins being produced in the system, possibly due to the presence of 2 mM DTT causing too strong a reducing environment for correct disulphide pairing leading to exposure of hydrophobic regions, or to the inherent instability of the anti-GPE scFv framework as discussed in Chapter 3.

An interesting difference was observed between display with C_H3 as spacer, which showed no RT-PCR bands, and display using C_L as spacer, with the latter constructs exhibiting bands (Figure 4.5.B). This does not necessarily mean that the C_L domain is better than the C_H3 for allowing the nascent protein to fold. For instance, the C_H3 domain could be allowing the scFvs to fold correctly but no bands are being seen because conditions in the wash step may be too harsh, and due to low affinity all binding scFvs are lost before they can be recovered. Reduction in wash strength (eg. lowering Tween-20 concentration) may assist if this was the case. Conversely, the C_L may be detrimental to proper folding of the scFvs and thus the bands seen are due to non-specific interactions of misfolded complexes. As the C_L domain naturally follows V_L in antibodies, and RT-PCR bands were being generated, it was decided to first pursue this C_L as the preferred spacer and attempt to reduce the non-specific binding observed. The comparison of the effectiveness of a selection of primers (Figure 4.6) revealed that the constant domain primer used was important in obtaining an RT-PCR band. The primer 5269 was the only one to display good bands and was the best in subsequent experiments, for reasons not investigated, although the annealing temperature used in the RT-PCR was low enough to accommodate the melting temperatures of all the primers. Secondary structures in the RNA are presumed to be a factor here in reducing access of certain primers to their homologous sequence.

Little success was observed for specific selection of the lysozyme binder 4T10. However, in using this construct as a control binder to the negative control antigen lysozyme, these experiments involved optimisation of conditions for selection of anti-GPE to IGF-I. This may therefore indicate that this ribosome display system needs to be independently optimised for different proteins.

4.9.2 Mutagenesis of anti-GPE scFv by error-prone PCR

It was a relatively simple process to employ the method of Leung *et al*., (1989) to achieve the amino acid mutation rate of 4.2 mutations per scFv based on the five randomly chosen clones sequenced (Figure 4.10). There appears to be a random spread of mutations throughout the genes. The rate of

mutation is consistent with early successful attempts at using this method to affinity mature scFvs (Gram *et al*., 1992; Hawkins *et al*., 1992). Daugherty *et al*., (2000) showed in a quantitative analysis that libraries with this level of random point mutation do indeed harbour functional clones, albeit at a reduced frequency than less mutated libraries, although the chances of finding greater affinity increases among these functional clones are higher. Thus, there is a tradeoff with such a library, with the presence of more non-functional and possibly unstable scFvs, which may lead to problems of non-specific selection seen for display of the wild type, but the potential to isolate scFvs with much improved affinity and possibly other characteristics such as stability and solubility. As these properties in the anti-GPE scFv were inherently poor, it was decided that such a library was needed to improve the chances of generating mutants with substantial improvements.

4.9.3 Ribosome display and selection of EPGPE

Application of ribosome display to selection of the EPGPE library looked promising based on the intensity of RT-PCR bands in the first round of selection but this intensity did not increase with subsequent rounds of display, as might be expected based on the increase in titres when enriching for binders in phage display (McCafferty *et al*., 1990). He and Taussig (1997) reported such an enrichment as evidenced by increasing intensity of bands in their eukaryotic ribosome display system, as did Hanes and Pluckthun (1997) in their *E. coli* S-30 system, although these instances were using 'spiked' libraries where the target scFv was included at a very low level in a pool of non-target scFvs, not a direct comparison with the random point mutation library displayed here. Nonetheless, their increasing RT-PCR band intensities did correlate with increasing numbers of binders, whereas ribosome display of EPGPE showed decreasing intensities against IGF-I and increasing intensities against lysozyme.

Possibly, in early display rounds, the proportion of non-specific proteins in the library is relatively low. These may nonetheless be artificially selected via non-specific interactions with the IGF-I surface, along with real functional binders, from the rest of the pool of non-functional molecules. These non-specific binders will then be taken through to the subsequent rounds of display and selection, and if their non-specific interactions are stronger or less likely to be disrupted in the wash step than the specific, weak affinity IGF-I-binders, they may 'out-compete' the real binders and gradually constitute a much higher proportion of the total pool of scFvs. As this proportion increases, this 'out-competing' of the real binders for antigen may eventually be manifested in the appearance of non-specific RT-PCR bands against the control antigen lysozyme becoming more intense, if these non-specific interactions are broad, such as a general hydrophobic interaction. A

reason for the presence of an abundance of non-specific proteins could be that the 2 mM DTT causes too strong a reducing environment for correct folding of most scFvs within this library, although presence of DTT in ribosome display has been used in selection for stability (Jermutus *et al*., 2001). Another explanation could be that the anti-GPE scFv is too inherently unstable as discussed in Chapter 3, and therefore a difficult framework on which to base a mutagenesis library. An alternative explanation for non-specific RT-PCR bands is that the RNA template, that either hasn't been associated with ribosomes, or has been involved with unselected complexes but has become detached, is not being washed away totally, and therefore being amplified by RT-PCR. Testing of the amount of mRNA that is associated with ribosomes could be achieved by radio-labelling of the input mRNA in a translation that is uncoupled from transcription, and then separation of the ribosome complexes after the reaction by centrifugation, so complexed and uncomplexed mRNA can be counted and compared. This would provide an indication of the stability of the complexes. The ideal situation for displaying of the highest diversity possible is for ribosome display complexes to be stable during the whole selection procedure so that both protein and mRNA remains attached to the ribosome.

4.9.4 Screening of selected EPGPE clones

The fact that the three purified scFvs from a sixth round of ribosome display all showed a strong propensity to aggregate rather than form monomeric species (described in 4.6) suggested that misfolded scFvs were making it through to this stage. The ELISA screening of 64 clones from a fourth round of ribosome display revealed mostly weak binders or binders with high background responses against the negative control antigens, showing very little enrichment had occurred at this stage, further implying that non-specific binders were being too easily selected. The sequences of the best binding (ELISA) error-prone PCR generated mutants revealed an amino acid mutation rate of 6.7 per scFv as opposed to 4.2 per scFv for the preselected library. This is contrary to the findings of Daugherty *et al*., (2000) who showed that selected scFvs from a highly mutated library tended to show fewer mutations than the average for the preselection library. This difference may again indicate selection bias here towards non-functional and non-specific scFvs due to their having more mutations than can be accommodated for retention of stability of the framework. Analysis of the sequences (Figure 4.18) of the best binding scFvs compared to anti-GPEwt – EP50, EP58, and EP62, showed a seemingly random spread of mutations occurring in both the framework and CDR regions and these were therefore purified for characterisation.

4.9.5 Expression and purification of the mutant scFvs

Most of the properties of the anti-GPEwt scFv are reflected in the error-prone PCR mutants. The amount of scFv detected in the culture supernatant (Figure 4.21) is an indication of its toxicity. This may be related to the amount seen in the aggregate fractions (Figures 4.19 and 4.21), and in insoluble precipitates (Figure 4.21), reflecting poor folding which may be causing the hydrophobic associations leading to aggregation and cell lysis (Georgiou and Valax, 1996; Suominen *et al*., 1987) or precipitation. Therefore it appears there has been no great improvement in reducing propensity to aggregate and toxicity or increasing solubility as a result of the mutations. There are subtle differences in the amount of soluble monomer produced between the mutants and the monomers (Figure 4.19). Point mutations leading to improvements in expression levels and solubility have been observed (Coia *et al*., 1997; Hall and Pluckthun, 1999; Chowdhury *et al*., 1998). However, the improvements seen here are minimal and significant amounts of all scFvs run as higher molecular weight species. Nonetheless enough of all mutants could be purified for analysis of binding on the BIAcore.

4.9.6 Characterisation of binding of selected scFvs

EP58 and EP62 only exhibited weak binding by BIAcore (data not shown) showing that the ELISA method here is only a rough guide for the screening of best binders. The ELISA responses of both these scFvs were similar to that of the wild type, suggesting that the signal is a function not only of monomer affinity, but also expression levels, avidity from multimeric species, and non-specific interactions. The BIAcore data for EP50 showed an improvement in affinity of 2.6-fold which is not remarkable. Hanes *et al*., (1998) showed an affinity improvement of up to 65-fold using their *E. coli* S-30 system, although the mutations in this case were introduced within the ribosome display system by use of low fidelity enzymes between cycles of selection. EP50 has 4 amino acid mutations. Three of these mutations are in CDRs - G to S in HCDR2, V to I in HCDR3, and R to Q in LCDR2. Most interesting of these is the HCDR2 mutation because of the unusual nature of this CDR as discussed in Chapter 3, and the HCDR3 mutation, as this is a crucial CDR in the binding of an antibody to its antigen (Chothia and Lesk, 1987). There is also a mutation in framework 1 of the heavy chain which cannot be discounted as such mutations away from the binding site are often crucial and have been observed as having significant effects over the affinity of an antibody (Hawkins *et al*., 1993; Deng *et al*., 1994; Daugherty *et al*., 2000). However, without structural information to enable identification of the disposition of these mutations with respect to binding interfaces, it is hard to make conclusions about the relative importance of any of these mutations. To isolate one weakly improved mutant from a screen of 64 round four clones suggests that the

ribosome display and selection system employed here has not been very efficient at this stage. One might expect to have a reasonable chance of isolating such a modestly improved mutant from a screen of clones from the preselected library.

It appears that improved binders are not being enriched over non-specific binders. Perhaps competitive elution, where bound complexes would be dissociated by the addition of soluble antigen, may be one way of improving the isolation of specific binders. Also, washing and binding steps may need to be further refined. A more stable framework or better spacer may be required, or perhaps the transcription and translation needs to be uncoupled. It is suggested that the DTT needs to go up to 10 mM to start having a negative effect (He *et al*., 1999) but this is probably protein dependent. Hanes *et al*., 1999 claimed that the uncoupled reticulocyte system was 100-fold less efficient than their optimised *E. coli* S-30 system and the coupled reticulocyte system 100-fold less efficient again during a side-by-side comparison. There is no doubt scope for improvement of the rabbit reticulocyte ribosome display system.

CHAPTER 5

ANTI-GPE AND NC10 CHIMAERIC SCFV LIBRARY CONSTRUCTION BY DNA SHUFFLING AND RIBOSOME DISPLAY OF THIS LIBRARY

5.1 Introduction

5.1.1 General

The objectives of the work in this chapter were to determine whether features of an anti-GPE scFv could be DNA shuffled with an NC10 scFv framework to create functional chimaeric antibodies by (i) grafting the CDRs from the anti-GPE antibody onto the framework of the NC10 scFv; (ii) creating a library of chimaeric scFvs by DNA shuffling of the anti-GPE scFv with this grafted NC10 scFv; and (iii) determining whether functional chimaeric proteins could be isolated from this library by ribosome display.

NC10 is an antibody with specificity for N9 neuraminidase (NA) of influenza virus (Colman *et al*., 1989). The scFv version of the antibody has been cloned and characterised previously and shown to be stable with good soluble expression levels (Malby *et al*., 1993). The NC10 scFv gene was therefore chosen for this study as a scaffold for shuffling with the anti-GPE scFv gene, exploring a novel means of creating diversity in an antibody framework. Initially, the NC10 scFv framework was used as host for the grafting of the CDRs from anti-GPE in place of its wild type CDRs. CDR grafting has been previously employed as a means of improving the stability of an scFv (Jung and Pluckthun, 1997), for humanisation (Jones *et al*., 1986), or for altering the specificity of an antibody-like molecule (Nuttall *et al*., 1999). This CDR grafting of NC10 was not expected to produce a functional anti-GPE scFv fragment in this case as the sequence and antibody subgroup differences between NC10 (V_H – subgroup IIB, V_L – subgroup V) and anti-GPE (V_H – subgroup IIA, V_L – subgroup II; Kabat, 1991) would most likely cause the grafted CDRs to assume the improper orientation for presentation to their cognate antigen. The purpose of shuffling this anti-GPE CDR-grafted version of NC10 against wild type anti-GPE was to produce a library of chimaeric scFvs, in which some members of this library would gain a mix of sequences from the parental fragments that would confer functionality (binding to IGF-I), and possibly good expression characteristics and stability. DNA shuffling has been shown to be a highly effective method for improvement of proteins such as enzymes (Crameri *et al*., 1998; Kumamaru *et al*., 1998; Christians *et al*., 1999). Shuffling of two scFvs has been demonstrated at the genetic level with no cloning

(Lorimer and Pastan, 1995). It has also been used to shuffle synthetic CDRs into a master scFv framework (Crameri *et al*., 1996) and to delineate useful from deleterious mutations in the selection of an scFv without disulphide bonds (Proba *et al*., 1998). To date, no cross-antibody shuffled scFv genes such as those described by Lorimer and Pastan (1995) have been cloned, their proteins expressed, or their function investigated. More recently, a functional scFv was reported to have been selected from a phage library produced by the DNA shuffling of pools of V_L domains, with a four-fold affinity improvement from a parental scFv (Huls *et al*., 2001). Likewise, van den Beuken *et al*., (2001) DNA shuffled a library of V_L domains to obtain functional binders. However, in neither case, was information reported to describe recombination events that would show these fragments were cross-antibody chimaeras.

In this chapter an scFv based on NC10 with grafted anti-GPE CDRs (NC10GPE) was produced. A DNA shuffling method for recombination between NC10GPE and anti-GPE was developed to produce the chimaera libraries GPENC and H2MNC. These libraries were subjected to ribosome display. Proteins were isolated from these libraries by selection utilising GPE peptide elution, GPE 10-mer elution, and selection utilising the BIAcore 1000. Sequences from clones isolated by all three of these selection strategies were genuine chimaeras. Best binding clones as measured by ELISA were expressed and purified for characterisation of binding, with one chimaera, selected using the BIAcore, shown to have a specific IGF-I-binding activity.

5.1.2 Antecedent work

The cloning of the NC10 antibody as an scFv has been described (Malby *et al*., 1993). The NC10 scFv gene was supplied in the phagemid vector pHFAsacNC10 1.16 by Dr. J. L. Atwell (CSIRO Molecular Science, Parkville).

5.2 Grafting of the anti-GPE CDRs onto the NC10 framework

5.2.1 Subcloning of NC10 scFv

The NC10 scFv gene was released from the pHFAsacNC10 1.16 vector by an *Sfi*I/*Not*I digest (2.1.7). This scFv gene was ligated (2.1.9) into likewise digested pGC. This ligation was transformed into electrocompetent *E. coli* HB2151 (2.1.11). Plasmids prepared from clones containing the insert DNA as identified by colony PCR (2.1.12) were DNA sequenced (2.1.14). Correct subcloning was checked by comparison of these sequences with the published sequence

data for the NC10 scFv (Malby *et al*., 1993). The DNA sequence and deduced amino acid sequence of NC10 cloned in pGC is shown in Figure 5.1.

5.2.2 Design of grafted construct

Each of the anti-GPE CDRs was grafted sequentially onto the NC10 framework by PCR. Primers were designed that coded for regions of homology to the NC10 framework adjacent to the CDRs, with overhangs that coded for the anti-GPE CDRs to be grafted. These primer sequences are shown in Table 2.1. For each CDR, two primers were designed. One primer was used to amplify a fragment of the gene from the 5′ end through to the CDR coding sequence. The other primer was used to amplify the fragment from the CDR coding sequence through to the 3′ end of the gene. These two fragments thus possessed overlapping homologous sequences that could be joined by PCR. The primers were designed to leave large overlapping complementary sequences so that SOE PCR could be performed with high annealing temperatures. Each newly grafted scFv could then be used as template for grafting of the next CDR. The forward and reverse primers 6227 and 6228 (Table 2.1) were designed with exact homology to the sequence of the subcloned NC10 scFv. 6227 also codes for a 5′ overhang containing an *Sfi*I site and 6228 codes for a 3′ overhang with a *Not*I site. The relative positions of annealing of each of the graft primers are indicated on the NC10 scFv sequence in Figure 5.1.

5.2.3 PCR construction of NC10GPE

The construction of NC10GPE is shown schematically in Figure 5.2.B. The PCRs to amplify each of the fragments for CDR grafting were performed under the standard conditions as described (2.1.4). The amplified fragments were separated by agarose gel electrophoresis (Figure 5.2.A) and gel-purified (2.1.6.1). The joining of the 2 overlapping fragments was performed using SOE PCR as described (2.1.4.2). The CDRs were grafted sequentially in the order HCDR3, HCDR1, HCDR2, LCDR1, LCDR2 and LCDR3 to give the series grafted NC10 scFvs, named respectively H3G, H1G, H2G, L1G, L2G, and the completed graft construct NC10GPE (Figure 5.2.B). Each sequential graft was cloned in pGC as described previously (3.2.5) and positive clones sequenced (2.1.14) to verify correct construction before use as template for the grafting of the next CDR.

5.2.4 Cloning and sequencing of NC10GPE

The final NC10 graft containing all anti-GPE CDRs (NC10GPE) was cloned into pGC as described (3.2.5) and confirmed by DNA sequencing (2.1.14). The sequence of NC10GPE is shown in Figure 5.3.

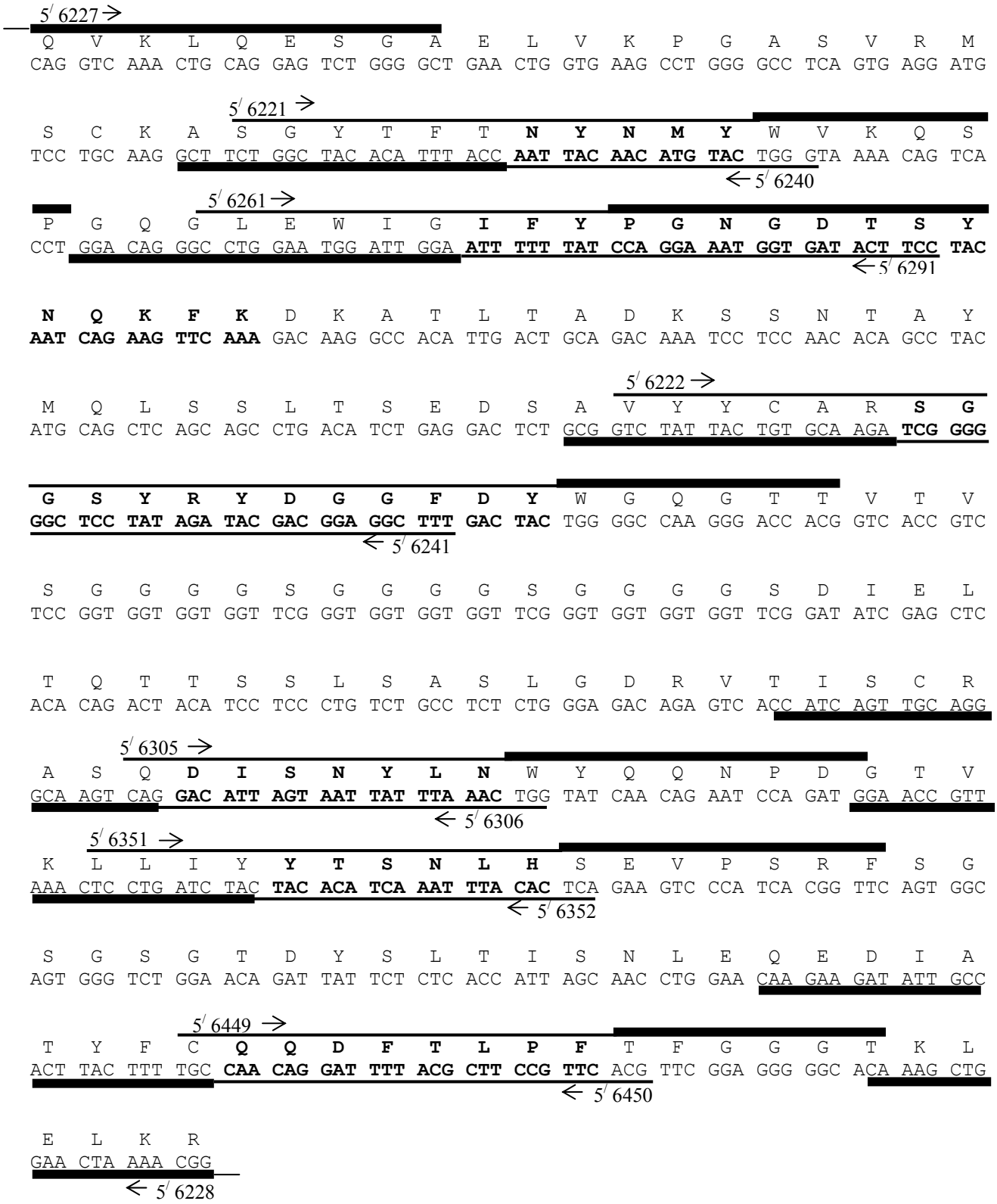

Figure 5.1 Nucleic acid sequence and deduced amino acid sequence of NC10 scFv and the annealing positions of the anti-GPE CDR grafting primers. Thick lines show areas for PCR annealing to NC10. Thin lines show areas of primers encoding anti-GPE CDR sequences. Forward primers are above the sequence and reverse primers are below. CDRs in bold.

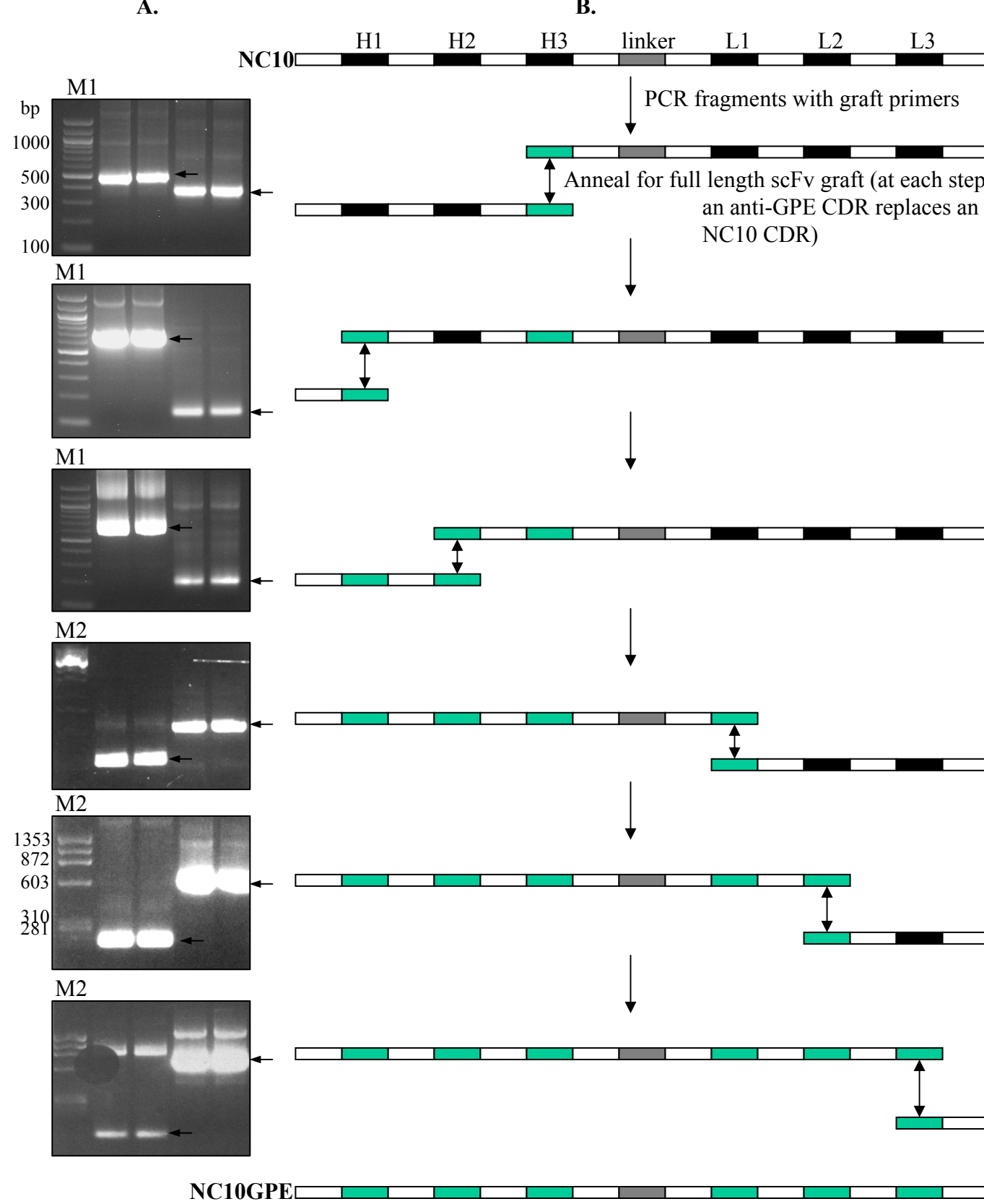

Figure 5.2 Agarose electrophoresis (A) and schematic of gene fragments (B) of the PCR construction of NC10GPE. Arrowed gel bands correspond to the schematic gene fragments opposite. NC10 framework in white; NC10 CDRs in black; anti-GPE CDRs in green. M1, 100bp

```
 Q   V   K   L   Q   E   S   G   A   E   L   V   K   P   G   A   S   V   R   M
CAG GTC AAA CTG CAG GAG TCT GGG GCT GAA CTG GTG AAG CCT GGG GCC TCA GTG AGG ATG

 S   C   K   A   S   G   Y   T   F   T  D   Y   T   M   H   W   V   K   Q   S
TCC TGC AAG GCT TCT GGC TAC ACA TTT ACC GAT TAC ACC ATG CAC TGG GTA AAA CAG TCA

 P   G   Q   G   L   E   W   I   G  G   I   I   P   G   N   G   D   T   S   Y
CCT GGA CAG GGC CTG GAA TGG ATT GGA GGT ATT ATT CCA GGA AAT GGT GAT ACT TCC TAC

 N   Q   K   F   K   D   K   A   T   L   T   A   D   K   S   S   N   T   A   Y
AAT CAG AAG TTC AAA GAC AAG GCC ACA TTG ACT GCA GAC AAA TCC TCC AAC ACA GCC TAC

 M   Q   L   S   S   L   T   S   E   D   S   A   V   Y   Y   C   A   R   N   Y
ATG CAG CTC AGC AGC CTG ACA TCT GAG GAC TCT GCG GTC TAT TAC TGT GCA AGA AAT TAC

 Y   G   V   D   W   F   F   D   V   W   G   Q   G   T   T   V   T   V   S   G
TAC GGA GTG GAC TGG TTC TTC GAT GTC TGG GGC CAA GGG ACC ACG GTC ACC GTC TCC GGT

 G   G   G   S   G   G   G   G   S   G   G   G   G   S   D   I   E   L   T   Q
GGT GGT GGT TCG GGT GGT GGT GGT TCG GGT GGT GGT GGT TCG GAT ATC GAG CTC ACA CAG

 T   T   S   S   L   S   A   S   L   G   D   R   V   T   I   S   C   R   A   S
ACT ACA TCC TCC CTG TCT GCC TCT CTG GGA GAC AGA GTC ACC ATC AGT TGC AGG GCA AGT

 Q   S   I   V   H   R   N   G   N   T   Y   L   E   W   Y   Q   Q   N   P   D
CAG AGC ATT GTA CAT AGA AAT GGA AAC ACC TAT TTA GAG TGG TAT CAA CAG AAT CCA GAT

 G   T   V   K   L   L   I   Y   K   V   S   N   R   F   S   E   V   P   S   R
GGA ACC GTT AAA CTC CTG ATC TAC AAA GTT TCC AAC CGA TTT TCA GAA GTC CCA TCA CGG

 F   S   G   S   G   S   G   T   D   Y   S   L   T   I   S   N   L   E   Q   E
TTC AGT GGC AGT GGG TCT GGA ACA GAT TAT TCT CTC ACC ATT AGC AAC CTG GAA CAA GAA

 D   I   A   T   Y   F   C   F   Q   G   S   H   V   P   W   T   F   G   G   G
GAT ATT GCC ACT TAC TTT TGC TTT CAA GGT TCA CAT GTT CCG TGG ACG TTC GGA GGG GGC

 T   K   L   E   L   K   R
ACA AAG CTG GAA CTA AAA CGG
```

Figure 5.3 The nucleotide sequence and deduced amino acid sequence of NC10GPE. The CDR regions are in bold.

5.3 Expression and Characterisation of NC10 graft clones

5.3.1 Expression and purification

Once the sequences of all the NC10 graft scFvs had been verified, characterisation of their expression and binding was undertaken. All scFvs were detectable with antibodies to the C-terminal FLAG tag by Western blot (2.3.2) of periplasmic extracts (2.2.2) from small-scale cultures (2.2.1) (data not shown). Analysis of binding of the graft clone scFvs from freshly transformed small-scale culture supernatant was performed by ELISA (2.3.12). The ELISA data (Figure 5.4) shows that there are quite low ELISA signals (A_{405nm} = 0.2 - 0.5) and substantial cross-reactivity with negative antigens, particularly lysozyme. The four clones with the strongest ELISA signal and best specificity, H1G, H3G, L2G and NC10GPE, were chosen for further analysis.

These clones were all grown in 1 L cultures (2.2.1) for expression of monomeric scFv as described for wild type anti-GPE (3.3). Periplasmic extracts (2.2.2) from cells harvested 2 h post-induction were applied to an anti-FLAG column for affinity purification (2.3.8). Protein eluted from the anti-FLAG column was dialysed against TBS (2.3.8), concentrated to ~1 mL (2.3.9) and then subjected to gel filtration chromatography (2.3.10) using either Superose 12 or Superdex 200 columns equilibrated in HBS/P20. Substantial oligomer and aggregate levels can be seen in the L2G and H1G preparations (Figure 5.5; NC10GPE data not shown). Peaks corresponding to expected retention times for scFv monomer were collected. These were concentrated and applied again to the same column for secondary collection to attempt to achieve higher purity for BIAcore analysis.

5.3.2 Binding of graft scFvs by BIAcore

The binding of purified graft scFvs produced as described in 5.3.1 was investigated by surface plasmon resonance using the BIAcore 1000. The protein concentrations were estimated (2.3.11) and analyses performed against immobilised IGF-I, des(1-3)IGF-I, and lysozyme (2.3.13.2). NC10GPE exhibited negligible binding to IGF-I (data not shown). Weak responses were seen for the other three scFvs but the nature of these interactions appeared to be non-specific as shown in Figure 5.6 where L2G shows a greater response binding to lysozyme than the other antigens. Large refractive index changes suggest the possibility of heterogenous samples due to misfolded species within the collected peaks. These bulk refractive effects have been subtracted from the curves in Figure 5.6 for ease of analysis. The same non-specificity was seen for both H1G and H3G although the responses were even weaker (data not shown). It therefore appears that the NC10 framework gains no appreciable affinity for binding to IGF-I in a specific manner by the grafting of any of the anti-GPE

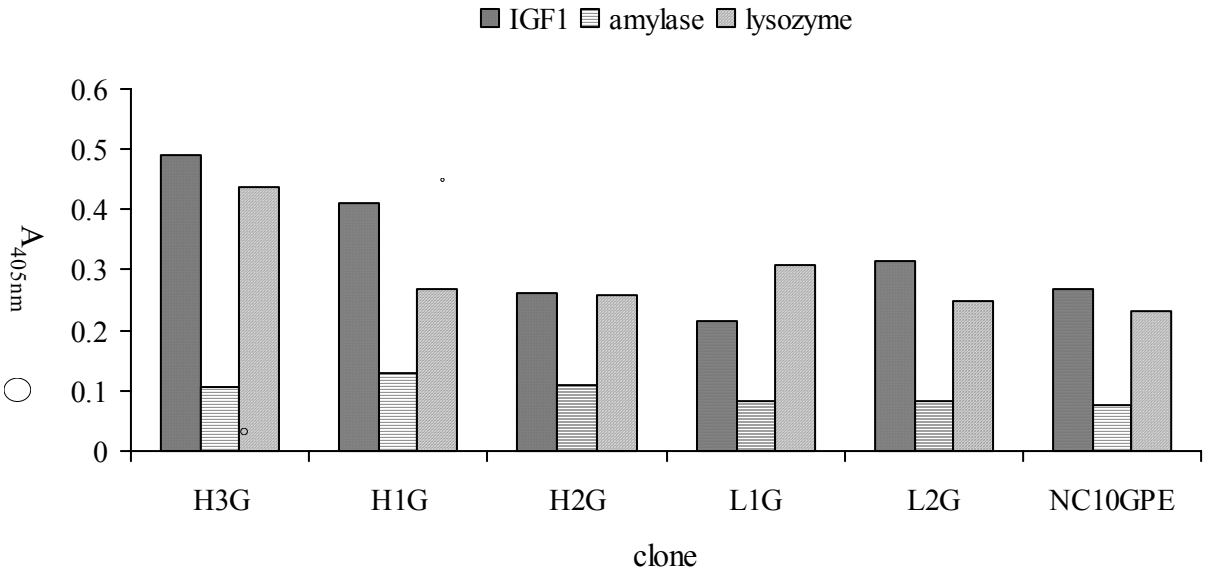

Figure 5.4 ELISA of binding of graft clone scFvs.

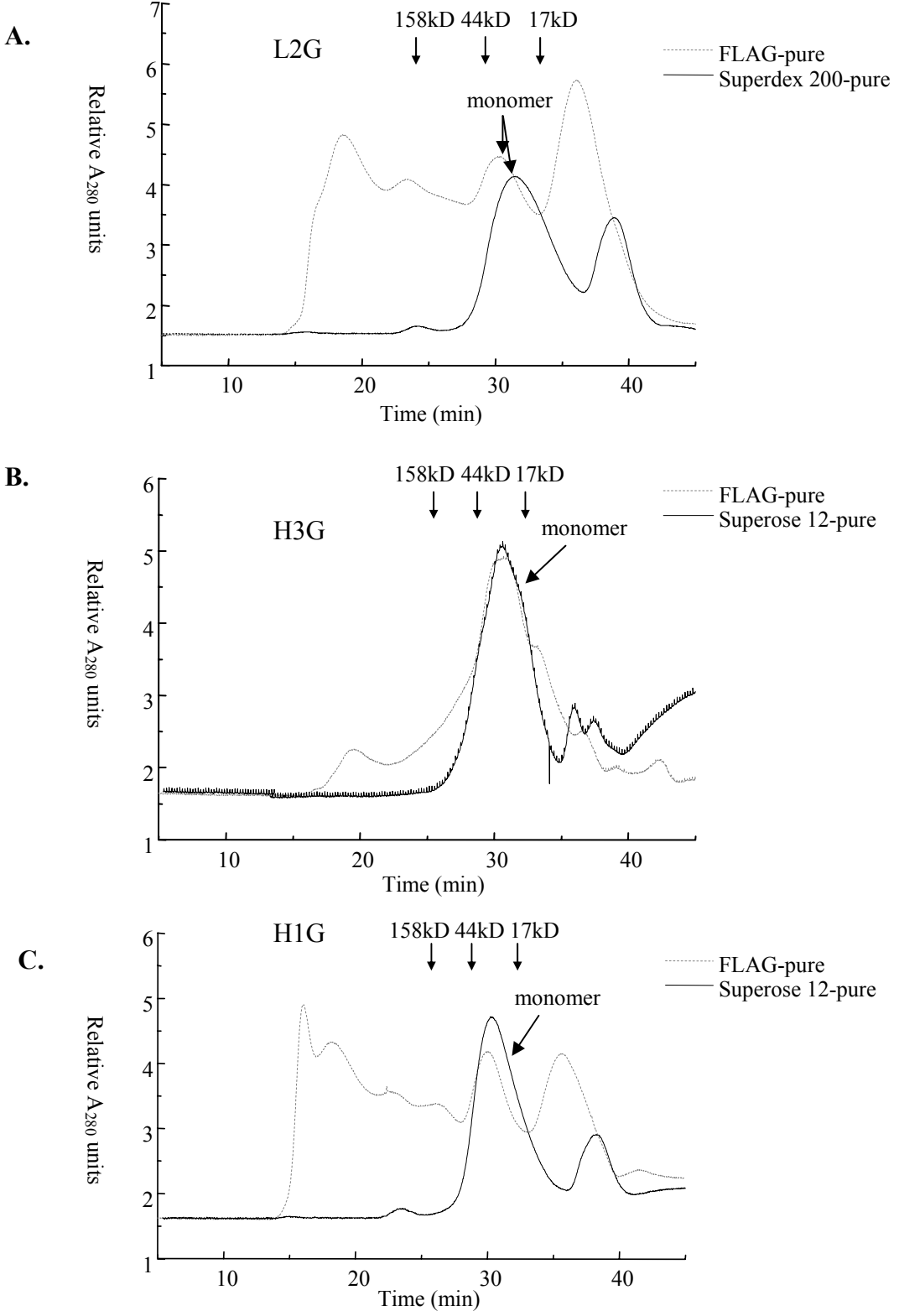

Figure 5.5 Gel-filtration chromatography purification of monomeric graft scFvs. A. L2G on Superdex 200; B. H3G on Superose 12; and C. H1G on Superose 12. The grey dashed curves show the profiles after FLAG affinity purification of expression culture periplasm. The black curves show the profile after monomer was collected, concentrated and reloaded onto the column. Retention times of BioRad molecular weight standards are indicated with arrows.

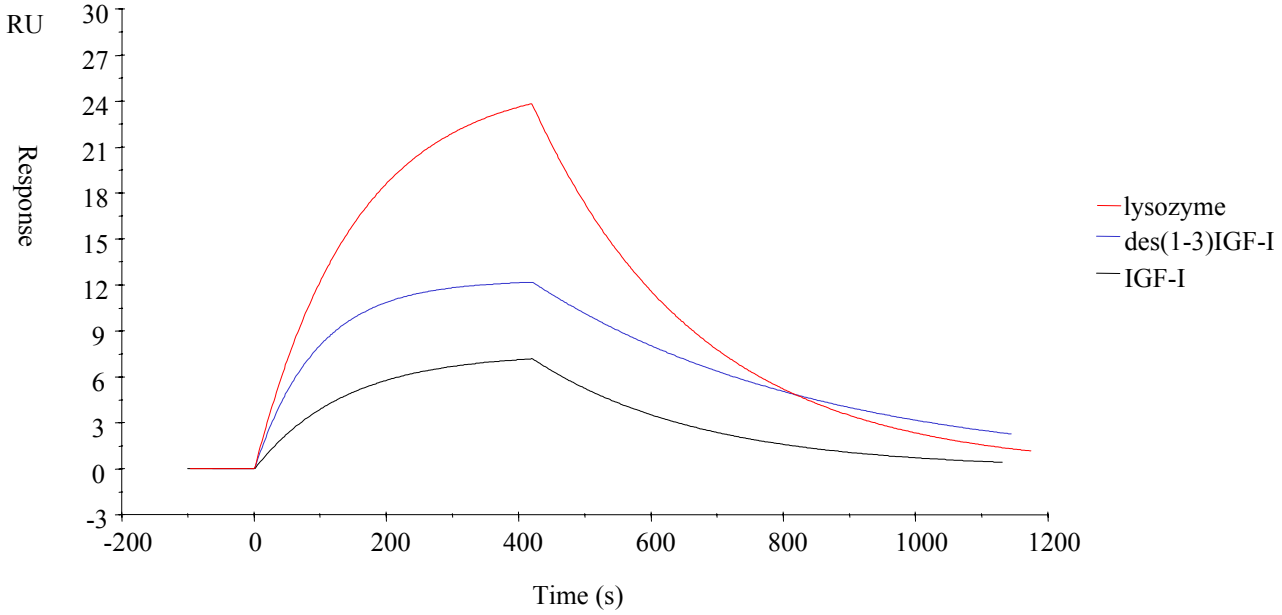

Figure 5.6 Overlaid BIAcore sensorgrams of binding of 1 μM L2G to immobilised antigens. Bulk refractive index changes have been subtracted from these curves.

CDRs. It could be argued that the weak binding to both IGF-I and des(1-3)IGF-I shows a shift in specificity away from the GPE epitope. However, the response against lysozyme appears to discount this and confirms the non-specificity seen in the ELISA results. The grafting may prevent proper folding of the framework, and therefore proper presentation of the CDRs to antigen, or the CDRs on properly folded framework may not be displayed in the ideal orientation for binding to the epitope.

5.4 DNA shuffling

5.4.1 DNaseI fragmentation of genes

The DNA shuffling protocol developed is described in 2.1.16 and was adapted from that published by Stemmer (1994a). The gene fragments to be shuffled were prepared by PCR amplification (2.1.4) and these scFvs were gel purified (2.1.6) and quantitated (2.1.8). In developing the DNA shuffling method, DNaseI enzymes from a number of commercial sources were tried before choosing the Boehringer Mannheim enzyme, as its activity in digesting the DNA was more controllable and reproducible. DNA to be shuffled was digested to approximately 50 bps in length with the extent of digestion assessed by agarose gel electrophoresis (2.1.16.1). To achieve digestion to this desired level of fragmentation (Figure 5.7, lanes 1 and 2), it was found that 25 min digestion with 1 unit of Boehringer Mannheim DNaseI at room temperature was sufficient. Initially the total sample of DNaseI-digested fragments was electrophoresed in agarose for good visualisation of the bands with the DNA then electroeluted from the agarose and ethanol precipitated. However, it was difficult to achieve good regeneration of genes from fragments prepared in this way in the subsequent PCR steps. Therefore, in subsequent experiments, a portion of the DNaseI-digested DNA (30-40%) was analysed on an agarose gel, and the rest was desalted by applying to G25 columns (2.1.15).

5.4.2 Primerless PCR reassembly of genes

The next stage in producing a shuffled gene was to generate DNA in a primerless PCR (2.1.16.2), where regions of homology in the DNaseI digested fragments were able to prime off each other, leading to DNA fragments of increasing length being constructed, visualised as the smear by agarose electrophoresis. It generally took 45 cycles of primerless PCR on substantial amounts of fragment template (~ 0.2 – 0.5 μg), with around 20 - 30 μL of the reaction loaded on an agarose gel to visualise a smear spanning full-length gene size (Figure 5.7.B, lanes 3-5). The annealing

temperature employed at this point is important. For shuffling point mutated versions of the same parent gene, an annealing temperature of 50°C or more should be adequate, as the fragments will be priming off each other with regions of nearly 100% homology. This was done with shuffling of two point-mutated variants of anti-GPE (5.6) generated by the error-prone PCR described in Chapter 4. Shuffling of anti-GPE with NC10GPE would require a lower annealing temperature to encourage fragments of lower homology (i.e. from different antibody sequences) to prime off each other. *Taq* polymerase was used in this PCR to increase the possibility for incorporation of point mutations.

5.4.3 Full-length gene amplification

The final step in producing shuffled genes is to amplify the full-length genes using the forward and reverse primers to the parent gene and encoding restriction sites for cloning, achieved by a standard PCR amplification using primerless PCR product as template (2.1.16.3), generating a discrete scFv band for subsequent cloning and analysis. Around 20 – 25 cycles of PCR was ample to attain this. Again, *Taq* polymerase was used for this step, but other enzymes with higher fidelity could also have been used.

5.5 DNA shuffling of anti-GPE scFv with NC10 scFv

5.5.1 Shuffling of the genes

Initially this procedure was used for the shuffling of anti-GPE scFv with the parent NC10 scFv (ungrafted) genes. Annealing in the primerless PCR (2.1.16.2) was performed at 35°C to encourage chimaerogenesis. This low annealing temperature was used due to the significant sequence variation between the two genes (64.7% homology at amino acid level, 68.7% homology at the nucleic acid level). A visible smear was regenerated in the primerless PCR (Figure 5.7.A, lanes 3 and 4) but there was no peak of intensity in the smear at the approximate size of a full-length scFv, suggesting a high proportion of irregular-size shuffled products was being constructed. PCR for full length gene amplification (2.1.16.3), using a cocktail of primers encoding both the anti-GPE and NC10 parent genes, yielded scFv-sized bands but also significant smearing (Figure 5.7.A, lanes 5-8), again suggesting that this PCR may have been picking up irregularly constructed shuffle products and therefore heterogeneity in size of these products.

5.5.2 Cloning and sequencing of the shuffled genes

The PCR amplified shuffled scFv bands were gel-purified (2.1.6.1), *Sfi*I/*Not*I digested (2.1.7), ligated into likewise digested pGC (2.1.9) and transformed into electrocompetent *E. coli* (2.1.11).

Four clones were randomly selected for scFv DNA sequencing (2.1.14). The deduced amino acid sequences (Figure 5.8) showed that rearrangement of the genes had occurred. Both GPNC1 and GPNC4 comprise sequence regions from both parental genes. Data for a middle section of GPNC3 could not be obtained but it can be seen that the gene is also a chimaera. GPNC2 appears to be a truncated gene resulting from the hybridisation of a small fragment from framework 1 of NC10, an eight-residue fragment of unknown origin, and small V_L framework three fragments from both genes. Such low fidelity hybridisation could be expected under such a low annealing temperature (35^0C) and is possibly reflected in the abovementioned smearing (Figure 5.7.A. lanes 5-8). These results showed that, although the procedure may be fairly inefficient, as indicated by the low intensity and sharpness of scFv bands (Figure 5.7.A lanes 5-8), it could indeed generate chimaeras from low homology genes without homologous CDRs (such as in NC10GPE) that would be expected to provide a convenient location for crossovers.

5.6 DNA shuffling of two error-prone PCR point mutated anti-GPE scFvs

5.6.1 Shuffling of the genes

Two of the clones that had been prepared by the error-prone PCR mutation strategy described in Chapter 4 were shuffled to assess if the procedure developed was effective at a higher annealing temperature on sequences with closer homology. The clones – EP1-4 and EP1-8 had six and five point mutations respectively as determined from the sequencing of these clones described in 4.4.3. Strong smears with a peak in intensity about the size of an scFv gene, indicating efficient shuffling, were generated with primerless PCR (2.1.16.2), using three different template concentrations at an annealing temperature of 50^oC, as can be seen in Figure 5.7.B (lanes 3-5). Strong, discrete scFv bands were amplified (2.1.16.3) from this DNA smear (Figure 5.7.B lanes 6-9).

5.6.2 Cloning and sequencing of the shuffled genes

These shuffled scFv bands were cloned as described for the previous shuffle (5.5.2). Sequencing (2.1.14) of five random clones revealed that the original point mutations of the parent mutants were now spread randomly through each of these (Figure 5.9). Furthermore, the process had led to additional amino acid point mutations (4.2 per scFv) being incorporated into the genes. This result provided evidence that the DNA shuffling protocol was effective and thus the low efficiency seen for anti-GPE/NC10 shuffling was a function of the lower annealing temperature and/or lesser degree of homology of the genes.

5.7 DNA shuffling of anti-GPE and anti-GPE H2M scFvs with NC10GPE scFv

5.7.1 Shuffling of the genes

Both the anti-GPE wild type and anti-GPE H2M scFvs were shuffled independently with the NC10GPE scFv. The annealing temperature was set at 50^{o}C taking into account homology of gene fragments due to the grafted CDRs on NC10GPE. It would be expected that formation of chimaeras incorporating NC10 framework sequences might often be detrimental to presentation of anti-GPE CDRs by shuffled scFv framework for reasons mentioned before (5.1.1). Thus, *Taq* polymerase was used in the PCR for the incorporation of point mutations to allow the shuffled framework to evolve towards correct presentation of CDRs to antigen. Figure 5.7.C shows the progress of this process, which appears more efficient than that achieved for shuffling with NC10 wild type (Figure 5.7.A), with smears peaking in density at scFv size and regenerated full length fragments sharper in intensity.

5.7.2 Cloning and sequencing of the shuffled genes

To analyse the effectiveness of the shuffling procedure both pools of shuffled genes – anti-GPEwt with NC10GPE and anti-GPE H2M with NC10GPE – were cloned as described in 5.5.2 for the previous shuffles. Sequencing (2.1.14) was performed on five random clones from each pool. The sequence data shows that shuffling was successful with all clones sequenced being chimaeric. These sequence alignments are shown in Figure 5.10 for the shuffling of anti-GPEwt with NC10GPE. These clones were given the names GPENC1, GPENC2 etc. The exact site of recombination was not possible to be determined by observation at the amino acid level, so the shuffled genes were analysed at the nucleotide level and the crossover point estimated to be midway between the last definitive anti-GPE base and the first definitive NC10 base. As expected, the homology of the CDRs provided a convenient place for recombination that was often utilised by the fragments for annealing. For instance, in GPENC clone 1, the gene is made up of four NC10 segments and three anti-GPE segments. Therefore there are six crossover events in creating this chimaera. Three of these appear to have occurred in a CDR (HCDR1, LCDR1 and LCDR2), and a fourth has occurred at the linker, an area of strong homology. Likewise for GPENC clone 2, of the five crossovers, three appear to have occurred in CDRs (HCDR3, LCDR2 and LCDR3). Also the process has introduced a number of point mutations, again at an average of 4.2 per gene. This is similar to the rate for the error-prone PCR of anti-GPE described in 4.4.3. This shows that the DNA shuffling procedure alone, without any altering of PCR conditions, enhances the infidelity of Taq polymerase. A deletion of three nucleotides within the codons for Glu and Leu of GPENC5 has led

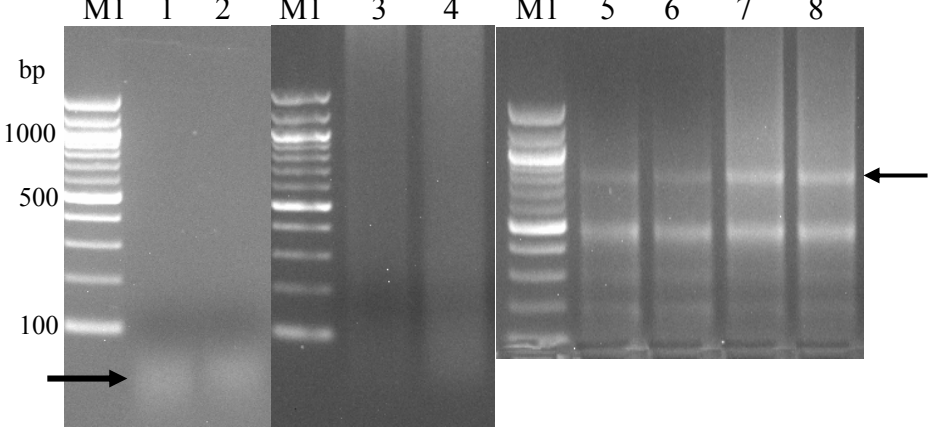

Figure 5.7.A Agarose electrophoresis of the DNA shuffling of anti-GPE with NC10 scFv. M1, 100 bp DNA ladder. Lanes 1 and 2, DNaseI-digested anti-GPE and NC10 genes respectively; lanes 3 and 4, primerless PCR-generated smears from varying template levels; lanes 5-8 flanking primer PCR for full-length scFv. Left arrows – DNaseI fragments. Right arrows – full length scFvs.

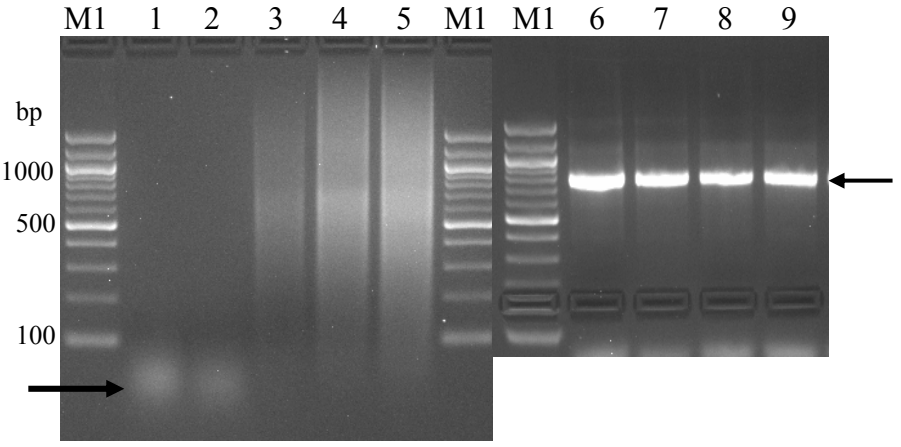

Figure 5.7.B Agarose electrophoresis of the DNA shuffling of EP1-4 with EP1-8 scFvs. M1, 100 bp DNA ladder. Lanes 1 and 2, DNaseI-digested genes EP1-4 and EP1-8 respectively; lanes 3-5, primerless PCR-generated smears from varying template levels; lanes 6-9, flanking primer PCR for full-length scFv. Arrows as in Figure 5.7.A.

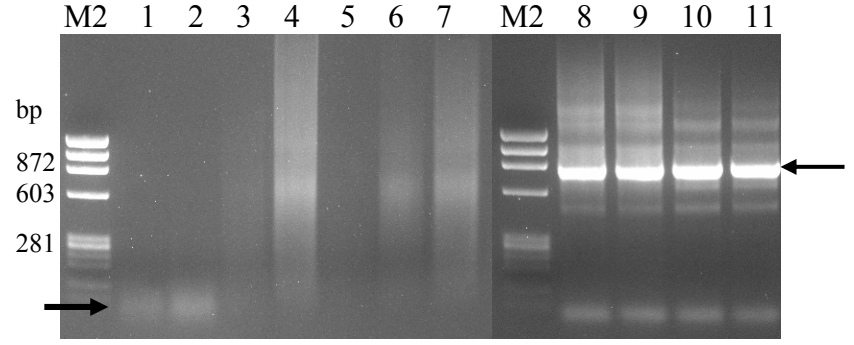

Figure 5.7.C Agarose electrophoresis of the DNA shuffling of anti-GPE and anti-GPE H2M with NC10GPE scFv. M2, ϕX174 DNA markers. Lanes 1, 2 and 5, DNaseI-digested genes - anti-GPE, NC10GPE and anti-GPE H2M respectively; lanes 3 and 4, primerless PCR-generated smears for anti-GPE/NC10GPE, and lanes 6 and 7, for anti-GPE H2M/NC10GPE from varying template levels; lanes 8 and 9, flanking primer PCR for full-length anti-GPE/NC10GPE scFv, and lanes 10 and 11, for anti-GPE H2M/NC10GPE scFv. Arrows as in Figure 5.7.A.

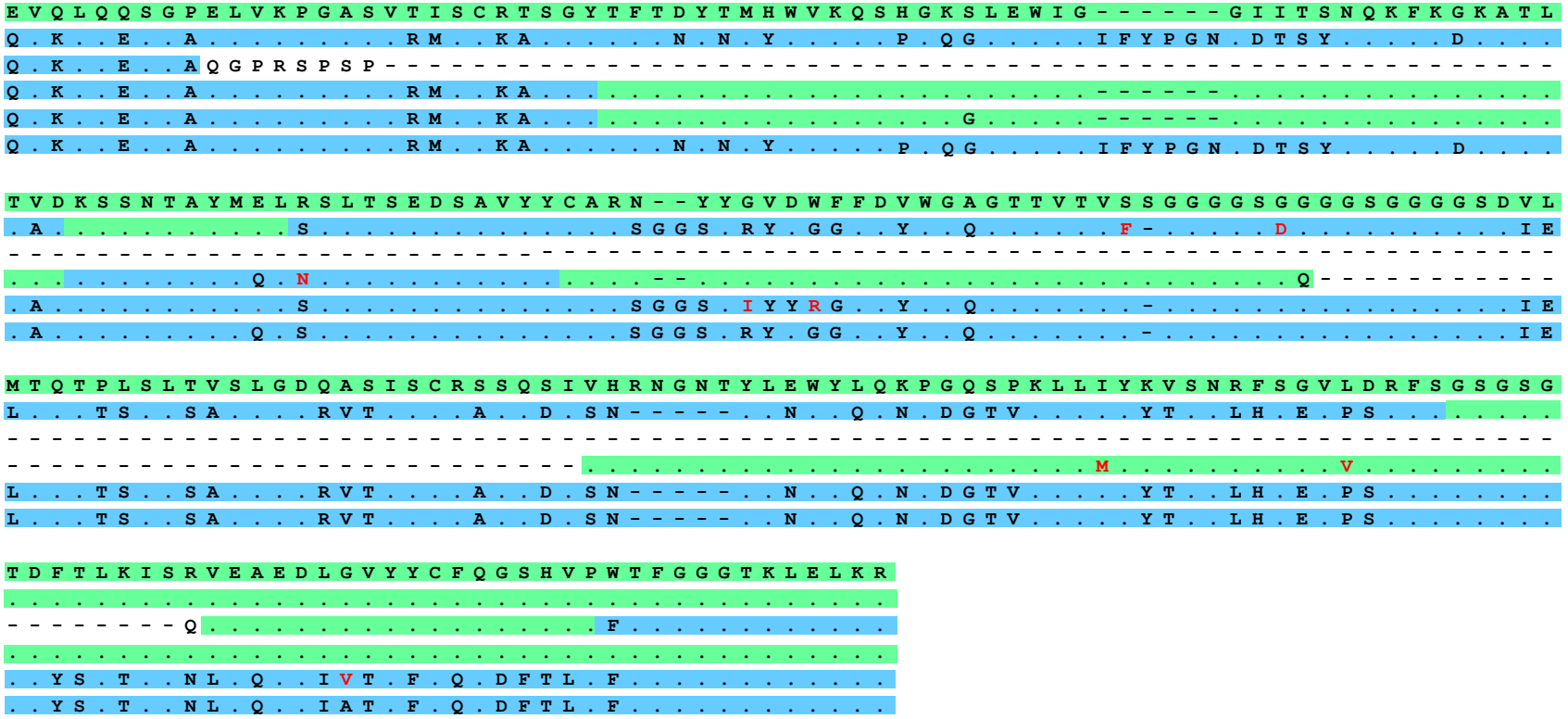

Figure 5.8 Deduced amino acid sequences of scFvs constructed by DNA shuffling of anti-GPE and NC10 sequences. Anti-GPE segments in green. NC10 segments in blue. Point mutations in red. Only residues differing from the anti-GPE wild type sequences are shown. Residues the same as anti-GPE indicated by '.' and residues missing at a position indicated by '-' .

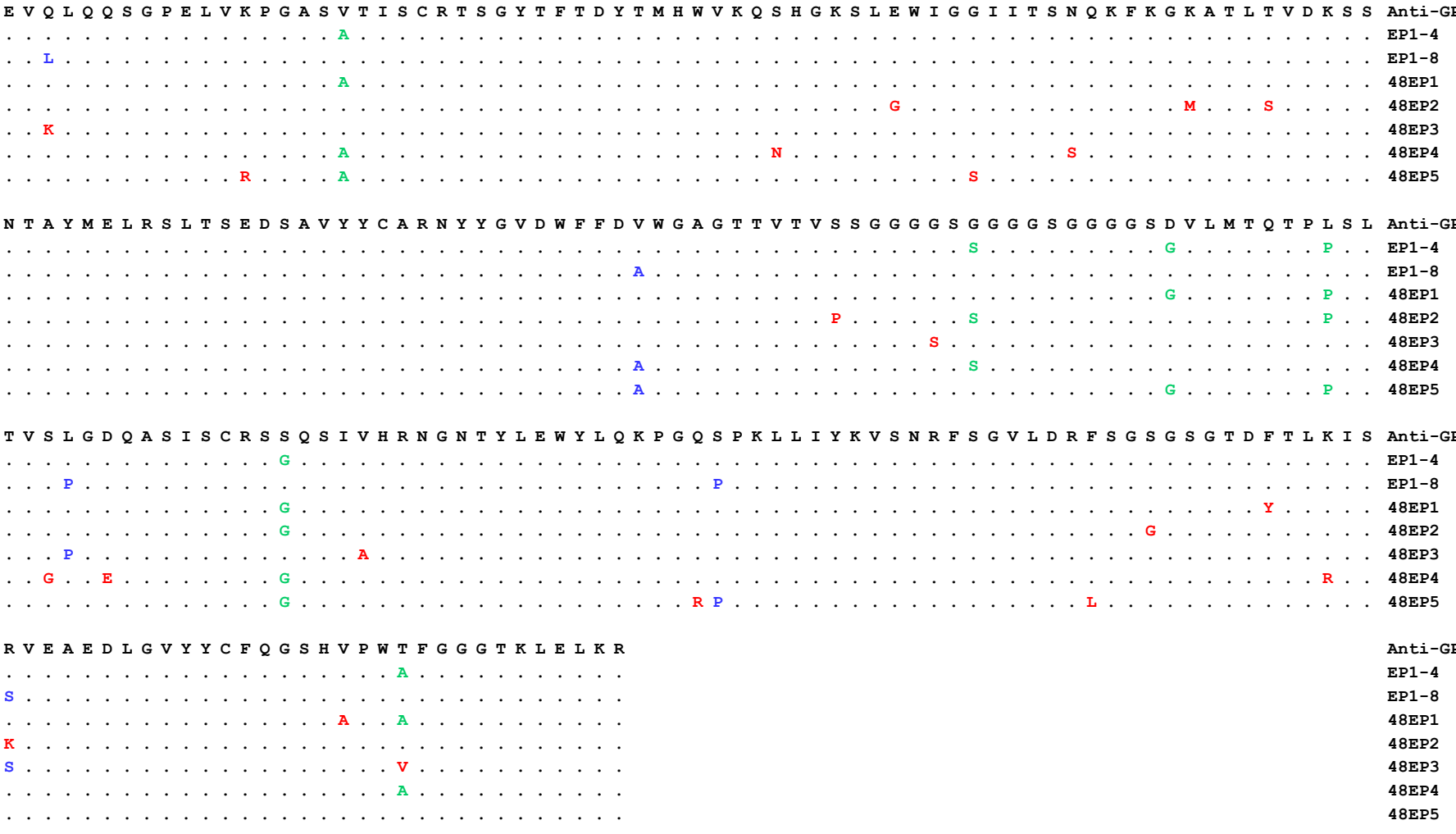

Figure 5.9 Deduced amino acid sequences of scFvs constructed by DNA shuffling of anti-GPE point-mutated variants – EP1-4 and EP1-8. Mutations of EP1-4 in green. Mutations of EP1-8 in blue. Mutations generated during DNA shuffling in red. Only residues differing from the anti-GPE wild type sequences are shown. Residues the same as anti-GPE indicated by '.'

```
1     QVKLQGSGAELVKPGASVRMSCKASRYTFTDYTIHWVKQSHGKSLEWIGGII-----TS-NQKFKGKATLTADKSSNTAYMQLSSLTSEDSAVYYCARNYYGVDWFFDV
1     WGQGTTVTVS-GGGGSGGGGSGGSGSDVLMTQTPLSLTVSLGDQASISCRSSQSIVHRNGNTYLEWYQQNPDGTVKLLIHKVSNRFSGVLDRFSGSGSGADYSLTISNL
1     EQEDIATYFCFQGSHVPWTFGGGTKLELKR

2     QVKLQESGAELVKPGASVRMSCKASGYTFTDYTMHWVKQSPGQGLEWIGGIIPGNGDTSYNQKFKDKATLTADKSSNTAYMQLSSLTSEDSAVYYCARNYYGVDWFFDV
2     WGAGTTVTVSSGGGGSGGGGSGGGGSDVLMTQTPLSLTVSLGDRVTISCRASQSIVHRNGNTYLEWYQQNPDGTVKLLIYKVSN*FSGVLDRFSGSGSGTDYSLTISNL
2     EQEDIATYFCFQGSHVPWTFGGGTKLELKR

3     QVKLQESGAELVKPGASVRMSCKAPGYTFTNYTMHWVKQSPGQGLEWIGGIIPGNGDTSYNQKFKDKATLTADKSSNTAYMELRSLTSEDSAVYYCARNYYGVDWFFDV
3     WGAGTTVTVSSGGGGSGGGGSGGGGSDVLMTQTPLSLTVSLGDQASISCGSSQSIVHRNGNTYLEWYLQKPGQSPKLLIYKVSNRFSGVLDRFSGSGSGTDFTLKISRV
3     EAEDLGVYYCFQGSHVPWTFGGGTKLELKR

4     QVKLQESGAELVKPRASVRMSCKASGYTFTDYTMHWVKQSPGQGLEWIGGIIPGNGDTSYNQKFKDKATLTADKSSNTAYMQLSSLTSEDSAVYYCARNYYGVDWFFDV
4     WGQGTTVTVSSGGGGSGGGGSGGGRSDVLMTQTPLSLTVGLGDQASISRRSSQSIVHRNGNTYLEWYQQNPDGTVKLLIYKVSNRFSEVPSRFSGSGSGTDYSLTISNL
4     EQEDIATYFCFQGSHVPWTFGGSTKLELKR

5     QVKLQESGAELVKPGASVRMSCKASGYTFTDYTMHWVKQSHGKSLEWIGGII-----TS-NQKFKGKATLTVDKSSNTAYMELRSLTSEDSAVYYCARNYYGVDWFFDV
5     WGQGTMVTVP-GGGGSGGGGSGGGGSDVLMTQTPLSLTVSLGDQASISCRSSQSIVHRNGNTYLVWYLQKPGQSPKLLIYKVSNRFSGVLDKFSGSGSGTDYSLTISNL
5     EQEDIATYFCFQGSHVPWTFGGGTKL_TKT
```

Figure 5.10 Deduced amino acid sequences of scFvs constructed by DNA shuffling of anti-GPE with NC10GPE. NC10 segments in green, anti-GPE segments in black, CDRs in dark red, and point mutations in blue. * - stop codon. Residues missing at a position indicated by '-'. Deletion indicated by '_'.

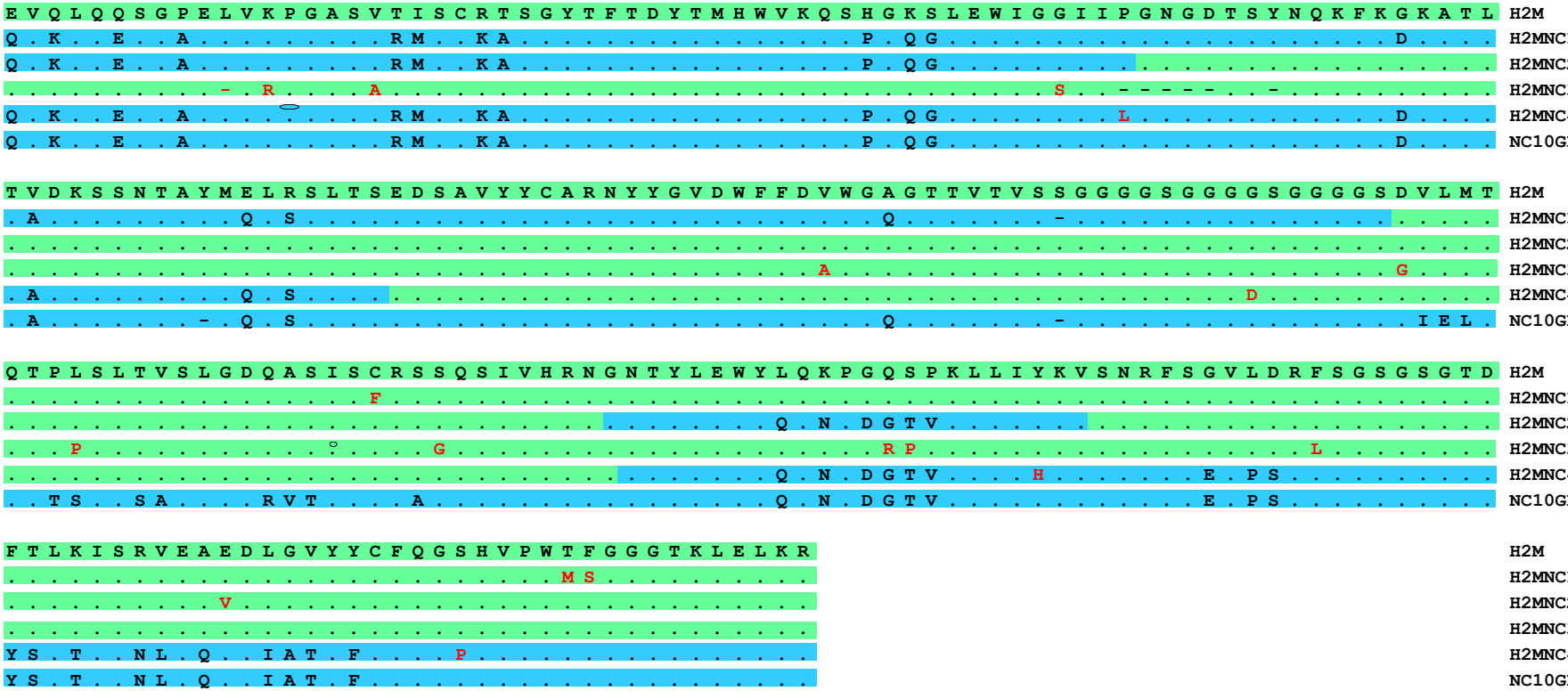

Figure 5.11 Deduced amino acid sequences of scFvs constructed by DNA shuffling of anti-GPE H2M and NC10GPE sequences. Anti-GPE segments in green. NC10GPE segments in blue. Point mutations in red. Only residues differing from the anti-GPE wild type sequences are shown. Residues the same as anti-GPE indicated by '.' and residues missing at a position indicated by '-' .

to a deletion of one amino acid and the reading of the remaining codon as Thr. An insertion of an A within the last two codons of this clone has mutated the last residue from Arg to Thr. An alignment is shown for the shuffling of anti-GPE H2M with NC10GPE (Figure 5.11). These clones are named H2MNC1 etc. and again it can be seen that a variety of chimaeric genes has been produced. H2MNC3 appears to be anti-GPE wild type with deletion of V_H residue 11. The high number of mutations suggests that this gene has been generated by the shuffling process and so the anti-GPE wt may have existed as a contaminant in the original pool of anti-GPE H2M. A fifth sequence not shown in Figure 5.11 was also a chimaera. The resultant libraries from these two shuffles were named GPENC and H2MNC.

5.8 Ribosome display of GPENC and H2MNC chimaera libraries

The ribosome display of the GPENC and H2MNC libraries was performed with two main differences in the selection procedure from that used for the display of EPGPE as described in Chapter 4. The transcription and translation coupled reaction was performed essentially as for EPGPE as described (2.4.2). Alterations to the procedure were an attempt to overcome the occurrence of significant non-specific binding which was difficult to eliminate in the display and selection of EPGPE. This was possibly caused by proteins that were misfolded or unfolded, exposing 'sticky' hydrophobic regions that could non-specifically associate with antigen. The main differences in the selection procedure (2.4.3) were that BSA was used as the blocking reagent instead of skim milk, and that specific peptide elution was used instead of elution with EDTA (2.4.4). This elution was attempted with the GPE tripeptide, the whole IGF-I molecule, and the 10-mer GPE peptide used in the raising of the anti-GPE monoclonal antibody (3.1.2; Craven, 1999). Peptide elution may aid in separating the specific binders from the mass of bound material, all of which would be eluted with EDTA. Such specific elution has been successful in phage display of antibody fragments (Pereira *et al*., 1997; Chames *et al*., 1998; Goletz *et al*., 2002).

5.8.1 Preparation of ribosome display templates

The PCR generated GPENC and H2MNC chimaera libraries were *Sfi*I/*Not*I digested (2.1.7) and ligated (2.1.9) at a 3:1 molar ratio into the likewise digested pGC-C_L vector, prepared for ribosome display (4.2). Ribosome display templates were then amplified from this vector with a forward 5′ primer mix to the anti-GPE gene (5998) and NC10 gene (6904) encoding the T7 promoter and RBS, and reverse C_L primers (refer to Figure 4.3; sequences shown in Table 2.1). Amplified templates were gel purified (2.1.6.1) and quantitated (2.1.8) in preparation for ribosome display.

5.8.2 Display of GPENC and HM2NC libraries with GPE peptide elution

Selection of ribosome displayed GPENC and H2MNC libraries with GPE peptide elution was performed on IGF-I and lysozyme coated on well surfaces and blocked with 2% BSA / 100 μg/mL RNA (2.4.3). Blocking reagent was also included in the binding step at 0.67% BSA / 33 μg/mL RNA and Tween 20 was included in the washes at 0.5 % (2.4.3). The full-length GPENC and H2MNC libraries (amplified with C_L primer 6322) were displayed. An empirical study of concentrations of the GPE peptide used 100 fM, 10 pM, 1 nM and 100 nM consecutively to elute interacting species, referred to as "binders" (2.4.4). Agarose electrophoresis of RT-PCR on these peptide eluates (2.4.4) using a $5^{/}$ primer cocktail of 5998 and 6904 and $3^{/}$ C_L primer 5269 (Table 2.1) shows most mRNA appeared to be eluted by the initial, lower concentrations of GPE (Figure 5.12). Virtually no further material was recovered by even the strongest (100 nM) GPE elution. Additionally, RT-PCR bands produced using eluates from selection against IGF-I were more intense than those from selection against lysozyme, through all elution concentrations. However, the efficacy of elution by low concentrations suggested that the binders were not strong binders. RT-PCR on the same eluates was undertaken with the primer 6322, producing very little recovery of DNA bands (data not shown), possibly due to the mRNAs still being attached to the ribosome, thereby preventing access of this outermost C_L primer, however, the 48^0C incubation step in the RT-PCR would be expected to dissociate the ribosome complexes. Alternatively, some degradation of mRNAs at the $3^{/}$ end, or blocking due to secondary structures may be occurring.

Display of the chimaera libraries with the shorter 5269 C_L primer fragment was compared with display of the full-length 6322 C_L fragments as shown above. In this experiment, the concentration of blocking reagent included in the binding step (2.4.3) was doubled to 1.33% BSA / 66 μg/mL RNA to attempt to reduce further the non-specific bands observed above (Figure 5.12). Also, a "blank" elution (i.e. PBS / 5 mM Mg Acetate with no added peptide) was included prior to the series of peptide elutions (2.4.4). The display and selection of the longer 6322 fragments was more effective than the shorter 5269 fragments as measured by intensity and specificity of RT-PCR (2.1.4.3) DNA bands (Figure 5.13). The intensity of the non-specific bands (selection against lysozyme) was reduced in this instance, possibly due to the increase in blocking agent concentration in the selection, but there was also an overall reduction in the intensity of the bands. Again, the 100 fM elution gave the strongest recovery of bands with negligible recovery of DNA from the "blank" elution, suggesting the peptide elution may be effective.

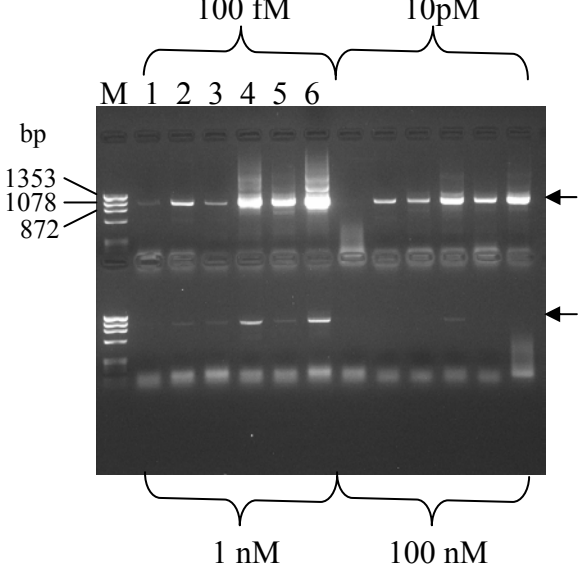

Figure 5.12 Ribosome display of chimaeric libraries with 6322 C_L spacer. Agarose electrophoresis of RT-PCR with 5269 C_L primer on GPE peptide eluates. Elution concentrations are indicated on the figure. M, ϕX174 DNA markers. Lane 1, anti-GPE wt against lysozyme and lane 2, against IGF-I; lane 3, GPENC against lysozyme and lane 4, against IGF-I; lane 5, H2MNC against lysozyme and lane 6, against IGF-I.

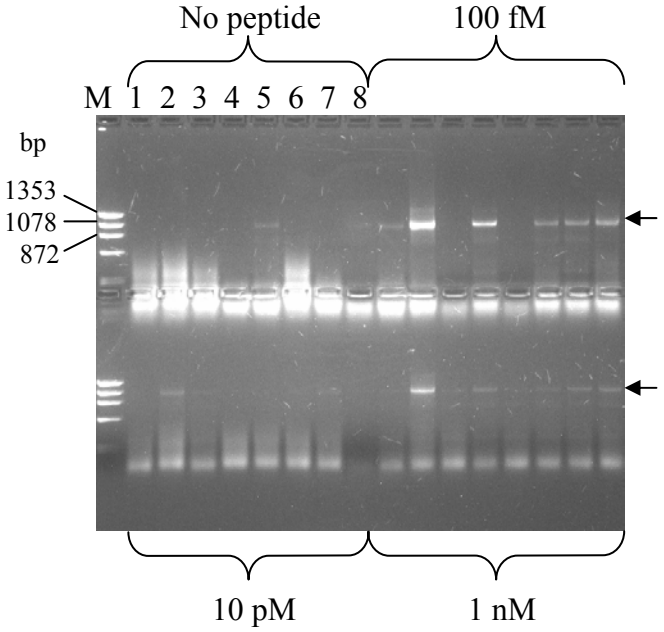

Figure 5.13 Ribosome display of chimaeric libraries comparing display of 6322 and 5269 fragments. Agarose electrophoresis of RT-PCR with 5269 C_L primer on GPE peptide eluates. Elution concentrations are indicated on the figure. M, ϕX174 DNA markers. Lane 1, GPENC (6322) against lysozyme and lane 2, against IGF-I; lane 3, H2MNC (6322) against lysozyme and lane 4, against IGF-I; lane 5, GPENC (5269) against lysozyme and lane 6, against IGF-I; lane 7, H2MNC (5269) against lysozyme and lane 8, against IGF-I.

RT-PCR (2.1.4.3) on the 100 fM eluates using C_L primer 5269 for both GPENC and H2MNC produced DNA for a second round of display and selection as performed for the initial first round experiment. The RT-PCR for this display (Figure 5.14) shows that ribosome selection against lysozyme produces more intense bands than against IGF-I. This is opposite to what was expected based on the result obtained for the first round display. If the DNA retrieved from the first round selection was predominantly specific for IGF-I then one would expect this enrichment to be seen in the second round RT-PCR.

It was postulated that the 5269 fragments might be more prone to misfolding on the ribosome, thereby facilitating non-specific selection against lysozyme. Therefore, the original successful first round 100 fM elution was used as template for an RT-PCR with the 5267 C_L primer to obtain full length C_L fragments (Figure 5.15) for a second round display to test whether this length of spacer is more conducive for folding of scFvs on the ribosome into functional molecules. It can be seen that RT-PCR cDNA sequences from this selection can be efficiently recovered using primer 5267. The new second round display and selection was performed as for the first round. RT-PCR on GPE peptide eluates was performed with the C_L primer 5268 (Figure 5.16) and 5269 (data not shown) but neither showed successful selection, with only bands against lysozyme recovered. Amplification of more template DNA by PCR (2.1.4), as opposed to RT-PCR as above, for a further attempt at this second round display gave a similar result (data not shown).

The use of primer 6322 fragments for a second round display was also attempted. Like 5267, the 6322 primer codes all the way to the $3^{/}$ end of C_L, but has a much shorter overhang of 15 nucleotides (codes for *Sac*2 site) compared with the 27 nucleotide overhang (codes for FLAG peptide) of 5267. Display with the 6322 fragments gave the best results for the first round display. The 5267 fragments amplified above were used as template for PCR amplification (2.1.4) using primer 6322. This DNA was used for ribosome display as performed for the first round. RT-PCR on GPE peptide eluates (100 fM – 100 nM) again failed to produce specific bands for IGF-I (Figure 5.17.A). This second round display of 6322 fragments was also performed with a series of peptide elution concentrations through to 1 mM GPE peptide to determine whether stronger concentrations may show elution of stronger, more specific binders. This approach was also unsuccessful with all binders eluted at lower concentrations of the peptide (Figure 5.17.B). Due to the difficulty in taking the chimaeric libraries beyond one round of selection it was decided to analyse the binders selected from each library with the 100 fM elution from the first round (see below, 5.10).

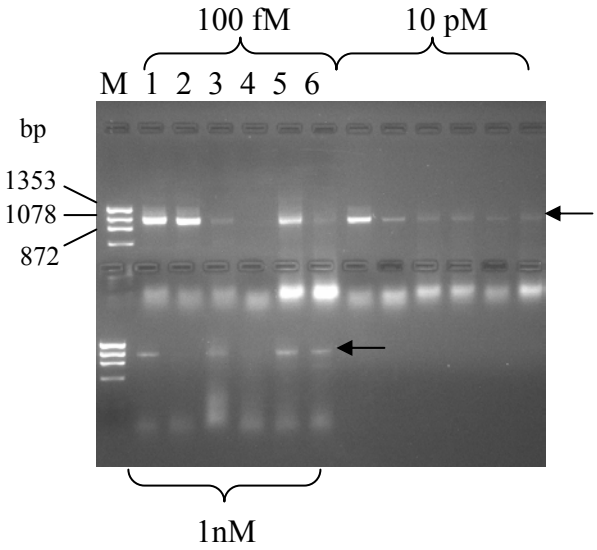

Figure 5.14 Second round of ribosome display of chimaeric libraries as 5269 fragments. Agarose electrophoresis of RT-PCR on GPE peptide eluates. Elution concentrations are indicated on the figure. M, ϕX174 markers. Lane 1, anti-GPE wt against lysozyme and lane 2, against IGF; lane 3, GPENC against lysozyme and lane 4, against IGF-I; lane 5, H2MNC against lysozyme and lane 6, against IGF-I.

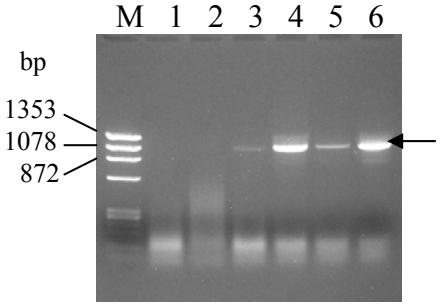

Figure 5.15 First round of ribosome display of chimaeric libraries with primer 5267 RT-PCR. Agarose electrophoresis of RT-PCR with 5267 C_L primer on 100 fM eluates. Display was of the 6322 fragments. M, ϕX174 DNA markers. Lane 1, anti-GPE wt against lysozyme and lane 2, against IGF-I; lane 3, GPENC against lysozyme and lane 4, against IGF-I; lane 5, H2MNC against lysozyme and lane 6, against IGF-I.

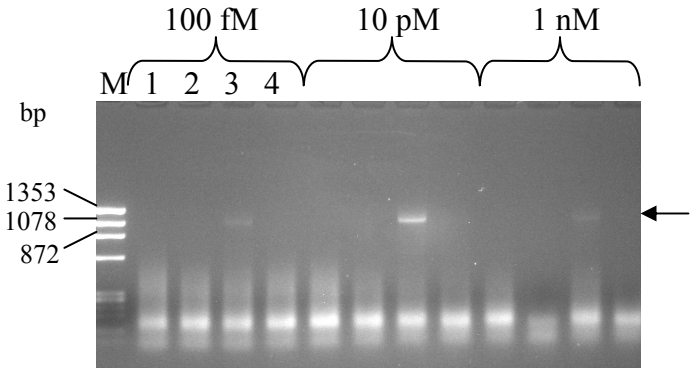

Figure 5.16 Second round of ribosome display of chimaeric libraries as 5267 fragments. Agarose electrophoresis of RT-PCR with C_L primer 5268 on GPE peptide eluates. Elution concentrations are indicated on the figure. M, ϕX174 DNA markers. Lane 1, GPENC against lysozyme and lane 2, against IGF-I; lane 3, H2MNC against lysozyme and lane 4, against IGF-I.

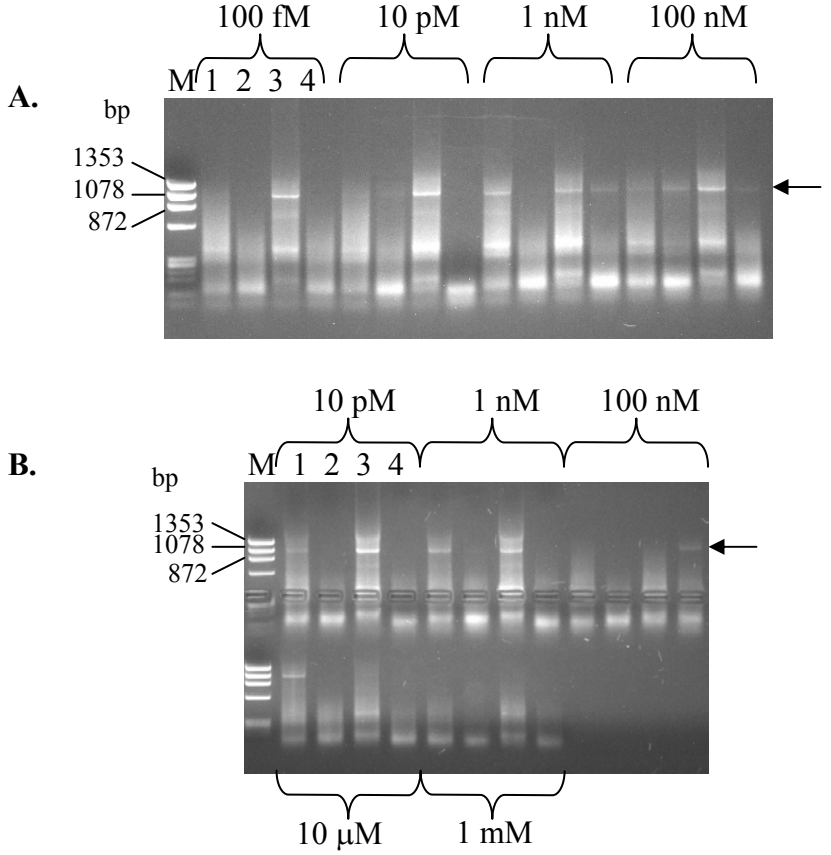

Figure 5.17 Second round of ribosome display of chimaeric libraries as 6322 fragments. Agarose electrophorsis of RT-PCR with C_L primer 5269 on GPE peptide eluates. Elution concentrations are indicated on the figure. M – ϕX174 DNA markers. Lane 1, GPENC against lysozyme and lane 2, against IGF-I; lane 3, H2MNC against lysozyme and lane 4, against IGF-I. A. 100 fM – 100 nM elution series. B. 10 pM – 1 mM elution series.

5.8.3 Display of GPENC and H2MNC libraries with IGF-I elution

Ribosome display of the chimaeric libraries was performed to determine if specific elution of selected complexes could be achieved with IGF-I. The display and selection against IGF-I and lysozyme was performed as previously described for the chimaeric libraries (round 1) with GPE peptide elution (5.8.2). The elution was carried out with a series of IGF-I concentrations at 13 fM, 1.3 pM, 130 pM, 13 nM and 1.3 μM. RT-PCR on the eluates (Figure 5.18) showed similar results to those in the second round display with peptide elution, with very faint bands being retrieved for selection against IGF-I but much stronger bands against lysozyme, and so it was decided not to pursue this approach further.

5.8.4 Display of GPENC and H2MNC libraries with GPE 10-mer peptide elution

Ribosome display and selection of the chimaeric libraries to determine the effectiveness of elution using the 10-mer GPE peptide (GPE($_{\beta}$A)$_3$DYKC) originally used to raise the anti-GPE Mab was performed as described for the first round experiments using GPE peptide elution (5.8.2). The elution series used was 100 fM, 10 pM, 1 nM, 100 nM and 10 μM. Non-specific recovery of bands was seen in the RT-PCR result (Figure 5.19). This consistent selection of non-specific binders to lysozyme was obviously hampering efforts to isolate IGF-I binders and perform multiple rounds of selection and display. Increasing the stringency of washing at this stage was not an option as recovery of bands against IGF-I was already very low. It was postulated that the lysozyme being used here as a negative control antigen may not be ideal for these experiments. Due to their hybrid nature, the chimaeric libraries would be expected to contain many proteins that may not fold correctly, possibly exposing hydrophobic regions. This may present a surface compatible for association with hydrophobic parts of the coated lysozyme molecule that may be present. It was therefore decided to test subsequent display and selection with the use of a different negative control – in this case the enzyme α-amylase – which might allow more efficient washing off of non-specifically interacting complexes.

Display and selection of the chimaera libraries using α-amylase as the negative antigen was performed as for display with GPE peptide elution (5.8.2) but with a decrease in stringency of the washes by reducing the concentration of Tween 20 from 0.5% to 0.1% (2.4.3). The elution series started at GPE 10-mer peptide concentration of 1 nM, then 100 nM and 10 μM, attempting to select for tighter specific binders and was followed by a 20 mM EDTA elution to release all remaining mRNAs (2.4.4). RT-PCR on the eluates (Figure 5.20.A) shows that most complexes were eluted at

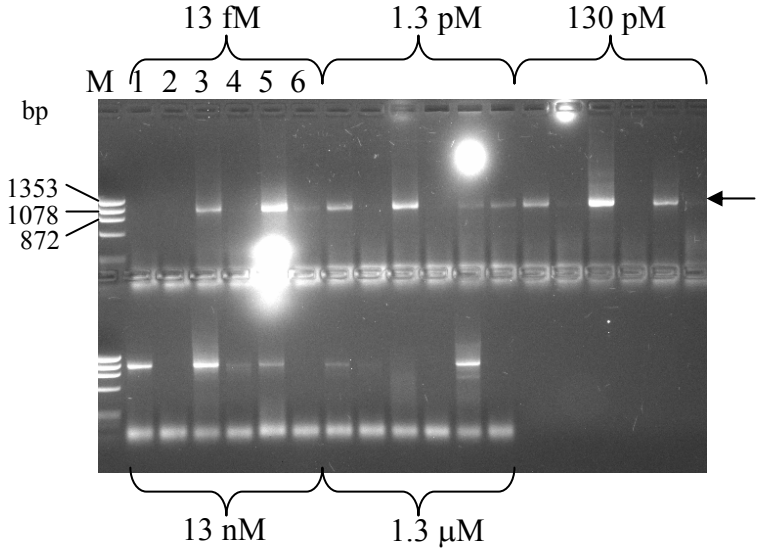

Figure 5.18 Ribosome display of chimaeric libraries with IGF-I elution. Agarose electrophoresis of RT-PCR with 5269 C_L primer on eluates. Elution concentrations are indicated on the figure. M, ϕX174 DNA markers. Lane 1, anti-GPE wt against lysozyme and lane 2, against IGF-I; lane 3, GPENC against lysozyme and lane 4, against IGF-I; lane 5, H2MNC against lysozyme and lane 6, against IGF-I.

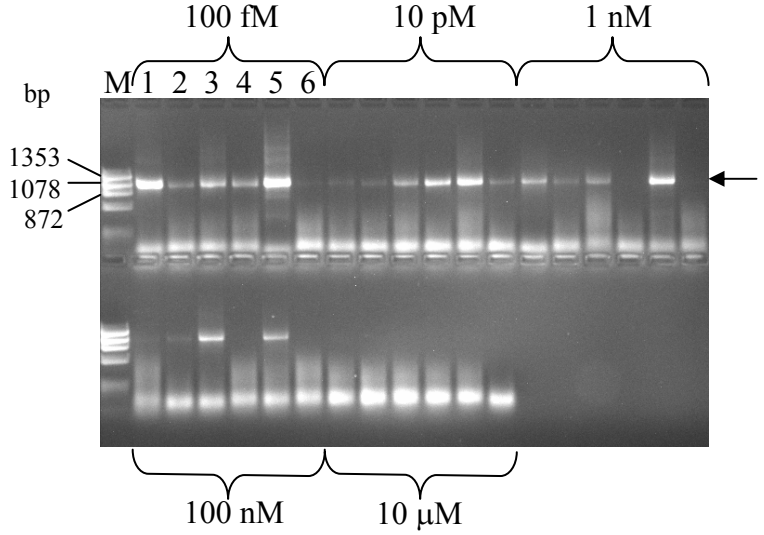

Figure 5.19 Ribosome display of chimaeric libraries with GPE 10-mer peptide elution. Agarose electrophoresis of RT-PCR with 5269 C_L primer on GPE 10-mer peptide eluates. Elution concentrations are indicated on the figure. M, ϕX174 DNA markers. Lane 1, anti-GPE wt against lysozyme and lane 2, against IGF-I; lane 3, GPENC against lysozyme and lane 4, against IGF-I; lane 5, H2MNC against lysozyme and lane 6, against IGF-I.

1 nM. The reduced stringency of washing allowed more IGF-I-selected RNAs to be recovered. No DNA was seen for the EDTA elutions, showing that all complexes, specific or non-specific, were eluted by the peptide. Bands against α-amylase were generally less strong than those against IGF-I.

A number of experimental measures were taken to reduce the non-specific binding to α-amylase. The concentration of the blocking reagent was increased to 3% BSA / 100 μg/mL RNA for blocking of the well surface, blocking reagent in the binding step was increased to 2 % BSA / 66 μg/mL RNA, and the concentration of Tween 20 in the wash was increased to 0.2% (2.4.3). The elution series was started from 10^4-fold lower concentration than the previous display. The increased stringency lead to a reduction overall in the intensity of RT-PCR bands, including elimination of anti-GPE wt bands, and a reduction in non-specific binding to α-amylase (Figure 5.20.B), suggesting that the intensity of the bands in the previous display was due chiefly to non-specific or very low affinity binders. Specific RT-PCR bands were obtained in the 100 fM elution of GPENC against IGF-I (Figure 5.20.B, lane 4), and in the 10 pM elution of H2MNC against IGF-I (Figure 5.20.B, lane 6), and these DNAs were purified (2.1.6.1) and used as template for PCR amplification (2.1.4) of sufficient DNA for a second round of display and selection.

The second round of display of GPENC and H2MNC was performed using fragments generated by both C_L primers 5268 and 5269 (Figure 4.3, Table 2.1), with selection conditions the same as for the first round display experiment that generated these fragments except that blocking reagent in the binding step was 1% BSA / 33 μg/mL RNA. RT-PCR on eluates (Figure 5.21) showed weak bands for specific selection of H2MNC (5268) against IGF-I with the 100 fM and 10 pM elutions. Display and selection of the other fragments (GPENC) showed nil, very weak, or non-specific recovery of DNA bands. Further attempts at a second round of display of these fragments making alterations to the blocking, selection and washing buffers for reduced stringency yielded no improvements in selection (data not shown). It was therefore decided to analyse the material selected from the first round of display for GPENC (100 fM) and H2MNC (10 pM) and in the second round of display for H2MNC (100fM and 10 pM). This is described in section 5.10.

5.9 Use of BIAcore for selection of binders from ribosome-displayed chimaera libraries

BIAcore selection of binders from ribosome-displayed libraries may provide a kinetic based and controlled means of isolating proteins with desired dissociation characteristics. This section

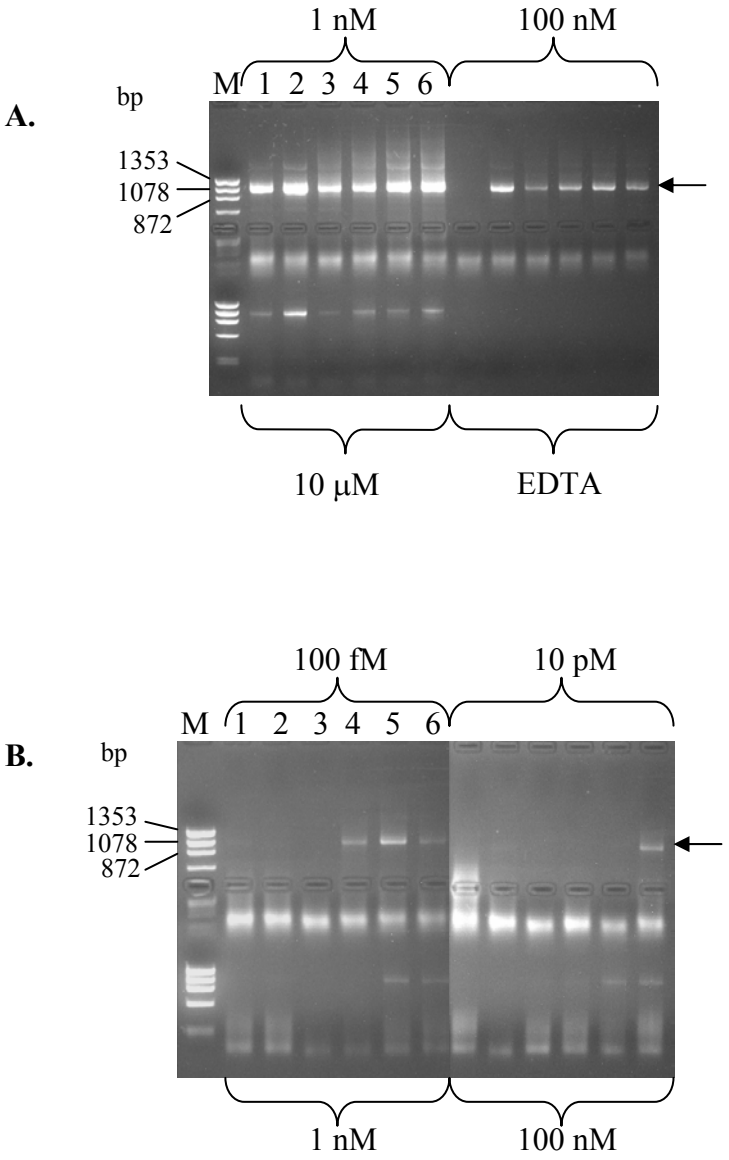

Figure 5.20 Ribosome display of chimaeric libraries with GPE 10-mer peptide elution using α -amylase as negative control antigen. Agarose electrophoresis of RT-PCR with 5269 C_L primer on GPE 10-mer peptide eluates. Elution concentrations are indicated on the figure. M, ϕX174 DNA markers. Lane 1, anti-GPE wt against α-amylase and lane 2, against IGF-I; lane 3, GPENC against α-amylase and lane 4, against IGF-I; lane 5, H2MNC against α -amylase and lane 6, against IGF-I. A. Lower stringency with elution series 1nM – 10μM, EDTA. B. Higher stringency with elution series 100 fM-100 nM.

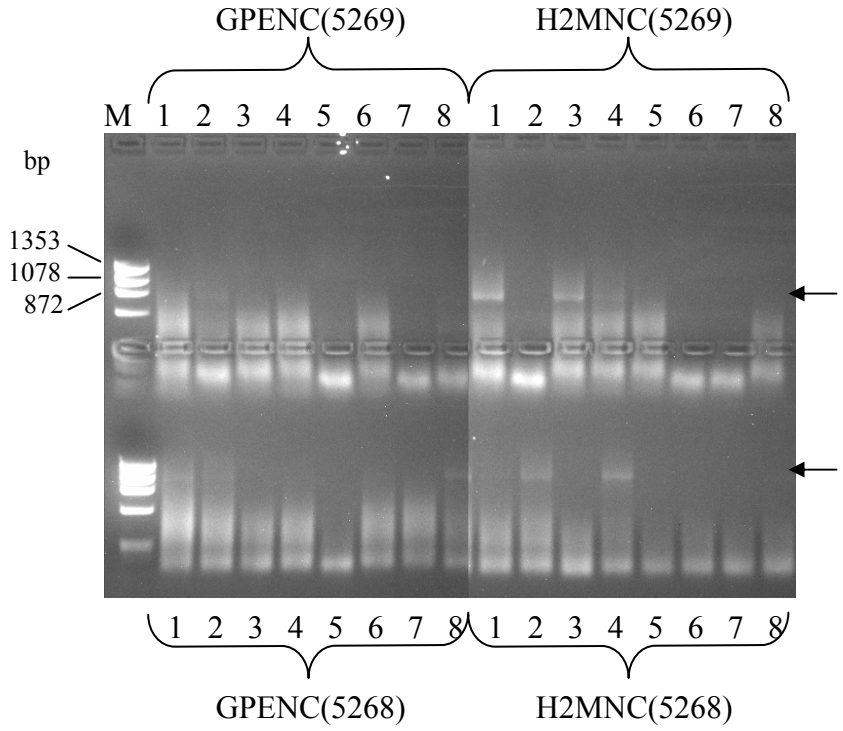

Figure 5.21 Second round ribosome display of chimaeric libraries with GPE 10mer peptide elution. Agarose electrophoresis of RT-PCR on GPE 10mer peptide eluates. For 5269 fragments, reverse primers VLF1 and 6228 were used. For 5268 fragments, reverse primer 5269 was used. M, ϕX174 DNA markers. Lanes 1and 2, 100 fM elution; lanes 3 and 4, 10 pM elution; lanes 5 and 6, 1 nM elution; lanes 7 and 8, 100 nM elution. Lanes 1, 3, 5, and 7, selection against α-amylase; Lanes 2, 4, 6, and 8, selection against IGF-I.

explores the feasibility of using the BIAcore 1000 in this mode. The use of the BIAcore has been previously reported as a tool for selection in phage display, as a guide to monitor successful enrichment of binders (Schier and Marks, 1996), and as a direct selection surface (Malmborg *et al*., 1996). It was postulated that the sensor chip surface with immobilised IGF-I might be less prone to the non-specific binding of proteins that appeared to be occurring in selection on well surfaces. The BIAcore has a fraction collection function where proteins released from the sensorchip surface during the dissociation phase can be retrieved. It was therefore decided to investigate whether collection of such mRNA/ribosome/protein complexes could be effective in improving the chances of recovery of functional scFvs. BIAcore selection was investigated in the ribosome display of the GPENC and H2MNC chimaera libraries.

The effect of injecting ribosome complexes over antigen immobilised on BIAcore sensorchips and the ability to retrieve the message from interacting complexes using the fraction collection system was tested using ribosome display of anti-GPE wt. Coupled transcription and translation of anti-GPE scFv was performed as described (2.4.2). Prior to selection the BIAcore was subjected to the desorb function of the machine to clean out any residual proteins in the system, and an RNasin treatment (2.4.5) to attempt to inactivate any RNases that may be present in the system. The anti-GPE transcription/translation reactions were injected over immobilised IGF-I (2.4.5). The sensorgram from this injection showed a very large initial refractive index change that would be expected when considering the heterogeneity of the sample (Figure 5.22). There was then a gradual rise in RUs on the chip during the association phase, not typical of a normal binding event. A second injection was performed with an identical transcription/translation mix without the addition of anti-GPE template (2.4.5) to look at the effect of untranslated ribosomes in comparison with the translated complexes. After the large refractive index change, a much smaller rise in RUs was seen compared with the translated ribosomes (figure 5.22). This observed difference in response was a promising result but it could not be assumed that this was due to specific binding of mRNA/ribosome/protein complexes to the immobilised IGF-I. The first eight 5 μL (15 s) dissociation fractions were collected for each of these injections (2.4.5) with RT-PCR (2.1.4.3) performed on the first three of these fractions (2.4.5) to determine if RNA from selected complexes could be detected. Strong DNA bands were recovered for all fractions (Figure 5.23). The fact that bands were recovered in the fractions for the injection of the untranslated ribosomes suggested that an extended dissociation phase would be needed between injections to allow all interacting complexes to wash off, or a regeneration step would be required. Another possibility was that

autonomous RNAs, separated from ribosomes, were non-specifically sticking to the chip. Injections of purified anti-GPE wt and H2M scFvs over the chip (2.3.13.2) to assess activity of the immobilised IGF-I after this procedure showed negligible binding (data not shown) suggesting that the procedure was harsh to the antigen.

In an attempt to partly quantify the effects of this procedure on the flow cell surface, IGF-I was immobilised (2.3.13.1) on a new sensorchip flow cell and a series of samples were injected, with fraction collection and RT-PCR to monitor the recovery of mRNA, in the following order:

1. Purified anti-GPE scFv (1 μM) to check initial surface activity (2.3.13.2).
2. Untranslated ribosomes with three fractions collected (2.4.5; Figure 5.24, lanes 1, 2).
3. Translated ribosomes (anti-GPE) with three fractions collected (2.4.5; Figure 5.24, lanes 3-7).
4. Regeneration (25 mM HCl; 2.3.13.2), then a "blank" HBS/P20 injection with three fractions collected (Figure 5.24, lane 8).
5. Translated ribosomes (EPGPE) with 12 fractions collected (2.4.5; Figure 5.24, lanes 9-12).
6. Purified anti-GPE scFv (1 μM) to check final surface activity (2.3.13.2).

No regeneration step is included after binding of purified scFv as the response returns to baseline relatively quickly during the dissociation phase of this interaction. RT-PCR (2.1.4.3) was performed on the collected dissociation fractions. Agarose gel electrophoresis of a selection of these RT-PCR products is shown in Figure 5.24. As seen previously, strong bands are recovered for display of anti-GPE (lanes 3 – 7). The regeneration step is only partially effective (lane 8) suggesting that either stronger regeneration or more time for dissociation needs to be allowed. Bands are seen in early fractions for display of EPGPE (lanes 9, 10), but interestingly most complexes appear to have dissociated by fractions 11 and 12 (lanes 11 and 12), as evidenced by very weak bands, possibly because fewer functional proteins would be expected to be found in the mutated library, but also possibly due to loss of activity on the chip surface. This loss seems to be confirmed when comparing the initial (step 1) anti-GPE scFv maximum response of ~ 70 RUs with the final (step 6) response of ~ 4 RUs (data not shown) which equates to about a 95% loss of IGF-I activity.

It would therefore appear that there are elements within this procedure that are detrimental to the IGF-I immobilised on the chip surface. For example, the DTT present in the transcription/translation mix may be sufficient to cause some unfolding of the IGF-I, or there may be other substances within the coupled reaction mix that reduce activity on the chip surface,

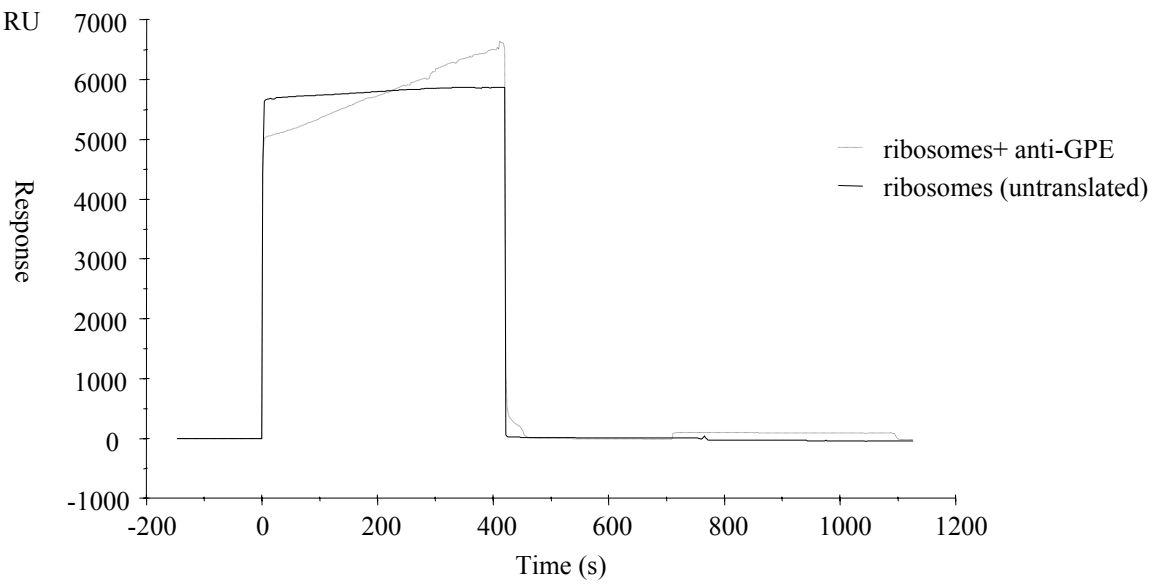

Figure 5.22 BIAcore sensorgrams of transcription/translation mixes injected over IGF-I.

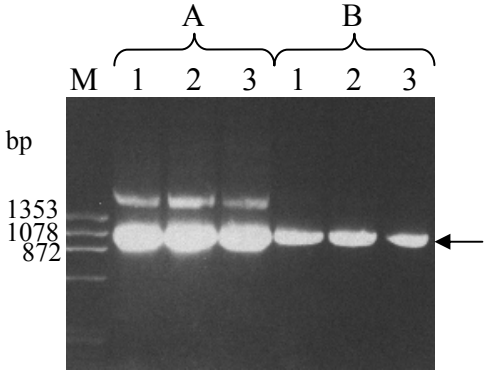

Figure 5.23 Agarose electrophoresis of RT-PCR on dissociation fractions collected after transcription/translation mixes injected over IGF-I. M, ϕX174 DNA markers; A. first three fractions of anti-GPE-translated ribosomes; B. first three fractions of untranslated ribosomes.

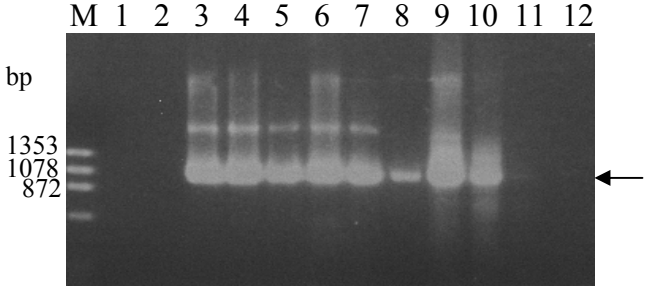

Figure 5.24 Agarose electrophoresis of RT-PCR on dissociation fractions collected after injections to determine the effect of the ribosome display and selection procedure on the IGF-I surface. M, ϕX174 DNA markers. Lanes 1 and 2, untranslated ribosomes fraction 2; lanes 3 and 4, anti-GPE-translated ribosomes fraction 2, and lanes 5-7, fraction 3; lane 8, post-regeneration fraction 2; lane 9, EPGPE translated ribosomes fraction 1, lane 10, fraction 2, lane 11, fraction 11, and lane 12, fraction 12.

including the ribosomes themselves. To investigate this further, IGF-I was immobilised (2.3.13.1) on three parallel flow cells of a new sensorchip. The samples injected over the first flow cell were as follows:

1. Purified 0.25 μM anti-GPE H2M scFv (2.3.13.2; Figure 5.25.A, 1st injection).
2. Injection of RNasin solution (2.4.5).
3. Purified 0.25 μM anti-GPE H2M scFv (2.3.13.2; Figure 5.25.A, 2nd injection).
4. Untranslated ribosomes (2.4.5; Figure 5.25.B).
5. Regeneration with 25 mM HCl.
6. Purified 0.25 μM anti-GPE H2M scFv (2.3.13.2; Figure 5.25.A, 3rd injection).

The results of these injections can be seen in the sensorgrams of Fig 5.25.A. The initial activity of the immobilised IGF-I on the chip surface is represented by a maximum response of ~ 68 RUs for the first anti-GPE H2M injection. After the RNasin injection the binding of anti-GPE H2M only reached 48 RUs, a significant drop in activity, suggesting that this step, possibly due to the presence of DTT, is harmful. After the injection of the untranslated ribosome mix (Figure 5.25.B) a further loss of activity on the flow cell surface to a maximum response of 36 RUs was seen (Figure 5.25.A, 3rd injection), and also the baseline was now drifting downwards (data not shown), suggesting permanent damage to the surface IGF-I.

On the second IGF-I flow cell surface the following injections were performed:

1. Purified 0.25 μM anti-GPE H2M scFv (2.3 13.2; Figure 5.26, 1st injection).
2. Translated ribosomes (anti-GPE) with three fractions collected (2.4.5; Figure 5.28).
3. Regeneration with 25 mM HCl then a "blank" HBS/P20 injection with three fractions collected.
4. Purified 0.25 μM anti-GPE H2M scFv (2.3.13.2; Figure 5.26, 2nd injection).

The results can be seen in the sensorgrams in Figure 5.26 with the IGF-I surface losing significant activity (~51 RUs to 33 RUs) between the first and second injections of anti-GPE H2M, suggesting that this loss of activity occurs whether untranslated (as shown Figure 5.25.A) or translated ribosome complexes are passed over the chip. Also, this reduction in response has occured without the RNasin injection containing DTT at 1 mM as done for results shown in Figure 5.25.A. The final concentration of DTT in the injected transcription/translation mix is lower than this at ~ 0.22 mM (2.4.5) but it is unclear whether this or other factors are responsible for the reduction of IGF-I activity.

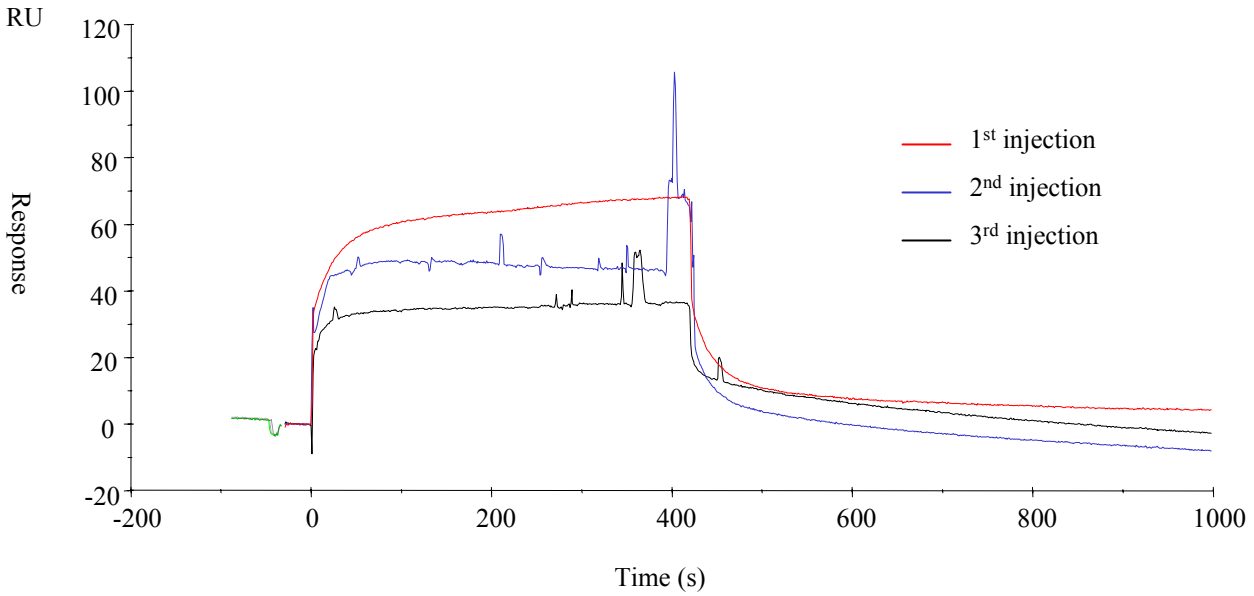

Figure 5.25.A Overlaid sensorgrams of anti-GPE H2M scFv binding to freshly immobilised IGF-I showing loss of IGF-I activity on chip. 1st injection – initial activity, 2nd injection – after RNasin solution, 3rd injection - after transcription/translation mix.

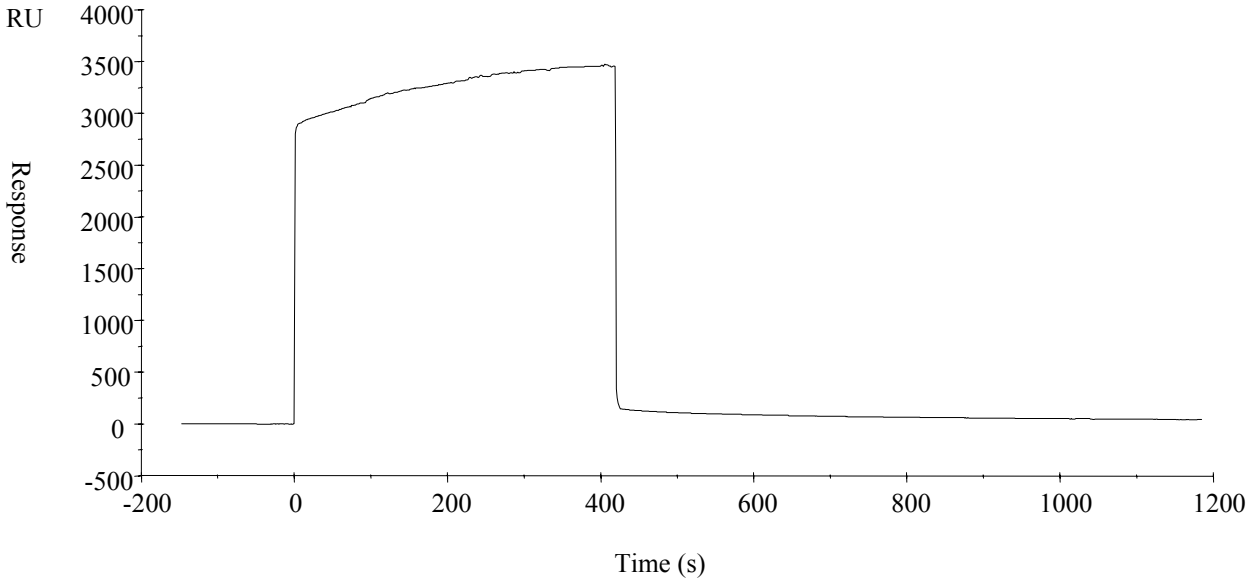

Figure 5.25.B Sensorgram showing injection of transcription/translation mix on freshly immobilised IGF-I after two anti-GPE H2M scFv injections and an RNasin injection.

The third IGF-I flow cell surface was used to determine if removal, by dialysis, of DTT or other harmful factors from the transcription/translation reaction mix could reduce the loss of activity to the immobilised IGF-I. To achieve this, a standard transcription/translation of anti-GPE was performed (2.4.2), and then this was dialysed against HBS/P20/0.5 mM MgAcetate (2.4.5). The samples injected were as follows:

1. Purified 0.25 μM anti-GPE H2M scFv (2.3.13.2; Figure 5.27, 1st injection)
2. Dialysed translated ribosomes (anti-GPE) with three fractions collected (2.4.5; Figure 5.28).
3. Regeneration with 25 mM HCl then a "blank" HBS/P20 injection with three fractions collected.
4. Purified 0.25 μM anti-GPE H2M scFv (2.3.13.2; Figure 5.27, 2nd injection).

Much less loss of activity appears to occur after this dialysis of the mix with a decrease in maximum response reached between positive control binding injections of anti-GPE H2M of ~ 16% (Figure 5.27) compared to 30-40% seen in the examples without dialysis (Figures 5.25.A and 5.26). This is a good improvement and gives more confidence that the chip is active for selection during injection. Completely eliminating loss of activity from the immobilised IGF-I on the chip after these injections is probably not possible as the reticulocyte lysate is a crude extract that includes unknown components. Even with the improvements made with this dialysis, at the rate of loss of activity observed (Figure 5.27), a chip may only be able to be used for 2 – 3 selections before a fresh surface may need to be used. It is unknown whether the stability of the translated complexes is reduced by this dialysis, although the sensorgrams show that there is a better response with the dialysed mix compared to the undialysed mix (Fig 5.28), which suggests that the dialysis may not be detrimental. The RT-PCRs from all these collected fractions showed strong recovery of DNA from selected complexes (data not shown) as seen previously (Figures 5.23 and 5.24).

The interaction of anti-GPE-translated complexes was tested on another antigen, in this case freshly immobilised BSA, in parallel with freshly immobilised IGF-I (2.4.5). No significant differences could be seen in the sensorgrams of these interactions (data not shown). RT-PCR was performed on the first 10 dissociation fractions (2.4.5) from each of these sensorgrams and shows that the recovery of mRNA is as effective with selection against BSA as it for IGF-I (Figure 5.29). These results suggest that non-specific binding and dissociation can also be a problem with BIAcore selection as seen with the methods involving selection off ELISA well surfaces described previously. This observed non-specificity, along with the observed harshness of the process to the

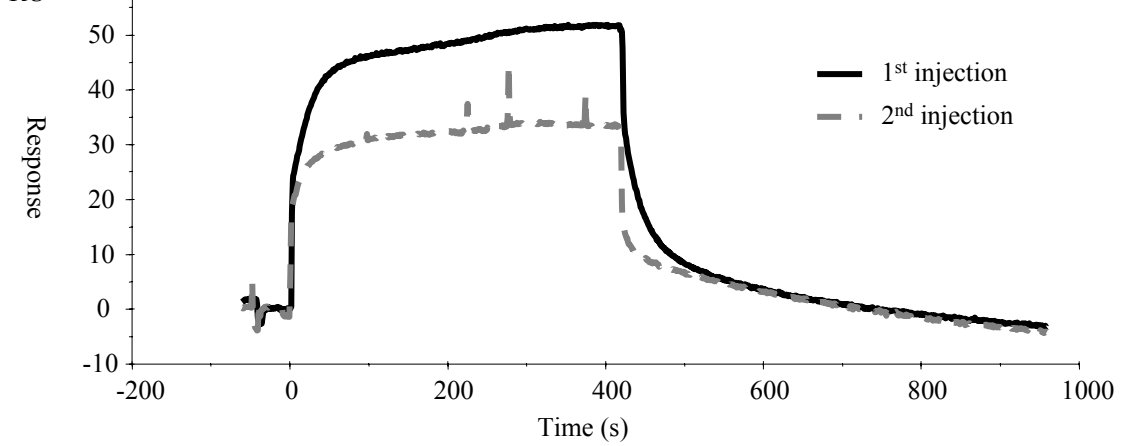

Figure 5.26 Overlaid sensorgrams of anti-GPE H2M scFv binding to immobilised IGF-I showing loss of IGF-I activity after injection of undialysed anti-GPE-translated ribosomes.

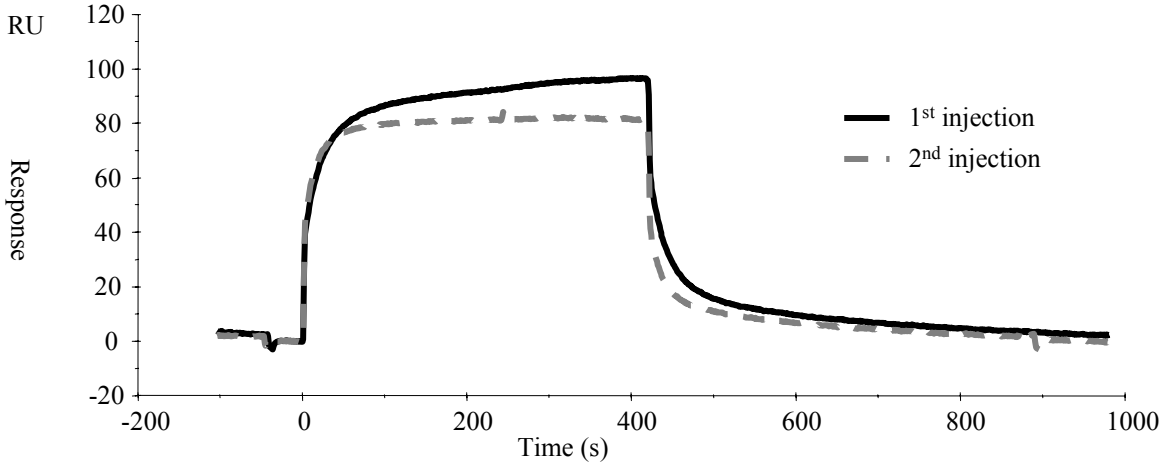

Figure 5.27 Overlaid sensorgrams of anti-GPE H2M scFv binding to immobilised IGF-I showing loss of IGF-I activity after injection of dialysed anti-GPE-translated ribosomes.

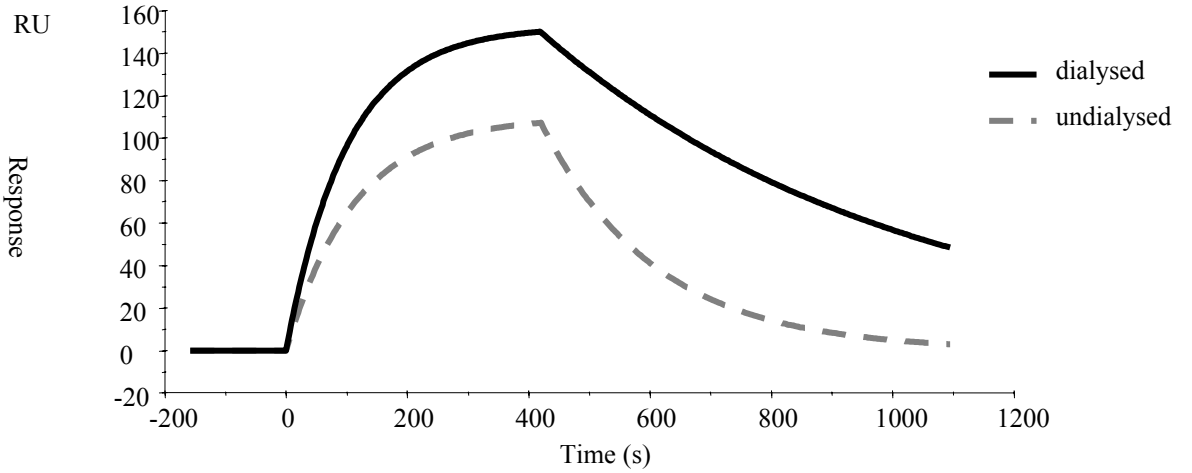

Figure 5.28 Overlaid sensorgrams showing injection of dialysed and undialysed anti-GPE-translated ribosome mixes over immobilised IGF-I. Bulk refractive index changes have been subtracted from the curves using BIAevaluation 3.0 software.

immobilised IGF-I, reduces the likelihood that using the BIAcore for specific selection of ribosome associated scFvs will be effective.

Despite the apparent non-specific interaction of translated ribosome complexes (anti-GPE) with the BSA surface, suggesting that most isolated scFvs will, in turn, be non-specific, it could not be ruled out that positive binders to IGF-I may be isolated by this selection strategy. The ribosome display and BIAcore selection of the GPENC and H2MNC chimaera libraries was pursued to test if specific binders could be isolated from within the pool of non-specific binders by this process. These libraries were transcribed, translated, and then dialysed prior to selection undertaken on freshly immobilised antigen using the BIAcore as described (2.4.5). GPENC was selected against both IGF-I and des(1-3)IGF-I with the large bulk refractive index changes of these interactions subtracted from the sensorgrams using the BIAevaluation 3.0 software to allow easier comparison (Figure 5.30) showing a slightly greater response for binding to des(1-3)IGF-I than IGF-I. It was anticipated that the opposite of this might occur, indicating specificity towards IGF-I, since the original scFv displays such selectivity (Figure 3.9.B). It is possible that this may represent a shift in specificity away from the GPE epitope amongst library members, or it may be a reflection of general non-specificity of selection within this system, as described above for the interaction of anti-GPE-translated ribosomes with BSA (Figure 5.29). Similar results were obtained for H2MNC chimaeras (Figure 5.32), where it was also noted that significant interactions were occurring on a blank flow cell (a flow cell with no immobilised antigen). There was also variability between IGF-I runs on different flow cells but this could be due to differing activities on the flow cell surfaces. Attempts to fit the data to a 1:1 binding scenario using the Langmuir model in the BIAevaluation software 3.0 (2.3.13.3) were unsuccessful, suggesting other interactions with the surface were occurring besides specific scFv binding. RT-PCR was performed on ten dissociation fractions from each of these library selections against IGF-I and des(1-3)IGF-I (Figures 5.31 and 5.33). Despite the apparent lack of discrimination of binders by the different surfaces it was decided to analyse the later IGF-I fractions as these may provide a greater chance of isolating stronger binders whose off rates may be expected to be slower than scFvs eluting in the earlier fractions. As binding curves were seen for injections against des(1-3)IGF-I and a blank flow cell (Figure 5.30, 5.32), and DNA bands were produced in the RT-PCR of fractions from these injections (data not shown), there may be substantial numbers of non-specific binders within these fractions. For GPENC, fractions 8-10 and the regeneration fraction were chosen and their RT-PCR bands excised from the gel (Figure 5.31) for cloning and analysis. The same was done for fractions 6-9 for H2MNC (Figure 5.33).

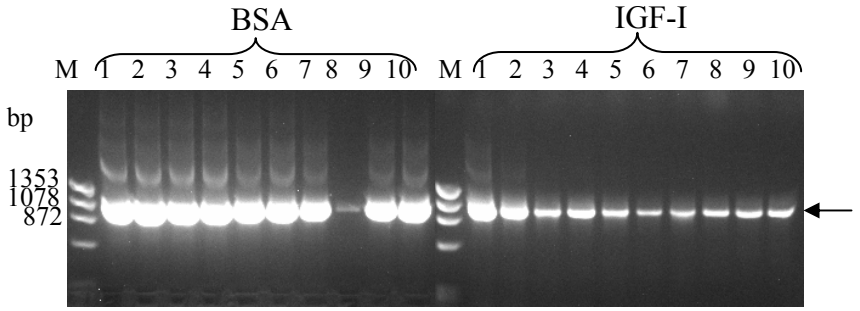

Figure 5.29 Agarose electrophoresis of RT-PCR bands retrieved from the first 10 dissociation fractions of selection of anti-GPE-translated ribosomes against BSA and IGF-I. M, ϕX174 DNA markers.

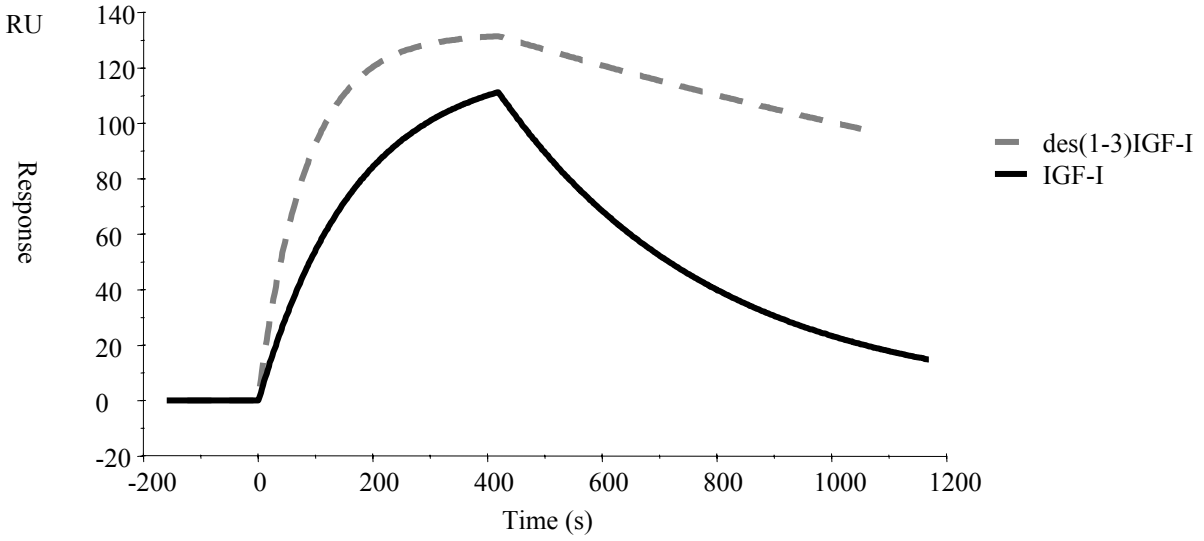

Figure 5.30 Overlaid sensorgrams showing interaction of GPENC-translated ribosomes with different antigens during BIAcore selection. Bulk refractive index change has been subtracted from the curves using BIAevaluation software.

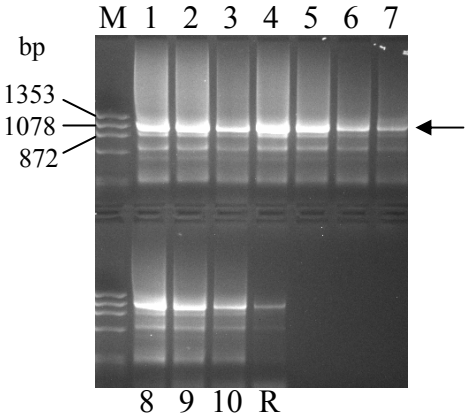

Figure 5.31 Agarose electrophoresis of RT-PCR on dissociation fractions from BIAcore selection of GPENC against IGF-I. M, ϕX174 DNA markers; 1-10, dissociation fractions; R, fraction recovered during regeneration step.

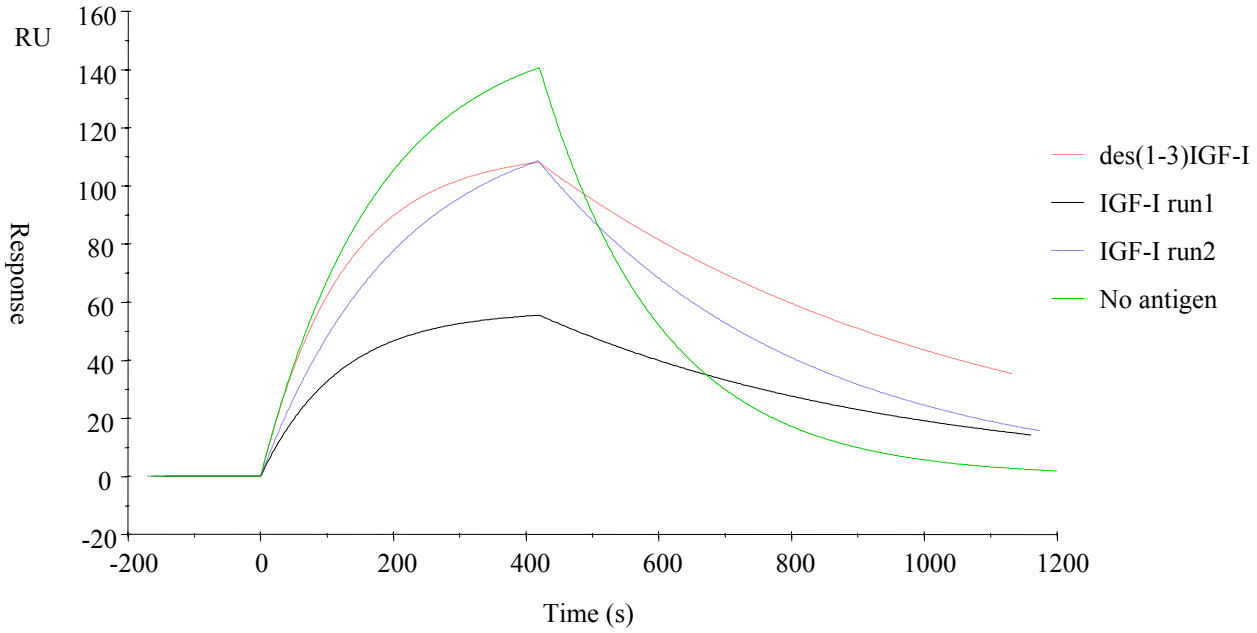

Figure 5.32 Overlaid sensorgrams showing interaction of H2MNC-translated ribosomes with different antigens during BIAcore selection. Bulk refractive index change has been subtracted from the curves using BIAevaluation software.

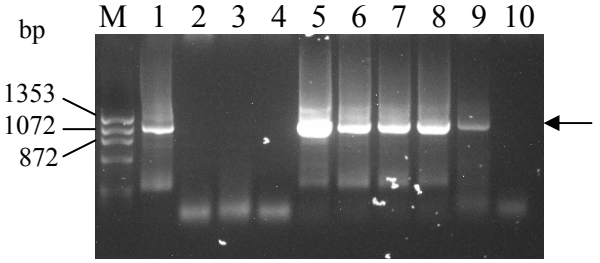

Figure 5.33 Agarose electrophoresis of RT-PCR on dissociation fractions from BIAcore selection of H2MNC against IGF-I. M, ϕX174 DNA markers; 1-10, dissociation fractions

5.10 Cloning and screening for isolation of IGF-I binders

5.10.1 Cloning selected DNAs

The RT-PCR generated DNAs from each of the five ribosome display selections on microtiter well surfaces described above – GPENC and H2MNC with GPE elution (5.8.2; Figure 5.13), GPENC and H2MNC round 1 with GPE 10-mer peptide elution (5.8.4; Figure 5.20.B), and H2MNC round 2 with GPE 10mer peptide elution (5.8.4; Figure 5.21) - were cloned into expression vector pGC as described previously for screening for binders (4.6). This cloning was also undertaken for the two pools of BIAcore-selected RT-PCR generated DNAs from GPENC and H2MNC described above (5.9). These selected DNAs were amplified by standard PCR with *Sfi*I and *Not*I primers (2.1.4) and then digested with these restriction enzymes (2.1.7). The digested DNA was purified (2.1.6.2), quantitated (2.1.8), and ligated (2.1.9) into likewise digested pGC at a molar ratio of 3:1. Ligations were transformed (2.1.11) into electrocompetent HB2151. Ten colonies for each of the seven clonings were screened for inserted scFv sequence by colony PCR (2.1.12; data not shown), most of which were positive.

5.10.2 ELISA screening of colonies

For each of the seven cloned selections, ELISA screening (2.3.12) on culture supernatants from induced cultures grown in microtiter wells (2.2.3) was used to screen multiple colonies (70-95) for binding to IGF-I. Colonies whose supernatants gave the best signals in this ELISA (data not shown) were then chosen for further ELISA analysis. The clones from selection of the H2MNC library on IGF-I-coated microtiter wells gave weak to negligible ELISA signals and so were not pursued any further. Colonies from the GPENC library selected on microtiter wells that gave reasonable signals (14 clones from each of the GPE peptide and GPE 10mer peptide elutions) were further analysed. Likewise, some colonies from the BIAcore-selected GPENC and H2MNC libraries gave significant initial ELISA signals and so 12 of these were further analysed. The chimaera clones were again grown in microtiter wells (2.2.3), along with an anti-GPE wt scFv clone, for ELISA analysis of supernatants (2.3.12). The ELISA results are shown in Figure 5.34 for the ribosome display selections on microtiter wells with peptide elution, and Figure 5.35 for the BIAcore selections. While all colonies showed a significant degree of non-specific binding to lysozyme and α-amylase, the best three clones from each ELISA for the microtiter well-selected clones, based on strength of signal against IGF-I compared to the other antigens, were chosen for further analysis. Clones 29, 42 and 68 from the GPE 10mer peptide elution were chosen and named GN10m29, GN10m42 and

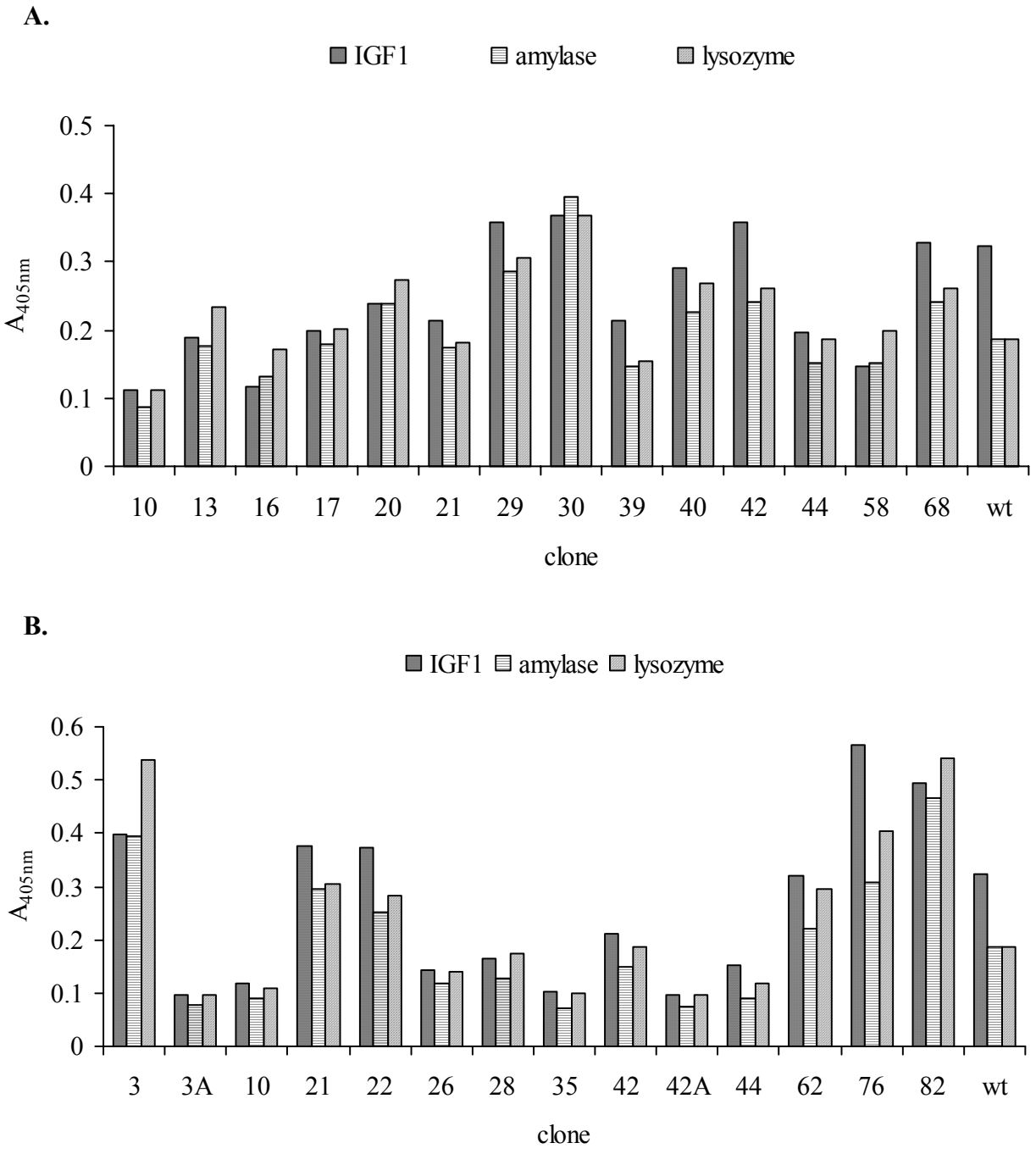

Figure 5.34 ELISA of binding of selected clones from GPENC chimaera library. A. The highest binding clones selected with GPE 10-mer peptide elution. B. The highest binding clones selected with GPE peptide elution.

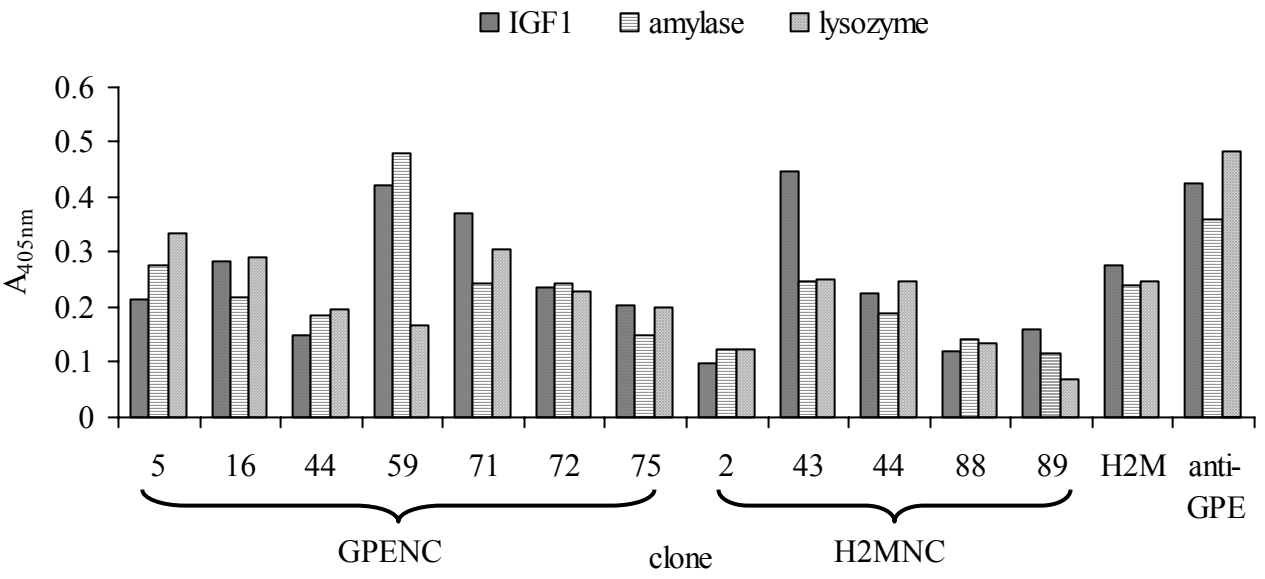

Figure 5.35 ELISA of binding of BIAcore-selected clones from GPENC and H2MNC chimaera libraries.

GN10m68. The best clones from the GPE peptide elutions were named GNpep21, GNpep22 and GNpep76. The best six BIAcore-selected clones were likewise chosen for further analysis and were named GNBIA16, 59, 71, 75 and HNBIA43 and 44 respectively.

5.10.3 Sequencing of selected chimaeras

Plasmid preparations (2.1.12) were made from these best-binding clones described above (5.10.2) and the gene inserts were DNA sequenced (2.1.13) with most found to be chimaeras of the anti-GPE and NC10GPE scFvs. The sequence alignments are shown in Figures 5.36 and 5.37. GN10m29, GNpep22 and GNpep76 are all generated from just one crossover event. The GN10m29 may in fact be the anti-GPE wt that has been amplified by the forward primer for the NC10 scFv (6227) as there is only a small NC10 segment at the 5/ end of this chimaera and the rest is anti-GPE. GNpep22 and GNpep76 appear to have been created by the shuffling of the same two fragments. However, they vary significantly due to the amino acid point mutations that have been introduced into these genes – seven and six respectively. Due to this mutation, GNpep76 has lost a Cysteine residue from both the V_H and V_L domains. The overall point mutation rate of 5.5 amino acid changes per scFv for the microtiter well-selected clones (Figure 5.36) is slightly higher than the 4.2 observed for the chimaera library prior to ribosome display selection. This higher post-selection mutation rate was also observed for the selection of EPGPE (4.6). GN10m42 and GN10m68 have the most crossovers (three) of these clones, being created from two NC10GPE and two anti-GPE fragments. The BIAcore-selected clones were all found to be unique chimaeras (Figure 5.37). For example, GNBIA71 is created from six crossover events, one of which has led to the linker being reduced from 15 to 10 residues. GNBIA16 has a deletion of the first two residues. HNBIA43 is a truncated gene. GNBIA75 and HNBIA44 have lost Cysteine residues due to point mutation. All sequences show NC10 residues at the 5/ end suggesting that the 6227 primer preferentially amplifies over the 5325 anti-GPE primer at the annealing temperature used.

5.11 Expression and purification of selected chimaeric scFvs

5.11.1 Expression and affinity purification

Five clones - GNpep22, GNpep76, GN10m42, GN10m68 and GNBIA71- chosen on the basis of ELISA signal strength and their sequences (eg. CNBIA43 was not pursued as the sequence was truncated) were grown in 1 L cultures (2.2.1) as done previously for anti-GPE wt scFv (3.3). Cells were harvested 2 h after induction due to the fact that, as seen with expression of the wild type, cell densities were beginning to decline at this point in the expression (data no shown). Periplasmic

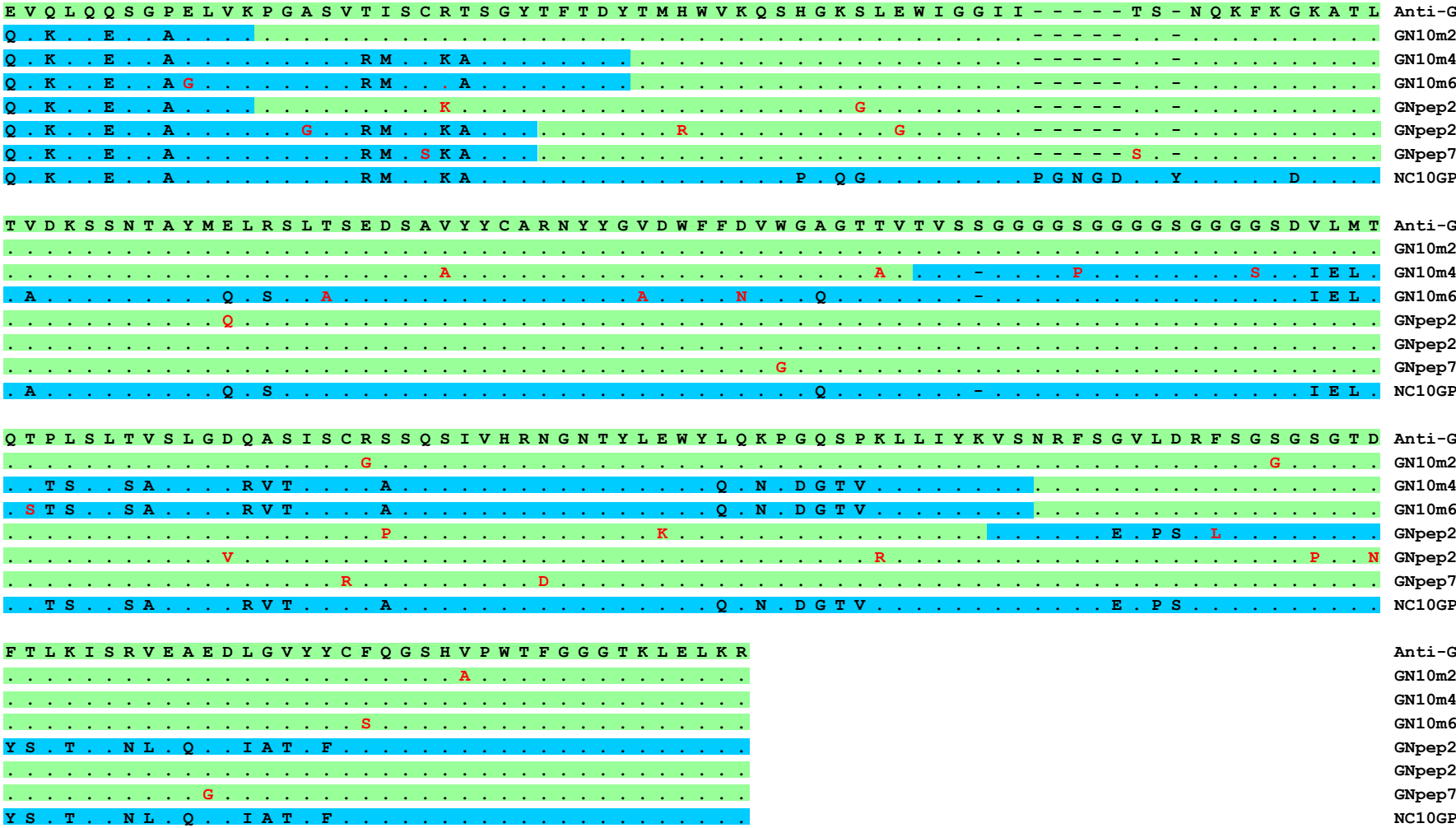

Figure 5.36 Deduced amino acid sequences of scFvs selected with peptide elution from GPENC library. Anti-GPE segments in green. NC10GPE segments in blue. Point mutations in red. Only residues differing from the anti-GPE wild type sequences are shown. Residues the same as anti-GPE indicated by '.' and residues missing at a position indicated by '-' .

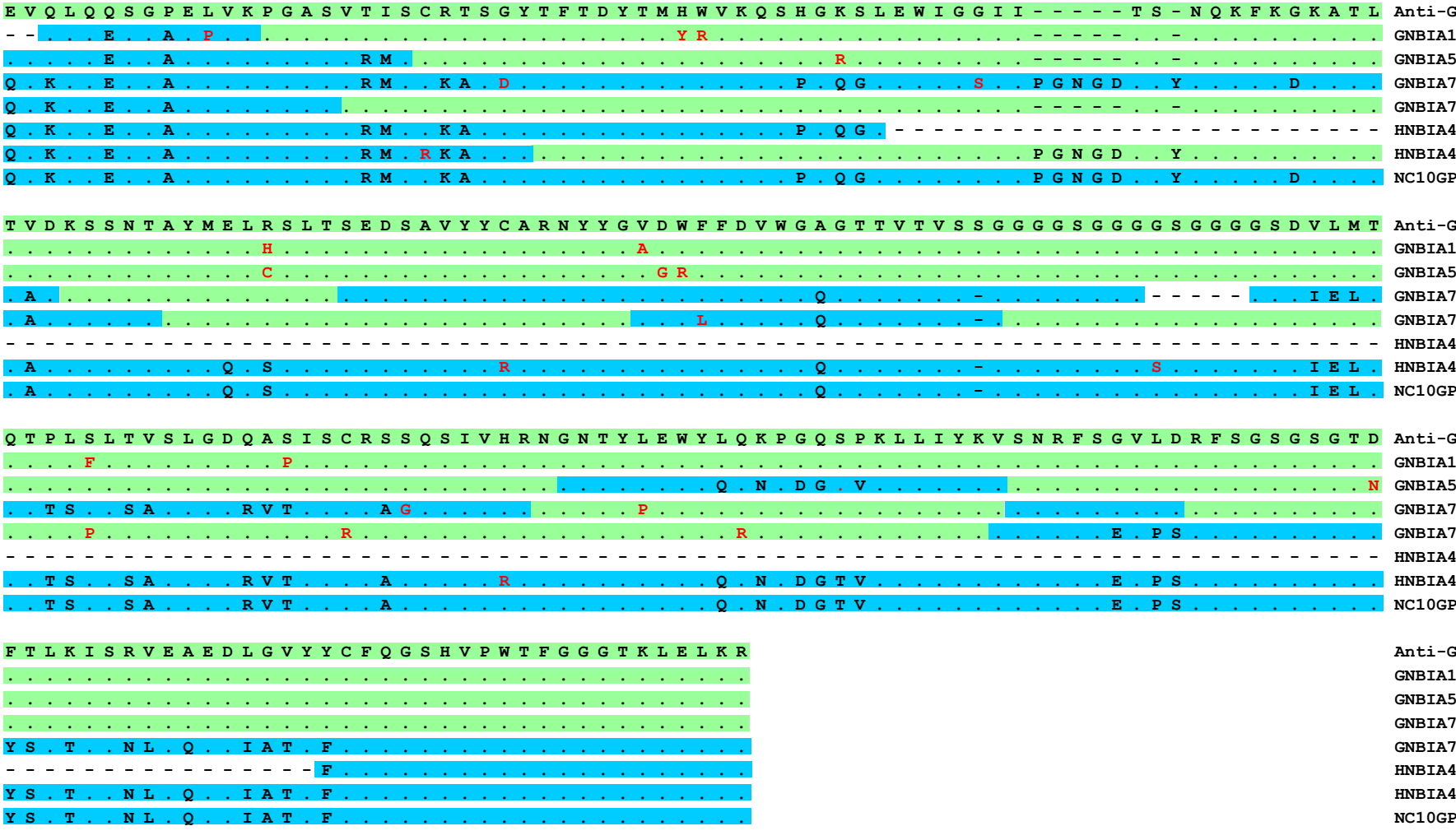

Figure 5.37 Deduced amino acid sequences of scFvs selected from GPENC library using the BIAcore. Anti-GPE segments in green. NC10GPE segments in blue. Point mutations in red. Only residues differing from the anti-GPE wild type sequences are shown. Residues the same as anti-GPE indicated by '.' and residues missing at a position indicated by '-' .

extracts were produced (2.2.2) and these were subjected to anti-FLAG affinity chromatography (2.3.8). Protein eluted from the FLAG column was dialysed into TBS (2.3.8) and this was concentrated (2.3.9) from ~ 15 mL to ~ 1 mL. Significant amounts of all these scFvs precipitated during dialysis and concentration as shown by SDS-PAGE and Western blot where these reduced precipitates were shown to resolve as scFv-sized bands (data not shown).

5.11.2 Gel filtration chromatography

The soluble affinity purified protein samples were applied to either Superose 12 or Superdex 200 columns equilibrated with HBS/P20 for analysis and peak purification by gel filtration chromatography (2.3.10). Chromatographic profiles are shown in Figures 5.38 and 5.39. The FLAG-purified samples were loaded on these columns and peaks corresponding to the expected retention time for scFv monomer were collected. These were concentrated and reapplied to the same column for a secondary collection to attempt to achieve further purity. The same was also done for an oligomeric peak eluting at ~ 26 min for GNBIA71 that was possibly a dimer, trimer, or a mix of the two. The profiles of all these clones show much of the preparations existing as oligomeric forms and aggregate, all of which when collected and subjected to reducing SDS-PAGE and Western blot resolved as scFv monomer (data not shown). GNBIA71 appears to show greater tendency for oligomerisation than the other clones due probably to the shortened linker (Holliger *et al*., 1993; Kortt *et al*., 1997). The secondary runs allowed clearer collection of scFv although some shift towards a smaller, possibly breakdown product was detected at a retention time of about 33 min on Superose 12 (Figure 5.38) and 37 min on Superdex 200 (Figure 5.39). The collected scFv peaks are quite broad as opposed to a sharp peak that would be expected from a highly pure protein. This is most likely due to the material within these peaks being a heterogeneous mix. The peaks may contain correctly folded scFv along with misfolded and unfolded species.

5.12 Binding of chimaeric scFvs by BIAcore

The purified chimaeric scFvs were quantitated (2.3.11) and then applied to the BIAcore for analysis of binding to immobilised IGF-I, as well as to des(1-3)IGF-I, and in some instances lysozyme and NA (2.3.13.2). The general trend of these binding studies showed that indeed, selection appears to be occurring for non-specific protein interactions as was inferred from the ELISA results and to a certain extent, the poor solubility characteristics of these chimaeras observed during the purification process. Figure 5.40.A shows the binding of GNpep76 to three antigens. Bulk refractive index change is subtracted from each curve for ease of comparison. Despite the response against IGF-I

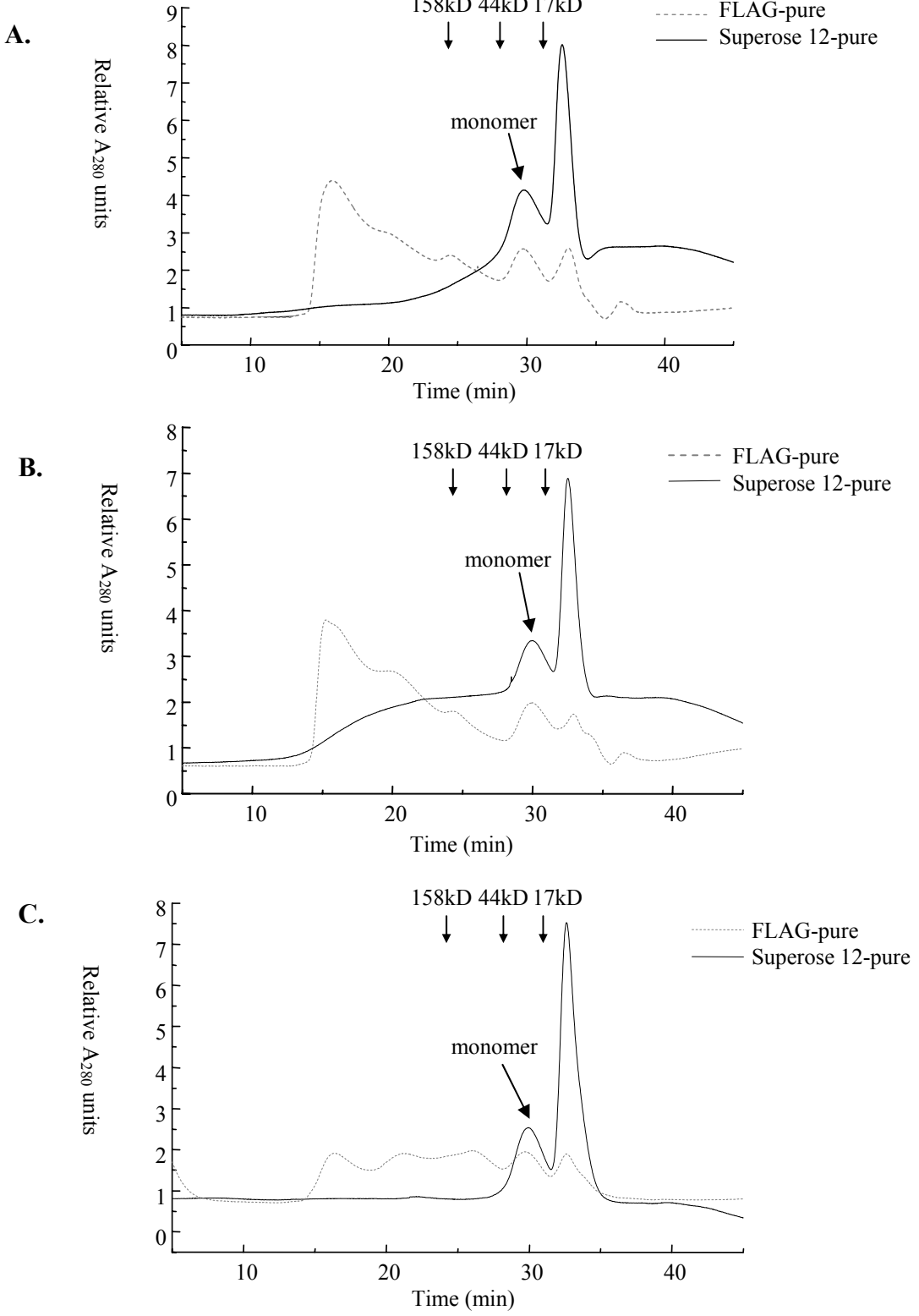

Figure 5.38 Gel-filtration chromatography purification of monomeric chimaeras using a Superose 12 column. A. GN10m42; B. GNpep22; and C. GN10m68 scFv. The grey dashed curves show the profile after FLAG affinity purification of expression culture periplasm. The black curves show the profile after monomer was collected, concentrated and reloaded onto the column. Retention times of BioRad molecular weight markers are indicated with arrows.

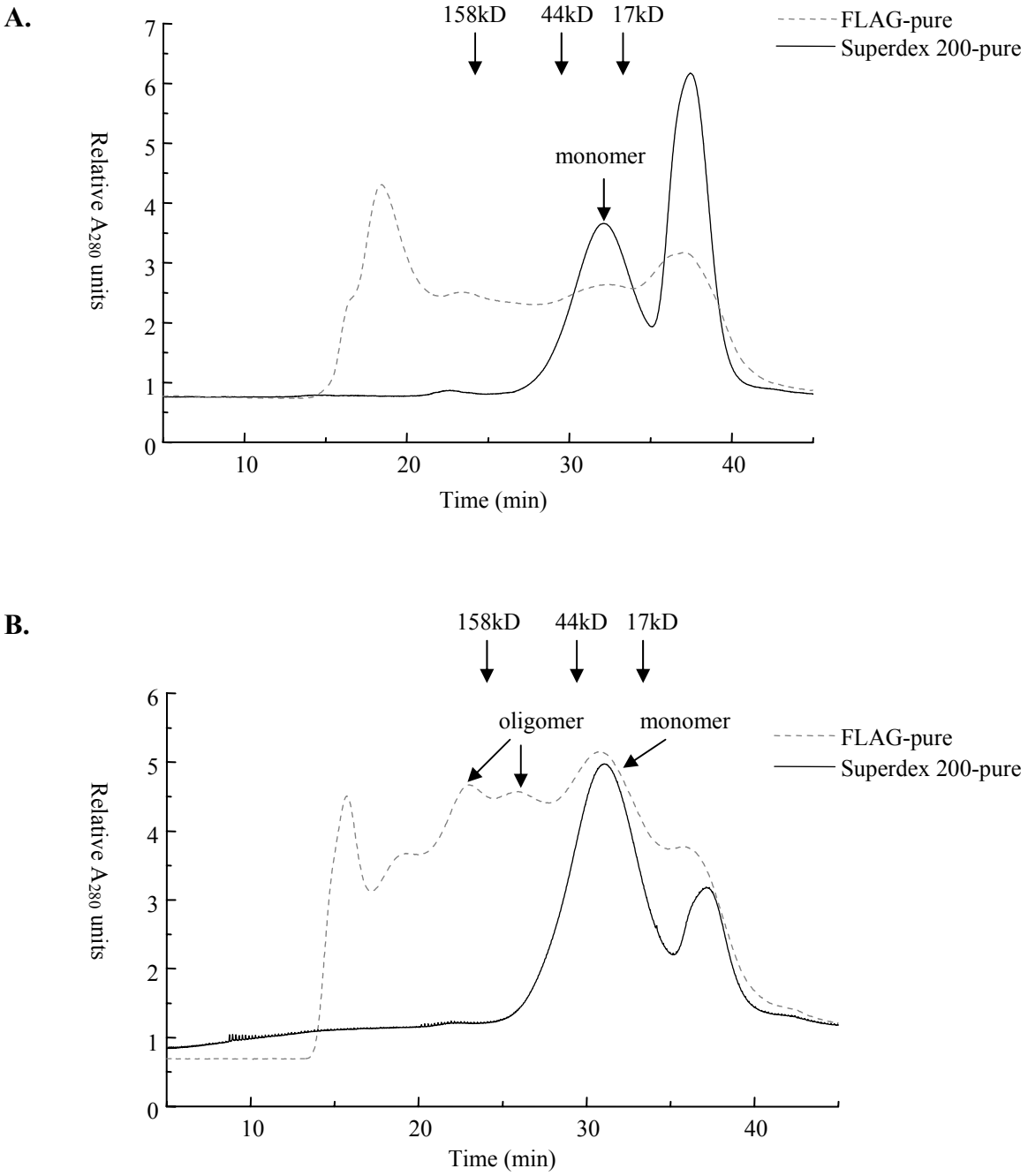

Figure 5.39 Gel-filtration chromatography purification of monomeric chimaeras using a Superdex 200 column. A. GNpep76; and B. GNBIA71. The grey dashed curves show the profile after FLAG affinity purification of expression culture periplasm. The black curves show the profile after monomer was collected, concentrated and reloaded onto the column. Retention times of BioRad molecular weight standards are indicated with arrows.

being the strongest of all the antigens, substantial cross-reactivity can be seen against both des(1-3)IGF-I and lysozyme, showing that this scFv does not possess a specific affinity for IGF-I. As this clone has lost a Cysteine from both domains and so has no stabilising disulphide bridges, it may be unable to fold correctly into a stable structure, which could explain the observed non-specificity in terms of general hydrophobic interactions from such exposed regions, although it has been reported that stable scFvs can be engineered lacking these bonds (Worn and Pluckthun, 1998). A similar result was seen for binding of GNpep22 (data not shown) but with lower overall responses. Overlaid sensorgrams are presented for binding of GN10m42 in Figure 5.40.B showing a weak non-specific response. This was also seen for GN10m68 (data not shown). The data were analysed for kinetics using BIAevaluation 3.0 (2.3.13.3) but fit poorly to the Langmuir 1:1 theoretical model and so kinetic constants were unable to be obtained.

Purified GNBIA71 was analysed for binding of its monomer to IGF-I (2.3.13.2) at 1, 2, 3 and 4 μM with the 1-3 μM runs shown overlaid in Figure 5.41. There appeared to be some cross-reactivity to other antigens (Figure 5.42.A) but there was a reasonable fit of the data to the Langmuir 1:1 model using BIAevaluation 3.0 (2.3.13.3) when analysing binding of the monomer to IGF-I (Table 5.1), whereas the data for binding to the other antigens did not fit this model. Only the 2 and 3 μM runs, fitted individually and globally (all shown in Table 5.1), were reliable, based on low χ^2 (under 1) and SE values, and visual analysis of closeness of fit to the model. The figure for dissociation constant, averaged from all fits, is 0.136 μM, which is an affinity improvement of about 27-fold on the anti-GPE wt scFv (K_D = 3.68 μM; Table 3.2). The improvement is mainly due to a slower off rate. This substantial improvement may be exaggerated as it is assumed that the broad monomer peak is not homogeneous, with the possible infiltration of some dimeric species and "sticky" non-specifically interacting species, which may be distorting the data towards a slower off-rate. The fact that the data were only reliable over a narrow concentration range (2-3 μM) also adds some uncertainty to the accuracy of the kinetic figures. However, the demonstration of some specific anti-IGF-I activity for the monomer suggests a truly chimaeric functional scFv has been produced. As an oligomeric form (possibly dimer and/or trimer) of GNBIA71 was quite prevalent (Figure 5.39.B, ~ 26 min), this was also analysed to see if an avidity effect due to multivalency could be observed. This oligomeric protein shows non-specificity (Figure 5.42.B) although it appears to have a higher apparent affinity than the monomer when binding to IGF-I (Figure 5.43), due probably to its avidity.

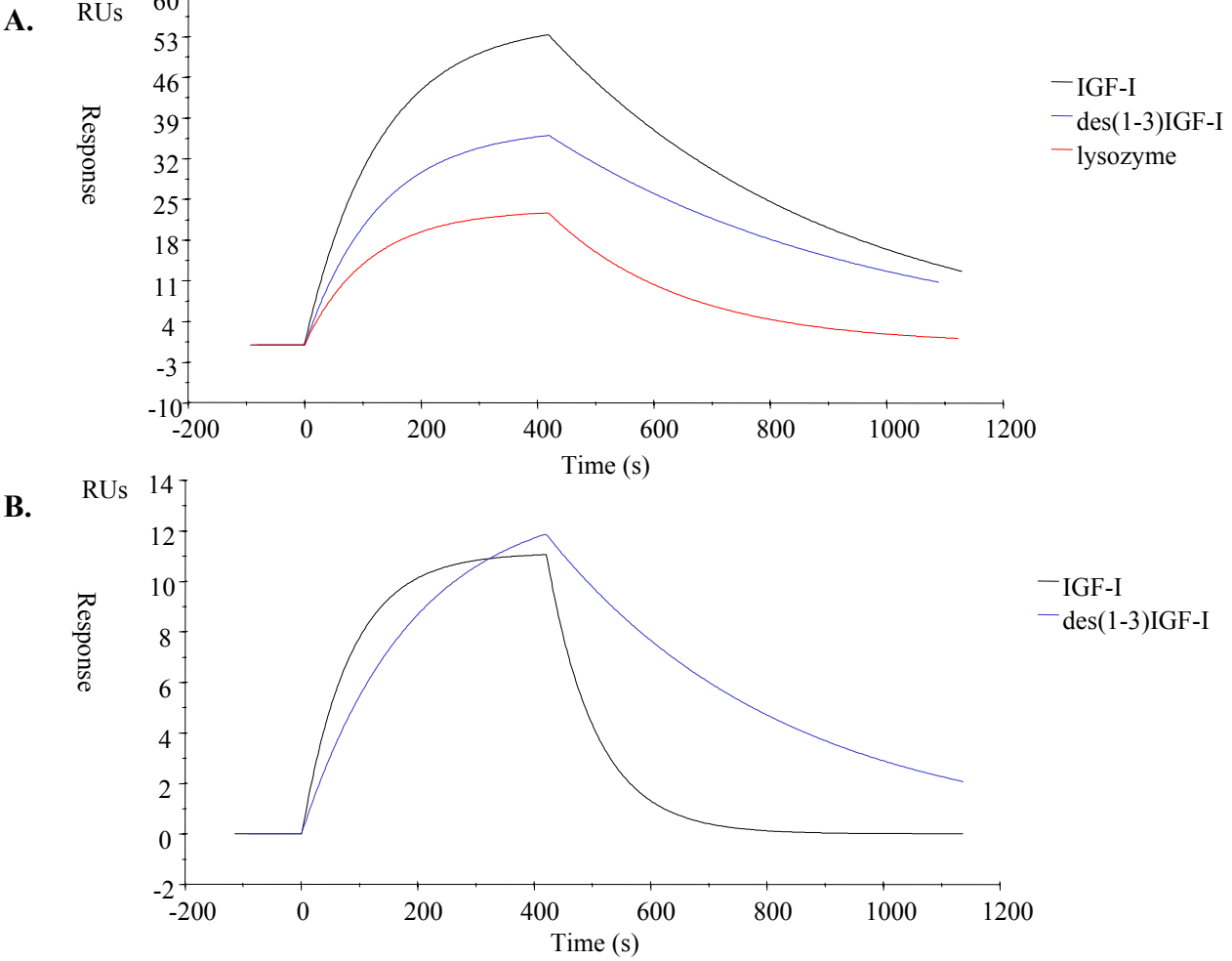

Figure 5.40 Overlaid BIAcore sensorgrams of selected chimaeras binding to different immobilised antigens. A. GNpep76 at 2 µM B. GN10m42 at 1.6 µM. Curves have had bulk refractive index changes subtracted.

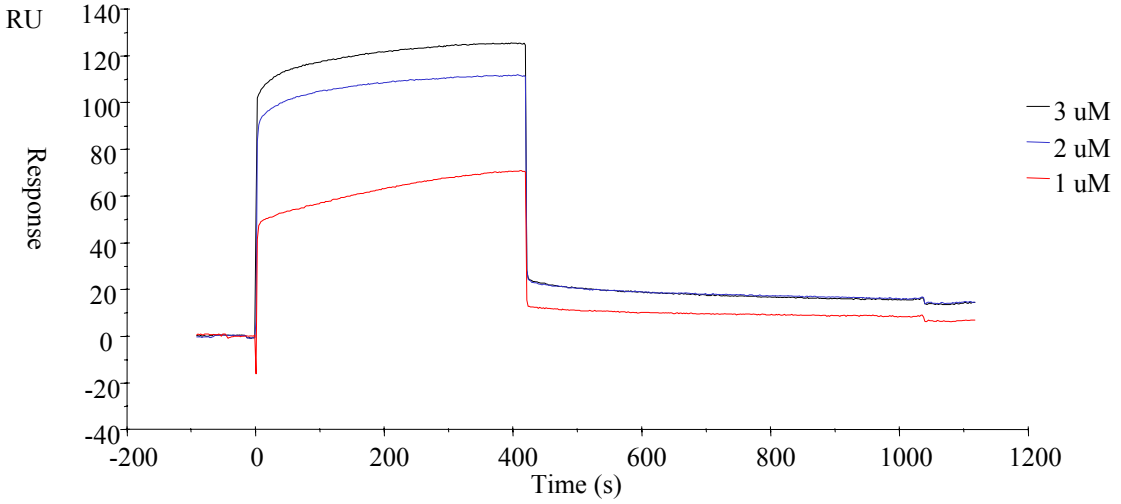

Figure 5.41 Overlaid BIAcore sensorgrams of a concentration series of GNBIA71 binding to immobilised IGF-I.

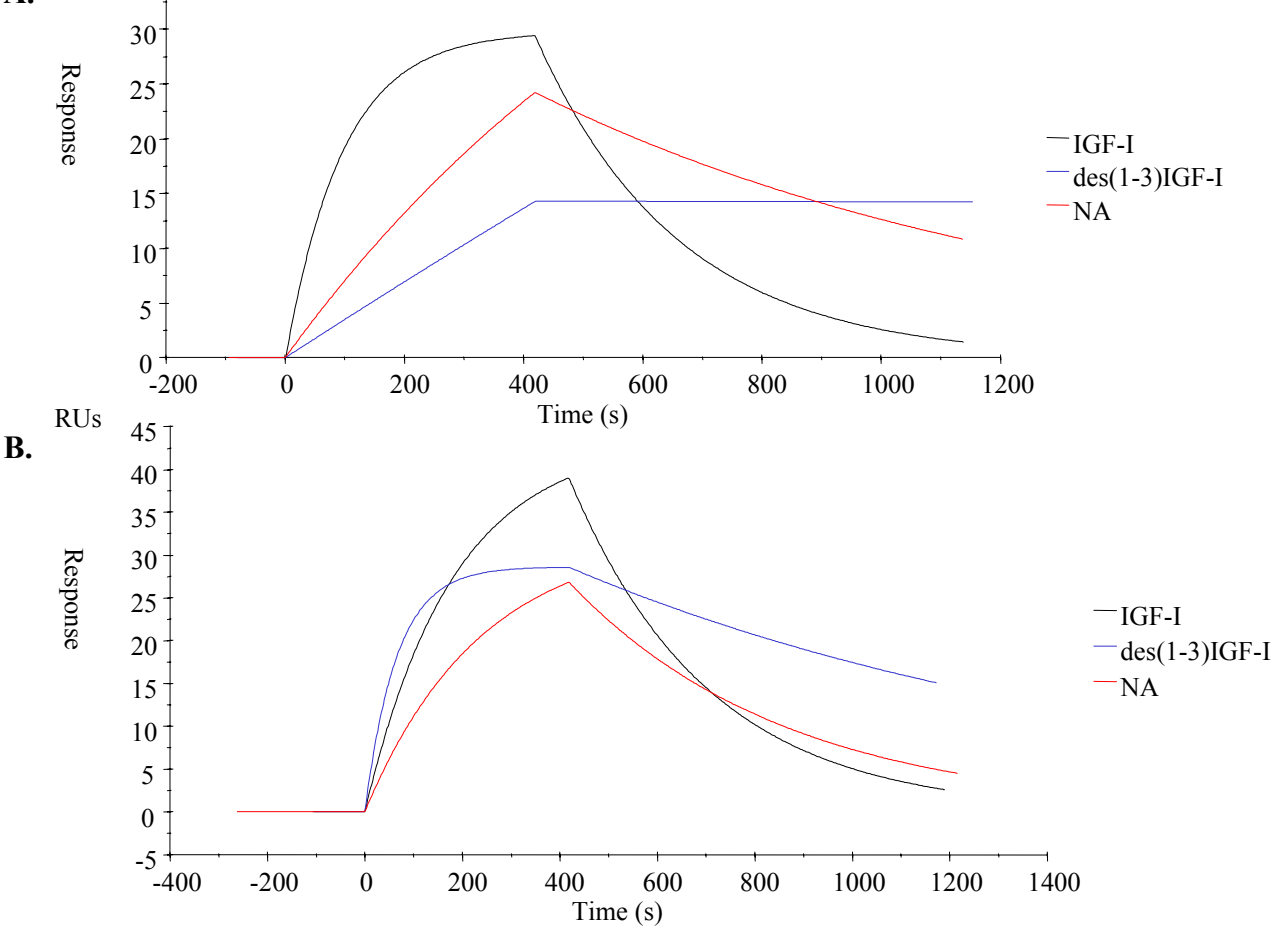

Figure 5.42 Overlaid BIAcore sensorgrams of GNBIA71 binding to different immobilised antigens. A. monomer at 2 μM B. dimer at 0.5 μM. Curves have had bulk refractive index changes subtracted.

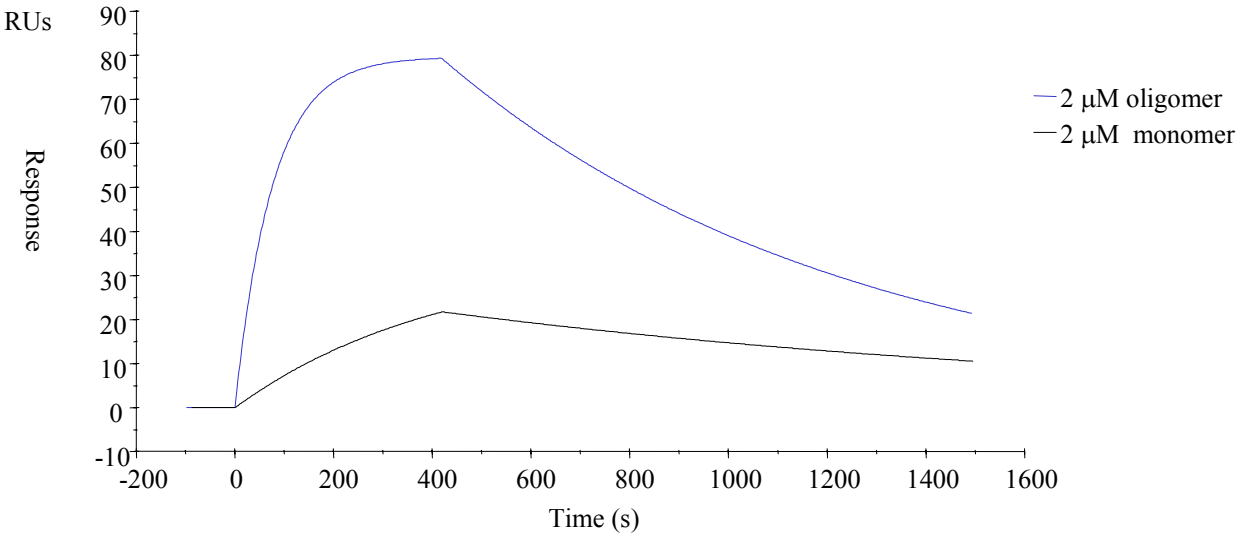

Figure 5.43 Overlaid BIAcore sensorgrams comparing monomeric and oligomeric forms of GNBIA71 binding to immobilised IGF-I.

Table 5.1 Kinetic data for interaction of GNBIA71 monomer with immobilised IGF-I.

[GNBIA71]	k_a(1/Ms)	SE*	k_d(1/s)	SE	K_D(μM)
2 μM	7.22×10^3	106	5.83×10^{-4}	1.55×10^{-5}	0.081
3 μM	3.29×10^3	52.7	6.46×10^{-4}	1.61×10^{-5}	0.196
2 μM/3μM	4.82×10^3	66.6	6.28×10^{-4}	1.54×10^{-5}	0.130

* standard errors for on and off rate calculations

5.13 Discussion

5.13.1 Cloning and characterisation of NC10GPE

The grafting strategy utilised here to construct NC10GPE has been used previously with the intent of reproducing the specificity of the CDR-donating scFv (Jung and Pluckthun, 1997), particularly in humanisation of fragments (Pulito *et al*., 1996), but structural information was used in these cases to select the appropriate framework. Also, multiple specificities have been produced by random introduction of natural CDRs to a single scFv framework (Soderlind *et al*., 2000), although this framework was chosen for its optimised expression and display characteristics. No such functionality was achieved for NC10GPE, despite favourable expression characteristics of the host (Malby *et al*., 1993), but this was expected due to the substantial sequence differences as discussed previously (5.1.1). However, it was seen as an interesting exercise to see if some anti-GPE affinity may have been acquired in any of the graft clones. The binding data (Figure 5.6) suggested weak non-specific protein interactions for all graft clones tested. If this was due to the grafting causing a propensity for the NC10 scFv to misfold and expose hydrophobic regions that may non-specifically interact with the antigen surface, then it could be suggested that it is not a robust framework for this sort of substitution. However, this may vary from antibody to antibody with the CDRs of some antibodies being a better 'fit' than others.

5.13.2 DNA shuffling

The choice of DNaseI enzyme whose activity was most easily controlled and reproduced was important to reduce the wastage of DNA template in reactions where the gene has been either over-digested or under-digested. The amount of template DNA required for primerless PCR to yield a

product appears to be far greater than that required for normal PCR. It was found that at least 0.2-0.5 μg was needed as template, consistent with the original reporting of the method (Stemmer, 1994), which in the case of a pool of fragments about 50 base pairs in length is over 10^{12} molecules. In theory, only one template molecule would be needed for standard PCR with specific flanking primers (Saiki *et al*., 1988). Such a large amount of template is probably required because, to anneal off each other, digested fragments would need to have a sufficient overhang of homology for the priming process to occur leading to polymerisation, and it is likely that many of the fragments in the pool would have insufficient complementary overhangs for this to occur, making them redundant to the shuffling process. Therefore, much of the pool would not be used, being "out-competed" by the more complementary fragments. The way these fragments were purified was also important. It was much easier to produce a primerless PCR smear from these fragments if they were purified directly from the DNaseI digest using desalting columns (2.1.15) compared with electroelution from agarose gel and then ethanol precipitation. This may have been due to poor yield from the electroelution and precipitation procedure. The temperature of annealing is also important. It is desirable to encourage crossover events between the gene fragments by using lower annealing temperatures, while not forcing this process to be over promiscuous, leading to production of genes that have deletions, insertions, or are truncated. Sequence information for the shuffled genes has revealed that some incomplete genes have been constructed (Figures 5.8 and 5.37). This is not totally avoidable as it has been shown theoretically that in attempts to attain a desired cross-over frequency there is a trade off with efficiency of gene reassembly that can lead to these "junk" sequences (Maheshri and Schaffer, 2003). Too high an annealing temperature may lead to crossovers only in the homologous CDRs for the shuffle of NC10GPE and anti-GPE, or may lead to the regeneration of parental genes predominating. A satisfactory mix of crossovers in both the CDR and framework regions is desired in this case to optimise diversity. This appears to have been achieved for GPENC (Figure 5.10) and H2MNC (Figure 5.11) although the experimental conditions for the shuffling process might have to be individually optimised for every different gene.

5.13.3 Ribosome display of the chimaera libraries

Either measures to improve folding of the scFvs on the ribosome in the reticulocyte lysate, or measures to prevent the association of unfolded species with antigen needed to be developed to reduce non-specific selection as seen for EPGPE (Chapter 4). Initially the latter approach was chosen, because in any mutated library there would be expected to be a reasonable proportion of non-functional proteins within the pool due to mutations that may be deleterious to proper folding,

especially in a chimaeric library like GPENC and H2MNC, and one based on an apparently unstable framework such as anti-GPE. Therefore BSA was used as an alternative blocking agent to the skim milk used in the work described in Chapter 4. Further, EDTA, used as the eluent in Chapter 4, was replaced by peptide, with the expectation that this would lead to more specific elution of binders. As only one of the two fragments shuffled had a functional affinity to IGF-I it would be expected that there would be a lower proportion of functional library members compared to a library created from shuffling of two functional fragments. However, DNA shuffling has been shown to produce proteins with new function (Raillard *et al*., 2001; Matsumura and Ellington, 2001; Liu *et al*., 1997) and so the desire was to select and enrich for these functional molecules from other non-functional, non-specific or misfolded species.

5.13.3.1 Selection with GPE peptide elution

Experiments using the GPE tripeptide for elution, previously shown to have an activity specific for the anti-GPE scFv in competing for binding with immobilised IGF-I on the BIAcore (3.5.3), were initially promising, as there appeared to be stronger recovery against IGF-I compared to lysozyme and the intensity of the RT-PCR bands could be seen to titrate out with increasing concentration of peptide (Figure 5.12 and 5.13). The elution concentration, however, was extremely low suggesting elution of very weak affinity binders, but the fact that a 'blank' elution with no peptide prior to the peptide elutions yielded no RT-PCR bands gave some confidence that the specific elution was occurring. The fact that little was eluted at higher concentrations of the peptide suggests that few tight binders were binding, however, strong binders might be expected to be rare in these libraries and it was desired, in the first instance, to isolate functional chimaeras even though they may have a low affinity.

Peptide specific elution was not apparent in the subsequent selection round, regardless of spacer length used (Figure 5.14, 5.16 and 5.17), and this suggests some problem with the RT-PCR or T7 polymerase steps applied to the primary eluate pool. Perhaps in between the first and second rounds of display, a mutation leading to loss of function or a deletion leading to a frameshift introduced by the RT-PCR or T7 polymerase had been propagated, although such mutations would be unlikely to knock out the whole pool of binders. It was therefore decided to analyse these GPE peptide-selected mutants from the first round where better specificity was observed.

5.13.3.2 Selection with GPE 10-mer peptide elution

Experiments performed with the GPE 10-mer peptide initially showed non-specific selection. It was therefore decided to investigate use of an alternative negative control antigen, α-amylase. Optimisation of selection using this antigen, by alteration of blocking and washing conditions, led to some specific selection being demonstrated by RT-PCR (Figure 5.20 and 5.21). Interestingly, the EDTA elution after the peptide elutions showed no RT-PCR bands, suggesting that either little non-specific protein from this library was associating with antigen or the blocking and washing protocol was sufficient to eliminate these interactions. It was also possible that non-specific proteins were dissociating in the earlier elutions. The lack of EDTA-eluted bands also suggested that few, if any high affinity binders existed in the library, as they were eluted by low concentrations of the peptide. The second round enrichment against lysozyme seen for selections using GPE tripeptide was not reflected in second round selections using GPE 10mer against α-amylase. It could not be determined whether this was a function of use of α-amylase or the GPE 10-mer. However, it was again difficult to enrich for IGF-I binders, in this second round, as evidenced by the weak RT-PCR bands, possibly due to their low affinities.

5.13.3.3 Selection using the BIAcore

The data obtained from using the BIAcore as a selection tool in ribosome display suggests that it is not an ideal system for this purpose. The IGF-I chip surface appears to have a short active life in this process and therefore antigen has to be constantly immobilised on fresh flow cells making it costly and laborious. Some other antigen surfaces may be more robust though. Strong RT-PCR bands were retrieved for runs against all antigens tested suggesting poor specificity with this system. It follows that the sensorgram curves seen are not reflective of binding of specific proteins attached to complexes and therefore are not a way of monitoring real dissociation during the selection process. The sensitivity of the BIAcore 1000 appears to be insufficient for detecting interactions of specific translated complexes and is masked anyway by non-specific interactions from within the transcription/translation mix. Non-specific complexes appear to be able to interact with the chip surface in a way that makes them slow to leave during dissociation. The BIAcore selection process, including the dialysis step introduced, may be detrimental to stability of the complexes, and therefore the retrieval of RT-PCR bands observed may in fact be due to residual mRNAs, detached from their ribosomes, that are slow to leave the chip surface. Measures to improve stability of complexes within this system such as the introduction of Mg Acetate into the

running buffer and doing runs at low temperature may assist specific selection. Addition of a blocking reagent into the binding step may also help reduce non-specific interactions.

5.13.4 Screening of selected chimaeras

ELISA data for 'selected' chimaera clones was not conclusive, with high background binding to non-IGF-I antigens (Figures 5.34 and 5.35). This suggested that perhaps there was a propensity for these proteins to misfold and aggregate, but could have also been due to other species in the culture supernatants. However, problems in gaining good ELISA data have been consistent throughout the work of this study. Presumably, this is partly due to the poor apparent affinity of the anti-GPE wt scFv. The bivalent parent monoclonal antibody binds well and specifically by the ELISA method used. It has been difficult to get a strong enough signal to gain a feel for relative affinities and possible improvements achieved in scFvs. Blocking using skim milk gave less background binding but signals too low for conclusions to be drawn. The protocol developed for use of BSA as a blocking agent enabled higher signals to be obtained but higher non-specific signals were produced in the process. It is possible that misfolded protein was responsible for this effect, since it has been shown that, in phage display, sequence motifs shown to bind to both unblocked and BSA-blocked plastic surfaces often have a prevalance of tyrosine and tryptophan residues (Adey *et al*., 1995), both of which are conserved in the hydrophobic core of antibody frameworks (Chothia *et al*., 1998). This may be one explanation for some non-specific selection observed. Thus, the few clones chosen for closer analysis were those with the best IGF-I ELISA signal and lowest signal against the negative control antigens (lysozyme and α-amylase), though none of the clones exhibited low cross-reactivity in ELISA. It was reasoned that it was worthwhile to look more closely at the properties of some of these selected proteins to show conclusively that selection was predominantly for non-specific proteins. The clones analysed for sequence (Figures 5.36 and 5.37) were genuine chimaeras, as seen for sequences of the library prior to selection (Figure 5.10 and 5.11). Shuffling and selection of full scFv chimaeras has not been reported before, although shuffling of large pools of V_L sequences (van den Beuken *et al*., 2001), or V_H and V_L separately (Huls *et al*., 2001) has been reported.

5.13.5 Expression and purification of chimaeras

The selected chimaeras all showed the same low solubility and low proportion of monomer that was observed for the wild type anti-GPE and mutants selected from EPGPE. These properties may reflect the observed ELISA cross-reactivity and poor specificity of ribosome display selection, due

to the interactions of misfolds, aggregates or insoluble species with the antigen surface. However, some monomer could be purified for analysis. The presence of DTT in the transcription/translation reaction is a possible reason for isolation of poor folding scFv with a consequent tendency to precipitate and aggregate, although selection in a reducing environment such as the bacterial cytoplasm (Martineau and Betton, 1999), or in the presence of DTT in ribosome display selection (Jermutus *et al*., 2001), have been used in selection of scFvs with improved stability. It was reasoned that improved frameworks with better solubility and stability may have been generated in the library, but these don't appear to have been selected. Methods to improve yield of soluble monomer such as refolding techniques or manipulation of expression conditions could be investigated further, although such techniques cannot modify the instrinsic folding stability of a protein that its solubility is often highly dependent on (Waldo, 2003). Use of ribosome display for selection and enrichment of folded soluble proteins by doing a preselection for misfolds has recently been reported (Matsuura and Pluckthun, 2003). Despite the fact that the collected peaks were broad and likely to be heterogeneous with unfolded species present, some BIAcore analysis was possible.

5.13.6 Binding of selected chimaeras

The BIAcore data generated for the chimaeric scFvs is indicative of non-specific interactions occurring with a variety of antigens. Most of the clones showed a poor fit to the theoretical model when analysed using BIAevaluation 3.0 suggesting that an scFv able to bind to its antigen in a 1:1 manner had not been produced, or that such an interaction was being masked by misfolded or other non-specific species present in the preparation. The data for GNBIA71, however, is promising as there is a reasonable fit to the Langmuir 1:1 model (albeit over a narrow concentration range) and the interaction of monomeric peak is more typical of a specific binding event for IGF-I as opposed to other antigens (Table 5.1; Figures 5.41 and 5.42.B). The dissociation constant generated of 0.136 μM, equating to an ~ 27-fold affinity improvement on the anti-GPE wt is good. The interpretation of the data is that functional anti-IGF-I chimaeric scFv exists within the peak-purified protein preparation that also included misfolds that may interact non-specifically, and dimeric species that may be skewing off rate data. Thus extra purification efforts to attempt to separate functional from spurious species, such as a further chromatographic step to purify based on affinity to IGF-I, or a chromatographic step to absorb hydrophobic species may be justified. Such a step may yield an scFv preparation that can be assigned a more accurate determination of protein concentration and provide better kinetic data, giving greater confidence in the measurement of affinity. The generation

of chimaeric scFv gene sequences reported by Lorimer and Pastan, (1995) has been achieved here with subsequent protein expression, purification, and binding analysis of some of these proteins. Recently, possible genuine cross antibody shuffling has been reported by DNA shuffling of large libraries of V_L domains (van den Beuken *et al*., 2001), however, functional fragments selected were low in affinity and possibly resulted from regenerated germline sequences. Similarly, scFv libraries produced by DNA shuffling of large pools of V_H and V_L domains separately, yielded functional clones with improved affinity and a different V_L sequence (Huls *et al*., 2001), although it was not clear from the report whether the V_L of this clone was genuinely chimaeric or an intact sequence. Detailed sequence information for the above two cases was not provided so the frequency of crossovers and relative use of parental sequences could not be determined. The method employed in these latter two reports could potentially be applied to anti-GPE, shuffling it against a large pool of scFvs, as the diversity generated may enhance the potential for selection of functional scFvs. There is potential for more work in the exploring of DNA shuffling as means of generating diversity for producing novel antibody sequences, as only a limited number of successes have so far been reported. The ribosome display and selection strategies employed here have not been highly successful in isolating scFvs chimaeras, although GNBIA71 appears to be a genuine functional chimaeric scFv. An improved ribosome display system would allow better assessment of the efficacy of the DNA shuffled chimaera libraries.

CHAPTER 6
OVERVIEW, CONCLUSIONS, FURTHER WORK

This thesis describes the construction and characterisation of an IGF-I-binding scFv (anti-GPE) and its use as a model for a number of antibody engineering approaches.

Initially the variable domain genes were isolated from the hybridoma cell line producing the anti-GPE monoclonal antibody. Cloning of these genes into an scFv format and subsequent DNA sequencing revealed that the CDR2 region of V_H was unusually short with no similar examples found in the literature. Comparison of deduced amino acid sequence for the cloned genes with N-terminal amino acid sequence data for the parent antibody heavy and light chains suggested that the correct genes had been cloned. Expression of the anti-GPE scFv and protein purification showed that the protein has poor solubility and stability. A low proportion of the expressed protein exists in a monomeric state. It is concluded that the unusually short V_H CDR2 is responsible for a large proportion of the produced scFv misfolding leading to the formation of precipitates and aggregates and also causing toxicity to *E. coli*. This conclusion was supported by the results from the construction of a mutant version of the anti-GPE scFv. This mutant (anti-GPE H2M) had six extra residues engineered in to the V_H CDR2 region to bring it to the length found in most mouse class IIA V genes. A number of differences observed supported the conclusion that the fuller length sequence folded more efficiently. Firstly, the toxic effect of the expressed protein on the host *E.coli* cells was less pronounced, suggesting reduction in the propensity to aggregate which is often a cause of cell lysis. Secondly, overall expression levels were higher. Thirdly, the proportion of monomer compared to higher order species was significantly improved in the mutant with nearly three-fold improved yield in purified monomer for the mutant.

Monomeric scFv could be purified in sufficient amounts to allow analysis of binding to immobilised IGF-I by surface plasmon resonance on the BIAcore. The scFv bound to IGF-I and was shown to retain the specificity of the parent antibody, namely binding to the N-terminal GPE domain of the IGF-I as negligible binding to immobilised des(1-3)IGF-I was detected. The calculated dissociation constant for the scFv binding to IGF-I of K_D = 3.68 μM is weak for an antibody. This affinity was easily an order of magnitude lower than that calculated for the Fab fragment of the parent antibody. It is concluded that the monomer peak collected is a heterogenous mix of properly folded scFvs and misfolds, thus the calculated protein concentration used in the

affinity evaluation is not that of the concentration of functionally active scFv present and therefore the apparent affinity reported is an underestimate of the actual affinity. This is again most likely a function of the low stability of the anti-GPE scFv. The anti-GPE H2M scFv was shown to retain binding to IGF-I with a slight affinity improvement (< 2-fold) however this is again an apparent affinity and may be reflective of a higher concentration of active monomer within the purified sample.

A model has been presented for the mechanism of deletion of residues for the germline sequence for the anti-GPE V gene. Further work to confirm that the cloned anti-GPE V gene has been generated in vivo and is not an artefact of cloning or PCR would be to confirm the amino acid sequence in the parent antibody. This would require some type of cleavage of the heavy chain fragment by enzymatic digestion and purification of the resulting fragments to gain closer access to the CDR2 region for N-terminal sequencing. Mass spectrometry could be used for this purpose. If indeed the causes of the poor biophysical characteristics of the anti-GPE scFv are sequence-related, then the pursuit of engineering approaches further to the site-directed mutagenesis of the V_H CDR2 was seen as the best approach to improve this framework, as opposed to manipulation of expression conditions and protein chemistry, and so subsequent experiments addressed this.

A ribosome display system was developed to show antigen-specific selection of anti-GPE scFv using a commercial rabbit reticulocyte lysate as a source of ribosomes. Fine optimisation of the blocking, binding and washing steps was required to achieve this selection. Such optimisation may be necessary for every new protein displayed. An error-prone PCR method was used to incorporate point mutations into the anti-GPE scFv gene. A pool of mutants (EPGPE) was created that had an average of 4.2 random amino acid changes per scFv. Ribosome display of these mutants was employed as an approach for isolation of proteins of improved affinity as well as characteristics such as stability and expression. In performing successive rounds of display and panning for enrichment of improved scFvs, the occurrence of non-specific selection was observed. The most likely explanation for this phenomenon is that many of the mutants were interacting with the selection surface in a non-specific manner, possibly through associations of hydrophobic regions exposed due to misfolding of the scFvs on the ribosome, and that these interactions were difficult to disrupt with washing steps. This was supported by ELISA data showing that many of the selected clones produced scFvs that bound in a nonspecific manner, and that the three mutants analysed from the sixth round of display and selection produced mostly aggregated protein. Of the 64 clones screened from a fourth round of display and selection, three were chosen for characterisation but

just one of these showed an improved affinity and none exhibited any significant improvement in expression or solubility. The matured mutant had a modest affinity improvement of 2.6-fold which is the first example of affinity maturation using this system.

The method of ribosome display and selection developed, in combination with error-prone PCR mutagenesis, was not a highly effective means of producing affinity-matured anti-GPE variants. Firstly, the mutagenesis rate may have been too high for the anti-GPE scFv framework. Further display experiments involving mutagenesis of anti-GPE would be best performed using a lower mutation rate. This may be more compatible with the low stability anti-GPE. This would reduce the chances of isolating highly improved mutants but may increase the proportion of functional and properly folded proteins within the library. An alternative would be to base the mutagenesis on a more stable framework such as the anti-GPE H2M mutant. Uncoupling the translation from the transcription, thereby eliminating the presence of DTT in this reaction, could be undertaken with the objective of increasing the proportion of properly folded proteins, therefore reducing the amount of non-specific interactions occurring within the system. As it is most likely impossible to totally rid the system of misfolds that non-specifically interact with the selection surface, measures to competitively elute specifically bound complexes from non-specific species, rather than total elution of mRNA with EDTA, could be utilised as a means of isolating a higher proportion of positive binding scFvs as measured by ELISA. Such an elution approach using GPE peptides was undertaken in the ribosome display experiments described in Chapter 5.

The grafting of the anti-GPE CDRs on to the framework of the NC10 scFv did not result in a functional IGF-I-binding chimaera but rather provided the partner for DNA shuffling with anti-GPE. DNA shuffling of these two species generated a pool of chimaeric scFvs with randomly recombined framework fragments. Ribosome display was employed to attempt to isolate functional chimaeric scFvs from the pool that may have attained a favourable combination of parental sequences from the DNA shuffling procedure. Elution of selected ribosome complexes with specific peptide was attempted to reduce the prevalence of non-specific scFvs seen in the display of EPGPE with EDTA elution. The same problems of non-specificity observed for EPGPE were seen in the selection and screening for the chimaera libraries. It is concluded that the chimaera libraries comprised a high proportion of non-functional species prone to non-specific interactions with the selection surface and that many of these were non-specifically eluted by the peptide. The chimaeras chosen for characterisation reflected this non-specificity in BIAcore studies. Use of the BIAcore itself for selection from the chimaera libraries also showed the same problems with non-specificity.

However, one characterised BIAcore-selected chimaera, GNBIA71, did appear to exhibit a binding specificity to whole IGF-I although this protein still retained poor expression characteristics. This genuine scFv chimaera showed some non-specific interaction with other immobilised antigens but a one to one specific interaction was only detectable for GNBIA71 binding to IGF-I from the BIAcore data. This is the first functional fully chimaeric DNA-shuffled scFv reported. Despite this, the BIAcore selection procedure is concluded to be not ideal, due to the harsh effects it has on the chip surface, and the tendency for non-specific interactions with this surface. The selection of the chimaera libraries against antigen coated on microtiter well surfaces was not efficient for isolation of specific binders, but several approaches for improvement of this system are apparent.

The data suggests, as seen for ribosome display of EPGPE, that an uncoupling of the transcription and translation steps needs to be investigated as a means of improving the system. This will allow DTT to be absent when protein folding is occurring and allow independent optimisation of the translation step. Stability of the complexes – keeping both mRNA and protein attached to the ribosome - is important. In this work, low temperature and magnesium was used for this purpose. Magnesium was used at a low concentration and levels may need optimisation. Also, the use of spacer sequences with motifs that may enhance retention of attachment of mRNA to the ribosome could be investigated. More stable ribosome complexes should assist the selection procedure for steps to eliminate or reduce non-specific interactions from misfolded species by washing. Additional blocking reagent components may also need to be investigated. Steps to promote efficient folding should also be investigated. Firstly, the removal of DTT from the translation by the uncoupling should assist. Also, the effects of substances such as PDI, chaperones, and glutathione could be examined. Steps to maximise folding efficiency should help to reduce occurrence of non-specific interactions in the system. This would help to support the conclusions postulated here as to why non-specific recovery was so prevalent in this work. Selection of antigen in solution may also help to reduce non-specificity and allow closer control of selection by management of the soluble antigen concentrations. The library construction itself can be addressed. The selection of GNBIA71 proves in principle that the creation of functional chimaeric scFvs derived from antibodies of significantly different sequence is possible, but a better library to create greater diversity would be achieved by DNA shuffling of the anti-GPE scFv sequence against a large pool of variant scFv sequences, such as a naïve library with oligonucleotides coding for the anti-GPE CDRs spiked into the primerless PCR. Such a chimaera library strategy, sourcing a greater variety of sequences, would enhance the chances of production of useful combinations of sequences than the limited example of two sequences as described in this work. Therefore the potential of improved library

construction and ribosome display methodologies as a means of creating and isolating useful binding reagents is largely untapped.

The anti-GPE scFv is not an ideal framework on which to base antibody engineering experiments due to its unusual sequence and poor biophysical characteristics as reported in this thesis. However, its use as a model in this study has allowed identification of approaches to improve ribosome display in a eukaryotic system. Further, its use in DNA shuffling has shown in principle that it is possible to create functional chimaeric scFvs.

References

Adey, N.B., Mataragnon, A.H., Rider, J.E., Carter, J.M. and Kay, B.K., **1995**. Characterization of phage that bind plastic from phage-displayed random peptide libraries. *Gene*. 156:27-31.

Alexi, T., Hughes, P.E., van Roon-Mom, W.M., Faull, R.L., Williams, C.E., Clark, R.G. and Gluckman, P.D., **1999**. The IGF-I amino-terminal tripeptide glycine-proline-glutamate (GPE) is neuroprotective to striatum in the quinolinic acid lesion animal model of Huntington's disease. *Exp. Neurol*. 159:84-97.

Almagro, J.C., Hernandez, I., del Carmen Ramirez, M. and Vargas-Madrazo, E., **1997**. The differences between the structural repertoires of VH germ-line gene segments of mice and humans: implication for the molecular mechanism of the immune response. *Mol. Immunol*. 34:1199-214.

Ames, R.S., Tornetta, M.A., McMillan, L.J., Kaiser, K.F., Holmes, S.D., Appelbaum, E., Cusimano, D.M., Theisen, T.W., Gross, M.S., Jones, C.S., et al. **1995**. Neutralizing murine monoclonal antibodies to human IL-5 isolated from hybridomas and a filamentous phage Fab display library. *J. Immunol*. 154:6355-64.

Amstutz, P., Pelletier, J.N., Guggisberg, A., Jermutus, L., Cesaro-Tadic, S., Zahnd, C. and Pluckthun, A., **2002**. *In vitro* selection for catalytic activity with ribosome display. *J. Am. Chem. Soc*. 124:9396-403.

Anlar, B., Sullivan, K.A. and Feldman, E.L., **1999**. Insulin-like growth factor-I and central nervous system development. *Horm. Metab. Res*. 31:120-5.

Babino, A., Pritsch, O., Oppezzo, P., Du Pasquier, R., Roseto, A., Osinaga, E. and Alzari, P.M., **1997**. Molecular cloning of a monoclonal anti-tumor antibody specific for the Tn antigen and expression of an active single-chain Fv fragment. H*ybridoma* 16:317-24.

Baca, M., Presta, L.G., O'Connor, S.J. and Wells, J.A., **1997.** Antibody humanization using monovalent phage display. *J. Biol. Chem.* 272:10678-84.

Baggio, R., Burgstaller, P., Hale, S.P., Putney, A.R., Lane, M., Lipovsek, D., Wright, M.C., Roberts, R.W., Liu, R., Szostak, J.W. and Wagner, R.W., **2002**. Identification of epitope-like consensus motifs using mRNA display. *J. Mol. Recognit*. 15:126-34.

Bagley, C.J., May, B.L., Szabo, L., McNamara, P.J., Ross, M., Francis, G.L., Ballard, F.J. and Wallace, J.C., **1989**. A key functional role for the insulin-like growth factor 1 N-terminal pentapeptide. *Biochem. J*. 259:665-71.

Barbas, C.F. 3rd, Kang, A.S., Lerner, R.A. and Benkovic, S.J., **1991.** Assembly of combinatorial antibody libraries on phage surfaces: the gene III site. *Proc. Natl. Acad. Sci. U.S.A.* 88:7978-82.

Barbas, C.F. 3rd, Bain, J.D., Hoekstra, D.M. and Lerner, R.A., **1992.** Semisynthetic combinatorial antibody libraries: a chemical solution to the diversity problem. *Proc. Natl. Acad. Sci. U.S.A.* 89:4457-61.

Barbas, C.F. 3rd, Hu, D., Dunlop, N., Sawyer, L., Cababa, D., Hendry, R.M., Nara, P.L. and Burton, D.R., **1994.** In vitro evolution of a neutralizing human antibody to human immunodeficiency virus type 1 to enhance affinity and broaden strain cross-reactivity. *Proc. Natl. Acad. Sci. U.S.A.* 91:3809-13.

Barbas, C.F. 3rd and Burton, D.R., **1996.** Selection and evolution of high-affinity human anti-viral antibodies. *Trends Biotech.* 14:230-4.

Barrick, J.E., Takahashi, T.T., Ren, J., Xia, T. and Roberts, R.W., **2001**. Large libraries reveal diverse solutions to an RNA recognition problem. *Proc. Natl. Acad. Sci. U.S.A*. 98:12374-8

Bartel, D. P. and Szostak, J.W., **1993**. Isolation of new ribozymes from a large pool of random sequences. *Science* 261:1411-18.

Bass, S., Greene, R. and Wells, J.A., **1990.** Hormone phage: an enrichment method for variant proteins with altered binding properties. *Proteins* 8:309-14.

Batori, V., Koide, A. and Koide, S., **2002**. Exploring the potential of the monobody scaffold: effects of loop elongation on the stability of a fibronectin type III domain. *Protein Eng*. 15:1015-20.

Baxter, R.C., Bayne, M.L. and Cascieri, M.A., **1992**. Structural determinants for binary and ternary complex formation between insulin-like growth factor-I (IGF-I) and IGF binding protein-3. *J. Biol. Chem*. 267:60-5.

Baxter, R.C., **1994**. Insulin-like growth factor binding proteins in the human circulation: a review. *Horm. Res*.42:140-4.

Bayne, M.L., Applebaum, J., Underwood, D., Chicchi, G.G., Green, B.G., Hayes, N.S. and Cascieri, M.A., **1989**. The C region of human insulin-like growth factor (IGF) I is required for high affinity binding to the type 1 IGF receptor. *J. Biol. Chem*. 264:11004-8.

Beaudry, A.A. and Joyce, G.F., **1992**. Directed evolution of an RNA enzyme. *Science* 257:635-41.

Beiboer, S.H., Reurs, A., Roovers, R.C., Arends, J.W., Whitelegg, N.R., Rees, A.R. and Hoogenboom, H.R., **2000**. Guided selection of a pan carcinoma specific antibody reveals similar binding characteristics yet structural divergence between the original murine antibody and its human equivalent. *J. Mol. Biol*. 296:833-49.

Bespalov, I.A., Bond, J.P., Purmal, A.A., Wallace, S.S. and Melamede, R.J., **1999**. Fabs specific for 8-oxoguanine: control of DNA binding. *J. Mol. Biol*. 293:1085-95.

Beste, G., Schmidt, F.S., Stibora, T. and Skerra, A., **1999**. Small antibody-like proteins with prescribed ligand specificities derived from the lipocalin fold. *Proc. Natl. Acad. Sci. U.S.A.* 96:1898-1903.

Better, M., Chang, C.P., Robinson, R.R. and Horwitz, A.H., **1988.** Escherichia coli secretion of an active chimeric antibody fragment. *Science* 240:1041-3.

Bieberich, E., Kapitonov, D., Tencomnao, T. and Yu, R.K., **2000**. Protein-ribosome-mRNA display: affinity isolation of enzyme-ribosome-mRNA complexes and cDNA cloning in a single-tube reaction. *Anal. Biochem*. 287:294-8.

Bird, R.E., Hardman, K.D., Jacobson, J.W., Johnson, S., Kaufman, B.M., Lee, S.M., Lee, T., Pope, S.H., Riordan, G.S. and Whitlow, M., **1988.** Single-chain antigen-binding proteins. *Science* 242:423-6.

Boder, E.T. and Wittrup, K.D., **1997**. Yeast surface display for screening combinatorial polypeptide libraries. *Nat. Biotech.* 15:553-557.

Boder, E.T. and Wittrup, K.D., **1998.** Optimal screening of surface-displayed polypeptide libraries. *Biotech. Prog.* 14:55-62.

Boder ET, Midelfort KS, Wittrup KD. **2000**. Directed evolution of antibody fragments with monovalent femtomolar antigen-binding affinity. *Proc Natl Acad Sci U S A*. 97(20):10701-5.

Boss, M.A., Kenten, J.H., Wood, C.R. and Emtage, J.S., **1984.** Assembly of functional antibodies from immunoglobulin heavy and light chains synthesised in e. Coli. *Nucleic Acids Res.* 12:3791-806.

Bourguignon, J. and Gerard, A., **1999**. Role of insulin-like growth factor binding proteins in limitation of IGF-I degradation into the N-methyl-D-aspartate receptor antagonist GPE: evidence from gonadotrophin-releasing hormone secretion in vitro at two developmental stages. *Brain Res*. 847:247-52.

Braisted, A.C. and Wells, J.A., **1996.** Minimizing a binding domain from protein A. *Proc. Natl. Acad. Sci. U.S.A.* 93:5688-92.

Brinkmann, U., Reiter, Y., Jung, S.H., Lee, B. and Pastan, I., **1993.** A recombinant immunotoxin containing a disulfide-stabilized Fv fragment. *Proc. Natl. Acad. Sci. U.S.A.* 90:7538-42.

Butcher, D. J., M. A. Kowalska, S. Li, Z. Luo, S. Shan, Z. Lu, S. Niewiarowski and Z. Huang., **1997**. A natural motif to protein design: a synthetic leucine zipper peptide mimcs the biological function of the platelet factor 4 protein. *FEBS Lett.* 409:183-87.

Cabilly, S., Riggs, A.D., Pande, H., Shively, J.E., Holmes, W.E., Rey, M., Perry, L.J., Wetzel, R. and Heyneker, H.L., **1984.** Generation of antibody activity from immunoglobulin polypeptide chains produced in escherichia coli. *Pro. Natl. Acad. Sci. U.S.A.* 81:3273-7.

Carter, P., L. Presta, C. M. Gorman, J. B. B. Ridgway, D. Henner, W. L. T. Wong, A. M. Rowland, C. Kotts, M. E. Carver and H. M. Shepard. **1992**. Humanisation of an anti-p185^{HER2} antibody for human cancer therapy. *Proc. Nat. Acad. Sci. U.S.A.* 89:4285-89.

Casson, L.P. and Manser, T., **1995**. Evaluation of loss and change of specificity resulting from random mutagenesis of an antibody V_H region. *J. Immunol*. 155:5647-54.

Chames, P., Coulon, S. and Baty, D., **1998**. Improving the affinity and the fine specificity of an anti-cortisol antibody by parsimonious mutagenesis and phage display. *J. Immunol*. 161:5421-9.

Chang, C.C., Chen, T.T., Cox, B.W., Dawes, G.N., Stemmer, W.P., Punnonen, J. and Patten, P.A., **1999**. Evolution of a cytokine using DNA family shuffling. *Nat Biotechnol*. 17(8):793-7.

Chen, G., Cloud, J., Georgiou, G. and Iverson, B.L., **1996**. A quantitative immunoassay utilizing *Escherichia coli* cells possessing surface-expressed single chain Fv molecules. *Biotech. Prog*. 12:572-4.

Chen, W. and Georgiou, G., **2002**. Cell-Surface display of heterologous proteins: From high-throughput screening to environmental applications. *Biotechnol. Bioeng*. 79:496-503.

Cheong, H.S., Chang, J.S., Park, J.M. and Byun, S.M., **1990.** Affinity enhancement of bispecific antibody against two different epitopes in the same antigen. *Biochem. Biophys. Res. Comm.* 173:795-800.

Chiang, Y.L., Sheng-Dong, R., Brow, M.A. and Larrick, J.W., **1989.** Direct cDNA cloning of the rearranged immunoglobulin variable region. *Biotechniques* 7:360-6.

Cho, B.K., Kieke, M.C., Boder, E.T., Wittrup, K.D. and Kranz, D.M., **1998**. A yeast surface display system for the discovery of ligands that trigger cell activation. *J. Immunol. Methods* 220:179-88.

Chothia, C. and Lesk, A.M., **1987.** Canonical structures for the hypervariable regions of immunoglobulins. *J. Mol. Biol.* 196:901-17.

Chothia, C., Lesk, A.M., Tramontano, A., Levitt, M., Smith-Gill, S.J., Air, G., Sheriff, S., Padlan, E.A., Davies, D., Tulip, W.R. Colman, P.M., Spinelli, S., Alzari, P.M. and Poljak, R.J., **1989.** Conformations of immunoglobulin hypervariable regions. *Nature* 342:877-83.

Chothia, C., Gelfand, I. and Kister, A. **1998**. Structural determinants in the sequences of immunoglobulin variable domain. *J. Mol. Biol*. 278:457-79.

Chowdhury, P.S., Vasmatzis, G., Beers, R., Lee, B. and Pastan, I., **1998**. Improved stability and yield of a Fv-toxin fusion protein by computer design and protein engineering of the Fv. *J. Mol. Biol*. 281:917-28.

Christians, F.C., Scapozza, L., Crameri, A., Folkers, G. and Stemmer, W.P., **1999**. Directed evolution of thymidine kinase for AZT phosphorylation using DNA family shuffling. *Nat. Biotechnol*. 17:259-64.

Christmann, A., Walter, K., Wentzel, A., Krätzner, R. and Kolmar, H., **1999**. The cystine knot of a squash-type protease inhibitor as a structural scaffold for *Escherichia coli* cell surface display of conformationally constrained peptides. *Protein Eng.* 12:797-806.

Christmann, A., Wentzel, A., Meyer, C., Meyers, G. and Kolmar, H., **2001**. Epitope mapping and affinity purification of monospecific antibodies by Escherichia coli cell surface display of gene-derived random peptide libraries. *J. Immunol. Methods* 257:163-173.

Clackson, T., Hoogenboom, H. R., Griffiths, A. D. and Winter, G., **1991**. Making antibody fragments using phage display libraries. *Nature* 352:624-28.

Clement, J.M., Jehanno, M., Popescu, O., Saurin, W. and Hofnung, M., **1996**. Expression and biological activity of genetic fusions between MalE, the maltose binding protein from *Escherichia coli* and portions of CD4, the T-cell receptor of the AIDS virus. *Protein Expr. Purif.* 8:319-31.

Coco, W.M., Levinson, W.E., Crist, M.J., Hektor, H.J., Darzins, A., Pienkos, P.T., Squires, C.H. and Monticello, D.J., **2001** .DNA shuffling method for generating highly recombined genes and evolved enzymes. *Nat. Biotechnol*. 19:354-9.

Coia, G., Hudson, P.J. and Lilley, G.G., **1996**. Construction of recombinant extended single-chain antibody peptide conjugates for use in the diagnosis of HIV-1 and HIV-2. *J. Immunol. Methods*. 192:13-23.

Coia, G., Ayres, A., Lilley, G.G., Hudson, P.J. and Irving, R.A., **1997**. Use of mutator cells as a means for increasing production levels of a recombinant antibody directed against Hepatitis B. *Gene*. 201:203-9.

Coia, G., Pontes-Braz, L., Nuttall, S.D., Hudson, P.J. and Irving, R.A., **2001**. Panning and selection of proteins using ribosome display. *J. Immunol. Methods*. 254:191-7.

Collet, T.A., Roben, P., O'Kennedy, R., Barbas, C.F. 3rd, Burton, D.R. and Lerner, R.A., **1992**. A binary plasmid system for shuffling combinatorial antibody libraries. *Proc. Natl. Acad. Sci. U.S.A*. 89:10026-30.

Colman, P.M., Tulip, W.R., Varghese, J.N., Tulloch, P.A., Baker, A.T., Laver, W.G., Air, G.M. and Webster, R.G., **1989**. Three-dimensional structures of influenza virus neuraminidase-antibody complexes. *Philos. Trans. R. Soc. Lond. B. Biol. Sci*. 323:511-8.

Coloma, M.J. and Morrison, S.L., **1997.** Design and production of novel tetravalent bispecific antibodies. *Nature Biotech.* 15:159-63.

Cook, J. and Barber, B.H., **1997**. Recombinant antibodies with conformationally constrained HIV type 1 epitope inserts elicit glycoprotein 160-specific antibody responses *in vivo*. *AIDS Res. Hum. Retroviruses* 13:449-60.

Coulon, S., Pellequer, J.L., Blachere, T., Chartier, M., Mappus, E., Chen Sw, S.W., Cuilleron, C.Y. and Baty, D., **2002**. Functional characterization of an anti-estradiol antibody by site-directed mutagenesis and molecular modelling: modulation of binding properties and prominent role of the V(L) domain in estradiol recognition. *J. Mol. Recognit*. 15:6-18.

Crameri, A. and Stemmer, W.P., **1995.** Combinatorial multiple cassette mutagenesis creates all the permutations of mutant and wild-type sequences. *Biotechniques* 18:194-6.

Crameri, A., Cwirla, S. and Stemmer, W.P., **1996a.** Construction and evolution of antibody-phage libraries by DNA shuffling. *Nature Medicine* 2:100-2.

Crameri, A., Whitehorn, E.A., Tate, E and Stemmer, W.P.C., **1996b**. Improved green fluorescent protein by molecular evolution using DNA shuffling. *Nature Biotech.* 14:315-19.

Crameri, A., Dawes, G., Rodriguez, E.Jr., Silver, S. and Stemmer, W.P.C., **1997**. Molecular evolution of an arsenate detoxification pathway by DNA shuffling. *Nature Biotech.* 15:436-38.

Crameri, A., Raillard, S., Bermudez, E. and Stemmer, W.P.C., **1998**. DNA shuffling of a family of genes from diverse species accelerates directed evolution. *Nature* 391:288-291.

Craven, C., **1999**. Mechanisms of Maturation of Insulin-Like Growth Factor-1. *Ph.D thesis, QUT.*

Crissman, J.W. and Smith, G.P., **1984**. Gene-III protein of filamentous phages: evidence for a carboxy-terminal domain with a role in morphogenesis. *Virology* 132:445-55.

Cwirla, S.E., Peters, E.A., Barrett, R.W. and Dower, W.J., **1990.** Peptides on phage: a vast library of peptides for identifying ligands. *Proc. Nat. Acad. Sci. U.S.A.* 87:6378-82.

Czerwinski, M., Krop-Watorek, A., Siegel, D.L. and Spitalnik, S.L., **1999**. A molecular approach for isolating high-affinity Fab fragments that are useful in blood group serology. *Transfusion* 39:364-71.

Daugherty, P.S., Chen, G., Olsen, M.J., Iverson, B.L. and Georgiou, G., **1998**. Antibody affinity maturation using bacterial surface display. *Protein Eng* 11:825-832.

Daugherty, P.S., Chen, G., Iverson, B.L. and Georgiou, G., **2000**. Quantitative analysis of the effect of the mutation frequency on the affinity maturation of single chain Fv antibodies. *Proc. Natl. Acad. Sci. U.S.A*. 97:2029-34.

Davies, J. and Riechmann, L., **1995**. Antibody V_H domains as small recognition units. *Bio/Technology* 13:475-479.

Davies, J. and Riechmann, L., **1996**. Single antibody domains as small recognition units: design and in vitro antigen selection of camelized, human V_H domains with improved protein stability. *Protein Eng.* 9:531-537.

de Haard, H.J., Kazemier, B., van der Bent, A., Oudshoorn, P., Boender, P., van Gemen, B., Arends J.W. and Hoogenboom, H.R., **1998**. Absolute conservation of residue 6 of immunoglobulin heavy chain variable regions of class IIA is required for correct folding. *Protein Eng*. 11:1267-76.

De Jonge, J., Brissinck, C., Heirman, C., Demanet, C., Leo, O., Moser, M. and Thielemans, K., **1995**. Production and characterisation of bispecific single-chain antibody fragments. *Mol. Immunol.* 33:1405-12.

Dekruif, J. and Logtenberg, T., **1996.** Leucine zipper dimerized bivalent and bispecific scFv antibodies from a semi-synthetic antibody phage display library. *J. Biol. Chem.* 271:7630-7634.

Delagrave, S., Catalan, J., Sweet, C., Drabik, G., Henry, A., Rees, A., Monath, T.P. and Guirakhoo, F., **1999**. Effects of humanization by variable domain resurfacing on the antiviral activity of a single-chain antibody against respiratory syncytial virus. *Protein Eng*. 12:357-62.

Deng, S.J., MacKenzie, C.R., Sadowska, J., Michniewicz, J., Young, N.M., Bundle, D.R. and Narang, S.A., **1994**. Selection of antibody single-chain variable fragments with improved carbohydrate binding by phage display. *J. Biol. Chem*. 269:9533-8.

Dennis, M.S. and Lazarus, R.A., **1994**. Kunitz domain inhibitors of tissue factor-factor VIIa. *J. Biol. Chem.* 269:22129-22136.

De Pascalis, R., Iwahashi, M., Tamura, M., Padlan, E.A., Gonzales, N.R., Santos, A.D., Giuliano, M., Schuck, P., Schlom, J. and Kashmiri, S.V., **2002**. Grafting of "abbreviated" complementarity-determining regions containing specificity-determining residues essential for ligand contact to engineer a less immunogenic humanized monoclonal antibody. *J. Immunol*. 169:3076-84.

de Wildt, R.M., van Venrooij, W.J., Winter, G., Hoet, R.M. and Tomlinson, I.M., **1999**. Somatic insertions and deletions shape the human antibody repertoire. *J. Mol. Biol*. 294:701-10.

Dolezal, O., Pearce, L.A., Lawrence, L.J., McCoy, A.J., Hudson, P.J. and Kortt, A.A., **2000**. ScFv multimers of the anti-neuraminidase antibody NC10: shortening of the linker in single-chain Fv fragment assembled in V(L) to V(H) orientation drives the formation of dimers, trimers, tetramers and higher molecular mass multimers. *Protein Eng*. 13:565-74.

Dolezal, O., De Gori, R., Walter, M., Doughty, L., Hattarki, M., Hudson, P.J. and Kortt, A.A., **2003**. Single-chain Fv multimers of the anti-neuraminidase antibody NC10: the residue at position 15 in the V(L) domain of the scFv-0 (V(L)-V(H)) molecule is primarily responsible for formation of a tetramer-trimer equilibrium. *Protein Eng*.16:47-56.

Dougan, D.A., Malby, R.L., Gruen, L.C., Kortt, A.A. and Hudson, P.J., 1998. Effects of substitutions in the binding surface of an antibody on antigen affinity. *Protein Eng*. 11:65-74.

Duenas, M. and Borrebaeck, C.A., **1994.** Clonal selection and amplification of phage displayed antibodies by linking antigen recognition and phage replication. *Bio/Technology* 12:999-1002.

Duenas, M., Ayala, M., Vazquez, J., Ohlin, M., Soderlind, E., Borrebaeck, C.A. and Gavilondo, J.V., **1995**. A point mutation in a murine immunoglobulin V-region strongly influences the antibody yield in *Escherichia coli*. *Gene*. 158:61-6.

Duenas, M., Malmborg, A.C., Casalvilla, R., Ohlin, M. and Borrebaeck, C.A.K., **1996.** Selection of phage displayed antibodies based on kinetic constants. *Mol. Immunol.* 33:279-85.

Essig, N.Z., Wood, J.F., Howard, A.J., Raag, R. and Whitlow, M., **1993.** Crystallization of single-chain Fv proteins. *J Mol. Biol.* 234:897-901.

Fedorov A.N. and Baldwin, T.O., **1997**. Cotranslational protein folding. *J Biol Chem*. 272:32715-8.

Figini, M., Marks, J.D., Winter, G. and Griffiths, A.D., **1994.** *In vitro* assembly of repertoires of antibody chains on the surface of phage by renaturation. *J. Mol. Biol.* 239:68-78.

Fowler, R.G., Degnen, G.E. and Cox, E.C., **1974**. Mutational specificity of a conditional *Escherichia coli* mutator, mutD5. *Mol. Gen. Genet*.133:179-91.

Francisco, J.A., Campbell, R., Iverson, B.L. and Georgiou, G., **1993**. Production and flow cytometry sorting of Escherichia coli expressing a single chain Fv antibody on its surface. *Proc. Natl. Acad. Sci. U.S.A*. 90:10444-10448.

Fuchs, P., Weichel, W., Dubel, S., Breitling, F. and Little, M., **1996**. Separation of *E. coli* expressing functional cell-wall bound antibody fragments by FACS. *Immunotechnology*. 2:97-102.

Galanis, M., Firth, S.M., Bond, J., Nathanielsz, A., Kortt, A.A., Hudson, P.J. and Baxter, R.C., **2001**. Ligand-binding characteristics of recombinant amino- and carboxyl-terminal fragments of human insulin-like growth factor-binding protein-3. *J. Endocrinol*. 169:123-33.

Garrard, L.J. and Henner, D.J., **1993**. Selection of an anti-IGF-1 Fab from a Fab phage library created by mutagenesis of multiple CDR loops. *Gene* 128:103-9.

Garrett, T.P., McKern, N.M., Lou, M., Frenkel, M.J., Bentley, J.D., Lovrecz, G.O., Elleman, T.C., Cosgrove, L.J. and Ward, C.W., **1998**. Crystal structure of the first three domains of the type-1 insulin-like growth factor receptor. *Nature*. 394:395-9.

Georgiou, G. and Valax, P., **1996**. Expression of correctly folded proteins in *Escherichia coli*. *Curr. Opin. Biotechnol*. 7:190-7.

Georgiou, G., Stathopoulos, C., Daugherty, P.S., Nayak, A.R., Iverson, B.L. and Curtiss, R., **1997**. Display of heterologous proteins on the surface of microorganisms: from the screening of combinatorial libraries to live recombinant vaccines. *Nat Biotech.* 15:29-34.

Gersuk G.M., Corey, M.J., Corey, E., Stray, J.E., Kawasaki, G.H. and Vessella, R.L., **1997**. High-affinity peptide ligands to prostate-specific antigen identified by polysome selection. *Biochem Biophys Res Commun*. 232:578-82.

Ghahroudi, M. A., Desmyter, A., Wyns, L., Hamers, R. and Muyldermans, S., **1997**. Selection and identification of single domain antibody fragments from camel heavy-chain antibodies. *FEBS lett.* 414: 521-526.

Gill, S.C. and von Hippel, P.H., **1989**. Calculation of protein extinction coefficients from amino acid sequence data. *Anal. Biochem*. 182:319-26.

Gillespie, C., Read, L.C., Bagley, C.J. and Ballard, F.J., **1990**. Enhanced potency of truncated insulin-like growth factor-I (des(1-3)IGF-I) relative to IGF-I in lit/lit mice. *J. Endocrinol*. 127:401-5.

Glockshuber, R., Malia, M., Pfitzinger, I. and Pluckthun, A., **1990.** A comparison of strategies to stabilize immunoglobulin Fv-fragments. *Biochemistry* 29:1362-7.

Glockshuber, R., Schmidt, T. and Pluckthun, A., **1992**. The disulfide bonds in antibody variable domains: effects on stability, folding in vitro, and functional expression in *Escherichia coli*. *Biochemistry* 31:1270-9.

Gluckman, P.D., Guan, J., Williams, C., Scheepens, A., Zhang, R., Bennet, L. and Gunn, A., **1998**. Asphyxial brain injury--the role of the IGF system. *Mol. Cell. Endocrinol*. 140:95-9.

Goletz, S., Christensen, P.A., Kristensen, P., Blohm, D., Tomlinson, I., Winter, G. and Karsten, U., **2002**. Selection of large diversities of antiidiotypic antibody fragments by phage display. *J. Mol. Biol*. 315:1087-97.

Gram, H., Marconi, L.A., Barbas, C.F. 3rd, Collet, T.A., Lerner, R.A. and Kang, A.S., **1992.** *In vitro* selection and affinity maturation of antibodies from a naive combinatorial immunoglobulin library. *Proc. Natl. Acad. Sci. U.S.A.* 89:3576-80.

Gramatikoff, K., Georgiev, O. and Schaffner, W., **1994**. Direct interaction rescue, a novel filamentous phage technique to study protein-protein interactions. *Nucleic Acids Res.* 22:5761-62.

Griffiths, A.D., Williams, S.C., Hartley, O., Tomlinson, I.M., Waterhouse, P., Crosby, W.L., Kontermann, R.E., Jones, P.T., Low, N.M., Allison, T.J. and et, al., **1994.** Isolation of high affinity human antibodies directly from large synthetic repertoires. *EMBO J.* 13:3245-60.

Griffiths, G.M., Berek, C., Kaartinen, M. and Milstein, C., **1984**. Somatic Mutation and Maturation of the Immune Response to 2-Phenyl Oxazolone. *Nature* 312:271-75.

Guan, J., Krishnamurthi, R., Waldvogel, H.J., Faull, R.L., Clark, R. and Gluckman, P., **2000**. N-terminal tripeptide of IGF-1 (GPE) prevents the loss of TH positive neurons after 6-OHDA induced nigral lesion in rats. *Brain Res*. 859:286-92.

Gunneriusson, E., Samuelson, P., Uhlen, M., Nygren, P.A. and Stahl S., **1996**. Surface display of a functional single-chain Fv antibody on staphylococci. *J. Bacteriol*. 178:1341-6.

Gunneriusson, E., Nord, K., Uhlen, M. and Nygren, P., **1999a**. Affinity maturation of a Taq DNA polymerase specific affibody by helix shuffling. *Protein Eng*. 12:873-8.

Gunneriusson, E., Samuelson, P., Ringdahl, J., Gronlund, H., Nygren, P.A. and Stahl, S., **1999b**. Staphylococcal surface display of immunoglobulin A (IgA)- and IgE-specific in vitro-selected binding proteins (affibodies) based on Staphylococcus aureus protein A. *Appl. Environ. Microbiol.* 65:4134-40.

Hamers-Casterman, C., Atarhouch, T., Muyldermans, S., Robinson, G., Hamers, C., Songa, E.B., Bendahman, N. and Hamers, R., **1993.** Naturally occurring antibodies devoid of light chains. *Nature* 363:446-8.

Hanes, J. and Pluckthun, A., **1997.** *In vitro* selection and evolution of functional proteins by using ribosome display. *Proc. Natl. Acad. Sci. U.S.A.* 94:4937-42.

Hanes, J., Jermutus, L., Weber-Bornhauser, S., Bosshard, H.R. and Pluckthun, A., **1998**. Ribosome display efficiently selects and evolves high-affinity antibodies in vitro from immune libraries. *Proc. Natl. Acad. Sci. U.S.A*. 95:14130-5.

Hanes, J., Jermutus, L., Schaffitzel, C. and Pluckthun, A., **1999**. Comparison of *Escherichia col*i and rabbit reticulocyte ribosome display systems. *FEBS Lett*. 450:105-10.

Hanes, J., Schaffitzel, C., Knappik, A. and Pluckthun, A., **2000**. Picomolar affinity antibodies from a fully synthetic naive library selected and evolved by ribosome display. *Nat. Biotechnol*. 18:1287-92.

Harbury, P.B., Zhang, Z., Kim P.S. and Alber, T., **1993**. A switch between two-, three- and four-stranded coiled coils in GCN4 Leucine zipper mutants. *Science* 262:1401-6.

Hawkins, R. E., Russell S. J. and Winter G. **1992**. Selection of phage antibodies by binding affinity. Mimicking affinity maturation. *J. Mol. Biol.* 226:880-896.

Hawkins, R.E., Russell, S.J., Baier, M. and Winter, G., **1993.** The contribution of contact and non-contact residues of antibody in the affinity of binding to antigen. The interaction of mutant D1.3 antibodies with lysozyme. *J. Mol. Biol.* 234:958-64.

Hayden, M. S., Linsley, P.S., Gayle, M.A., Bajorath, J., Brady, W.A., Norris, N.A., Fell, H.P., Ledbetter, J.A. and Gilliland, L.K., **1994**. Single-chain mono- and bispecific antibody derivatives with novel biological properties and antitumour activity from a COS cell transient expression system. *Therap. Immunol.* 1:3-15.

He, M. and Taussig, M.J., **1997**. Antibody-ribosome-mRNA (ARM) complexes as efficient selection particles for *in vitro* display and evolution of antibody combining sites. *Nucleic Acids Res*. 25:5132-4.

He, M., Menges, M., Groves, M.A., Corps, E., Liu, H., Bruggemann, M. and Taussig, M.J., **1999**. Selection of a human anti-progesterone antibody fragment from a transgenic mouse library by ARM ribosome display. *J. Immunol. Methods*. 231:105-17.

Heding, A., Gill, R., Ogawa, Y., De Meyts, P. and Shymko, R.M., **1996**. Biosensor measurement of the binding of insulin-like growth factors I and II and their analogues to the insulin-like growth factor-binding protein-3. *J. Biol. Chem*. 271:13948-52.

Hemminki, A., Niemi, S., Hautoniemi, L., Soderlund, H. and Takkinen, K., **1998**. Fine tuning of an anti-testosterone antibody binding site by stepwise optimisation of the CDRs. *Immunotechnology*. 4:59-69.

Hennecke, F., Krebber, C. and Pluckthun, A., **1998**. Non-repetitive single-chain Fv linkers selected by selectively infective phage (SIP) technology. *Protein Eng*. 11:405-10.

Holler, P.D., Holman, P.O., Shusta, E.V., O'Herrin, S., Wittrup, K.D. and Kranz, D.M., **2000**. In vitro evolution of a T-cell receptor with high affinity for peptide/MHC. *Proc. Natl. Acad. Sci. U.S.A.* 97:5387-5392.

Holliger, P., Prospero, T. and Winter, G., **1993.** 'Diabodies': small bivalent and bispecific antibody fragments. *Proc. Natl. Acad. Sci. U.S.A.* 90:6444-8.

Holliger, P., Brissinck, J., Williams, R.L., Thielemans, K. and Winter, G., **1996.** Specific killing of lymphoma cells by cytotoxic T-cells mediated by a bispecific diabody. *Prot. Eng.* 9:299-305.

Hoogenboom, H.R., Griffiths, A.D., Johnson, K.S., Chiswell, D.J., Hudson, P. and Winter, G., **1991.** Multi-subunit proteins on the surface of filamentous phage: methodologies for displaying antibody (fab) heavy and light chains. *Nucleic Acids Res.* 19:4133-7.

Hoogenboom, H.R. and Winter, G., **1992.** By-passing immunisation. Human antibodies from synthetic repertoires of germline V_H gene segments rearranged *in vitro*. *J. Mol. Biol.* 227:381-8.

Hoogenboom, H.R., **1997.** Designing and optimizing library selection strategies for generating high-affinity antibodies. *Trends Biotech.* 15:62-70.

Hopp, T.P., Prickett, K.S., Price, V.L., Libby, R.T., March, C.J., Cerretti, P., Urdal, D.L. and Conlon, P.J., **1988**. A short polypeptide marker sequence useful for recombinant protein identification and purification. *Bio/Technology*, 6:1204-1210.

Horton, R.M., Hunt, H.D., Ho, S.N., Pullen, J.K. and Pease, L.R., **1989**. Engineering hybrid genes without the use of restriction enzymes: gene splicing by overlap extension. *Gene* 77:61-8.

Huls, G., Gestel, D., van der Linden, J., Moret, E. and Logtenberg, T. **2001**. Tumor cell killing by *in vitro* affinity-matured recombinant human monoclonal antibodies. *Cancer Immunol. Immunother*. 50:163-71.

Huse, W.D., Sastry, L., Iverson, S.A., Kang, A.S., Alting-Mees, M., Burton, D.R., Benkovic, S.J. and Lerner, R.A., **1989.** Generation of a large combinatorial library of the immunoglobulin repertoire in phage lambda . *Science.* 246:1275-81.

Huston, J.S., Levinson, D., Mudgett-Hunter, M., Tai, M.S., Novotny, J., Margolies, M.N., Ridge, R.J., Bruccoleri, R.E., Haber, E., Crea, R. and *et al*., **1988.** Protein engineering of antibody binding sites: recovery of specific activity in an anti-digoxin single-chain Fv analogue produced in *Escherichia coli*. *Proc. Natl. Acad. Sci. U.S.A.* 85:5879-83.

Iliades, P., Kortt A.A. and Hudson P.J., **1997**. Triabodies: Single Chain Fv Fragments without a linker form trivalent trimers. *FEBS Lett.* 409(3):437-41.

Iliades, P., Dougan, D.A., Oddie, G.W., Metzger, D.W., Hudson, P.J. and Kortt, A.A., **1998**. Single-chain Fv of anti-idiotype 11-1G10 antibody interacts with antibody NC41 single-chain Fv with a higher affinity than the affinity for the interaction of the parent Fab fragments. *J. Protein Chem*. 17:245-54.

Inbar, D., Hochman, J. and Givol, D., **1972**. Localisation of Antibody-Combining Sites within the Variable Portions of Heavy and Light Chains. *Proc. Nat. Acad. Sci. U.S.A.* 69:2659-62.

Irving, R.A., Kortt, A.A. and Hudson, P.J., **1996.** Affinity maturation of recombinant antibodies using E. coli mutator cells. *Immunotechnology* 2:127-43.

Irving, R.A., Coia, G., Roberts, A., Nuttall, S.D. and Hudson, P.J., **2001**. Ribosome display and affinity maturation: from antibodies to single V-domains and steps towards cancer therapeutics. *J. Immunol. Methods*. 248:31-45.

Jackson, J.R., Sathe, G., Rosenberg, M. and Sweet, R., **1995**. *In vitro* antibody maturation. Improvement of a high affinity, neutralizing antibody against IL-1 beta. *J. Immunol*. 154:3310-9.

Jansson, M., Andersson, G., Uhlen, M., Nilsson, B. and Kordel, J., **1998**. The insulin-like growth factor (IGF) binding protein 1 binding epitope on IGF-I probed by heteronuclear NMR spectroscopy and mutational analysis. *J. Biol. Chem*. 273:24701-7.

Jermutus, L., Honegger, A., Schwesinger, F., Hanes, J. and Pluckthun, A., **2001**. Tailoring *in vitro* evolution for protein affinity or stability. *Proc. Natl. Acad. Sci. U.S.A*. 98:75-80.

Johnsson, B., Lofas, S. and Lindquist, G., **1991**. Immobilization of proteins to a carboxymethyldextran-modified gold surface for biospecific interaction analysis in surface plasmon resonance sensors. *Anal. Biochem*. 198:268-77.

Jonsson, U., Fagerstam, L., Ivarsson, B., Johnsson, B., Karlsson, R., Lundh, K., Lofas, S., Persson, B., Roos, H., Ronnberg, I., *et al*., **1991**. Real-time biospecific interaction analysis using surface plasmon resonance and a sensor chip technology. *Biotechniques* 11:620-7.

Jones, P.T., Dear, P.H., Foote, J., Neuberger, M.S. and Winter, G., **1986.** Replacing the complementarity-determining regions in a human antibody with those from a mouse. *Nature* 321:522-5.

Jung, H.C., Lebeault, J.M. and Pan, J.G., **1998**. Surface display of Zymomonas mobilis levansucrase by using the ice-nucleation protein of Pseudomonas syringae. *Nature Biotech.* 16:576-580.

Jung, S. and Pluckthun, A., **1997**. Improving in vivo folding and stability of a single-chain Fv antibody fragment by loop grafting. *Protein Eng*. 10:959-66.

Jung, S., Honegger, A. and Pluckthun, A. **1999**. Selection for improved protein stability by phage display. *J. Mol. Biol*. 294:163-80.

Kabat, E.A., Wu, T.T., Perry, H.M., Gottensman, K.S. and Foeler, C., **1991**. Sequences of proteins of immunological interest. *US Department of Health and Human Service*, US Public Health Service, NIH, Bethesda, MD.

Kang, A.S., Jones, T.M. and Burton, D.R., **1991.** Antibody redesign by chain shuffling from random combinatorial immunoglobulin libraries. *Proc. Natl. Acad. Sci. U.S.A.* 88:11120-3.

Kang, N., Hamilton, S., Odili, J., Wilson, G. and Kupsch, J., **2000**. *In vivo* targeting of malignant melanoma by 125Iodine- and 99mTechnetium-labeled single-chain Fv fragments against high molecular weight melanoma-associated antigen. *Clin. Cancer Res*. 6:4921-31.

Kettleborough, C.A., Saldanha, J., Heath, V.J., Morrison, C.J. and Bendig, M.M., **1991**. Humanisation of a mouse monoclonal antibody by CDR grafting: the importance of framework residues on loop conformation. *Protein Eng.* 4:773-83.

Keefe, A.D. and Szostak, J.W., **2001**. Functional proteins from a random-sequence library. *Nature* 410:715-8.

Kieke, M.C., Cho, B.K., Boder, E.T., Kranz, D.M. and Wittrup, K.D., **1997**. Isolation of anti-T-cell receptor scFv mutants by yeast surface display. *Protein Eng.* 10:1303-1310.

Kipriyanov, S.M., Breitling, F., Little, M. and Dubel, S., **1995.** Single-chain antibody streptavidin fusions: tetrameric bifunctional scFv-complexes with biotin binding activity and enhanced affinity to antigen. *Hum. Antibod. Hybridomas* 6:93-101.

Kipriyanov, S.M., Moldenhauer, G., Martin, A.C., Kupriyanova, O.A. and Little, M., **1997**. Two amino acid mutations in an anti-human CD3 single chain Fv antibody fragment that affect the yield on bacterial secretion but not the affinity. *Protein Eng*. 10:445-53.

Klein, U., Goossens, T., Fischer, M., Kanzler, H., Braeuninger, A., Rajewsky, K. and Kuppers, R., **1998**. Somatic hypermutation in normal and transformed human B cells. *Immunol. Rev*. 162:261-80.

Klimka, A., Matthey, B., Roovers, R.C., Barth, S., Arends, J.W., Engert, A. and Hoogenboom, H.R., **2000**. Human anti-CD30 recombinant antibodies by guided phage antibody selection using cell panning. *Br. J. Cancer*. 83:252-60.

Knappik, A. and Pluckthun, A., **1995**. Engineered turns of a recombinant antibody improve its *in vivo* folding. *Protein Eng.* 8:81-9.

Knappik, A., Ge, L., Honegger, A., Pack, P., Fischer, M., Wellnhofer, G., Hoess, A., Wolle, J., Pluckthun, A. and Virnekas, B., **2000**. Fully synthetic human combinatorial antibody libraries (HuCAL) based on modular consensus frameworks and CDRs randomized with trinucleotides. *J. Mol. Biol*. 296:57-86.

Kohler, G. and Milstein, C., **1975.** Continuous cultures of fused cells secreting antibody of predefined specificity. *Nature* 256:495-97.

Koide, A., Bailey, C.W., Huang, X. and Koide, S., **1998**. The fibronectin type III domain as a scaffold for novel binding proteins. *J. Mol. Biol.* 284:1141-1151.

Koide, A., Jordan, M.R., Horner, S.R., Batori, V. and Koide, S., **2001**. Stabilization of a fibronectin type III domain by the removal of unfavorable electrostatic interactions on the protein surface. *Biochemistry* 40:10326-33.

Komar, A.A., Kommer, A., Krasheninnikov, I.A. and Spirin, A.S., **1997**. Cotranslational folding of globin. *J Biol Chem*. 272(16):10646-51.

Kortt, A.A., Lah, M., Oddie, G.W., Gruen, C.L., Burns, J.E., Pearce, L.A., Atwell, J.L., McCoy, A.J., Howlett, G.J., Metzger, D.W., Webster, R.G. and Hudson, P., **1997.** Single-chain Fv Fragments of anti-neuraminidase antibody NC10 containing five- and ten-residue linkers form dimers and with zero-residue linker a trimer. *Protein Eng.* 10:423-33.

Krebber, C., Spada, S., Desplancq, D. and Pluckthun, A., **1995.** Co-selection of cognate antibody-antigen pairs by selectively-infective phages. *FEBS Lett.* 377:227-31.

Krebber, C., Spada, S., Desplancq, D., Krebber, A., Ge, L.M. and Pluckthun, A., **1997.** Selectively-infective phage (SIP) - a mechanistic dissection of a novel *in vivo* selection for protein-ligand interactions. *J. Mol. Biol.* 268:607-18.

Kudlicki, W., Chirgwin, J., Kramer, G. and Hardesty, B., **1995**. Folding of an enzyme into an active conformation while bound as peptidyl-tRNA to the ribosome. *Biochemistry*. 34:14284-7.

Kumamaru, T., Suenaga, H., Mitsuoka, M., Watanabe, T. and Furukawa, K., **1998**. Enhanced degradation of polychlorinated biphenyls by directed evolution of biphenyl dioxygenase. *Nature Biotech*. 16:663-666.

Kurucz, I., Titus, J.A., Jost, C.R., Jacobus, C.M. and Segal, D.M., **1995.** Retargeting of CTL by an efficiently refolded bispecific single-chain Fv dimer produced in bacteria. *J. Immunol.* 154:4576-82.

Kurz, M., Gu, K. and Lohse, P.A., **2000**. Psoralen photo-crosslinked mRNA-puromycin conjugates: a novel template for the rapid and facile preparation of mRNA-protein fusions. *Nucleic Acids Res*.28:E83.

Laemmli, U.K., **1970**. Cleavage of structural proteins during the assembly of the head of bacteriophage T4. *Nature* 227:680-5.

Lamla, T. and Erdmann, V.A., **2001**. *In vitro* selection of other proteins than antibodies by means of ribosome display. *FEBS Lett*. 502:35-40.

Lamminmaki, U., Pauperio, S., Westerlund-Karlsson, A., Karvinen, J., Virtanen, P.L., Lovgren, T. and Saviranta, P., **1999**. Expanding the conformational diversity by random insertions to CDRH2 results in improved anti-estradiol antibodies. *J. Mol. Biol*. 291:589-602.

Lantto, J. and Ohlin, M., **2002**. Uneven distribution of repetitive trinucleotide motifs in human immunoglobulin heavy variable genes. *J. Mol. Evol*. 54:346-53.

Lee, J.S., Shin, K.S., Pan, J.G. and Kim, C.J., **2000**. Surface-displayed viral antigens on Salmonella carrier vaccine. *Nat Biotech.* 18:645-648.

Lerner, R.A., Kang, A.S., Bain, J.D., Burton, D.R. and Barbas, C.F. 3d., **1992.** Antibodies without immunization. *Science.* 258:1313-4.

Leung, D.W., Chen, E. and Goeddel, D.V., **1989.** A method for random mutagenesis of a defined DNA segment using a modified polymerase chain reaction. *J. Methods Cell Mol. Biol.* 1:11-15.

Lilie, H., Schwarz, E. and Rudolph, R., **1998**. Advances in refolding of proteins produced in *E. coli*. *Curr. Opin. Biotechnol*. 9:497-501.

Liu, D.R., Magliery, T.J., Pastrnak, M. and Schultz, P.G., **1997**. Engineering a tRNA and aminoacyl-tRNA synthetase for the site-specific incorporation of unnatural amino acids into proteins *in vivo*. *Proc. Natl. Acad. Sci. U.S.A*. 94:10092-7.

Lorimer, I.A.J. and Pastan, I., **1995**. Random recombination of antibody single chain Fv sequences after fragmentation with DNaseI in the presence of Mn2+. *Nucleic Acids Res*. 23:3067-3068.

Low, N.M., Holliger, P. and Winter, G., **1996.** Mimicking somatic hypermutation - affinity maturation of antibodies displayed on bacteriophage using a bacterial mutator strain. *J. Mol. Biol.* 260:359-68.

Mack, M., Riethmuller, G. and Kufer, P., **1995**. A small bispecific antibody construct expressed as a functional single-chain molecule with high tumor cell cytotoxicity. *Proc. Natl. Acad. Sci. U.S.A*. 92:7021-25.

Maheshri, N. and Schaffer, D.V., **2003**. Computational and experimental analysis of DNA shuffling. *Proc. Natl. Acad. Sci. U.S.A*. 100:3071-6.

Makeyev, E.V., Kolb, V.A. and Spirin, A.S., **1996**. Enzymatic activity of the ribosome-bound nascent polypeptide. *FEBS Lett*. 378:166-70.

Malby, R.L., Caldwell, J.B., Gruen, L.C., Harley, V.R., Ivancic, N., Kortt, A.A., Lilley, G.G., Power, B.E., Webster, R.G. and Colman, P.M., *et al*., **1993**. Recombinant antineuraminidase single chain antibody: expression, characterization, and crystallization in complex with antigen. *Proteins* 16:57-63.

Malby, R.L., Tulip, W.R., Harley, V.R., McKimm-Breschkin, J.L., Laver, W.G., Webster, R.G. and Colman, P.M., **1994**. The structure of a complex between the NC10 antibody and influenza virus neuraminidase and comparison with the overlapping binding site of the NC41 antibody. *Structure* 2:733-46.

Mallender, W.D., Ferreira, S.T., Voss, E.W. and Coelho-Sampaio, T., **1994**. Inter-active-site distance and solution dynamics of a bivalent-bispecific single-chain antibody molecule. *Biochemistry* 33:10100-10108.

Malmborg, A.C., Duenas, M., Ohlin, M., Soderlind, E. and Borrebaeck, C.A., **1996**. Selection of binders from phage displayed antibody libraries using the BIAcore biosensor. *J. Immunol. Methods*. 19851-7.

Malmborg, A.C., Soderlind, E., Frost, L. and Borrebaeck, C.A., **1997**. Selective phage infection mediated by epitope expression on F pilus. *J. Mol. Biol*. 273:544-51.

Markland, W., Ley, A.C., Lee, S.W. and Ladner, R.C., **1996**. Iterative optimization of high-affinity protease inhibitors using phage display. 1. Plasmin. *Biochemistry* 35:8045-8057.

Marks, J.D., Hoogenboom, H.R., Bonnert, T.P., McCafferty, J., Griffiths, A.D. and Winter, G., **1991.** By-passing immunization. Human antibodies from V-gene libraries displayed on phage. *J. Mol. Biol.* 222:581-97.

Marks, J. D., Griffiths, A.D., Malmqvist, M., Clackson, T.P., Bye J.M. and Winter, G., **1992**. By-passing immunization: Building high affinity human antibodies by chain shuffling. *Bio/Technology* 10:779-83.

Martin, F., Toniatti, C., Salvati, A.L., Venturini, S., Ciliberto, G., Cortese, R. and Sollazzo, M., **1994.** The affinity-selection of a minibody polypeptide inhibitor of human interleukin-6. *EMBO J.* 13:5303-9.

Martin, F., Toniatti, C., Salvati, A.L., Ciliberto, G., Cortese, R. and Sollazzo, M., **1996.** Coupling protein design and in vitro selection strategies: improving specificity and affinity of a designed beta-protein IL-6 antagonist. *J. Mol. Biol.* 255:86-97.

Martin, F., Volpari, C., Steinkühler, C., Dimasi, N., Brunetti, M., Biasiol, G., Altamura, S., Cortese, R., De Francesco, R. and Sollazzo, M., **1997**. Affinity selection of a camelized V_H domain antibody inhibitor of hepatitis C virus NS3 protease. *Protein Eng.* 10: 607-614.

Martineau, P. and Betton, J.M., **1999**. *In vitro* folding and thermodynamic stability of an antibody fragment selected in vivo for high expression levels in *Escherichia coli* cytoplasm. *J. Mol. Biol*. 292:921-9.

Matsuura, T. and Pluckthun, A., **2003**. Selection based on the folding properties of proteins with ribosome display. *FEBS Lett*. 539:24-8.

Matsumura, I. and Ellington, A.D., **2001**. *In vitro* evolution of beta-glucuronidase into a beta-galactosidase proceeds through non-specific intermediates. *J. Mol. Biol*. 305:331-9.

Mattheakis, L.C., Bhatt, R.R. and Dower, W.J., **1994**. An in vitro polysome display system for identifying ligands from very large peptide libraries. *Proc. Nat. Acad. Sci. U.S.A.* 91:9022-26.

Mattheakis, L.C., Dias, J.M. and Dower, W.J., **1996**. Cell-free synthesis of peptide libraries displayed on polysomes. *Methods Enzymol.* 267:195-207.

McCafferty, J., Griffiths A.D., Winter, G. and Chiswell, D.J., **1990**. Phage antibodies: filamentous phage displaying antibody variable domains. *Nature* 348:552-54.

Mcguinness, B.T., Walter, G., Fitzgerald, K., Schuler, P., Mahoney, W., Duncan, A.R. and Hoogenboom, H.R., **1996.** Phage diabody repertoires for selection of large numbers of bispecific antibody fragments. *Nature Biotech.* 14:1149-54.

McKean, D., Huppi, K., Bell, M., Staudt, L., Gerhard, W. and Weigert, M., **1984**. Generation of antibody diversity in the immune response of BALB/c mice to influenza virus hemagglutinin. *Proc. Nat. Acad. Sci. U.S.A.* 81:3180-3184.

Milstein, C. and Cuello, A.C., **1983**. Hybrid hybridomas and their use in immunohistochemistry. *Nature* 305:537-40.

Minsky, A., Summers, R.G. and Knowles, J.R., **1986**. Secretion of beta-lactamase into the periplasm of *Escherichia coli*: evidence for a distinct release step associated with a conformational change. *Proc. Natl. Acad. Sci. U.S.A*. 83:4180-4.

Miyazaki, C., Iba, Y., Yamada, Y., Takahashi, H., Sawada, J. and Kurosawa, Y., **1999**. Changes in the specificity of antibodies by site-specific mutagenesis followed by random mutagenesis. *Protein Eng*. 12:407-15.

Moore, J.C., Jin, H.M., Kuchner, O. and Arnold, F.H., **1997**. Strategies for the *in vitro* evolution of protein function-enzyme evolution by random recombination of improved sequences. *J. Mol. Biol.* 272:336-47.

Müller, H.N. and Skerra, A., **1994**. Grafting of a high-affinity Zn(II)-binding site on the β-barrel of retinol-binding protein results in enhanced folding stability and enables simplified purification. *Biochemistry* 33:14126-14135.

Nagahira, K., Fukuda, Y., Oyama, Y., Kurihara, T., Nasu, T., Kawashima, H., Noguchi, C.,Oikawa, S. and Nakanishi, T., **1999**. Humanization of a mouse neutralizing monoclonal antibody against tumor necrosis factor-alpha (TNF-alpha). *J. Immunol. Methods*. 222:83-92.

Nemoto, N., Miyamoto-Sato, E., Husimi, Y. and Yanagawa, H., **1997**. *In vitro* virus: bonding of mRNA bearing puromycin at the 3'-terminal end to the C-terminal end of its encoded protein on the ribosome *in vitro*. *FEBS Lett*. 414:405-8.

Neri, D., Momo, M., Prospero, T. and Winter, G., **1995.** High-affinity antigen binding by chelating recombinant antibodies (CRAbs). *J. Mol. Biol.* 246:367-73.

Ness, J.E., Welch, M., Giver, L., Bueno, M., Cherry, J.R., Borchert, T.V., Stemmer, W.P. and Minshull, J., **1999**. DNA shuffling of subgenomic sequences of subtilisin. *Nat. Biotechnol*. 17:893-6.

Neuberger, M.S., **1983.** Expression and regulation of immunoglobulin heavy chain gene transfected into lymphoid cells. *EMBO J.* 2:1373-78.

Newton, S.M.C., Jacob, C.O. and Stocker, B.A.D., **1989**. Immune response to cholera toxin epitope inserted in *Salmonella* flagellin. *Science* 244:70-72.

Nieba, L., Honegger, A., Krebber, C. and Pluckthun, A., **1997**. Disrupting the hydrophobic patches at the antibody variable/constant domain interface: improved in vivo folding and physical characterization of an engineered scFv fragment. *Protein Eng*. 10:435-44.

Nilsson-Hakansson, L., Civalero, I., Zhang, X., Carlsson-Skwirut, C., Sara, V.R. and Nordberg, A., **1993**. Effects of IGF-1, truncated IGF-1 and the tripeptide Gly-Pro-Glu on acetylcholine release from parietal cortex of rat brain. *Neuroreport* 4:1111-4.

Nisinoff, A. and Mandy, W.J., **1962**. Quantitative estimation of the hybridisation of rabbit antibodies. *Nature*. 194:355-58.

Nissim, A., Hoogenboom, H.R., Tomlinson, I.M., Flynn, G., Midgley, C., Lane, D. and Winter, G., **1994.** Antibody fragments from a 'single pot' phage display library as immunochemical reagents. *EMBO J.* 13:692-8.

Nord, K., Gunneriusson, E., Ringdahl, J., Stahl, S., Uhlen, M. and Nygren, P-A., **1997**. Binding proteins selected from combinatorial libraries of an alpha-helical bacterial receptor domain. *Nature Biotech.* 15:772-77.

Nuttall, S.D., Rousch, M.J.M., Irving, R.A., Hufton, S.E., Hoogenboom, H.R. and Hudson, P.J., **1999**. Design and expression of soluble CTLA-4 variable domain as a scaffold for the display of functional polypeptides. *Proteins Struct. Funct. Genet.* 36:217-227.

Nuttall, S.D., Krishnan, U.V., Hattarki, M., De Gori, R., Irving, R.A. and Hudson, P.J., **2001**. Isolation of the new antigen receptor from wobbegong sharks, and use as a scaffold for the display of protein loop libraries. *Mol. Immunol*. 38:313-26.

O'Connor, S.J., Meng, Y.G., Rezaie, A.R. and Presta, L.G., **1998**. Humanization of an antibody against human protein C and calcium-dependence involving framework residues. *Protein Eng*. 11:321-8.

O'Shea, E.K., Klemm, J.D., Kim, P.S. and Alber, T., **1991**. X-ray structure of the GCN4 leucine zipper, a two stranded, parallel coiled-coil. *Science* 254:539-44.

Ohlin, M. and Borrebaeck, C.A., **1998**. Insertions and deletions in hypervariable loops of antibody heavy chains contribute to molecular diversity. *Mol. Immunol*. 35:233-8.

Oi, V.T., Morrison, S.L., Herzenberg, L.A. and Berg, P., **1983.** Immunoglobulin gene expression in transformed lymphoid cells. *Proc. Natl. Acad. Sci. U.S.A.* 80:825-9.

Orlandi, R. Gussow D.H. Jones P.T. and Winter G. **1989**. Cloning immunoglobulin variable domains for expression by the polymerase chain reaction. *Proc. Natl. Acad. Sci.* U.S.A. 86:3833-37.

Osbourn, J.K., Field, A., Wilton, J., Derbyshire, E., Earnshaw, J.C., Jones, P.T., Allen, D. and McCafferty, J., **1996**. Generation of a panel of related human scFv antibodies with high affinities for human CEA. *Immunotechnology* 2:181-96.

Pack, P. and Pluckthun, A., **1992.** Miniantibodies: use of amphipathic helices to produce functional, flexibly linked dimeric F_V fragments with high avidity in *Escherichia coli*. *Biochemistry* 31:1579-84.

Pack, P., Muller, K., Zahn, R. and Pluckthun, A., **1995.** Tetravalent miniantibodies with high avidity assembling in *Escherichia coli*. *J. Mol. Biol.* 246:28-34.

Palmer, J.L., Mandy, W.J. and Nisinoff, A., **1962**. Heterogeneity of rabbit antibody and its subunits. *Proc. Nat. Acad. Sci. U.S.A.* 48:49-53.

Parmley, S.F. and Smith, G.P., **1988.** Antibody-selectable filamentous fd phage vectors: affinity purification of target genes. *Gene.* 73:305-18.

Patten, P.A., Howard, R.J. and Stemmer, W.P.C., **1997**. Applications of DNA shuffling to pharmaceuticals and vaccines. *Curr. Opin. Biotech*. 8:724-733

Pedrazzi, G., Schwesinger, F., Honegger, A., Krebber, C. and Pluckthun, A., **1997.** Affinity and folding properties both influence the selection of antibodies with the selectively infective phage (SIP) methodology. *FEBS Lett*. 415(3):289-93.

Pereira, S., Van Belle, P., Elder, D., Maruyama, H., Jacob, L., Sivanandham, M., Wallack, M., Siegel, D. and Herlyn, D., **1997**. Combinatorial antibodies against human malignant melanoma. Hybridoma. 16:11-6.

Perisic, O., Webb, P.A., Holliger, P., Winter, G. and Williams, R.L., **1994.** Crystal structure of a diabody, a bivalent antibody fragment. *Structure* 2:1217-26.

Pluckthun, A. and Pack, P., **1997.** New protein engineering approaches to multivalent and bispecific antibody fragments. *Immunotechnology.* 3:83-105.

Poljak, R J., Amzel, L.M., Avey, H.P., Chen, B.L., Phizackerley, R.P. and Saul, F., **1973**. Three-dimensional structure of the Fab' fragment of a human immunoglobulin at 2.8-A resolution. *Proc. Nat. Acad. Sci. U.S.A.* 70:3305-10.

Porter, R.R., **1973**. Structural studies of immunoglobulins. *Science* 180:713-16.

Power, B.E., Ivancic, N., Harley, V.R., Webster, R.G., Kortt, A.A., Irving, R.A. and Hudson, P.J., **1992**. High-level temperature-induced synthesis of an antibody V_H-domain in *Escherichia coli* using the PelB secretion signal. *Gene*. 113:95-9.

Press, E.M. and Hogg, N.M., **1969**. Comparitive study of two immunoglobulin G Fd-fragments. *Nature* 223:807-10.

Proba, K., Worn, A., Honegger, A. and Pluckthun, A., **1998**. Antibody scFv fragments without disulfide bonds made by molecular evolution. *J. Mol. Biol*. 275:245-253.

Pulito, V. L., Roberts, V.A., Adair, J.R., Rothermal, A.L., Collins, A.M., Varga, S.S., Martocello, C., Bodmer, M., Jolliffe L.K. and Zivin, R.A., **1996**. Humanisation and molecular modeling of the anti-CD4 monoclonal antibody, OKT4A. *J. Immunol.* 156:2840-2850.

Rader, C. and Barbas, C.F., **1997**. Phage display of combinatorial antibody libraries. *Curr. Opin. Biotech.* 8:503-8.

Raillard, S., Krebber, A., Chen, Y., Ness, J.E., Bermudez, E., Trinidad, R., Fullem, R., Davis, C., Welch, M., Seffernick, J., Wackett, L.P., Stemmer, W.P. and Minshull, J., **2001**. Novel enzyme activities and functional plasticity revealed by recombining highly homologous enzymes. *Chem. Biol*. 8:891-8.

Regan, L. and DeGrado, W.F., **1988**. Characterisation of a helical protein designed from first principles. *Science.* 241:976-78.

Rheinnecker, M., Hardt, C., Ilag, L.L., Kufer, P., Gruber, R., Hoess, A., Lupas, A., Rottenberger, C., Pluckthun, A. and Pack, P., **1996.** Multivalent antibody fragments with high functional affinity for a tumor-associated carbohydrate antigen.

*J.Immunol.*157:2989-97.

Riechmann, L., Clark, M., Waldmann, H. and Winter, G., **1988**. Reshaping human antibodies for therapy. *Nature.* 332:323-27.

Riechmann, L. and Holliger, P., **1997**. The C-terminal domain of tolA is the coreceptor for filamentous phage infection of *E. coli. Cell* 90:351-60.

Roberts, B.L., Markland, W., Ley, A.C., Kent, R.B., White, D.W., Guterman, S.K. and Ladner, R.C., **1992**. Directed evolution of a protein: selection of potent neutrophil elastase inhibitors displayed on M13 fusion phage. *Proc. Natl. Acad. Sci. U.S.A.* 89:2429-2433.

Roberts, R.W. and Szostak, J.W., **1997**. RNA-peptide fusions for the *in vitro* selection of peptides and proteins. *Proc. Natl. Acad. Sci. U.S.A*. 94:12297-302.

Rode, H.J., Little, M., Fuchs, P., Dorsam, H., Schooltink, H., de Ines, C., Dubel, S. and Breitling, F., **1996**. Cell surface display of a single-chain antibody for attaching polypeptides. *Biotechniques*. 21:650-658.

Roguska, M.A., Pedersen, J.T., Keddy, C.A., Henry, A.H., Searle, S.J., Lambert, J.M., Goldmacher, V.S., Blattler, W.A., Rees, A.R. and Guild, B.C., **1994.** Humanization of murine monoclonal antibodies through variable domain resurfacing. *Proc. Natl. Acad. Sci. U.S.A.* 91:969-73.

Roguska, M.A., Pedersen, J.T., Henry, A.H., Searle, S.M., Roja, C.M., Avery, B., Hoffee, M., Cook, S., Lambert, J.M., Blattler, W.A., Rees, A.R. and Guild, B.C., **1996**. A comparison of two murine monoclonal antibodies humanized by CDR-grafting and variable domain resurfacing. *Protein Eng*. 9:895-904.

Roitt, I.M., Brostoff, J. and Male, D.K., **1993**. Immunology 3rd Ed. *Mosby-Year Book Europe Ltd.*

Ross, M., Francis, G.L., Szabo, L., Wallace, J.C. and Ballard, F.J., **1989**. Insulin-like growth factor (IGF)-binding proteins inhibit the biological activities of IGF-1 and IGF-2 but not des-(1-3)-IGF-1. *Biochem. J*. 258:267-72.

Rothenfluh, H.S. and Steele, E.J., **1993**. Origin and maintenance of germ-line V genes. *Immunol. Cell. Biol*. 71:227-32.

Rothenfluh, H.S., Blanden, R.V. and Steele, E.J., **1995**. Evolution of V genes: DNA sequence structure of functional germline genes and pseudogenes. *Immunogenetics* 42:159-71.

Saiki, R.K., Gelfand, D.H., Stoffel, S., Scharf, S.J., Higuchi, R., Horn, G.T., Mullis, K.B. and Erlich, H.A., **1988**. Primer-directed enzymatic amplification of DNA with a thermostable DNA polymerase. *Science* 239:487-91.

Saldanha, J.W., Martin, A.C. and Leger, O.J., **1999**. A single backmutation in the human kIV framework of a previously unsuccessfully humanized antibody restores the binding activity and increases the secretion in cos cells. *Mol. Immunol*. 36:709-19.

Sambrook, J., Fritsch, E.F. and Maniatis, T., **1989**. Molecular Cloning: A Laboratory Manual. (Nolan, C., Ed., 2nd ed.), *Cold Spring Harbour Laboratory Press*, Cold Spring Harbour, New York.

Sara, V.R., Carlsson-Skwirut, C., Bergman, T., Jornvall, H., Roberts, P.J., Crawford, M., Hakansson, L.N., Civalero, I. and Nordberg, A., **1989**. Identification of Gly-Pro-Glu (GPE), the aminoterminal tripeptide of insulin-like growth factor 1 which is truncated in brain, as a novel neuroactive peptide. *Biochem. Biophys. Res. Commun*. 165:766-71.

Sastry, L., Alting-Mees, M., Huse, W.D., Short, J.M., Sorge, J.A., Hay, B.N., Janda, K.D., Benkovic, S.J. and Lerner, R.A., **1989.** Cloning of the immunological repertoire in *Escherichia coli* for generation of monoclonal catalytic antibodies: construction of a heavy chain variable region-specific cDNA library. *Proc. Natl.Acad. Sci. U.S.A.* 86:5728-32.

Saura, J., Curatolo, L., Williams, C.E., Gatti, S., Benatti, L., Peeters, C., Guan, J., Dragunow, M., Post, C., Faull, R.L., Gluckman, P.D. and Skinner, S.J., **1999**. Neuroprotective effects of Gly-Pro-Glu, the N-terminal tripeptide of IGF-1, in the hippocampus in vitro. *Neuroreport* 10:161-4.

Saviranta, P., Pajunen, M., Jauria, P., Karp, M., Pettersson, K., Mantsala, P., Lovgren, T., **1998**. Engineering the steroid-specificity of an anti-17beta-estradiol Fab by random mutagenesis and competitive phage panning. *Protein Eng*. 11:143-52.

Schaffitzel, C., Berger, I., Postberg, J., Hanes, J., Lipps, H.J. and Pluckthun, A., **2001**. *In vitro* generated antibodies specific for telomeric guanine-quadruplex DNA react with *Stylonychia lemnae* macronuclei. *Proc. Natl. Acad. Sci. U.S.A*. 98:8572-7.

Scheepens, A., Williams, C.E., Breier, B.H., Guan, J. and Gluckman, P.D., **2000**. A role for the somatotropic axis in neural development, injury and disease. *J. Pediatr. Endocrinol. Metab*.13 Suppl 6:1483-91.

Schier, R., Bye, J., Apell, G., McCall, A., Adams, G.P., Malmqvist, M., Weiner, L.M. and Marks, J.D., **1996a.** Isolation of high-affinity monomeric human anti-c-erbB-2 single chain Fv using affinity-driven selection. *J. Mol. Biol.* 255:28-43.

Schier, R., Mccall, A., Adams, G.P., Marshall, K.W., Merritt, H., Yim, M., Crawford, R.S., Weiner, L.M., Marks, C. and Marks, J.D., **1996b.** Isolation of picomolar affinity anti-c-erbB-2 single-chain Fv by molecular evolution of the complementarity determining regions in the center of the antibody binding site. *J. Mol. Biol.* 263:551-67.

Schier, R. and Marks, J.D., **1996c**. Efficient in vitro affinity maturation of phage antibodies using BIAcore guided selections. *Hum. Antibodies Hybridomas* 7:97-105.

Schlehuber, S., Beste, G. and Skerra, A., **2000**. A novel type of receptor protein, based on the lipocalin scaffold, with specificity for digoxigenin. *J. Mol. Biol.* 297:1105-1120.

Schmidt, M., Hynes, N.E., Groner, B. and Wels, W., **1996**. A bivalent single-chain antibody-toxin specific for erbB-2 and the EGF receptor. *Int. J. Cancer.* 65:538-46.

Schodin, B.A. and Kranz, D.M., **1993**. Binding affinity and inhibitory properties of a single-chain anti-T cell receptor antibody. *J. Biol. Chem.* 268:25722-27.

Schreuder, M.P., Brekelmans, S., van den Ende, H. and Klis, F.M., **1993**. Targeting of a heterologous protein to the cell wall of *Saccharomyces cerevisiae*. *Yeast.* 9:399-409.

Scott, J.K. and Smith, G.P., **1990.** Searching for peptide ligands with an epitope library. *Science* 249:386-90.

Shao, Z., Zhao, H., Giver, L. and Arnold, F.H., **1998**. Random-priming *in vitro* recombination: an effective tool for directed evolution. *Nucleic Acids Res*. 26(2):681-3.

Shusta, E.V., VanAntwerp, J. and Wittrup, K.D., **1999**. Biosynthetic polypeptide libraries. *Curr. Opin. Biotech.* 10:117-122.

Sizonenko, S.V., Sirimanne, E.S., Williams, C.E. and Gluckman, P.D., **2001**. Neuroprotective effects of the N-terminal tripeptide of IGF-1, glycine-proline-glutamate, in the immature rat brain after hypoxic-ischemic injury. *Brain Res*. 922:42-50.

Skerra, A. and Pluckthun, A., **1988**. Assembly of a functional immunoglobulin Fv Fragment in *Escherichia coli*. *Science* 240:1038-41.

Skerra, A., **2000**. Engineered protein scaffolds for molecular recognition. *J. Mol. Recognit*. 13:167-87.

Smith, G.P., **1985.** Filamentous fusion phage: novel expression vectors that display cloned antigens on the virion surface. *Science* 228:1315-7.

Smith, J.W., Tachias, K. and Madison, E.L., **1995.** Protein loop grafting to construct a variant of tissue-type plasminogen activator that binds platelet integrin $\alpha_{IIb}\beta_3$. *J. Biol. Chem.* 270:30486-90.

Soderlind, E., Strandberg, L., Jirholt, P., Kobayashi, N., Alexeiva, V., Aberg, A.M., Nilsson, A., Jansson, B., Ohlin, M., Wingren, C., Danielsson, L., Carlsson, R. and Borrebaeck, C.A., **2000**. Recombining germline-derived CDR sequences for creating diverse single-framework antibody libraries. *Nat. Biotechnol*. 18:852-6.

Spada, S., Honegger, A. and Pluckthun, A., **1998**. Reproducing the natural evolution of protein structural features with the selectively infective phage (SIP) technology. The kink in the first strand of antibody kappa domains. *J. Mol. Biol*. 283:395-407.

Steele, E.J., Rothenfluh, H.S. and Blanden, R.V., **1997**. Mechanism of antigen-driven somatic hypermutation of rearranged immunoglobulin V(D)J genes in the mouse. *Immunol. Cell. Biol*. 75:82-95.

Stemmer, W.P., **1994a.** Rapid evolution of a protein *in vitro* by DNA shuffling. *Nature* 370:389-91.

Stemmer, W.P., **1994b**. DNA shuffling by random fragmentation and reassembly: in vitro recombination
for molecular evolution. *Proc Natl Acad Sci U S A*. 91(22):10747-51.

Suominen, I., Karp, M., Lahde, M., Kopio, A., Glumoff, T., Meyer, P. and Mantsala, P., **1987**. Extracellular production of cloned alpha-amylase by *Escherichia coli*. *Gene* 61:165-76.

Takahashi, F., Ebihara, T., Mie, M., Yanagida, Y., Endo, Y., Kobatake, E. and Aizawa, M., **2002**. Ribosome display for selection of active dihydrofolate reductase mutants using immobilized methotrexate on agarose beads. *FEBS Lett*. 514:106-10.

Teurk, C. and Gold, L., **1990**. Systematic evolution of ligands by exponential enrichment: RNA ligands to bacteriophage T4 DNA polymerase. *Science* 249:505-10.

Thompson, J., Pope, T., Tung, J.S., Chan, C., Hollis, G., Mark, G. and Johnson, K.S., **1996.** Affinity maturation of a high-affinity human monoclonal antibody against the third hypervariable loop of human immunodeficiency virus - use of phage display to improve affinity and broaden strain reactivity. *J. Mol. Biol.* 256:77-88.

Thompson, J.E., Vaughan, T.J., Williams, A.J., Wilton, J., Johnson, K.S., Bacon, L., Green, J.A., Field, R., Ruddock, S., Martins, M., Pope, A.R., Tempest, P.R. and Jackson, R.H., **1999**. A fully human antibody neutralising biologically active human TGFbeta2 for use in therapy. *J. Immunol. Methods*. 227:17-29.

Tonegawa, S., **1983.** Somatic generation of antibody diversity. *Nature* 302:575-81.

Towbin, H., Staehelin, T. and Gordon, J., **1979**. Electrophoretic transfer of proteins from polyacrylamide gels to nitrocellulose sheets: procedure and some applications. *Proc. Natl. Acad. Sci. U.S.A*. 76:4350-4.

Tramontano, A., Bianchi, E., Venturini, S., Martin, F., Pessi, A. and Sollazzo, M., **1994.** The making of the minibody: an engineered beta-protein for the display of conformationally constrained peptides. *J. Mol.Recognition* 7:9-24.

VanAntwerp, J.J. and Wittrup, K.D., **2000**. Fine affinity discrimination by yeast surface display and flow cytometry. *Biotech. Prog.* 16:31-37.

van den Beucken, T., van Neer, N., Sablon, E., Desmet, J., Celis, L., Hoogenboom, H.R. and Hufton, S.E., **2001**. Building novel binding ligands to B7.1 and B7.2 based on human antibody single variable light chain domains. *J. Mol. Biol*. 310:591-601.

van der Linden, R.H., de Geus, B., Frenken, G.J., Peters, H. and Verrips, C.T., **2000**. Improved production and function of llama heavy chain antibody fragments by molecular evolution. *J. Biotechnol*. 80:261-70.

Vaughan, T. J., Williams, A.J., Pritchard, K., Osbourn, J.K., Pope, A.R., Earnshaw, J.C., McCafferty, J., Hodits, R.A., Wilton, J. and Johnson, K.S., **1996**. Human antibodies with sub-nanomolar affinities isolated from a large non-immunized phage display library. *Nature Biotech.* 14:309-13.

Vita, C., Roumestand, C., Toma, F. and Menez, A., **1995.** Scorpion toxins as natural scaffolds for protein engineering. *Proc. Natl. Acad. Sci. U.S.A*. 92:6404-8.

Vita, C., Vizzavona, J., Drakopoulou, E., Zinn-Justin, S., Gilquin, B. and Ménez, A., **1998**. Novel miniproteins engineered by the transfer of active sites to small natural scaffolds. *Biopolymers* 47:93-100.

Waldo, G.S., **2003**. Genetic screens and directed evolution for protein solubility. *Curr. Opin. Chem. Biol*. 7:33-8.

Wall, J.G. and Pluckthun, A., **1999**. The hierarchy of mutations influencing the folding of antibody domains in *Escherichia coli*. *Protein Eng*. 12:605-11.

Ward, E. S., Gussow, D., Griffiths, A.D., Jones, P.T. and Winter, G., **1989**. Binding activities of a repertoire of single immunoglobulin variable domains secreted from Escherichia coli. *Nature* 341:544-46.

Ward, E.S., **1995**. V_H shuffling can be used to convert an Fv fragment of anti-hen egg lysozyme specificity to one that recognises a T cell receptor V alpha. *Mol. Immunol.* 32:147-56.

Waterhouse, P., Griffiths, A.D., Johnson, K.S. and Winter, G., **1993.** Combinatorial infection and *in vivo* recombination: a strategy for making large phage antibody repertoires. *Nucleic Acids Res.* 21:2265-6.

Westerlund-Wikstrom, B., **2000**. Peptide display on bacterial flagella: principles and applications. *Int. J. Med. Microbiol.* 290:223-230.

Whitlow, M., Filpula, D., Rollence, M.L., Feng, S.L. and Wood, J.F., **1994.** Multivalent Fvs: characterization of single-chain Fv oligomers and preparation of a bispecific Fv. *Protein Eng.* 7:1017-26.

Wilson, P.C., de Bouteiller, O., Liu, Y.J., Potter, K., Banchereau, J., Capra, J.D. and Pascual, V., **1998**. Somatic hypermutation introduces insertions and deletions into immunoglobulin V genes. *J. Exp. Med*. 187:59-70.

Wilson, D.S., Keefe, A.D. and Szostak, J.W., **2001**. The use of mRNA display to select high-affinity protein-binding peptides. Proc. Natl. Acad. Sci. U.S.A. 98:3750-5.

Winter, G. and Milstein, C., **1991.** Man-made antibodies. *Nature.* 349:293-9.

Wittrup, K.D., **2001**. Protein engineering by cell-surface display. *Curr. Opin. Biotechnol*. 12:395-9.

Worn, A. and Pluckthun, A., **1998**. An intrinsically stable antibody scFv fragment can tolerate the loss of both disulfide bonds and fold correctly. *FEBS Lett*. 427:357-61.

Wu, A.M., Chen, W., Raubitschek, A., Williams, L.E., Neumaier, M., Fischer, R., Hu, S.Z., Odom-Maryon, T., Wong, J.Y. and Shively, J.E., **1996**. Tumor localization of anti-CEA single-chain Fvs: improved targeting by non-covalent dimers. *Immunotechnology* 2:21-36.

Wu, H., Nie, Y., Huse, W.D. and Watkins, J.D., **1999**. Humanization of a murine monoclonal antibody by simultaneous optimization of framework and CDR residues. *J. Mol. Biol*. 294:151-62.

Xu, L., Aha, P., Gu, K., Kuimelis, R.G., Kurz, M., Lam, T., Lim, A.C., Liu, H., Lohse, P.A., Sun, L., Weng, S., Wagner, R.W. and Lipovsek, D., **2002**. Directed evolution of high-affinity antibody mimics using mRNA display. *Chem. Biol*. 9:933-42.

Yang, W.P., Green, K., Pinz-Sweeney, S., Briones, A.T., Burton, D.R. and Barbas, C.F. 3rd., **1995.** CDR walking mutagenesis for the affinity maturation of a potent human anti-HIV-1 antibody into the picomolar range. *J. Mol. Biol.* 254:392-403.

Young, N. M., MacKenzie, C.R., Narang, S.A., Oomen, R.P. and Baenziger, J.E., **1995**. Thermal stabilization of a single-chain Fv antibody fragment by introduction of a disulphide. *FEBS Lett.* 377:135-39.

Zaghouani, H., Steinman, R., Nonacs, R., Shah, H., Gerhard, W. and Bona, C., **1993**. Presentation of a viral T cell epitope expressed in the CDR3 region of a self immunoglobulin molecule. *Science* 259:224-27.

Zanetti, M. **1992**. Antigenised antibodies. *Nature* 355:476-77.

Zanetti, M., Filaci, G., Lee, R.H., del Guercio, P., Rossi, F., Bachetta, R., Stevenson, F., Barnaba, V. and Billetta, R., **1993**. Expression of conformationally constrained adhesion peptide in an antibody CDR loop and inhibition of natural killer cell cytotoxic activity by an antibody antigenised with the RGD motif. *EMBO J.* 12:4375-84.

Zeder-Lutz, G., Benito, A. and Van Regenmortel, M.H., **1999**. Active concentration measurements of recombinant biomolecules using biosensor technology. *J. Mol. Recognit*. 12:300-9.

Zhang, J.H., Dawes, G. and Stemmer, W.P., **1997.** Directed evolution of a fucosidase from a galactosidase by DNA shuffling and screening. *Proc. Natl. Acad. Sci. U.S.A.* 94:4504-9.

Zhao, H. and Arnold, F.H., **1997a**. Optimisation of DNA shuffling for high fidelity recombination. *Nucleic Acids Res.* 25 :1307-8.

Zhao, H. and Arnold, F.H., **1997b**. Functional and nonfunctional mutations distinguished by random recombination of homologous genes. *Proc. Nat. Acad. Sci. U.S.A.* 94:7997-8000.

Zhao, H., Giver, L., Shao, Z., Affholter, J.A. and Arnold, F.H., **1998**. Molecular evolution by staggered extension process (StEP) in vitro recombination. *Nat Biotechnol*. 16(3):258-61.

Zhou, H., Fisher, R.J. and Papas, T.S., **1994**. Optimization of primer sequences for mouse scFv repertoire display library construction. *Nucleic Acids Res*. 22:888-9.

Zhou, J.M., Fujita, S., Warashina, M., Baba, T. and Taira, K., **2002**. A novel strategy by the action of ricin that connects phenotype and genotype without loss of the diversity of libraries. *J. Am. Chem. Soc*. 124:538-43.

Zhu, Z., Zapata, G., Shalaby, G., Snedecor, B., Chen, H. and Carter, P., **1996**. High level secretion of a humanized bispecific diabody from *Escherichia coli*. *Bio/Technology* 14:192-96.